UNIVERSITÀ DEGLI STUDI DI MILANO

Ph.D. School in Molecular and Cellular Biology – XXXII cycle

Department of Pharmacological and Biomolecular Sciences

Targeting the Lipopolysaccharide Transport to Develop Novel Antimicrobial Drugs

Bio/19

Elisabete Cristina Cardoso Mendes Moura

Scientific supervisor: Alessandra Polissi

Co-supervisors: Jean-Pierre Simorre, Antonio Molinaro

Ph.D. Programme Coordinator: Martin Kater

2019/2020

This project has received funding from the European Union's Horizon 2020 research and innovation programme under the Marie Skłodowska-Curie grant agreement No 721484.

A scientist in his laboratory is not a mere technician: he is also a child confronting natural phenomena that impress him as though they were fairy tales.

Marie Curie

ACKNOWLEDGMENTS

Thank you to the people from my lab,

To Alessandra, for granting me this opportunity, for all the help you gave me with the university bureaucracy, for all you taught me, for the patience, for all the encouragement and criticism that has shaped me into a better scientist.

To Paola, your generosity is immeasurable. You always find the time to help even when you have a million other things to do. Thank you for all the knowledge you have shared with me and for the great scientific discussions.

To Ale, for all the times you had to translate something to English, for all the cappuccinos, for all the fun stories, for all that you have taught me at the lab and the experiments you suggested.

To Carlos, for that first beer and for immediately making me feel at home in a completely new place. We had our ups and downs, but it was great sharing this Ph.D. programme with you.

Obrigada à família e amigos de Portugal,

Aos meus pais, obrigado por sempre se interessarem pelo meu trabalho e fazerem perguntas mesmo quando não entendem as respostas.

À minha mãe, por ter sempre compreendido a minha vontade de trabalhar lá fora. Por me receber e deixar ir de braços abertos.

Ao meu pai, pelas inúmeras viagens que fez ao aeroporto.

À família na França, por me terem ajudado enquanto eu procurava um doutoramento. Agradeço pela generosidade de então, pela de hoje e pela de amanhã.

Às minhas amigas de Portugal, aquela família que tive a sorte de encontrar e que a distância não enfraquece.

Às professoras Célia e Conceição da universidade, por me terem incutido bons valores de investigação e por tudo o que aprendi com vocês. O rigor científico da química analítica é algo que pratico ainda hoje.

Thank you to the friends I met in Milan,

To Michael, for very patiently doing the mammoth task of proofreading this thesis. After these three years, I will take with me something even more special than a Ph.D., and I would not change any decision that has brought me here.

To Amogha, for the mountain trips, dinners, all the interesting conversations. From you, I learned a lot and I value your tenacity and optimism.

To D'arcy, for making that first year so colourful. It was friendship at first sight!

To Marina, for all the cupcakes and movie nights, for making our house a great place to live. Being at home was always fun.

Thank you. Grazie. Obrigada.

TABLE OF CONTENTS

ABSTRACT

The emergence of multidrug-resistant strains of Gram-negative pathogens that rapidly spread in the clinic is of great concern, since the range of antibiotics still effective against these organisms is limited and will continue to diminish. Therefore, the identification of novel and unexplored drug targets is an urgent need. Dissecting the biogenesis of the outer membrane (OM) and gaining insights into the multiprotein machineries that assemble this structure is vital if we want to succeed in developing innovative antibiotic compounds that can target these machineries. This thesis focuses on the machinery that transports lipopolysaccharide (LPS) to the cell surface: the LPS transport (Lpt) machinery. Due to its crucial role in cell physiology, the Lpt system represents a good target for the development of novel antimicrobial drugs.

Gram-negative bacteria possess an OM with highly selective permeability properties due to its asymmetric structure with LPS in the outer leaflet and phospholipids in the inner leaflet. The LPS layer is tightly packed and, by virtue of the amphipathic nature of the LPS molecule, hinders the passage of both lipophilic and hydrophilic compounds. LPS assembly at the cell surface relies on the activity of the Lpt transenvelope multiprotein complex comprising, in *Escherichia coli*, seven essential proteins (LptA-G). The LPS transport is powered by the ABC transporter $LptB_2FGC$ that extracts LPS from the IM and transfers it to LptA. LptA is the periplasmic protein that bridges the soluble β-jellyroll domains of LptC and LptD. At the OM, the LptDE translocon receives LPS from LptA and assembles it in the outer leaflet.

Recently, a host-defence antimicrobial peptide named thanatin was shown to cause defects in membrane assembly and to bind to the N-terminal β-strand of LptA *in vitro*. Since this region is involved in both LptA dimerization and interaction with LptC, we implemented the Bacterial Adenylate Cyclase Two-Hybrid (BACTH) system to detect these interactions in the periplasm and probe which is the target of thanatin (Manuscript 1). With this technique, we found that thanatin targets both interactions and has a stronger inhibitory effect on the LptC-LptA interaction. Further demonstrating a direct effect upon the LPS transport, we observed in thanatin-treated cells the degradation of LptA and the accumulation of LPS decorated with colanic acid (CA), both of which have been previously reported to be indicative of LPS transport defects (Manuscript 1).

We further explored how thanatin affects the integrity of the cell envelope by testing if this β-hairpin peptide could induce promoters regulated by envelope-specific stress response systems, such as the *lptAp1* promoter, and the promoters of *eptA* and *ldtD* (Additional

unpublished data). The *lptAp1* is a non-canonical σ^E-dependent promoter specifically activated by LPS biogenesis defects, and *eptA* belongs to the PmrAB regulon. PmrAB is a two-component system that regulates the expression of EptA and ArnT, which modify the phosphates of lipid A with phosphoethanolamine (PEtN) and aminoarabinose (L-Ara4N), respectively. The expression of LdtD is regulated by the Cpx stress response system and was recently shown to be induced by defects in LPS synthesis and transport to the OM. The LD-transpeptidase activity of LdtD remodels the peptidoglycan to strengthen it and avoid cell lysis when the OM is severely compromised.

We found that thanatin induces all the three tested promoters and, surprisingly, that thanatin cannot activate *lptAp1* in cells unable to synthesize CA (Additional unpublished data), thus suggesting a link to the Rcs stress response. Thanatin also induces the expression of EptA, therefore likely causing the modification of LPS with PEtN, and LdtD, possibly leading to the remodelling of the peptidoglycan cell wall.

Recent structural work on the IM complex $LptB_2FGC$ has shown that LptC has a regulatory role on the transporter by modulating the ATPase activity and coupling with the transport of LPS. Nevertheless, LptC can tolerate several mutations and it is still unclear why its role in LPS transport is essential. In a genetic selection designed to clarify the functional role of LptC, our group previously isolated viable mutants lacking LptC, which all carried amino acid substitutions at the residue R212 in the periplasmic domain of LptF. The substitution R212G was shown to restore cell viability and OM permeability to a nearly wild-type level; therefore, in this work, we performed a biochemical characterization of this suppressor mutant (*lptF*^{R212G}) (Manuscript 2). By means of *in vivo* pull-down assays, we showed that $LptF^{R212G}$ allows the assembly of a functional six-component machinery and we observed by UV-photocrosslinking that $LptF^{R212G}$ directly interacts with LptA. Interestingly, we found by assessing the ATPase activity of $LptB_2F^{R212G}G$ and $LptB_2FG$ that the maximum phosphate concentration released by the mutant is lower than the wild type. Moreover, unlike the wild type, the activity of $LptB_2F^{R212G}G$ was not stimulated when we tried to assemble the bridge by adding soluble LptC and LptA. By analysing the interaction networks around the residue R212 of LptF, we also proposed a putative mechanism adopted by the Lpt transporter to regulate LPS transfer from $LptB_2FGC$ to LptA.

ABBREVIATIONS

ABC	ATP binding cassette
ACP	acyl carrier protein
AMP	antimicrobial peptide
ATP	adenosine triphosphate
Bam	β-barrel assembly machinery
BLI	β-lactamase inhibitor
CA	colanic acid
CL	cardiolipin
Cpx	conjugative pilus expression
CRAB	carbapenem-resistant *Acinetobacter baumannii*
CRAP	carbapenem-resistant *Pseudomonas aeruginosa*
CRE	carbapenem-resistant *Enterobacteriaceae*
DBO	diazabicyclooctane
DNA	deoxyribonucleic acid
EDTA	ethylenediaminetetraacetic acid
EMA	European Medicines Agency
ESBL	extended-spectrum β-lactamase
ESBL-PE	ESBL-producing *Enterobacteriaceae*
ESR	envelope stress response
FDA	U.S. Food and Drug Administration
FIC	fractional inhibitory concentration
FIC_I	FIC index
IM	inner membrane
Kdo	3-deoxy-ᴅ-*manno*-oct-2-ulosonic acid
Lol	localization of lipoproteins
LOS	lipooligosaccharide
LPS	lipopolysaccharide
Lpt	lipopolysaccharide transport
L-Ara4N	4-amino-4-deoxy-L-arabinose
MAMP	microbial-associated molecular pattern
MBL	metallo-β-lactamase
mcr	mobilized colistin resistance
MDR	multidrug-resistant

MD2	myeloid differentiation factor 2
MIC	minimal inhibitory concentration
Mla	maintenance of lipid asymmetry
NBD	nucleotide-binding domain
NMR	nuclear magnetic resonance
OM	outer membrane
OMP	outer membrane protein
OMPTA	outer membrane protein targeting antibiotics
PBP	penicillin-binding protein
PE	phosphatidylethanolamine
PEtN	phosphoethanolamine
PG	peptidoglycan
PL	phospholipid
PMB	polymyxin B
pmf	proton motive force
POTRA	polypeptide transport-associated
Rcs	regulator of capsule synthesis
RNA	ribonucleic acid
RND	resistance-nodulation-division
rRNA	ribosomal RNA
SLP	surface lipoprotein
TCS	two-component system
TLR4	toll-like receptor 4
TM	transmembrane helix
TMD	transmembrane domain
WHO	World Health Organisation
XDR	extensively drug-resistant

PART I. INTRODUCTION

CHAPTER 1. Antimicrobial resistance: why are Gram-negative pathogens a major concern?

1.1 The gap in antibiotic discovery

The discovery of penicillin in 1928 by Alexander Fleming is a hallmark in the history of medicine. The advent of antibiotics represents one of the greatest advances in health care, enabling not only the treatment of infections but also other medical interventions such as complex care, surgeries, and cancer treatment. However, over the last few decades, antibiotic discovery has dropped dramatically accompanied by the emergence and global spread of antimicrobial resistance causing life-threatening infections with no available treatment [1, 2]. Most of the antibiotics used in patients today have derived from classes discovered more than 35 years ago. This is worrisome because when resistance to one antibiotic rises, it often leads to resistance to multiple drugs in the same class, given the similar chemical structure. Nevertheless, current research is largely focused on modifying these existing classes to overcome bacterial resistance [3]. Ever since the "golden age" of antibiotic discovery, new starting points for the development of innovative antibiotic classes have become harder to find.

The difficulty in the discovery and development of novel antibiotic chemical scaffolds, the challenges in running the clinical trials and proving superior drug efficacy comparing to already existing treatments, and the diminishing revenue on investments have led Big Pharma companies to scale down or abandon their antibacterial research programmes [2, 4]. The development of new antibiotics, drugs with a low market value that should ideally only be used as a last-resort treatment against multidrug-resistant pathogens, is not attractive from an economical point of view to the large pharmaceutical companies. Thus, a lot of the initial discovery work is performed by smaller biotechnology enterprises and basic research is mostly performed by the academic community [5].

The wide spread of antimicrobial resistance, the decline of drug approvals and poor prospects on the discovery of novel classes of antibiotics have rendered a future that has been referred to by the World Health Organisation (WHO) as a "post-antibiotic era", where common infections may kill again [6]. In 2016, in order to concentrate global efforts and guide scientists to where action is urgently needed, the WHO was commissioned by its member states with the task of compiling data and selecting which pathogens were more critical according to mortality

and health-care burden, the increase in antibiotic resistance, the availability of effective treatments and prospects of successful new therapies [7, 8]. The WHO priority pathogens list indicates that, aside from multidrug-resistant tuberculosis, antibacterial research and development should mainly focus on multidrug-resistant (MDR) and extensively drug-resistant (XDR) Gram-negative infections. In the top category, classified as a critical concern, are carbapenem-resistant *Acinetobacter baumannii*, carbapenem-resistant *Pseudomonas aeruginosa*, carbapenem- and third generation cephalosporin-resistant *Enterobacteriaceae* [7]. These pathogens cause infections with very limited treatment options and high morbidity and mortality rates [9].

1.2 The Gram-negative cell envelope

The cell envelope is a multi-layered structure surrounding the cytoplasm that protects the bacterial cell from the environment [10]. The structural differences in the cell envelope allow the phylogenetic division between bacteria surrounded by a single membrane, the monoderms, and with a double membrane, referred to as diderms [11]. Gram-negative bacteria fall into the latter group, possessing two membranes with distinct permeability properties that antibiotics need to cross to access an intracellular target. This sophisticated double-barrier maintains nutrient uptake and extrusion of waste products while protecting the cell from toxic compounds [12].

The Gram-negative cell envelope is composed of an inner membrane (IM), a thin peptidoglycan layer, and an outer membrane (OM) (**Figure 1**) [10]. Gram-positive bacteria, on the other hand, lack an OM and are surrounded with many interconnected layers of peptidoglycan bound to lipoteichoic acid, that retain the crystal violet stain in the Gram staining procedure [13]. The absence of that extra selective permeation barrier in Gram-positive organisms results in a higher susceptibility to antibiotics.

Escherichia coli, a Gram-negative bacterium belonging to the *Enterobacteriaceae* family and commonly found in the human gut, is the model organism in scientific research and it has been extensively studied over the years, being one of the most well-understood organisms nowadays [14, 15].

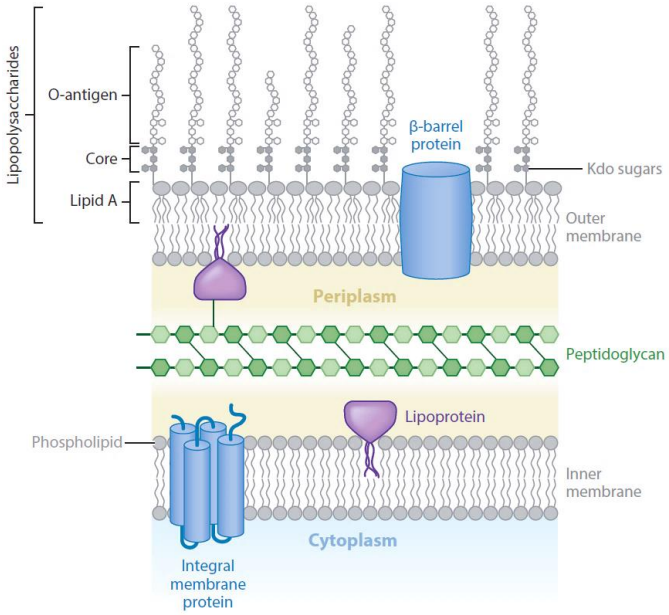

Figure 1. The Gram-negative cell envelope architecture (from [16]). For clarity, only integral proteins embedded in the membranes and lipoproteins are depicted. See text for details.

1.2.1 Inner membrane (IM)

The cytoplasmic IM is a symmetrical bilayer of phospholipids with very low permeability to polar molecules. In *E. coli*, it is mainly composed of phosphatidylethanolamine, phosphatidylglycerol, and cardiolipin [10, 17]. Integral proteins span the membrane with one or more transmembrane α-helical domains, while lipoproteins are inserted into the outer leaflet. Peripheral membrane proteins may be associated with either the inner or the outer leaflet, or may be present as part of protein complexes that contain integral membrane proteins [18].

The cytoplasmic membrane features respiratory complexes that maintain the proton motive force required for energy production, and transport systems that regulate the passage of nutrients, waste products and secretion of proteins. Other IM protein complexes are involved in envelope biogenesis and cell division; moreover, receptors of signalling systems sensing the environment and linking external stimuli to changes in gene transcription are also present [10, 18].

1.2.2 Peptidoglycan cell wall

In Gram-negative bacteria, the IM and the OM delimit what is called the periplasm, an aqueous compartment densely packed with proteins and containing the peptidoglycan cell wall, structure that confers shape and osmotic stability to the cell. Antibiotics that damage the peptidoglycan cause cell lysis due to the cytoplasmic turgor pressure [10, 19].

The peptidoglycan, also known as murein, is composed of repeating units of the disaccharide *N*-acetyl glucosamine (GlcNAc)–*N*-acetyl muramic acid (MurNAc) linked by β-1,4 glycosidic bonds and with a pentapeptide side chain attached to the carboxyl group of the MurNAc moiety. In *E. coli* and other *Enterobacteriaceae*, this side chain is composed of *L*-alanine, *D*-glutamic acid, *L*-*meso*-diaminopimelic acid, and two *D*-alanines [20, 21]. The linear glycan strands are covalently linked directly or through a short peptide bridge between the carboxyl group of the *D*-Alanine residue at position 4 and the amino group of the diaminopimelic acid at position 3 of an adjacent strand. The cross-linking forms the characteristic net structure of the peptidoglycan sacculus surrounding the IM. In *E. coli*, the cell wall was determined to have a thickness of 6.35±0.53 nm by cryo-TEM [22]. The extent of the cross-linking and the length of the glycan strands vary with bacterial species, strains and growth conditions [19].

In *E. coli*, the peptidoglycan is covalently attached to the inner leaflet of the OM by a lipoprotein called Lpp, or Braun's lipoprotein [23, 24]. Lpp is the determinant of the size of the cell envelope and helps maintaining its integrity [25-27]. By covalently binding the OM to the peptidoglycan sacculus, it works as a tether and prevents the OM from tearing apart from the cell. Lpp is the most abundant protein in *E. coli* and homologous lipoproteins have been identified in several other γ-Proteobacteria [26, 28]. In some Gram-negative species however, such as *Proteus mirabilis* and *Pseudomonas fluorescens*, a covalently PG-bound lipoprotein is not present [28, 29].

1.2.3 Outer membrane (OM): a protective barrier

The OM is an asymmetrical lipid bilayer containing nearly exclusively phospholipids in the inner leaflet and lipopolysaccharide (LPS) in the outer leaflet, which confers unique permeability properties [10]. The phospholipid composition of the inner leaflet is similar to that of the cytoplasmic membrane [10, 17].

LPS can be divided in three major domains: the lipid A (with the acyl groups inserted into the outer leaflet), the core phosphorylated oligosaccharide (with Kdo sugars linked to the lipid A), and the O antigen formed by repeating oligosaccharide units (**Figure 1**) [30]. LPS is a potent activator of the host immune response and is responsible for the endotoxic shock associated with septicemia in Gram-negative infections, which results from excessive inflammation. LPS structure, function, and biosynthesis will be thoroughly discussed in Chapter 2.

The LPS leaflet is a very effective permeability barrier [12, 30]. LPS molecules strongly interact with each other through bridging by divalent cations (Mg^{2+} and Ca^{2+}) and H-bonding. Divalent cations bind the negatively charged phosphate groups avoiding repulsion and maintaining OM integrity. Moreover, the acyl chains of LPS are all saturated enabling tight packing and each lipid molecule is linked to many fatty acid chains, both contributing to a reduced fluidity of the hydrocarbon region. LPS polar structure combined with the nonfluid gel-like nature of the LPS layer greatly hamper the permeation of lipophilic molecules such as detergents, bile salts, dyes, and antibiotics.

Proteins in the OM include lipoproteins and integral proteins. Lipoproteins are anchored to the membrane by N-terminally attached lipids and they can either be present at the periplasmic side or exposed at the cell surface [31, 32]. Integral membrane proteins, referred as OMPs (OM proteins), fold into antiparallel β-barrels, unlike IM integral proteins that have hydrophobic α-helices. OmpA, a major OMP in *E. coli*, plays an important role in the maintenance of membrane integrity by non-covalently binding the peptidoglycan through its C-terminal periplasmic domain, thus stabilizing the position of the cell wall in the periplasm [33-37].

Among the most abundant OMPs are the porins. These proteins are water-filled open channels consisting of transmembrane antiparallel β-strands with alternating hydrophobic and hydrophilic amino acids facing, respectively, outwards and inwards in the β-barrel [12, 38, 39]. Based on their activity, porins can be divided in general porins, determining membrane

permeability, and substrate-specific porins. General porins allow the passive diffusion of small hydrophilic molecules (< 600 Da), like mono- and disaccharides and amino acids, with no substrate specificity, albeit with some selectivity towards the substrate charge or size. The porins OmpF and OmpC prefer cations, with OmpF allowing diffusion of slightly larger solutes. PhoE, on the other hand, favours anions and is expressed under phosphate starvation. LamB, also strongly induced when needed, is a specific porin that mediates the uptake of maltose and maltodextrins. Large substrates such as iron-siderophore complexes or vitamin B_{12} are transported by using TonB-dependent receptors at the OM (e.g., FhuA, FepA, and BtuB), larger β-barrels functioning as gated channels with high affinity to the ligands [12, 39].

While the LPS outer layer is an efficient obstacle for the passage of hydrophobic compounds, porins limit the diffusion of large hydrophilic or charged molecules, making the OM an outstanding permeability barrier.

1.3 Antimicrobial resistance

Gram-negative bacteria are intrinsically resistant to many antibiotics due to the complex architecture of their cell envelope. Nearly all licensed antibacterial agents need to penetrate the OM to reach their target. Hydrophilic drugs can cross the OM by diffusion through porins (e.g., β-lactams, fluoroquinolones) or by self-promoted uptake (e.g., aminoglycosides), while lipophilic drugs enter the cell by diffusion through the lipid bilayer (e.g., macrolides, novobiocin) [12]. Antibiotics that succeed in penetrating the OM and reaching the periplasm are then accessible to efflux pumps, that bind them and expel them from the cell [40].

Porins are known to play a role in antibiotic resistance and membrane integrity [37, 41]. They can limit the influx of drugs by size-exclusion, hydrophobicity, and charge repulsion. Gram-negative bacteria can alter their expression and function, resulting in changes in antibiotic sensitivity. In *E. coli*, OmpF was shown to be the main route for the permeation of many antibiotics, including β-lactams and fluoroquinolones, and OmpC was also reported to facilitate the entry of β-lactams [37, 42-46]; therefore, decreased expression levels of these porins or mutations that impair their transport function can lead to clinical resistance *via* a reduced antibiotic influx. In *A. baumannii*, the deletion of OmpA increases susceptibility to several antibiotics, possibly due to impaired membrane integrity given the OmpA structural

role [47]. Specific porins, on the other hand, have minor importance in the transport through the OM, although a few have been reported, like the OprD of *P. aeruginosa* that facilitates the diffusion of carbapenems into the cell [48]. The loss of this specific porin or its down-regulation decreases the susceptibility of *P. aeruginosa* to these antibiotics. Through functional loss or production of modified porins, the rate of entry of drugs can be decreased. However, lower antibiotic permeation alone does not completely halt influx and, therefore, does not account for a high level of antibiotic resistance.

The intracellular concentration of an antibacterial agent is a fine balance between influx and efflux [49]. Efflux pumps regulate the active transport of toxic compounds (e.g., detergents, bile acids, solvents, and dyes) to the external medium and they strongly affect antimicrobial resistance [40]. The bacterial efflux transporters can be divided into five classes: the major facilitator superfamily (MFS), the small multidrug resistance (SMR) family, the multidrug and toxic compound extrusion (MATE) family, the resistance-nodulation-division (RND) superfamily, and the adenosine triphosphate (ATP)-binding cassette (ABC) superfamily. The ABC-type systems use ATP hydrolysis as the energy source, whereas the others are driven by the proton-motive force thus being secondary transporters [40]. The RND superfamily of efflux pumps is a major participant in intrinsic multidrug resistance in Gram-negative bacteria. They form tripartite systems that span the cell envelope and expel drugs, which have either entered through the OM or have been extruded from the cytoplasm, from the periplasm to the exterior of the cell (**Figure 2**). An RND efflux system comprises the RND transporter at the IM (the pump), a periplasmic membrane fusion protein (MFP), and an OM channel protein (OMP). The main RND efflux systems constitutively expressed in *E. coli* and *P. aeruginosa* are AcrAB-TolC and MexAB-OprM, respectively, conferring resistance to an incredibly wide range of antibiotics.

It is the specificity and efficiency of multidrug efflux pumps, combined with the slow permeation of antibiotics through the OM, that determines the intracellular concentration of drugs and differences in antibiotic susceptibility among strains. The synergistic effect between the two independent mechanisms, that select antibiotics based on different physicochemical properties, results in a reduced intracellular antibiotic accumulation [50-52].

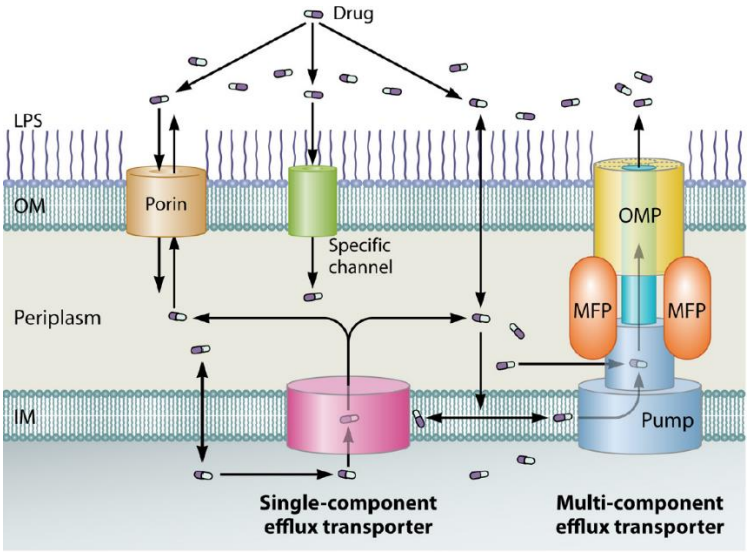

Figure 2. Drug intracellular concentration is an equilibrium between influx and efflux (from [40]). Antibiotics can enter the cell by diffusion through the lipid bilayer or through protein channels. Extrusion occurs through efflux transporters existing as (i) single-component pumps, that sequester drugs from the cytoplasmic side and expel them into the periplasm, or (ii) multi-component pumps, expelling drugs directly outside the cell from the periplasm and IM.

Another key resistance mechanism involves drug-inactivation by β-lactamases or aminoglycoside-modifying enzymes (AMEs), which can be intrinsically expressed in certain species or acquired through horizontal transfer of mobile genetic elements [53, 54]. The recent emergence of plasmid-mediated tetracycline-inactivating enzymes, capable of degrading all tetracyclines, is of increasing concern [55, 56].

In *Enterobacteriaceae*, resistance to third-generation cephalosporins was conferred by plasmid-borne extended-spectrum β-lactamases (ESBLs), and it has quickly spread since the 1980s when it was first described [57]. Carbapenems are a first-line choice of treatment for severe infections caused by ESBL-producing *Enterobacteriaceae* (ESBL-PE). However, resistance to carbapenems has been reported worldwide, both in hospital settings and the wider community, mainly due to the widespread acquisition of carbapenemase genes [58, 59]. The KPC, OXA-48, and the metallo-β-lactamases IMP, VIM and NDM are the most relevant in determining carbapenem resistance. Carbapenem-resistant *Enterobacteriaceae* (CRE) are of great concern since they have become resistant to nearly all currently licensed therapies.

Colistin is a last-resort antibiotic for infections caused by carbapenemase-producing Gram-negative bacilli [60]. Polymyxins, such as colistin (polymyxin E) and polymyxin B, are antimicrobial peptides that bind to the LPS, competitively displacing the divalent cations and inserting themselves into the OM, thus disrupting its integrity. The exact killing mechanism,

whether it is through pore formation at the OM or by an alternative mechanism taking place at the cytoplasm, is still unknown [61]. Reports of clinical isolates with decreased susceptibility to these antimicrobial peptides have been increasing [62]. Resistance can arise from chromosomal mutations in genes coding for LPS biosynthesis or in regulatory genes controlling the expression of enzymes that decorate LPS reducing its net negative charge, hence lowering its affinity to the positively charged polymyxins [63]. These modifications frequently include the addition of phosphoethanolamine (e.g., in *A. baumannii*) or aminoarabinose (e.g., in *P. aeruginosa*) or both (e.g., in *E. coli*) to the lipid A moiety of LPS. In *A. baumannii*, resistance can also occur through complete loss of LPS production, caused by either mutations or insertional inactivation of genes encoding the lipid A biosynthesis [64, 65].

Until recently, colistin resistance was solely chromosomally mediated and, therefore, not transmissible. However, in November 2015, the emergence of plasmid-mediated resistance due to the *mcr-1* (mobilized colistin resistance) gene was described for the first time [66]. This gene encodes a transferase that catalyses the addition of phosphoethanolamine to the lipid A, and it often co-carries other resistance genes (i.e., β-lactamase and carbapenemase genes) [67]. Worldwide dissemination of *mcr* and its detection in carbapenemase-producing bacteria is now greatly threatening the clinical utility of polymyxins. Furthermore, plasmids carrying *mcr* and genes encoding metallo-β-lactamases (e.g., bla_{NDM-1}) may also carry genes coding for tetracycline-inactivating enzymes, such as Tet(X3) and Tet(X4), rendering co-resistance to the remaining last-resort antibiotics colistin and tigecycline, and thus creating XDR strains [55, 56].

1.4 A new arsenal or a bleak pipeline?

Multidrug-resistant strains of Gram-negative pathogens can cause some of the most difficult-to-treat infections and are globally spreading at alarmingly increasing rates, representing one of the biggest threats to public health [68]. Their cell envelope, with its double membrane structure combined with efflux pumps, hinders the research attempts in finding effective antibiotics. Moreover, they are very efficient at upregulating or acquiring new genes encoding diverse resistance mechanisms. Worldwide efforts should, therefore, concentrate on

tackling the problem of antimicrobial resistance in order to meet the urgent need of new antimicrobials active against these pathogens.

Antibiotics currently used in the clinic mainly act on the cell wall synthesis, protein synthesis and nucleic acid synthesis [69]. The β-lactams are a large class of antibacterial molecules that share the β-lactam ring as the pharmacophore and include, e.g., the penicillins, cephalosporins, and carbapenems. The β-lactam antibiotics bind the penicillin-binding proteins (PBPs) to inhibit the cross-linking between peptidoglycan layers, and resistance arises with the production of β-lactamases that hydrolyse the β-lactam ring. Tetracyclines and aminoglycosides inhibit protein synthesis by binding to the 16S rRNA of the 30S ribosomal subunit, and resistance occurs through drug inactivation or *via* ribosome-protection mechanisms. Antibiotics inhibiting the synthesis of nucleic acids include, among other compounds, the fluoroquinolone class that targets the bacterial topoisomerase, the DNA gyrase, thus disrupting DNA replication, and resistance mechanisms include chromosomal target mutation or target protection.

In the last ten years, seven agents with activity against MDR Gram-negative bacteria have obtained market authorization by the EMA and/or FDA [70, 71]. These new antibiotics are all improved derivatives of existing classes and, in chronological order of approval, they are the following: ceftolozane/tazobactam, ceftazidime/avibactam, meropenem/vaborbactam, plazomicin, eravacycline, imipenem/cilastatin+relebactam, and cefiderocol. The first two cephalosporin/β-lactamase inhibitor combinations are effective against MDR *P. aeruginosa* and ESBL-PE. All the other agents are active against CRE, with the eravacycline also being effective against carbapenem-resistant *A. baumannii* (CRAB).

The ceftolozane, used in combination with the established β-lactamase inhibitor (BLI) tazobactam, is a novel fifth-generation cephalosporin with a modified side chain that increases the affinity to some PBPs, thus presenting more potent antibacterial activity [72]. The BLIs have evolved from the first generation comprising β-lactam-derived molecules (clavulanic acid, sulbactam, tazobactam) to novel classes based on non-β-lactam structures, such as the diazabicyclooctanes (DBOs) and the boronates, with an extended spectrum of activity [72]. From the recently approved drugs, DBO-based BLIs include the avibactam, the first of its class, and relebactam. Ceftazidime is an established third-generation cephalosporin paired with avibactam that covalently binds, with slow regeneration through recyclization, to β-lactamases inhibiting their action [72, 73]. Relebactam in combination with imipenem, a β-lactam cell wall inhibitor, and cilastatin, a dehydropeptidase inhibitor that prolongs the antibiotic effect of imipenem, has a synergistic effect that restores *P. aeruginosa* susceptibility to imipenem in

otherwise resistant isolates [70, 72]. Boronate-based BLIs, with a wider inhibitory spectrum that includes some metallo-β-lactamases (MBLs), resemble a transition state intermediate formed upon the degradation of the β-lactam ring by β-lactamases [72, 74]. Vaborbactam is a cyclic boronate used in combination with the broad-spectrum meropenem to protect it from degradation by carbapenemases, excluding MBLs and OXA enzymes [70].

Plazomicin is a new aminoglycoside with activity against *Enterobacteriaceae* containing aminoglycoside-modifying enzymes [75]. Although also active against CRE, strains that produce NDM-1 MBL or OXA-48 are often resistant to plazomicin because of the co-production of ribosomal methyltransferases (16S rRNA methylases) that modify plazomicin's target [76, 77].

Eravacycline is a synthetic tetracycline analogue of the tigecycline with a wider spectrum of activity [78]. This new fluorocycline demonstrated a potent broad-spectrum activity against Gram-negative species including ESBL-PE and CRAB, with the exception of *P. aeruginosa* [78, 79]. Eravacycline is not susceptible to the tetracycline-specific efflux and its activity is not affected by ribosomal protection mechanisms; however, it is degraded by plasmid-mediated tetracycline-inactivating enzymes [55].

Cefiderocol, a siderophore cephalosporin that uses the iron transport mechanism in addition to porin channels to enter the bacterial periplasmic space, has a broad spectrum of activity against all three critical-priority pathogens, although it still exhibits substantial cross-resistance with existing classes [70, 80]. It is the only recently patented antibacterial agent stable to hydrolysis by MBLs [81].

There is only a small number of agents acting on critical Gram-negative bacteria in the current clinical development pipeline, comprising all phases of human clinical testing [3, 71]. Furthermore, the pipeline is dominated by derivatives of established antibacterial classes, mostly β-lactam/β-lactamase inhibitor combinations, which are not innovative enough to overcome pre-existing cross-resistance. These agents are mainly active against specific pathogens, or subsets of resistant strains, and the majority targets ESBL, KPC and OXA-48 producing *Enterobacteriaceae*, with a major gap in effectivity against MBL-producers. In Phase 3 clinical trials, only one product targets CRAB, the sulbactam+durlobactam, and just a single agent has activity against MBL-producing CRE, the cefepime+taniborbactam. There are no products in later stages of the pipeline effective against MDR *P. aeruginosa*; however, in Phase 1 development, a promising polymyxin nonapeptide derivative shows activity against CRE, CRAB and CRAP.

According to the WHO database of 2019, there are 252 antibacterial agents targeting priority pathogens in the preclinical development pipeline, that includes products beyond the lead generation phase, with remarkably diverse structures and modes of action [5]. Direct-acting small molecules, i.e., traditional antibiotics directly inhibiting or killing bacteria, account for the majority of the pipeline, with most representing new chemical classes and/or new targets, followed by non-traditional approaches and antimicrobial peptides. The cell envelope remains an attractive target with most of the antibacterial agents acting on the cell wall synthesis or the membrane. The non-traditional therapies are varied and include phages, potentiators, anti-virulence approaches, immunomodulators, and microbiome-modifying therapeutics. The preclinical pipeline is marked by a shift towards pathogen-specific strategies, which seems to reflect efforts in directing the research to WHO critical pathogens and will raise the need for complementary diagnostics.

The clinical development pipeline certainly falls short when it comes to innovation regarding novel antibacterial classes, targets or modes of action. In preclinical development, however, the research is much more diverse, holding a promising and encouraging innovative potential. Since most of the preclinical projects are predicted to fail, large numbers of drug candidates in pre-clinical stages are needed to guarantee that some ultimately reach health care. Far more work and funding are required to progress innovative approaches into effective treatments that can enter the clinic and join the fight against MDR pathogens. For now, despite increased awareness, the clinical antibacterial pipeline remains insufficient to meet the needs of current and future patients.

CHAPTER 2. Outer membrane biogenesis: building an extra protective coat

The unique architecture of the OM protects Gram-negative bacteria from remarkably diverse toxic molecules. Composing this barrier are phospholipids, LPS, OMPs, and lipoproteins [16, 82]. The OM components are synthesized at the cytoplasm or at the IM, and then transported to the OM by multiprotein machineries: the phospholipid transport systems, and the Lpt (LPS transport), Bam (β-barrel assembly machinery), and Lol (localization of lipoproteins) pathways (**Figure 3**). After translocation across the IM, the hydrophobic moieties of the amphipathic OM components have to be shielded in the aqueous periplasmic compartment, either by chaperones (e.g., lipoproteins) or, in the case of LPS, through a multiprotein-bridge with a hydrophobic lumen; moreover, transport and final assembly at the OM is conducted without an energy source, since there is no ATP outside of the cytoplasm. There is some degree of interdependence between the distinct pathways, since both Lpt and Bam complexes contain β-barrel and lipoproteins. Therefore, the assembly of the OM requires a tight coordination between the various transport processes.

This chapter will overview the protein machineries involved in building the OM and present a comprehensive review on the LPS transport to the cell surface. Due to LPS's fundamental structural and immunological role, its function and biosynthesis will also be discussed.

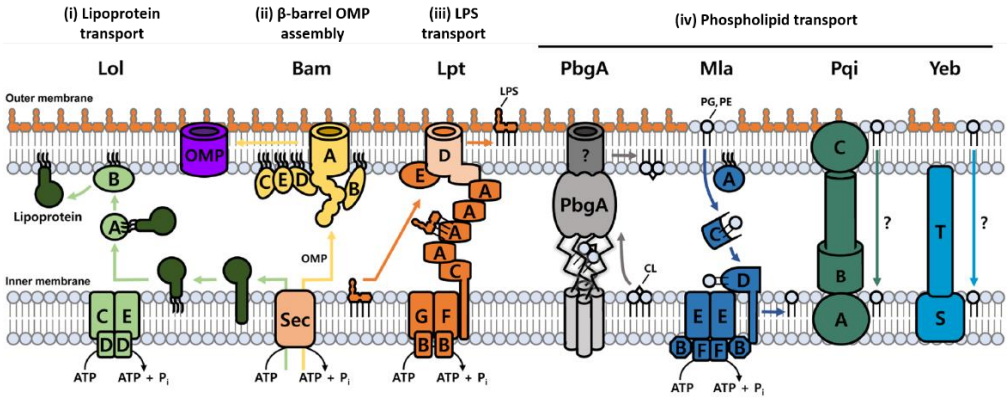

Figure 3. Assembly machineries of the *Escherichia coli* outer membrane (OM) (adapted from [83]). (i) The Lol pathway transports and inserts lipoproteins at the OM. (ii) The Bam complex folds and inserts β-barrel proteins into the OM (referred to as OM proteins, OMPs). (iii) The lipopolysaccharide transport (Lpt) machine is responsible for lipopolysaccharide (LPS) transport and assembly at the OM outer leaflet. (iv) Phospholipid transport systems carry phospholipids and maintain OM asymmetry.

2.1 LPS biogenesis

2.1.1 Structure and function of LPS

As described in Chapter 1, LPS is a large glycolipid presenting a tripartite structure: the lipid A, the core oligosaccharide, and the O antigen (**Figure 4A**) [30].

Lipid A, an acylated β-1',6-linked glucosamine disaccharide, is the hydrophobic moiety forming the OM outer monolayer and the most conserved domain of LPS. In *E. coli*, the glucosamines are linked to saturated acyl chains at the 2, 3, 2', and 3' positions, by an amide or ester bond, and are phosphorylated at the 1 and 4' positions. The fatty acids of the distal glucosamine are typically further acylated on their two hydroxyl groups; thus, mature lipid A is mostly hexa-acylated. Although lipid A is conserved within species, it can be altered in response to environmental stresses [84].

The core oligosaccharide, which can be further divided in an inner and outer core, is bound to the lipid A and consists of non-repeating sugar residues [30, 85]. While the outer core is more variable, comprising mostly hexoses, the inner core is more conserved within isolates of the same species and usually contains 3-deoxy-ᴅ-*manno*-oct-2-ulosonic acid (Kdo) and heptose residues, to which phosphates and other substituents, such as phosphoethanolamine, can be added [86, 87].

The O antigen is a long chain of oligosaccharide repeating units, each composed of two to eight sugar residues, attached to the core domain of LPS [88]. It is a remarkably diverse structure, presenting variations amongst strains within a species and, in some Gram-negative bacteria, the O antigen is even absent (e.g., *Neisseria meningitidis, Bordetella pertussis*) [89-91]. The laboratory *E. coli* strain K-12 derivatives do not synthesize the O antigen, due to an insertion mutation in the *rfb* locus, and produces an LPS referred to as "rough", as opposed to the wild-type "smooth" LPS [92]. Rough LPS can also be termed lipooligosaccharide, since it lacks the long O antigen.

Bacteria can alter LPS structure and regulate its synthesis in response to the environmental conditions [12]. Although a major structural OM component, LPS-null mutants have been isolated in *A. baumannii*, *N. meningitidis,* and *Moraxella catarrhalis* [64, 93, 94]. LPS seems to be non-essential in some organisms; nevertheless, its loss is not inconsequential, and LPS-deficient strains are less virulent and more susceptible to antibiotics routinely used to treat only

Gram-positive infections [64, 95]. The essentiality of LPS is complex and varies considerably with bacterial genera, species and even strain background, depending on several factors such as the cellular context and how the removal of LPS affects other metabolic processes [96], for example, given that several OMPs require LPS for proper assembly and function [97-99], LPS would be indispensable when specific porins are necessary to meet particular nutrient requirements of the bacterium.

The structural role of LPS in establishing an effective permeability barrier was discussed in Chapter 1. The densely packed acyl chains not only prevent the permeation of hydrophilic molecules but also hamper the passive diffusion of lipophilic compounds. Moreover, the hydrophilic core domain and O antigen further hinder the entrance of lipophilic molecules into the bacterial cell.

LPS plays a key role in host-microbe interactions by modulating the host immune response [100, 101]. Lipid A, also known as endotoxin, is a microbial-associated molecular pattern (MAMP) and, therefore, is mainly responsible for the biological toxicity. The innate immune system responds primarily to this most conserved part of LPS, and activation of the immune response mainly occurs through signalling *via* the toll-like receptor 4 (TLR4), a pattern recognition receptor present on many cell types including macrophages and endothelial cells.

LPS released from the bacterial cell surface into the circulation binds the LBP (LPS-binding protein) [102]. Then, LPS is delivered to CD14 that mediates the recognition of LPS as well as its transfer to the TLR4/myeloid differentiation factor 2 (MD2) complex, which triggers signalling cascades that ultimately result in the transcription of a variety of proinflammatory mediators, such as TNF-α and IL-1β. Production of cytokines is essential for clearance of the infection and TLR4 polymorphisms are associated with an increased susceptibility to severe Gram-negative infections [103-105]. Excessive levels of cytokine induction, however, can lead to septic shock with intravascular coagulation and multiple organ failure [30]. This immune crisis can be exacerbated by antibiotics that cause bacterial cell lysis and the consequent release of high amounts of LPS and intracellular toxins into the systemic circulation [106, 107].

The outcome of infection is affected by the lipid A structure, which can differ in the degree of acylation or phosphorylation to become more or less immunostimulatory [101, 108]. These structural alterations can reduce recognition by TLR4/MD2 or alter downstream signalling, thus many bacteria upregulate lipid A modifications during infection. While the hexa-acylated and bis-phosphorylated lipid A from *E. coli* strongly activates TLR4/MD2 [109], *Helicobacter pylori*, for instance, produces a dephosphorylated and tetra-acylated lipid A to allow long-term

colonization of the gastric mucosa [110, 111]; and *P. aeruginosa* is also known for modulating the number of acyl chains during chronic lung infection [112, 113]. The production of a less immunogenic lipid A allows bacteria to evade the immune response.

The O antigen, although not required for bacterial growth, is important in pathogenicity. The long polysaccharide chain allows bacteria to avoid phagocytosis and protects them from the lytic action of the complement system [114-116]. This highly variable LPS moiety has also been shown to protect some bacteria from immune recognition by the host by masking the more conserved domains, which impairs LPS uptake and delays immune response activation [117, 118]. Given the structural diversity and antigenicity, with the immune system producing specific antibodies for each type of O antigen, this domain is the basis for serogroup classification in the clinic [119]. In *E. coli* alone, there are more than 180 identified O-antigen serogroups [120].

2.1.2 Biosynthetic pathways

The biosynthesis of LPS takes place in different cellular compartments (i.e., cytoplasm, IM and periplasm) and the distinct pathways involved in the synthesis of the lipid A, Kdo residues, oligosaccharide core, and the O antigen, all need to coordinate to produce a full-length LPS molecule (**Figure 4B**) [30].

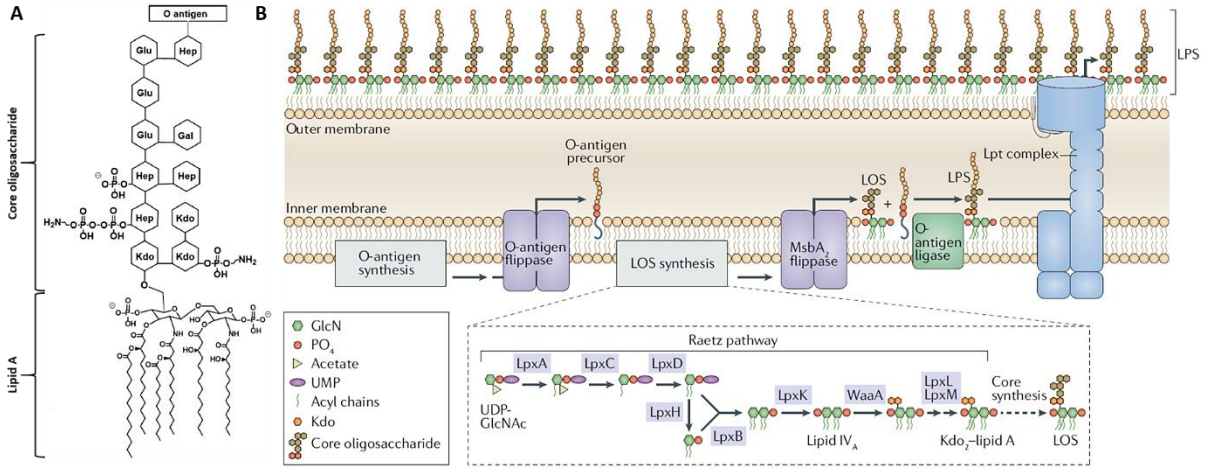

Figure 4. Structure and biogenesis of the LPS produced in *Escherichia coli* (adapted from [108, 121]). **(A)** Structure of the *E. coli* LPS (adapted from [121]). The depicted core-lipid A is typical of the K-12 strain. In strains that produce the O antigen, this is attached to the final heptose of the core oligosaccharide. **(B)** Biosynthesis of a full-length LPS involves diverse and independent pathways that converge to produce a mature molecule (adapted

from [108]). The synthesis of the core-lipid A portion takes place in the cytoplasm and on the inner surface of the IM. The Kdo_2-lipid A moiety is first synthesized by the Raetz pathway, followed by the addition of sugar units that will compose the core domain. This lipooligosaccharide (LOS) is flipped into the periplasm by MsbA, and the O antigen, synthesized *via* a separate pathway, is ligated to the outer core. The full-length LPS is transported from the IM to the cell surface by the Lpt complex.

The biosynthetic pathway of the Kdo_2-lipid A moiety, also known as the Raetz pathway, is the most conserved part of the LPS synthesis and it has been extensively characterized in *E. coli* and *Salmonella* [30, 122]. It occurs in the cytoplasm, where reactions are catalysed by soluble enzymes (i.e., LpxA, LpxC, and LpxD), and at the IM inner leaflet. The pathway starts with the acylation of the precursor molecule *N*-acetylglucosamine linked to a nucleotide carrier (UDP-GlcNAc) by LpxA, that uses the *R*-3-hydroxymyristoyl acyl carrier protein (ACP) as a donor [123, 124]. The equilibrium constant for this reaction is unfavourable, hence the first committed step of the pathway is the following deacetylation performed by the zinc metalloenzyme LpxC [124, 125]. This step is a major control point and is regulated by the FtsH protease in tandem with the heat-shock protein LapB (formerly YciM) [126, 127]. After a second acylation performed by LpxD, also using the *R*-3-hydroxymyristoyl-ACP as donor, LpxH is the pyrophosphatase that removes the sugar nucleotide carrier to form 2,3-diacylglucosamine-1-phosphate (lipid X) [128-130]. Then, LpxB adds lipid X to the product of LpxD, the UDP-2,3-diacylglucosamine, to generate the β-1',6-linked lipid A disaccharide with the release of the UDP nucleotide carrier [131]. This product is phosphorylated at the 4' position by LpxK to produce lipid IV_A, to which two Kdo residues from activated Kdo (CMP-Kdo) are sequentially added by the WaaA enzyme [132, 133]. Two further acylations of the distal glucosamine are catalysed in sequence by LpxL and LpxM, using substrates carried by ACP, to generate the hexa-acylated Kdo_2-lipid A, which concludes the lipid A synthesis [134-136]. For the synthesis of a complete core oligosaccharide, additional sugar groups are added by specific glycosyltransferases to the mature lipid A, which contains the first two Kdo residues of the inner core [30, 137, 138]. The core-lipid A molecule is then translocated across the IM by the MsbA ABC (ATP binding cassette) transporter and, in O antigen producing strains, a long polysaccharide chain is then added to the final heptose of the core domain [137, 139, 140].

The outermost component of LPS is synthesized independently from the core-lipid A moiety [30, 88, 89]. The sugar residues composing the O units are synthesized in the cytoplasm and the O antigen is built on the undecaprenyl diphosphate lipid anchor. The polymerization of the O units can occur at the periplasm or cytoplasm depending on the biosynthetic pathway

used: Wzy-, ABC-, or synthase-dependent pathway. Most O antigens appear to be synthesized *via* a Wzy-dependent assembly mechanism, where polymerization by Wzy occurs after each single O unit linked to the lipid carrier is flipped to the periplasmic side of the IM by the Wzx flippase [88]. In all the three pathways, the mature O antigen is transferred in the periplasm to the outer core oligosaccharide *via* the WaaL ligase, and the lipid carrier undecaprenyl diphosphate is recycled [30].

The pathways for the biosynthesis of LPS and phospholipids share the precursor molecule *R*-3-hydroxymyristoyl-ACP as a substrate for the enzymes LpxA and FabZ, respectively [126]. Therefore, a balanced synthesis of LPS and phospholipids is crucial for bacterial viability.

Although the enzymes for lipid A and Kdo biosynthesis are constitutively expressed, the biosynthesis of the Kdo_2-lipid A moiety is post-transcriptionally regulated at the first committed step catalysed by LpxC [30, 122, 141]. FtsH, an essential membrane-anchored metalloprotease, controls the turnover of LpxC and has also been shown to degrade WaaA, thus regulating the concentration of both lipid A and the sugar moiety (Kdo residues) to maintain a balanced LPS synthesis [142, 143]. This regulation correlates with the cellular growth rate, with LpxC being degraded by FtsH during slow growth [144]. LapB, a heat shock bitopic IM protein, regulates the FtsH-dependent proteolysis of LpxC [127, 145, 146]. In the absence of this protein, LpxC accumulates, causing toxicity due to the imbalance between LPS and phospholipids. This effect can be compensated by the overexpression of the *fabZ* gene, which leads to an increased formation of membrane phospholipids [127]. LapB was found to copurify with LPS transport (Lpt) proteins and WaaC, the first enzyme to add an heptose residue to the Kdo_2 moiety, suggesting that it could function as a docking site for various LPS biosynthetic enzymes, such as glycosyltransferases, to ensure that only completely synthesized LPS is translocated [127].

It is believed that the feedback signal responsible for the regulation of LPS biogenesis is either LPS or one of the precursor molecules [121]. However, how exactly the cell senses an imbalance between phospholipids and LPS and how this translates to LpxC being degraded or not by FtsH was not known until very recently. PbgA (YejM), an IM protein previously implicated in cardiolipin transport [147, 148], was recently found to be the LPS signal transducer in *E. coli*, regulating the biogenesis of LPS by controlling the stability of LpxC [149-152]. PbgA regulates the activity of LpxC by interacting with LapB. When LPS is in excess in the cell, it accumulates in the IM where it binds to PbgA, which prevents PbgA from inhibiting LapB-FtsH interaction and consequently allows the degradation of LpxC.

2.1.3 Translocation across the IM

The core-lipid A moiety of LPS synthesized in the cytoplasmic leaflet of the IM is translocated to the periplasmic side by MsbA, a conserved IM protein belonging to the ubiquitous ATP-binding cassette (ABC) transporter superfamily [153]. MsbA was first identified in *E. coli* as a multicopy suppressor of the loss of LpxL (formerly HtrB) activity in a thermosensitive mutant and it was named accordingly (multicopy suppressor of *htrB* A) [154]. *lpxL* null mutants, in non-permissive temperature, presented an altered cellular morphology and accumulated phospholipids and tetra-acylated lipid A in the IM [139, 140]. These knockout phenotypes could be suppressed by the overexpression of *msbA*, which appeared to facilitate the transport of immature LPS [140]. Moreover, MsbA depleted cells were found to accumulate hexa-acylated lipid A at the IM [140]. The flippase activity was later demonstrated by the evidence that aminoarabinose and phosphoethanolamine modifications of LPS, occurring at the IM outer leaflet, were MsbA-dependent [155].

MsbA functions as a homodimer of two 64.3 kDa subunits and each monomer presents a cytoplasmic nucleotide-binding domain (NBD) and a transmembrane domain (TMD) containing six transmembrane helices [156, 157]. The NBDs bind and hydrolyse ATP and the TMDs compose the substrate translocation pathway. Structural studies with cryo-electron microscopy (cryo-EM) where *E. coli* MsbA was reconstituted into lipid nanodiscs [158], reflecting a more native environment compared to detergent micelles used in previous crystallography studies [156], revealed how MsbA transports the lipooligosaccharide (LOS), which corresponds to the core-lipid A molecule, across the IM. LOS binds deeply inside a hydrophobic pocket formed by the TMDs, establishing extensive hydrophilic and hydrophobic interactions, with the acyl chains already located at the height of the IM outer leaflet, although still in an un-flipped orientation [158]. From the cryo-EM structures, the authors proposed a "trap and flip" mechanism for MsbA-mediated flipping of the core-lipid A moiety. LOS enters the cavity in MsbA through an opening between TM4 and TM6 of the two different monomers, and the binding of LOS aligns the NBDs for ATP binding. LOS flipping is induced by conformational changes upon ATP binding that weaken the interaction of the TMDs with LOS and allow the acyl chains to enter the periplasmic leaflet through the path formed by TM1 and TM3 of different monomers. The MsbA rearrangement and translocation of the core-lipid A lead to ATP hydrolysis and, with the release of LOS, the TM helices form a compact bundle.

With the release of phosphate, MsbA re-adopts the inward-facing conformation (resting state) that allows another LOS molecule to enter from the cytoplasmic side.

Although we cannot rule out that other lipophilic substrates are transported by MsbA, the substrate specificity towards LOS is achieved by interactions with the phosphorylated glucosamines and the acyl chains [159]. Within the MsbA cavity, the phosphoglucosamines of lipid A are surrounded by arginine residues that form a selectivity filter; moreover, the cavity favours the accommodation of the shorter acyl chains characteristic of LPS (12-carbon and 14-carbon), hence discriminating against glycerophospholipids, with typical 18-carbon chains. MsbA is also the most efficient when flipping across the IM hexa-acylated substrates, with densely packed hydrocarbon chains, evidencing the role of MsbA as a quality control checkpoint for LPS export to the OM that primarily contains a single form of lipid A [140, 159]. The Kdo_2-lipid A molecule as the minimal requirement for cell viability reflects the preference of MsbA for hexa-acylated substrates, since the addition of the last two acyl chains to the lipid A anchor, by the "late" acyltransferases LpxL and LpxM, occurs after the transfer of the two Kdo residues [160-164].

MsbA has also been associated with multidrug transport [165, 166]. Lipid A and amphipathic drugs were found to simultaneously bind MsbA, suggesting two distinct binding sites in the protein [167]. Recently, MsbA antagonists were shown to target an architecturally conserved transmembrane pocket, instead of competing directly with the transported substrate [159]. This could be an allosteric site for natural ligands, lipids, partner proteins or even other small molecules designed for the modulation of ABC transporters.

2.1.4 LPS modifications and regulation

In response to their surroundings, bacteria can modify the LPS structure by altering the number or type of acyl chains and the overall charge of the molecule, through the removal of phosphates or the addition of positively charged groups. Modifications of the conserved core-lipid A moiety mainly occur at the periplasmic leaflet of the IM, downstream from MsbA-mediated LPS flipping, and they can affect a variety of physiological processes such as the permeability or fluidity of the OM, the resistance to antimicrobial peptides (AMPs), the recognition by the immune system, and the formation of OM vesicles [108]. Environmental factors like temperature, concentration of metal ions, or the presence of cationic antimicrobials

can lead to LPS modifications, which often occur during host colonization [84]. In *E. coli*, LpxP is active at low temperatures and substitutes for LpxL, which is expressed at higher temperatures, to add a 16-carbon palmitoyl group instead of the 12-carbon lauroyl group [84]. This is thought to compensate for the decrease in membrane fluidity caused by a lower temperature. Most of the LPS modifications, nonetheless, are made in response to the concentration of cations and the presence of cationic AMPs in the environment.

Several two-component systems (TCS) have been described for the transcriptional regulation of lipid A modification enzymes, e.g., PhoPQ and PmrAB systems in *E. coli* and *Salmonella* spp., and the ParRS, ColRS and CprRS systems in *P. aeruginosa* [168-172]. These TCS comprise a sensor kinase that auto-phosphorylates a histidine residue in response to a signal, and a cognate response regulatory protein controlling gene expression, to which the phosphate group is transferred.

The PhoPQ two-component regulatory system primarily responds to acidic pH, low levels of divalent cations, the presence of AMPs, and osmotic shock [173]. These stimuli activate the IM kinase PhoQ to phosphorylate PhoP that, in turn, activates the transcription of genes coding for lipid A-modifying enzymes (**Figure 5**). Divalent cations (e.g., Mg^{2+} and Ca^{2+}) favour PhoQ in an off conformation and when their concentration decreases, or AMPs bind the periplasmic sensor domain of PhoQ, it causes a conformational change that favours auto-phosphorylation [174]. Changes in pH are detected by the cytoplasmic domain and, in *Salmonella enterica* serovar Typhimurium (*S.* Typhimurium), the IM protein UgtL is known to bind PhoQ and stimulate auto-phosphorylation in response to acidic pH [175, 176].

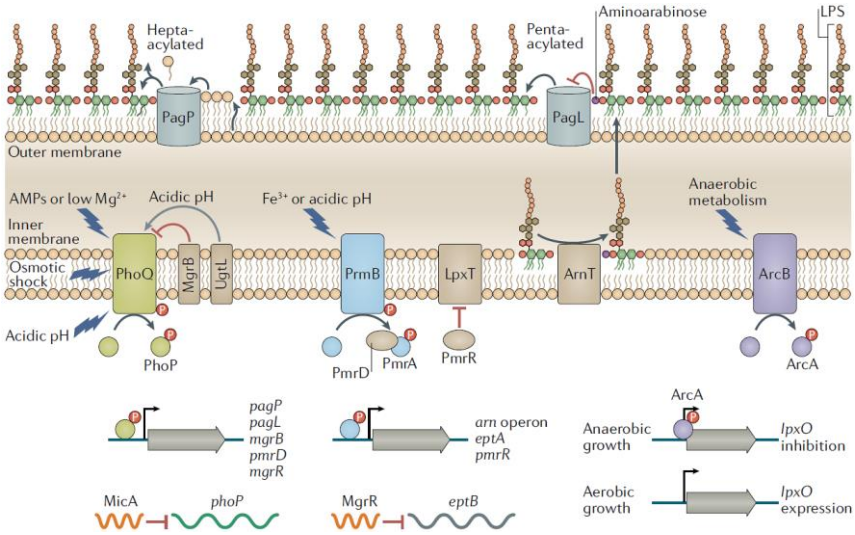

Figure 5. Regulatory systems of lipid A modifications in *Salmonella enterica* serovar Typhimurium (from [108]). The PhoPQ two component system (TCS) responds to environmental signals and regulates accordingly the

transcription of genes encoding enzymes that modify the lipid A acylation (PagP, PagL). This TCS couples with PmrAB *via* the PmrD protein, which is upregulated by PhoPQ. PmrAB upregulates the transcription of the genes *arnT* and *eptA* that encode enzymes that modify the phosphates of lipid A with aminoarabinose and phosphoethanolamine, respectively. Aminoarabinose-modified lipid A inhibits PagL deacylation. LpxT competes with EptA to modify the same site on LPS and is inhibited by PmrR, in turn activated by PmrAB. ArcAB regulates LpxO that hydroxylates an acyl chain of lipid A in an oxygen-dependent manner. The small RNAs MgrR and MicA are linked to PhoPQ regulation, with the latter inhibiting the translation of PhoP. At the IM, MgrB provides negative feedback into the PhoPQ TCS, and UgtL amplifies PhoQ autophosphorylation in response to acidic pH.

Among the lipid A-modifying enzymes controlled by PhoPQ TCS is PagP, an OMP that catalyses the addition of a palmitate residue to LPS (**Figure 6**), using as donor phospholipids mislocalized to the OM outer leaflet [177]. The hepta-acylated LPS has been implicated in resistance to AMPs. Additional modulators of the degree of acylation are PagL and LpxR, which are present in *Salmonella* but not in *E. coli* K-12 [178-180]. These OMPs remove the fatty acids linked at the 3 and 3' positions, respectively, thus regulating the immunogenicity of lipid A.

The PhoPQ, through the regulation by the PmrAB TCS, also modulates modifications to the phosphates of the lipid A glucosamines. The coupling between these two systems is mediated by the protein PmrD that, when upregulated by the activation of PhoPQ, binds and protects the phosphorylated PmrA from deactivation by the phosphatase activity of PmrB (**Figure 5**) [181-183]. PmrB is the IM sensor kinase that directly responds to acidic pH and elevated levels of metals such as Fe^{3+}, Al^{3+}, and Zn^{2+} [184, 185]. Activation of PmrB leads to the phosphorylation of PmrA that upregulates the *arn* operon and the *eptA* gene coding for enzymes that decorate lipid A with aminoarabinose (L-Ara4N) and phosphoethanolamine (PEtN), respectively. The IM enzyme ArnT adds an L-Ara4N primarily to the 4'-phosphate, while EptA prefers transferring PEtN to the 1-phosphate, although either phosphate group can be modified with either substituent (**Figure 6**) [186, 187]. PmrAB TCS also activates PmrR, a negative regulator of the phosphotransferase LpxT that competes with EptA to modify the 1-phosphate [188, 189]. The modification of lipid A with positively charged groups at the IM and loss of the additional phosphate transferred by LpxT are associated with an increased resistance to AMPs, due to an overall reduced negative charge of LPS which lowers the affinity to cationic peptides.

To modulate the extent of PhoPQ activation, the IM protein MgrB, upregulated itself by PhoP, binds and inhibits PhoQ, thus providing a negative feedback on this TCS [190]. Small RNAs linked to PhoPQ regulation include MicA, an inhibitor of the translation of PhoP, and

MgrR, which is upregulated by PhoP and represses the expression of the enzyme EptB [191, 192]. EptB is thus negatively regulated by PhoPQ but, when induced by high levels of Ca^{2+}, it transfers PEtN to the second Kdo sugar of the core oligosaccharide [193, 194]. An OM containing lipid A unmodified by enzymes upregulated by the PhoPQ TCS seems to be a more efficient barrier in high Mg^{2+} or Ca^{2+} concentrations [195].

One of the lipid A fatty acids can undergo an oxygen-dependent hydroxylation carried out by LpxO, an enzyme not present in *E. coli* [196, 197]. This oxygenase has been recently described in *S.* Enteritidis to be regulated by the ArcAB TCS, that responds to oxygen availability [198].

In addition to modifications in the lipid A moiety, and since the outer core oligosaccharide is more variable, other modifications described in the literature mainly localise to the inner core and they include addition of sugar groups (e.g., Kdo, rhamnose, galactose) and PEtN, which may confer resistance to AMPs [121]. In the case of the O antigen, it is worth noting that it can be replaced in its entirety by another O antigen serotype, *via* horizontal gene transfer of the biosynthetic locus, or even by a completely different polysaccharide [121].

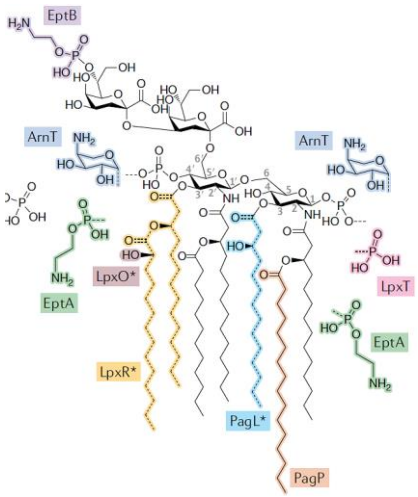

Figure 6. Schematic representation of Kdo_2-lipid A modifications and responsible enzymes in *Salmonella enterica* subspp. (from [108]). Removal of acyl chains is represented with a dotted line. Expression of PagP and PagL is directly under the control of PhoPQ two-component system (TCS). ArnT and EptA are upregulated by PmrAB. EptB and LpxT are transcriptionally and post-translationally negatively regulated by PhoPQ and PmrAB, respectively. LpxO and LpxR are not regulated by either of these TCS. LpxO, LpxR and PagL are LPS-modifying enzymes not present in *E. coli* K-12.

2.2 LPS export to the cell surface: the Lpt machinery

In the past two decades, the components required for the LPS transit across the cell envelope were discovered [199-210]. The mature LPS molecule, assembled with the O antigen after the flipping of the core-lipid A moiety by MsbA, needs to be extracted from the IM, transported through the aqueous periplasmic compartment, and inserted in the outer layer of the OM. Responsible for these steps is the LPS transport (Lpt) machinery comprising, in *E. coli*, seven essential proteins (LptA-G) spanning the cell envelope (**Figure 7**) [209, 211]. The transport is unidirectional against a concentration gradient and is powered by ATP hydrolysis in the cytoplasm [212, 213]. The IM ABC transporter $LptB_2FGC$ powers the LPS detachment from the IM and the transport along the periplasmic bridge, formed by the LptA protein linking the C-terminal and N-terminal periplasmic domains of LptC and LptD, respectively [212-217]. This protein-bridge, with a β-jellyroll fold shared by all the intervenient protein domains, shields the acyl moieties of LPS in the hydrophilic environment of the periplasm, while it transits towards the OM for final assembly in the outer leaflet *via* LptDE translocon [216, 218-221]. The conserved structurally homologous jellyroll domain, shared by all Lpt proteins with the exception of LptB and LptE [216, 220-223], establishes a continuous path for LPS transport across the periplasm; thus, this "Lpt fold" is a key element for protein-protein interactions within the machinery and for LPS transport as it accommodates the lipid A hydrophobic moiety [217, 224].

The PEZ model for the Lpt-mediated LPS transport has been proposed to explain how the energy harnessed at the cytoplasm is used to power the transport [217]. The Lpt machinery works like a PEZ candy dispenser, where a spring at the bottom pushes up a stack of candies through the central channel of the dispenser, so that a candy is always present at the top. Likewise, $LptB_2FG$ pushes a continuous stream of LPS molecules, using the energy derived from ATP hydrolysis, through the Lpt bridge by constantly loading new LPS into the channel formed by LptCAD. This channel allows the transit of LPS providing a route to the cell surface where the LptDE translocon, much like the head of the PEZ dispenser, opens to deliver LPS to the OM. *In vitro* reconstitution of the LPS transport, using proteoliposomes containing the IM and OM Lpt sub-complexes connected by LptA, combined with the fact that LPS molecules are always present at their respective binding sites in LptC and LptA, provide further evidence supporting a PEZ-like transport [211, 212, 216, 217].

The Lpt transenvelope complex operates as a single device since the depletion of any component or disruption of protein interactions within the machinery leads to the accumulation of LPS at the IM outer leaflet, which is toxic for the cells [96, 205, 206, 215, 225]. Bacteria with impaired LPS transport arrest growth and present increased OM permeability and OM defects.

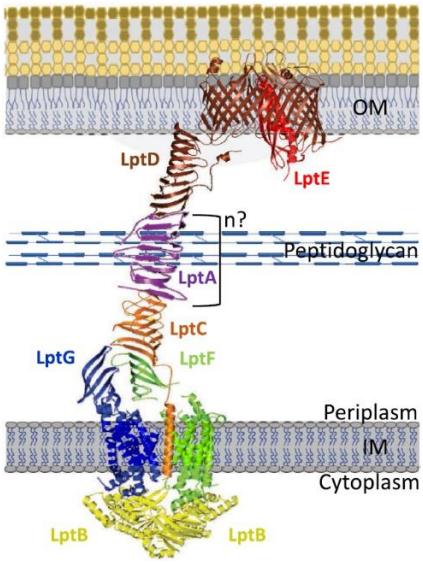

Figure 7. The lipopolysaccharide transport (Lpt) machinery (from [226]). The number of LptA molecules in the transenvelope bridge is still unknown. The structures of $LptB_2FGC$, LptA, and LptDE were determined separately from each other (see [213], [221], and [227]).

2.2.1 Detachment of LPS from the IM

The first step in the transport of the fully formed LPS is its extraction from the IM periplasmic leaflet powered by the atypical ABC transporter $LptB_2FGC$. The LptB dimer at the cytoplasm together with the polytopic proteins LptF and LptG form the ABC transporter, where the LptB subunits constitute the NBDs and LptFG correspond to the TMDs [207]. LptC is a bitopic auxiliary protein that strongly associates with $LptB_2FG$ [207, 209, 224]. $LptB_2FG$ is an unconventional ABC transporter since it extracts LPS from the IM periplasmic leaflet and delivers it to LptC rather than translocating its substrate across the membrane. Moreover, LptF and LptG folds are unprecedented and, unlike other ABC transporters, they lack the helix swapping in the TMDs. Accordingly, $LptB_2FG$ has been classified as a novel class of ABC transporters, i.e., the type VI exporters [153].

LptB is the engine of the transporter and the hydrolysis of ATP is vital to power LPS trafficking to the OM and maintain cell viability, although not required for the assembly of the Lpt complex [228]. LptF and LptG each contain six transmembrane helices (TM1-6), a large periplasmic domain, between TM3 and TM4, that adopts a β-jellyroll architecture, and a coupling helix, between TM2 and TM3, that interacts with one monomer of LptB [222, 223]. In the $LptB_2FG$ transporter, the cytoplasmic coupling helices, interacting with groove regions in LptB, transmit conformational changes occurring at the NBDs upon ATP binding and hydrolysis to LptF and LptG, allowing the coupling of energy production by LptB with LPS extraction by LptFG [228, 229]. Interestingly, the hydrophobic antibiotic novobiocin, that targets the DNA gyrase by binding the ATP-binding site in the ATPase subunit, was shown to bind LptB at the interface with LptF and LptG coupling helices, stimulating the ATPase activity and subsequently the transport of LPS [230]. This suggests that the effect of LptFG upon the ATPase activity of LptB is mediated through their coupling interaction.

LptC contains one N-terminal transmembrane helix, shown to be dispensable for cell viability, and a large periplasmic domain with a β-jellyroll fold comprising 15 antiparallel β-strands [216, 224]. LptC interacts with $LptB_2FG$ and LptA *via* its N-terminal and C-terminal domains, respectively [224, 231, 232]. Not only is a soluble periplasmic variant of LptC functional and assembles the machinery [224], its C-terminal region can also be deleted upon overexpression of LptB, which may shift the equilibrium in favour of the full complex, hence stabilizing the C-terminally truncated LptC, and LPS could directly transit from $LptB_2FG$ to LptA [232]. Furthermore, mutants lacking LptC and carrying suppressor mutations in LptF are viable, provided that LptA is overexpressed [233]. Specific amino acid substitutions at a single residue (R212) in the periplasmic domain of LptF allow a functional six-component Lpt machinery, suggesting that LptF may physically interact with LptA in the suppressor mutants. Interestingly, the complete $LptB_2FGC$ complex displays substantially lower ATPase activity comparing to $LptB_2FG$ [211, 223]. Altogether, these findings point to a regulatory function of LptC, more than an essential structural role, in the machinery.

The crystal structures of the nucleotide-free $LptB_2FG$ from *P. aeruginosa* and *Klebsiella pneumoniae* provided the first structural insights into this ABC transporter, however, with no bound LPS substrate nor LptC, which is known to form a tight complex with $LptB_2FG$ [207, 222, 223]. These studies determined that the TMDs of LptF and LptG form an outward-facing V-shaped cavity containing highly conserved hydrophobic residues and that LPS may enter this cavity laterally [223]. Two lateral gates are formed at opposing sites in $LptB_2FG$, one between TM5 of LptG and TM1 of LptF, and another between LptG TM1 and LptF TM5, and

LPS could enter alternately through both [222, 223]. Based on protein surface charge, it was suggested that the lipid A acyl chains may locate deeply inside the cavity and the phosphate groups may interact with positively charged residues at the IM-periplasm interface, whereas the sugar portion of LPS stays in the periplasm [223]. Upon ATP hydrolysis, LPS is then expelled into the periplasmic domain of LptF or LptG, according to the alternating mechanism for LPS extraction [222].

Many LPS modifications take place at the IM periplasmic leaflet before export, which is advantageous since $LptB_2FG$ controls which molecules to transport by recognizing charges at the 1 and 4' positions of lipid A [234, 235]. Electrostatic interactions between a cluster of residues at the periplasmic end of LptG TM1 and the glucosamine disaccharide backbone of lipid A might drive the selection of which variant of LPS to transport [235]. In *E. coli*, this domain contains a positively charged residue (K34) that interacts with the unmodified phosphates [235]. This residue is not conserved amongst LptG orthologues and may have coevolved with the LPS variant in the respective species to accommodate the charges of the lipid A glucosamines. In *Burkholderia cenocepacia*, a species resistant to AMPs where the modification of lipid A with L-Ara4N is constitutive and essential for viability, the residue D31 of LptG seems to only interact with an aminoarabinose-modified substrate [234, 236].

Recently, the crystal and cryo-EM structures of the $LptB_2FGC$ complex were solved and helped clarify the role of LptC, which had remained poorly understood until now. These structural studies showed that the transmembrane anchor of LptC interdigitates between LptG TM1 and LptF TM5, which breaks the symmetry observed in the crystal structures of $LptB_2FG$ and rules out the previously proposed alternating mechanism for LPS extraction [213, 214]. Analysis of the structures also revealed that the soluble domains of LptF and LptC form a continuous β-jellyroll *via* an edge-to-edge interaction between their C- and N-terminal β-strands. The cryo-EM map from *E. coli* $LptB_2FGC$ confirmed the charge distribution observed in $LptB_2FG$ and the predicted interactions with LPS [214]. For the first time, an LPS molecule inside the TMDs was resolved, with the hydrophobic tails of lipid A localizing inside a cone-shaped hydrophobic pocket formed by the TMDs and the inner core being positioned above the level of the membrane and extending towards the periplasm. The 1-phosphate is accommodated by a ring of positively charged residues at the membrane-periplasm interface of LptG, including residues K34 and K41 on TM1, whereas the 4'-phosphate establishes fewer electrostatic interactions.

In the $LptB_2FGC$ transporter, LPS laterally enters a large outward-open cavity, between LptG TM1 and LptF TM5 where the LptC helix is located, and is recognized through relatively

weak interactions with the TMDs [213]. Upon ATP binding, LptB subunits dimerize and the TM of LptC moves away from the TM1LptG-TM5LptF interface, which facilitates the attachment of the β-jellyroll domain of LptC on top of the β-jellyroll of LptF and allows the TMDs to rearrange to tightly bind to LPS. This path for LPS entry is directly aligned with the concave surface of the continuous β-jellyroll of LptF and LptC. ATP hydrolysis causes the inward movement of the TMDs which collapses the LPS-binding cavity and leads to the expulsion of the LPS molecule pushing open a gate in the β-jellyroll of LptF (**Figure 8**), which then spontaneously closes behind the substrate, and LPS flows towards LptC. This gate may serve to prevent backward movement of LPS when the cavity reopens, ensuring unidirectional transit towards the OM. Although ATP is not required for the entry of LPS into the cavity, one hydrolysis step is required for the extraction of LPS from the IM to LptC and subsequent rounds of ATP hydrolysis push LPS molecules which are already in the periplasmic bridge towards the OM [211, 212, 217].

LPS enters the cavity in the transporter where LptC TM is localized and this domain prevents LptG TM1 and LptF TM5 from forming the optimal conformation for LPS binding [214]. Moreover, $LptB_2FG$ associated with a full-length LptC protein uses less energy for the transport than when in complex with just the β-jellyroll domain [213], presumably because the positioning of the TM of LptC in the complex interferes with conformational changes in the TMDs upon ATP binding, thus determining a decrease in the ATPase activity of $LptB_2FG$ [214]. Therefore, the transmembrane helix of LptC has an important regulatory role by modulating the hydrolysis of ATP to achieve a more efficient coupling between ATP hydrolysis and LPS movement [213, 214]. Although it can be deleted in laboratory conditions [224], this transmembrane domain provides such a fitness advantage that is conserved in the wild. $LptB_2FGC$ is a remarkable and unprecedented ABC transporter tightly regulated by the transmembrane domain of an associated protein to achieve highly efficient LPS transport with minimal energy waste. The function of the periplasmic domain of LptG, however, still needs to be clarified and one cannot exclude that it could have a vital structural role in the Lpt machinery of other organisms [222]. Also, whether LptC responds to modified forms of LPS has not been investigated yet.

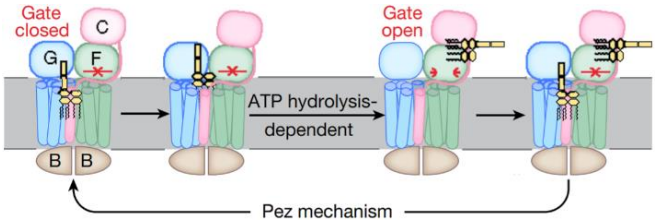

Figure 8. Mechanism for the extraction of LPS from the IM by the $LptB_2FGC$ transporter (from [213]). LPS enters the cavity between LptG TM1 and LptF TM5, where the TM of LptC is located. Upon ATP binding, the LptC TM moves away facilitating the stably association between the β-jellyroll domain of LptC with the β-jellyroll of LptF, and the TMDs of LptFG rearrange to interact strongly with LPS. Upon ATP hydrolysis, the TMDs move inwards and the cavity collapses expelling LPS that pushes open a gate in LptF (indicated by the red arrows), which promptly closes behind the substrate, and LPS slides towards LptC. Repeated extraction cycles continuously push LPS molecules through the periplasmic bridge to the OM according to the PEZ model.

2.2.2 Through the periplasm to the OM outer leaflet

$LptB_2FGC$ pushes LPS molecules into the periplasmic bridge formed by the C-terminal soluble domain of LptC, the soluble protein LptA, and the N-terminal periplasmic domain of LptD, which assemble *via* their homologous OstA-like β-jellyroll folds [217, 224]. The "Lpt fold" is a unique protein architecture and it was first identified in LptA [216, 220, 221, 227]. LptA contains 16 antiparallel β-strands folded in a slightly twisted β-jellyroll with a V-shaped hydrophobic core that opens slightly at the N- and C-termini [221]. LptA, the only soluble periplasmic protein in the machinery, fractionates with both IM and OM fractions in sucrose gradients and all the seven Lpt proteins can be copurified as a complex, evidencing a physical transenvelope bridge for LPS transport [208, 209]. The proteins assembling the Lpt bridge interact in a conserved manner *via* the edges of their β-jellyrolls (**Figure 7**): the C-terminal end of LptC interacts with the N-terminus of LptA, and the C-terminus of LptA interacts with the N-terminal β-strand of LptD [215, 231, 237]. The three periplasmic domains, architecturally very similar to each other but with different amino acid sequences, oligomerize in a head-to-tail orientation with a 90º twist per subunit, thus building a continuous multiprotein β-sheet with a spiralling hydrophobic groove that shields the lipid A portion of LPS from the aqueous periplasmic environment, whereas the hydrophilic oligosaccharide moiety remains exposed. Indeed, residues located in the interior of the LptA and LptC β-jellyrolls were shown to crosslink to LPS [212].

The apo crystal structures of LptC, LptA and LptD indicate that an extensive conformational change must occur for LPS to transit through their hydrophobic cavities, which are too small to accommodate the lipid A acyl chains [216, 221, 227]. This was demonstrated through electron paramagnetic resonance (EPR) spectroscopy experiments that showed that the entire LptA protein and the soluble domain of LptC undergo substantial structural rearrangement upon LPS binding, and the N-terminal end unfolds when LPS is present [238, 239]. The LPS affinity of LptC and LptA is not significantly different with values determined to be in the range of 11-28 and 7-34 μM, respectively [238, 239]. Therefore, it is unlikely that a differential affinity drives the transfer of LPS from LptC to LptA. LPS trafficking towards the OM through the Lpt β-jellyroll subunits could be a dynamic process where ripples of ordered-disordered transitions shuffle LPS along the periplasmic bridge, as opposed to the more passive mechanism for LPS transit proposed by the PEZ model [240].

LptA has a strong tendency to oligomerize in a head-to-tail fashion, forming long fibres in the presence of LPS and it forms oligomers *in vitro* in a concentration-dependent manner [221, 241, 242]. Nevertheless, the affinity between LptA and LptC is stronger than for LptA oligomerization (4 μM and 29 μM, respectively) [243]. The stoichiometry of LptA molecules in the periplasmic bridge is still unknown, thus the physiological relevance of LptA oligomerization is unclear. Interestingly, a monomeric version of LptA, lacking the C-terminal β-strand, can partially support cell growth [237]. A Lpt machinery with a single LptA molecule can bridge the typical *E. coli* periplasmic width of 10 nm, however this can vary with bacterial species and envelope stresses, such as osmotic stress [240]. LptA oligomerization could occur in response to changes in the IM-to-OM distance, thus granting the Lpt machinery the flexibility to adapt to alterations in the dimension of the cell envelope. Supporting this hypothesis is the presence of an additional σ^e stress response promoter upstream from the *lptA* gene that exclusively responds to conditions affecting LPS biogenesis [244]. Moreover, the Rcs stress response system in Enterobacteria is activated upon changes in the width of the periplasm, suggesting that essential envelope-spanning protein complexes are adapted to variations in envelope architecture [25].

LPS is delivered and assembled at the OM by the LptDE translocon [202]. LptD, the largest monomeric β-barrel protein identified in the OM of Gram-negative bacteria, contains a N-terminal periplasmic β-jellyroll domain with 11 antiparallel β-strands and a large C-terminal β-barrel domain comprising 26 antiparallel β-strands [219, 220, 227]. Each domain contains two cysteine residues and, for the LptDE complex to be functional, two disulfide bonds between non-consecutive cysteine residues are present (Cys31–Cys724 and Cys173–Cys725)

connecting the N-terminal and C-terminal domains of LptD [245]. Notably, the formation of at least one of these intramolecular bonds is sufficient for LptD functionality [245]. The disulfide bonds ensure the correct orientation of the periplasmic domain in relation to the β-barrel, which is important for the interaction with LptA and the insertion of the lipid A portion into the OM [231, 245]. LptD is a crenellated β-barrel where the first and last β-strands are not completely hydrogen-bonded and create a lateral gate through which LPS is inserted into the OM [219, 227]. The disulfide bond configuration, determinant of the position of the N-terminal domain, restricts the size of this lateral gate on the periplasmic side, which blocks the incorrect insertion of LPS into the OM inner leaflet. In LptD, the β-strands of the β-barrel domain are connected by shorter loops on the periplasmic side, and longer extracellular loops that fold over the lumen of the barrel, thus occluding most of the β-barrel's large cavity to maintain OM impermeability [219, 220, 227]. LptE is a lipoprotein, containing two α-helices packed against a four-stranded β-sheet, buried inside the barrel of LptD adopting a plug-and-barrel conformation (**Figure 7**) [208, 218]. This structural architecture was resolved from crystallography studies of the LptDE translocon from several microorganisms [219, 220, 227]. LptE has three major roles in the Lpt machinery: LptD assembly, LptD plugging, and LPS export. Interestingly, LptE is not essential for LPS transport in *N. meningitidis* [246].

While LptD is targeted to the OM by the β-barrel assembly machinery (Bam) pathway, LptE is inserted into the OM by the localization of lipoproteins (Lol) system [82]. Despite the different pathways, LptE is crucial in the assembly of a functional LptD protein [208, 210]. LptE assists in the assembly of LptD by the Bam complex and is essential for correct disulfide bond formation [210]. LptD folding involves extensive reshuffling of the disulfide bonds mediated by the periplasmic oxidase DsbA, and LptE is required to form a functional translocon with native disulfide bonds [247].

LptE binds the extracellular loops 4 and 8 of LptD that are located inside the barrel, thus blocking part of the extracellular opening [219, 220, 227]. LptE plugging of the otherwise too large LptD cavity is essential in preserving the permeability properties of the membrane. This is evidenced by the identification of a LptE mutant that presents increased OM permeability without hindering the assembly of LptD or the LPS export [248].

LptE was shown *in vitro* to bind LPS and disrupt LPS aggregates, *via* electrostatic interactions between its positively charged residues localized in the exposed loop connecting β-strands 2 and 3 and the negatively charged lipid A portion [208, 249]. In *E. coli*, mutations at this LPS-binding site diminish the ability of LptE to disaggregate LPS and lead to increased OM permeability without impairing LptD assembly [249]. These findings suggest that LptE

assists the LPS assembly at the OM by preventing LPS aggregation at the inner leaflet and facilitating the transfer to the outer leaflet.

From genetic and structural studies, the two-portal mechanism for LPS insertion into the OM outer leaflet has been proposed (**Figure 9**) [219, 220, 227, 250, 251]. The N-terminal domain of LptD receives LPS from LptA and delivers the lipid A moiety directly into the OM through an intramembrane hole, outside the LptD barrel, while the polysaccharide portion passes through the hydrophilic lumen of the barrel *via* a lateral gate that opens between β-strands 1 and 26. Then, the extracellular loop 4 moves to allow the exit of the saccharide moiety from the barrel, partially driven by electrostatic interactions with the divalent cations present at the outer leaflet [219, 227, 251]. The electrostatic gradient in the lumen of the barrel, which becomes increasingly negative near the extracellular surface, may also play a role in LPS insertion by creating a charge repulsion with the similarly charged LPS sugar domain, thus preventing the lodging of LPS molecules within the lumen [227]. LptE facilitates LPS transfer to the OM by providing a more favourable interaction between itself and LPS than between LPS molecules, which have the propensity to aggregate [249].

LptA binding to the LptDE translocon is a key regulatory checkpoint, since when LptDE is not correctly assembled, the interaction with LptA does not occur and the β-jellyroll oligomerization process for bridge formation is disrupted [231]. Only a functional OM translocon, with native disulfide bonds, connects *via* LptA with the IM ABC transporter [231]; this avoids the mistargeting of LPS which is toxic for the cells [96]. Likewise, only a correctly assembled $LptB_2FGC$ complex succeeds in recruiting LptA to connect the IM complex to the OM translocon [224]. Indeed, a LptC mutant described as defective in associating with $LptB_2FG$ *via* its periplasmic domain, although interacting with LptA *in vitro* [215], fails to assemble the transenvelope bridge [224]. LptA is more inclined to bind to LptDE than LptC [209], therefore it is likely recruited to the OM first and then binds its docking site at the IM, thereby ensuring that Lpt bridges do not couple to defective OM translocons which would mistarget LPS to the periplasm [231]. Moreover, the depletion of LptC and LptD/E components leads to LptA degradation, pointing to a quality control role for LptA-LptC and LptA-LptD interactions in the assembly of the Lpt transenvelope complex [215]. The LptDE translocon has another recently described role in LPS transport regulation: it can control the ATPase activity of $LptB_2FGC$ through negative feedback to arrest LPS transport [252]. It was shown with proteoliposomes containing the IM and OM complexes that when the proteoliposome mimicking the OM reaches a threshold concentration of LPS, the IM complex stops hydrolysing ATP to halt LPS transport and avoid energy waste.

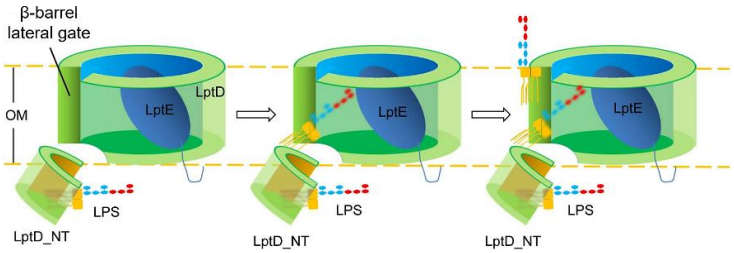

Figure 9. The two-portal mechanism for LPS insertion into the OM by the LptDE translocon (adapted from [220]). The N-terminal domain of LptD (LptD_NT) receives LPS from LptA and inserts the lipid A moiety (yellow) directly into the core of the membrane *via* an intramembrane hole, while the sugar portion of LPS (blue and red) passes inside the lumen of the β-barrel *via* a gate that opens laterally between strands β1 and β26.

2.3 Phospholipid transport

The phospholipid (PL) composition of the OM inner leaflet is similar to that of the cytoplasmic membrane. In *E. coli*, there are three major glycerophospholipids: the zwitterionic phosphatidylethanolamine (PE), accounting for 75% of the total lipid content; and the anionic PLs phosphatidylglycerol (PG), comprising 20%, and cardiolipin (CL), amounting to 5% [17]. The PLs are synthesised in the cytoplasm from a phosphatidic acid (PA) precursor *via* several enzymatic reactions and are presumably flipped across the IM by a transporter that has not yet been identified, since a spontaneous transbilayer diffusion of PLs is intrinsically slow [253].

In contrast to the LPS OM component, our understanding of how phospholipids are assembled into bacterial membranes is greatly lacking. The mechanism for phospholipid shuttling across the cell envelope remains elusive, but it would require shielding of the acyl chains. Mechanistic models proposed for intermembrane lipid trafficking involve either (i) proteins that function as chaperones or that form a protein bridge, in a process resembling the transport of lipoproteins and LPS, respectively, or (ii) a direct exchange of lipids between the IM and OM [254]. The latter could occur *via* a mechanism of vesicular budding from one membrane and fusion with the target membrane, or *via* lipid diffusion through membrane bridges connecting the periplasmic leaflets at sites of close juxtaposition of the membrane bilayers. However, no scientific evidence for such transport processes has emerged and, therefore, PL trafficking across the periplasm remains ambiguous and somewhat controversial. Vesicular transport is thought to be incompatible with the meshwork of the peptidoglycan cell wall with a pore radius of around 2 nm in *E. coli* [255], which is too small for the passage of

the typical 20 nm vesicles [256]; the existence of Bayer's junctions [257, 258], zones of adhesion between the inner and outer membranes, has also been challenged [259-261]. The translocation of PLs to the OM requires energy and, although ATP hydrolysis cannot be ruled out as an energy source, the transport of PE has been shown to be dependent on the proton motive force (pmf) across the IM [262]. In contrast to LPS and OM proteins, the transport of PLs across the periplasm is bidirectional [262-264].

To this date, after 40 years of research following the first studies on PL translocation [262, 263], no proteins clearly involved in the bulk transport of PLs to the OM have been identified. Transport systems implicated in the anterograde transport (IM-to-OM) are involved in the migration of discrete populations of PLs rather than in the bulk transport. The PbgA (YejM) is an IM tetrameric protein, with the transmembrane domain linked at the C-terminus to a non-essential periplasmic domain, suggested to have a role in the translocation of CL to the OM [147, 148]. Interestingly, the deletion of the periplasmic domain of PbgA, which is required for the OM enrichment in CL upon PhoPQ TCS activation in *S.* Typhimurium, results in OM permeability defects and reduced LPS levels [147, 265]. Very recent investigations refuted the claims that PbgA is a transporter of CL [149-152]. Surprisingly, PbgA was found to control the biosynthesis of LPS by modulating the levels of LpxC.

Several systems have been described for the retrograde transport (OM-to-IM) of PLs, such as the Tol-Pal complex and the OmpC-Mla pathway. The Tol-Pal complex has an established role in the maintenance of OM lipid homeostasis and it is also important during cell division for the invagination of the OM [266-268]. The Tol-Pal complex is the first molecular system implicated in bulk PL transport [266]. This system forms a transenvelope complex with the sub-complexes TolQRA and TolB-Pal at the IM and OM, respectively, interacting in a pmf-dependent fashion [269]. The five proteins connect the OM to both the peptidoglycan and IM layers, with TolQR controlling conformational changes in TolA and allowing interaction of the latter with Pal (peptidoglycan-associated lipoprotein) and the periplasmic TolB protein [266, 269-272]. How exactly the Tol-Pal system mediates the transport of PLs from the OM to the IM is not clear but it may be through a process of membrane hemifusion in regions where the transenvelope complex brings both membranes in close proximity and enables the formation of Bayer's bridges [254].

Maintaining the unique lipid asymmetry of the OM is essential for proper barrier function. The disruption of the LPS layer integrity can lead to a compensatory accumulation of PLs in the outer leaflet [12, 177]. These mislocalized PLs form patches that increase the membrane permeability to hydrophobic molecules, thus rendering the bacterial cell sensitive to detergents

and bile salts [273, 274]. In *E. coli*, several systems that restore the OM lipid asymmetry have been reported: the OM proteins PldA and PagP degrade surface-exposed PLs, and the Mla (maintenance of lipid asymmetry) system removes mislocalized PLs from the OM *via* retrograde trafficking. The OM phospholipase PldA is typically in an inactive monomeric conformation and the catalytically active dimer, that hydrolysis acyl ester bonds of PLs and lyso-PLs, is formed when phospholipids migrate to the outer leaflet [275, 276]. PldA also functions as a sensor of OM lipid asymmetry signalling to the cell to increase the production of LPS to restore lipid homeostasis [277]. The OM palmitoyltransferase PagP transfers a palmitate chain of the mislocalized surface PLs to the lipid A producing *sn*-1-lyso-PLs and hepta-acylated LPS [177]. The more hydrophobic form of LPS reduces lipid fluidity and presents stronger lateral interactions, which stabilizes the OM when the extracellular concentration of divalent cations is limiting [278, 279].

The OmpC-Mla system is a multiprotein complex with components in every cellular compartment: the ABC transporter MlaFEDB at the IM, the periplasmic protein MlaC, and the OM MlaA-OmpC complex [280, 281]. Although the Mla proteins are not essential, deletion of any member of the system results in PL accumulation at the OM outer leaflet, which causes permeability defects [280]. MlaC is the periplasmic lipid chaperone that interacts with both OM and IM sub-complexes to mediate the PL transport between the two membranes [282, 283]. The crystal structure of PL-bound MlaC revealed a hydrophobic pocket accommodating the acyl chains of the PL molecule [282, 283]. At the OM, the lipoprotein MlaA interacts with the trimeric porin OmpC to extract PLs from the outer leaflet [281]. Structural and biochemical studies suggest that MlaA is embedded in the inner leaflet and forms an amphipathic channel to deliver directly to MlaC the PLs removed from the outer leaflet in an energy-independent manner [284, 285]. The OmpC porin does not have a clear role in PL translocation and may serve as a scaffold for correct positioning of MlaA into the OM [281, 284, 285]. Phospholipids are inserted into the IM *via* the ABC transporter MlaFEDB that energizes the retrograde transport [286]. MlaC transfer PLs to MlaD within the IM complex, a protein shown to bind PLs [286], presumably in an energy-dependent manner, since MlaC has higher affinity towards PLs [283]. MlaD is a member of the mammalian cell entry (MCE) protein family forming a donut-shaped hexameric assembly that contains a central hydrophobic pore through which the PL acyl chains may transit [282].

In cells lacking the Tol-Pal complex, the overexpression of MlaC and the IM MlaFEDB complex can partially rescue defects in PL transport [266]. Moreover, PldA overexpression, which increases degradation of outer leaflet PLs, suppresses the OM permeability defects of

ompC-mla mutant strains [280]. These observations support a role of the OmpC-Mla system in retrograde PL transport. A MlaA variant with a dominant gain-of-function mutation termed *mlaA** endows the system with the exact opposite function facilitating the aberrant accumulation of PLs in the outer leaflet [287], due to the disruption of MlaA's donut shape which allows PLs to enter the amphipathic channel from the inner leaflet and flow into the outer leaflet [284].

Other putative lipid transporters involved in the maintenance of OM homeostasis have been reported in *E. coli*, such as PqiB and YebT [288, 289]. These putative systems contain mammalian cell entry (MCE) domains that assemble to form structures that span the periplasmic space and, potentially, mediate the transport of lipid substrates between the membranes to preserve the structural integrity of the OM [282].

2.4 Lipoprotein transport: the Lol pathway

The OM lipoproteins are essential components involved in the maintenance of envelope integrity, nutrient acquisition, and biofilm formation. They are soluble proteins anchored to the bilayer through N-terminally linked acyl groups, which are covalently attached *via* post-translational modifications [290].

Lipoproteins are synthesized in the cytoplasm in a precursor form with an N-terminal signal sequence that targets them for translocation across the IM by the SecYEG translocon, the major protein transport system in bacteria, or the twin-arginine transport (Tat) system, which translocates folded proteins [291, 292]. Lipoproteins contain at the C-terminus of their signal peptide a highly conserved lipobox motif of four amino acids where an invariant cysteine residue, immediately adjacent to the cleavage site of the signal peptide, undergoes acylation reactions after translocation [293, 294]. Whether the lipoproteins are sorted to the IM or the OM depends on the sequences following this conserved Cys residue. In *E. coli*, 90% of the lipoprotein species produced are targeted to the OM [295]. Lipoproteins retained at the IM contain the "Lol avoidance" signal, also known as the +2 rule, since it is determined by the identity of the amino acid adjacent to the conserved cysteine. The presence of a Asp residue at position +2 retains lipoproteins at the IM, while most other residues result in OM localization [296]; however, despite generally conserved in enterobacteria, this rule can vary with bacterial

species [290]. Following translocation, the maturation of lipoproteins occurs in a multistep process involving a series of modifications by enzymes that recognize the lipobox [290]. In *E. coli*, the IM enzyme Lgt adds diacylglycerol to the Cys residue, followed by the cleavage of the transmembrane signal peptide by Lsp. Lnt then attaches a third acyl group to the amino terminus of the cysteine generating the mature triacylated lipoprotein which is transported to the OM by the localization of lipoproteins (Lol) system (**Figure 10**) [297]. The Lol pathway comprises, in *E. coli*, five proteins located in each compartment of the cell envelope: the LolCDE complex, an ABC transporter, at the IM; the periplasmic chaperone LolA; and the OM lipoprotein LolB [297]. The mature lipoprotein is extracted from the IM by the LolCDE complex, transferred to the chaperone LolA for trafficking across the periplasm, and finally released to LolB at the OM that anchors the lipoprotein into the bilayer.

The degree of acylation of the lipoproteins is important for their export to the OM. Since the LolCDE complex presents in *E. coli* low affinity towards diacyl lipoproteins, the *N*-acylation of the Cys residue is determinant for lipoprotein interaction with the LolCDE complex and efficient release from the IM [298, 299]. The requirement for *N*-acylation, which is the final step in lipoprotein processing, may serve as a check-point mechanism preventing the secretion of immature lipoprotein intermediates. In other organisms, a homodimer of LolF replaces both LolC and LolE, and the LolDF complex does not require *N*-acylation for lipoprotein trafficking [300].

In the ABC transporter LolCDE, the homodimer of LolD corresponds to the NBD [301-303]. The transmembrane proteins LolC and LolE, despite the homology between their periplasmic domains, have distinct roles in the transporter: while LolC recruits LolA to the complex, LolE binds the lipoproteins [304-306]. In LolDF complexes, produced in certain pathogens such as *Neisseria gonorrhoeae* and *A. baumannii* [300], the LolF monomers must perform both functions. It is possible that dividing the labour between two distinct proteins, LolC and LolE, may optimize lipoprotein trafficking creating an unidirectional path for the substrate through the complex [31]. ATP binding to the LolD subunit induces the extraction of the lipoproteins from LolCDE, and the hydrolysis step is likely required for a complete release from the complex to the chaperone LolA [302]. LolA is recruited from the periplasm in an energy-independent fashion *via* a Hook-and-Pad architecture in the periplasmic domain of LolC, where the “Hook” corresponds to a solvent-exposed β-hairpin loop and the “Pad” comprises a trio of surface residues [305]. The lipoproteins are transferred from the IM complex LolCDE to the periplasmic chaperone LolA and then to the OM receptor LolB *via* a “mouth-to-mouth” exchange between the hydrophobic cavities of the Lol proteins [306].

In *E. coli*, the proteins involved in lipoprotein maturation and trafficking to the OM are conserved and essential. Lipoproteins are components of essential machines that build the peptidoglycan cell wall or that assemble the OM barrier, such as the Lpt and Bam complexes, hence, correct delivery of lipoproteins to the OM is critical [82, 307, 308]. Furthermore, the mislocalization of some lipoproteins can be toxic for the cell and severely disturb the cell envelope [309]. Nevertheless, LolA and LolB can be deleted under certain conditions, for instance, in *E. coli* cells lacking abundant OM lipoproteins, suggesting that an unknown alternate trafficking route must deliver lipoproteins to the OM to support cell viability [310]. The essentiality of LolAB in wild-type cells may be explained by a superior trafficking efficiency granted by these proteins that reduces toxicity events caused by mislocalized lipoproteins.

Some lipoproteins are translocated across the OM to become surface-exposed and their number varies with bacterial species [32]. Surface lipoproteins (SLPs) are involved in nutrient uptake, host immune evasion, cellular adhesion, and in stress response regulation; moreover, they have been explored as vaccine antigens. A few SLPs are known to use the Bam complex as a route towards the surface [311-313], and the Slam (surface lipoprotein assembly modulator) translocon has been described in the transport of SLPs in pathogenic *Neisseria* [314]. For most surface lipoproteins, the translocation pathway across the OM remains to be elucidated.

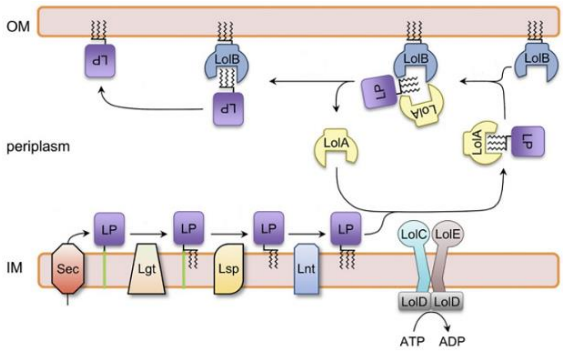

Figure 10. Lipoprotein processing and trafficking to the OM in *Escherichia coli* (from [305]). The preprolipoproteins are translocated across the IM by the Sec translocon, which recognizes the N-terminal signal peptide, and processed to their mature triacyl-form by the IM enzymes Lgt, Lsp and Lnt. The mature lipoproteins are recognized by the IM ABC transporter LolCDE that powers the extraction from the IM and the lipoprotein transfer to the periplasmic chaperone LolA. LolA delivers the lipoproteins *via* a mouth-to-mouth mechanism to the OM acceptor LolB for final insertion into the OM.

2.5 Integral OM proteins: the Bam-mediated assembly

OMPs have an important role in the maintenance of membrane integrity, OM biogenesis, nutrient uptake, and in the transport and secretion of diverse molecules, including drugs [82]. Bacterial OMPs possess at least eight β-strands arranged in an antiparallel configuration forming a cylindric β-sheet *via* hydrogen bond pairing between the first and last β-strands [315]. The internal surface of this barrel-like β-sheet is hydrophilic, while the external surface contains hydrophobic amino acids interacting with the OM lipid core, and the N- and C-termini face the periplasm. Like the lipoproteins, OMPs are synthesized in the cytoplasm and transported across the IM by the SecYEG translocon [82]. Following the cleavage of the signal peptide, the unfolded OMPs are escorted through the periplasm by chaperones (e.g., SurA and Skp in *E. coli*) and delivered to the β-barrel assembly machine (Bam) complex at the OM, which folds the OMPs into β-barrel structures and inserts them into the lipid bilayer. The Bam machine is an ubiquitous OM-associated heteromeric complex composed of BamA, itself a β-barrel protein, and four associated lipoproteins (BamB-E), the number of which can vary between species (**Figure 11**) [82]. In *E. coli*, the essential core components of the machine are BamA and BamD, while the remaining lipoproteins presumably have an accessory role and contribute to an optimal catalysis activity of the complex. Although BamB, BamC and BamE can be deleted, this causes defects in OM homeostasis and permeability [316-318].

BamA, a member of the Omp85 superfamily, is a highly conserved protein and it is essential for cell viability across all Gram-negative bacteria [319]. BamA contains a C-terminal β-barrel domain with 16 antiparallel β-strands, and extracellular loops that form a dome-shaped barrier at the top enclosing the lumen of the barrel from the passage of solutes [320-322]. The first and last barrel β-strands are only partially zipped creating a potential gate [323]. At this site, also referred as the seam, the height of the barrel is significantly shorter, which is thought to physically modify the local properties of the OM thus destabilizing it and facilitating OMP assembly [320, 324-326]. The N-terminal periplasmic moiety comprises five polypeptide transport-associated (POTRA) domains (P1-5) that scaffold BamA-interacting proteins to establish a native Bam complex [327, 328]. Despite being structurally homologous, the POTRA domains have distinct functions and, in *E. coli*, only P3-5 are essential [327]. BamA exists in two different conformations, i.e., the inward-open and outward-open. In the inward-open state, the P5 moiety is off-centred in relation to the barrel axis, which creates an open access from the periplasm to the lumen of the barrel; the extracellular loops form a dome on

top of the barrel; and β-strands 1 and 16 are partially hydrogen-bonded (closed lateral gate) [323]. In the outward-open configuration, P5 is shifted towards the central axis of the barrel occluding its access from the periplasm; the extracellular loops are reoriented; and the first eight β-strands of the barrel are rotated in a scissor-like movement that unzips the seam (open lateral gate) and exposes the barrel lumen [323, 329].

The essential proteins BamA and BamD interact to stabilize the sub-complexes BamAB and BamCDE. BamA interacts with BamD mainly *via* P5, while P3 and P1 are important for the interaction with BamB and the periplasmic chaperone SurA, respectively [327, 330, 331]. The POTRA domains together with the Bam lipoproteins assemble in a ring-like structure, with BamD and the POTRA domains forming the inner surface, that is positioned in parallel to the membrane plane under the BamA barrel [323, 329, 332, 333]. The Bam periplasmic ring, formed by essential subdomains, is believed to have a critical role in OMP assembly.

Although BamA is the central catalyst, BamD is also vital in the machinery [334]. While the POTRA domains may help with the formation of OMP secondary structure *via* β-strand augmentation [323, 327, 335, 336], BamD is involved in substrate recognition by binding the sorting signal for β-barrel assembly into the OM [337-339]. This so-called β-signal generally corresponds to the last C-terminal β-strand of the unfolded OMP and its sequence is relatively similar amongst different organisms, with a few exceptions such as the *Neisseriales*, and *Helicobacter* spp., which present noteworthy differences in their C-terminal recognition motif sequences [340, 341]. The interaction between BamD and P5 of BamA allows both proteins to coordinate their activities during the β-barrel assembly cycle [330, 342, 343]. BamD is associated with the regulation of BamA's activity by linking substrate recognition with conformational changes in BamA [339]. Moreover, BamD is required for the assembly of BamA itself since the depletion of this lipoprotein results in BamA misfolding [344].

The precise function of nonessential lipoproteins, which are variably conserved, is unclear since they are not central for the Bam-catalysed process of OMP folding and insertion. BamCE associate with BamA *via* BamD and likely stabilize the BamA-BamD interaction [318, 334]. BamB, directly interacting with several POTRA domains, supports the efficient assembly of certain OMPs [329, 345-350]. BamB and BamD, for example, assist in the biogenesis of BamA by binding the unfolded BamA and accelerating its assembly into the OM [347]. According to several lines of evidence, the nonessential Bam lipoproteins may be required to assist in the assembly of specific substrates [82]. Considering the structural diversity of the Bam substrates, a specialized activity of the Bam complex may be required for their assembly, and the Bam

accessory lipoproteins may either be directly involved or indirectly assist in this process by enhancing the efficiency of the core components BamAD.

OMPs can spontaneously fold into a lipid bilayer, however this is an intrinsically slow process [351-353]. Bam complexes accelerate the folding kinetics of OMPs to enable OM biogenesis within physiologically appropriate timescales [354]. Although the mechanism of Bam-mediated OMP assembly remains unclear, three mechanist models have been proposed [355, 356]. According to the first suggested model, referred to as 'BamA-assisted' model, the folding of the β-barrel begins at the periplasm/OM interface, prior to membrane integration, and insertion into the OM occurs in vicinity to the BamA lateral gate where the lipid bilayer is thinner and destabilized [354]. The second mechanist model, the 'BamA-hybrid barrel' model (also known as the 'budding' model) proposes that the barrel structure of a nascent OMP forms directly in the OM beginning with the zipping of the C-terminal β-signal of the substrate with the first β-strand of BamA, and continuing with the sequential insertion of more N-terminal β-strands or β-hairpins near the last β-strand of BamA [356]. After the insertion of the final β-strand, the nascent OMP buds off laterally into the membrane to complete folding.

The third 'BamA-triggered barrel-elongation' model conciliates most of the experimental data obtained from biochemical and structural studies [355, 356]. The nascent OMP, delivered by molecular chaperones, interacts with the Bam periplasmic ring and triggers a laterally open BamA state that exposes β1 of the barrel. OMP assembly begins with the interaction between β1 of BamA and the C-terminal β-strand of the substrate creating a hybrid barrel [357-360]. Then, folding proceeds towards the most N-terminal β-strand *via* β-augmentation [357, 360]. In this process, existing β-strands perform as templates for the formation of new strands, possibly sequentially added in β-hairpin units, and the nascent β-sheet is probably positioned in the Bam periplasmic ring [361, 362]. The scissor-like movement of the first eight β-strands of BamA, coupled with the rotation of the periplasmic ring, would pull the nascent OMP into the OM and position its N-terminal β-strand close to the β16 of BamA [356].

Recent work probing the assembly of a LptD variant (LptD4213), which stalls on the Bam complex as a late-stage folding intermediate, has revealed that the interior wall of BamA serves as an active site for the assembly of β-strands, as N-terminal strands of the client protein fold inside the BamA barrel [359]. Moreover, another study has found that BamA and the substrate OMPs form an asymmetric hybrid-barrel: while it presents a rigid interface between BamA β1 and the substrate C-terminal β-strand, on the opposite side of the hybrid-barrel, between BamA β15/β16 and the first substrate β-strand, the interactions are weaker and conformationally heterogenous [358]. A mechanism for β-barrel closure and release has been recently proposed

based on structural work using late-stage folding intermediates of the *E. coli* Bam complex assembling BamA itself [360]. The N-terminal edge of the nascent OMP is not hydrogen-bonded with the C-terminal end of the BamA barrel and, instead, these edges face inward towards the lumen of the hybrid barrel, which facilitates the substrate release since no polar bonds need to be disrupted. Furthermore, the substrate presents a C-terminal overhang that protrudes inside the hybrid barrel to connect with its own N-terminal. For the closure of the substrate β-barrel, its N- and C-termini sequentially form hydrogen bonds while sequentially disrupting the hydrogen bonds established with the BamA catalyst. This stepwise exchange of hydrogen bonds promotes the substrate release into the OM.

The Bam complexes prevent substrate aggregation and off-pathway misfolding, and protect the OMPs from degradation [354]. In all the proposed models for OMP assembly, the Bam complex destabilizes the membrane lowering the kinetic barrier for membrane integration, thus accelerating the OMP folding reaction [355].

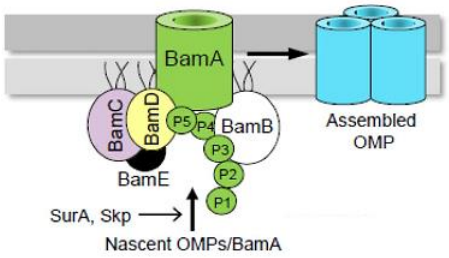

Figure 11. The β-barrel assembly of integral outer membrane proteins (OMPs) catalysed by the Bam complex (from [344]). The unfolded OMPs, including BamA, are delivered to the Bam complex at the OM by periplasmic chaperones, such as SurA and Skp. In *Escherichia coli*, the Bam complex is composed of four accessory lipoproteins (BamBCDE) and the central catalyst BamA, which contains a C-terminal β-barrel transmembrane domain and five N-terminal periplasmic POTRA domains. The Bam machine assists in the folding of OMPs and facilitates their insertion into the OM.

CHAPTER 3. Disrupting the OM biogenesis to counteract antibiotic resistance

The efficacy of antimicrobials against Gram-negative bacteria is greatly dependent on their ability to permeate the OM and access their target. The challenging architecture of the Gram-negative cell envelope, in tandem with an efficient ability to develop multidrug resistance, render the infections caused by these microorganisms difficult to treat and have hampered the search for innovative antibiotic classes over the last 50 years. Although the OM permeability represents a major hurdle in antibiotic discovery, the requirement of a robust OM makes it an interesting antimicrobial target. Elucidating the metabolic pathways for OM biogenesis and characterizing their essential components are essential in understanding how the OM barrier can be breached and broken down. The multiprotein machineries Lpt, Bam, and Lol represent attractive targets for antibiotic development since they are essential for the bacterial cell, working together to assemble the OM. Targeting the OM biogenesis could have a direct killing effect or sensitize the bacterial cell to the action of other antimicrobials otherwise unable to cross the outer barrier. New drug discovery or novel therapeutic drug combinations are paramount in overcoming the ever-growing problem of multidrug resistance. Despite the increased interest in exploring the many essential and highly conserved proteins that build the OM for the development of novel antibacterial agents, there are no antibiotics currently in clinical use that inhibit OM assembly.

This final chapter will review the compounds that target the essential OM assembly machines, and that act on the earlier steps of LPS biogenesis.

3.1 Targeting the LPS biosynthesis

Compounds interfering with LPS biosynthesis or transport have the potential to work in monotherapy as single agents, or as adjuvants by potentiating the permeation of other existing antibacterial agents normally excluded by the OM. Furthermore, the inhibition of LPS synthesis can reduce bacterial virulence, as bacteria become more vulnerable to the action of the complement system and phagocytosis [363]. The Kdo_2-lipid A moiety is the minimal

structural requirement for Gram-negative viability; therefore, the enzymes involved in the synthesis of this conserved part of LPS are attractive targets for drug development (**Figure 12**).

The enzyme LpxC has long been explored as a target in antibiotic discovery [364]. LpxC catalyses the first committed step of the LPS biosynthetic pathway and is broadly conserved across Gram-negative species [124]. The first ever identified LpxC inhibitor, discovered in the mid-1980s by Merck Research Laboratories, was the small oxazoline hydroxamic acid L-573,655 active against *E. coli* [365]. Using a strain hypersensitive to LpxC inhibitors, carrying the mutation H19Y in *lpxC*, British Biotech later discovered the potent hydroxamic acid derivatives BB-78484 and BB-78485, *via* a screen of a metalloenzyme inhibitor library [366]. Although possessing a wider spectrum of activity, these compounds were not active against *P. aeruginosa*. Research groups from the University of Washington and Chiron were able to discover inhibitors of *P. aeruginosa* growth using LpxC purified from this bacterial species in *in vitro* enzymatic assays [367]. This screening strategy was employed upon the discovery that LpxC inhibitors presented distinct activity against different LpxC orthologues [368]. Reports of LpxC inhibitors active against *P. aeruginosa* soon attracted interest from pharmaceutical companies and numerous research programs were initiated. Over a period of ten years, from 2004 until 2013, numerous patents were filed by companies such as Achaogen, AstraZeneca, Novartis, and Pfizer [364]. In 2005, the molecule CHIR-090 was reported as one of the most active compounds discovered by the University of Washington/Chiron, with an antibiotic activity comparable to that of ciprofloxacin against *E. coli* and *P. aeruginosa* [369]. Despite a favourable toxicity profile, the compounds identified by the University of Washington/Chiron presented high plasma-protein binding, and poor solubility and pharmacokinetic properties. Another promising LpxC inhibitor was the compound PF-5081090 from Pfizer with activity against several Gram-negative nosocomial pathogens (e.g., *E. coli*, *P. aeruginosa*, *K. pneumoniae*, *B. cepacia*, and *Stenotrophomonas maltophilia*) and with demonstrated efficacy in mouse infection models [364]. Despite all research efforts over the last 20 years, only one compound inhibiting LpxC, the ACHN-975 discovered by Achaogen, has advanced into clinical trials [364]. This molecule is active against *E. coli*, *P. aeruginosa*, and *K. pneumoniae*, and it was shown to be efficacious in a murine infection model. After entering human clinical trials in 2012, Phase 1 studies were discontinued due to inflammation at the injection site. The LpxC research programs are still encouraging examples of target-directed antimicrobial discovery where robust screening assays for *in vitro* activity can translate into *in vivo* potency and result in the identification of many antibiotic leads. Nowadays, investigators continue to

improve LpxC inhibitor molecules, designing novel hydroxamic acid derivatives with more desirable physicochemical and serum binding properties [370].

The other essential enzymes involved in the biosynthesis of LPS also represent attractive targets for antimicrobial development. Small peptides have been found to inhibit LpxA and LpxD, enzymes that catalyse the first and third steps, respectively, of the lipid A biosynthesis [371, 372]. The peptide RJPXD33, identified from a random peptide library screen targeting LpxD, presents dual *in vitro* target activity against both LpxD and LpxA [373]. The enzyme LpxD is an interesting target since its inhibition causes the potentially toxic accumulation of UDP-3-O-(R-3-hydroxyacyl) glucosamine, a detergent-like molecule [128, 129]. Structural studies revealed that this bioactive peptide is located at a conserved fatty acyl binding pocket present in both enzymes, explaining its multitarget inhibitory activity [374]. Derivatives of RJPXD33 with increased *in vitro* potency and with whole-cell activity, the latter achieved *via* conjugation with a cell-penetrating peptide, have been synthesized [374, 375]. Multitarget activity of a single molecule is intriguing since the inhibition of multiple LPS synthesis steps decreases the likelihood of resistance to arise.

Recent work has indicated that LpxH and LpxK are targets that antibiotic research should focus on. Inhibition of these enzymes leads to the toxic build-up of lipid A pathway intermediates, which is deleterious even for species that do not require LPS for viability, such as *A. baumannii* [376, 377]. Since LPS is not essential in this bacterium, the discovery of compounds active against this pathogen has been a challenge; therefore, inhibitors of such enzymes would be interesting drug candidates for the treatment of *A. baumannii* infections. In 2015, the first LpxH inhibitor was identified through a high-throughput screening assay of molecules inhibiting the cell wall synthesis [378]. This inhibitor is a sulfonyl piperazine with activity against an efflux-deficient *E. coli* strain but inactive against wild-type *E. coli*. More recently, a new high-throughput *in vitro* screening strategy for sulfonyl piperazine analogues has been developed [379]. LpxH is a promising target in antimicrobial therapy and further work is required, including the optimization of the discovered scaffolds or the development of more effective compounds.

As discussed in the previous chapter, the Kdo_2-lipid A moiety is the minimum requirement for cell growth. The Kdo biosynthesis pathway involves four enzymes and, although KdsD and KdsC are nonessential due to their redundancy, KdsA and KdsB perform essential steps and have been explored in antibacterial drug discovery [380-383]. Target-based design has produced various Kdo analogues inhibitors of KdsB [384, 385]. Unfortunately, these molecules are deficient in whole-cell activity because they cannot penetrate the IM. The same hurdle

limits the development of KdsA inhibitors; hence, although several molecules inhibiting this enzyme have been identified, only one compound named PD 404182 is active against wild-type *E. coli* [386]. Several strategies have been employed for the discovery of novel inhibitors of Kdo biosynthesis; nevertheless, their inability to permeate the cell remains a major obstacle [387, 388].

Once the synthesis of the core-lipid A moiety of LPS is completed, MsbA translocates this molecule across the IM to the periplasmic side, performing the first essential step in the LPS trafficking to the cell surface [155]. Since MsbA possesses easily assayable enzymatic activity, it enables the performance of high-throughput *in vitro* screenings of large libraries. From a library of about 3,000,000 small molecules, potent quinolone-like compounds inhibiting MsbA ATPase activity and the growth of *E. coli* and *K. pneumoniae* have been identified [159]. The scaffold of the inhibitor G592 was optimized to yield the more potent G907. Structural studies to unravel the mechanism behind G907 antagonism have found that it binds the architecturally conserved transmembrane pocket of MsbA, which traps MsbA in an inward-facing, LPS-bound conformation, and causes the structural and functional uncoupling of the NBDs [159]. The quinoline compounds, however, due to their high hydrophobicity, present very high levels of plasma protein binding, which results in a considerable loss of whole-cell growth inhibition [389]. The requirement for a hydrophobic scaffold that enables the binding to the transmembrane pocket of MsbA precludes the necessary chemical modifications that would reduce serum binding. For this reason, compounds targeting the membrane region of MsbA are not viable lead candidates. Nevertheless, these studies evidence MsbA as a valid drug target and ask for further efforts in identifying alternative inhibitor binding sites.

By exploiting the nonessentiality of LPS in certain pathogens, a cell-based screening assay has been developed for the discovery of inhibitors of the entire LPS biogenesis pathway, which includes both LPS biosynthesis and transport [390]. In this screening platform, compounds of interest are active against a wild-type *A. baumannii* strain but fail to inhibit the growth of an LPS-null strain. They identified one compound targeting MsbA that stimulated its ATPase activity, while decoupling it from LPS flipping. Accumulation of LPS at the IM was thought to interfere with other essential processes dependent on the normal state of the membrane. The binding site of this MsbA inhibitor has yet to be determined but it is likely to be different from that of the quinoline inhibitors. Although no compounds targeting any of the other enzymes involved in LPS biogenesis were discovered, this high-throughput cell-based platform holds great promise and further screens are warranted.

The development of compounds targeting LPS-modifying enzymes is another strategy in the fight against antibiotic resistance. LPS modifications are important for virulence and for the resistance against polymyxins. Encouragingly, molecules inhibiting lipid A modifications *via* the downregulation of PmrAB in *A. baumannii* and *K. pneumoniae* have been identified; moreover, these compounds were shown to suppress colistin resistance [391]. Substrate analogues inhibitors of ArnT have already been synthesized and they may also be useful in the future for the treatment of infections caused by pathogens resistant to polymyxins *via* a PmrAB-mediated mechanism [392]. Nevertheless, this type of compounds would still be ineffective against pathogens carrying plasmids harbouring *mcr* genes.

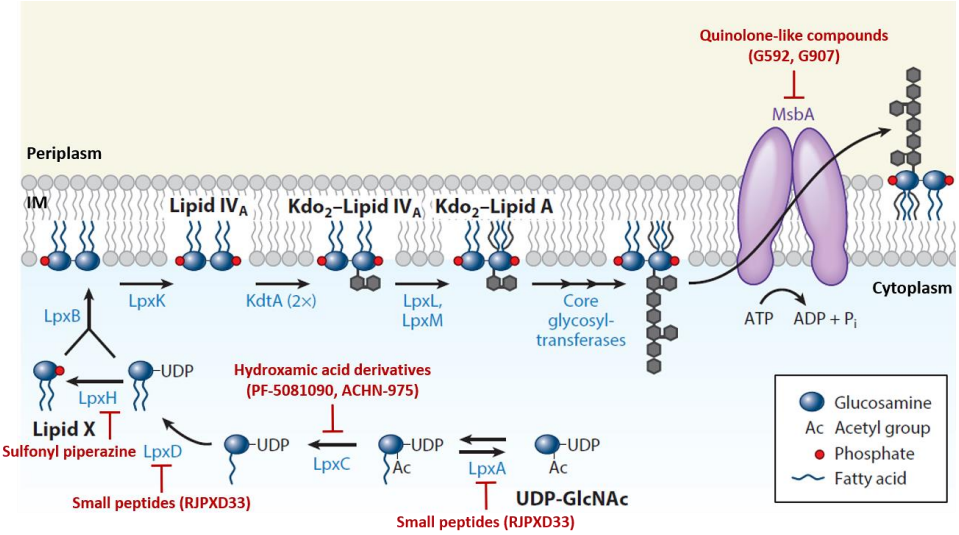

Figure 12. Inhibitors of lipopolysaccharide biosynthesis and translocation across the inner membrane (IM) (adapted from [16]). Blocked red arrows represent inhibition of enzymatic activity. See text for details.

3.2 Inhibiting the Lpt complex

All seven proteins composing the envelope-spanning Lpt complex are essential in organisms that require LPS for viability and pathogenicity [96, 205, 209]. Therefore, the disruption of this machinery is a promising strategy for the development of antimicrobials with a novel killing mechanism or to increase OM permeability (**Figure 13**). The blocking of LPS transport may also enable the use of polymyxins, considered as last-line antibiotics, with a safer toxicity profile by enabling a reduction in the administered dose without the loss of clinical efficacy.

The first identified OM assembly inhibitor was the macrocyclic peptide L27-11 developed by the optimization of β-hairpin mimetics of the cationic AMP protegrin I, a host-defence molecule shown to permeabilize membranes [393-395]. L27-11 does not lyse bacterial membranes and is potently and specifically active against *Pseudomonas* spp., including the opportunistic human pathogen *P. aeruginosa* [393]. Photoaffinity labelling studies allowed the identification of LptD from *P. aeruginosa* as its target; moreover, mutations conferring resistance mapped to the periplasmic β-jellyroll domain of LptD [393]. Further evidence of the mode of action of this peptidomimetic antimicrobial came from mechanist studies showing that it indeed inhibits the LPS transport function of LptD [396]. The optimization of the drug-like properties of L27-11 created the clinical candidate called murepavadin, also known as POL7080. Murepavadin is the pioneer molecule of the innovative chemical class of outer membrane protein targeting antibiotics (OMPTA) [397, 398]. Like L27-11, murepavadin is a pathogen-specific antibacterial agent with demonstrated high potency against *P. aeruginosa*, including MDR clinical isolates, and with poor activity against other Gram-negative bacteria. LptD structural differences amongst Gram-negative bacteria explain the unique species-selectivity of L27-11 and murepavadin [399]. In *Pseudomonas* spp., the periplasmic domain is longer than in most γ-proteobacteria, given the presence of an extra domain of ca 100 residues at the N-terminal. At present, this "insert" domain is of unknown structure and function. With photolabeling experiments, the peptidomimetics L27-11 and murepavadin were shown to bind the periplasmic segment of LptD, in proximity to both the β-jellyroll domain and the N-terminal insert domain [399]. Murepavadin was developed by the company Polyphor AG to meet the medical need for treatments against nosocomial pneumonia in cystic fibrosis patients. Although very promising as the first drug of an innovative antibiotic class, the Phase 3 clinical trials with the intravenous form of murepavadin were suspended due to unexpectedly high incidence of nephrotoxicity, and this molecule is currently in preclinical development for administration *via* inhalation [400, 401].

The first natural product discovered to target the Lpt machinery was thanatin, an inducible host-defence AMP [402]. Thanatin is a 21-residue peptide, with a β-hairpin conformation and a disulphide bond between Cys^{11} and Cys^{18}, originally isolated from the insect *Podisus maculiventris* (spined soldier bug) [403]. Thanatin possesses an extraordinarily large spectrum of antimicrobial activity, being both bactericidal and fungicidal, which suggests more than one mechanism of action; moreover, it exhibits low cytotoxicity towards human cells [403-405]. It is active against several Gram-negative strains, including *E. coli*, *S.* Typhimurium, and *K. pneumoniae*, with minimal inhibitory concentrations (MICs) of <1.5 μM, and presents weaker

activity against *P. aeruginosa* [403]. Thanatin also presents antibacterial activity against Gram-positive bacteria, with MICs of 1-5 μM. Its enantiomeric form (ᴅ-thanatin) loses much of its activity against Gram-negative bacteria, indicating a chiral target, and the peptide's disulphide bond is not required for activity [403, 404]. The first evidence pointing to thanatin's target in Gram-negative organisms came from *in vivo* photoaffinity labelling experiments performed in *E. coli* [402]. Three proteins, namely LptD, LptA, and BamA, were identified in this study, of which LptD and LptA were the most significantly labelled. Moreover, thanatin-resistant mutants with resistance mapping to LptA were isolated. Cells treated with thanatin presented defects in the membrane architecture and the accumulation of membrane-like material inside the cell, which is an effect characteristic of LPS transport defects caused by the depletion of Lpt proteins [402]. The interaction between thanatin and both LptA and the LptDE complex was demonstrated *in vitro*, and the thanatin-LptA complex was solved with NMR structural studies [402]. Thanatin binds to the N-terminal end of LptA, docking its N-terminal β-strand in a parallel orientation onto the first β-strand in the β-jellyroll of LptA. Thanatin's binding site therefore overlaps with the interaction site of LptA with another LptA subunit and with LptC, suggesting a possible mechanism for the antibacterial activity. Furthermore, modelling studies determined that the residues in thanatin's binding site in LptA are highly conserved at the N-terminus of the jellyroll of LptD, suggesting that thanatin could also interact at the same position in LptD. Overall, these results imply that thanatin may be able to disrupt multiple protein-protein interactions within the Lpt bridge formed by the continuous β-jellyroll fold shared by LptC, LptA, and LptD.

Another antibacterial compound targeting LptA is IMB-881 [406]. Its benzoxazine scaffold was originally identified in a high-throughput screening for small molecules active against *E. coli* and *P. aeruginosa*, and its mechanism of action had remained unknown [407]. Recently, through a yeast two-hybrid assay developed to detect the LptC-LptA interaction, IMB-881 was found to inhibit this interaction, and subsequent surface plasmon resonance experiments demonstrated that it binds specifically to LptA [406]. IMB-881 was also shown to possess antibacterial activity against clinical carbapenem-resistant *E. coli* strains (MICs of 6.25-12.5 μg/mL) and to be less potent against *P. aeruginosa* (MIC >32 μg/mL).

LptB is the only cytoplasmic protein of the machinery, requiring inhibitors to cross both OM and IM, and the only that possesses enzymatic activity. The ATPase activity of LptB has been proven suitable for high-throughput screening approaches, and two competitive inhibitors have been identified in a screen of a kinase inhibitor library [408]. Analogues of one of the discovered compounds, a 4-phenylpyrrolcabazole, displayed higher potency against LptB

alone than the complex $LptB_2FGC$ [409]. Moreover, none of the reported LptB inhibitors presented whole-cell activity and were only active against an *E. coli* strain with a compromised OM; likely because these compounds are too hydrophilic to permeate the outer barrier [409]. The well-described antibiotic novobiocin, a DNA gyrase inhibitor, was recently found to bind LptB, stimulating its ATPase activity and the LPS transport [230]. Novobiocin analogues lacking activity against the DNA gyrase and with enhanced LptB stimulatory activity have been synthesized [410]. Although LPS transport agonism does not inhibit bacterial growth by itself, boosting the transport worked synergistically with polymyxin B, increasing *A. baumannii* sensitivity to this AMP [410]. The stimulation of LPS transport is, therefore, a valid alternative strategy to target the Lpt machinery in antimicrobial discovery. Furthermore, combination therapies may allow the reduction of the dose of polymyxins required to treat bacterial infections, thus increasing both efficacy and safety.

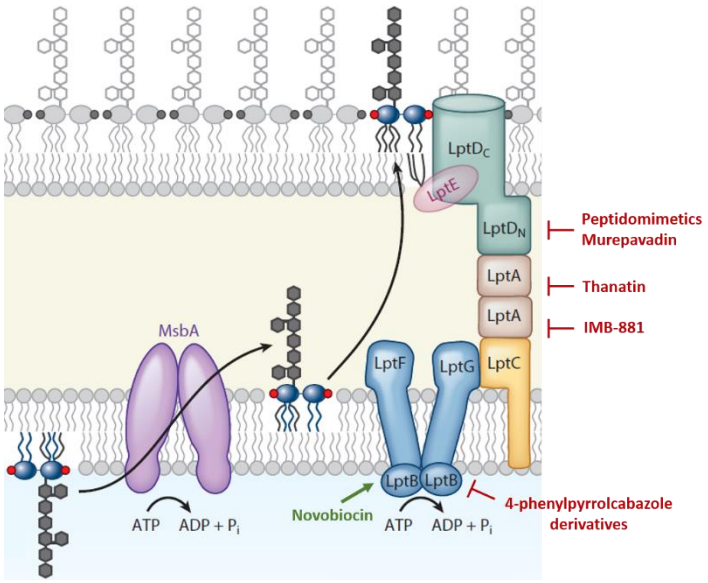

Figure 13. Compounds targeting lipopolysaccharide (LPS) transport (adapted from [16]). Blocked red arrows represent inhibition of LptB's enzymatic activity, and inhibition of LPS transport *via* binding to LptA or LptD. Green arrow represents stimulation of the ATPase activity of LptB and of LPS transport. See text for details.

3.3 Targeting other multiprotein molecular machines: Bam and Lol

Disrupting the assembly of OMPs can hinder a variety of cellular functions and interfere with the Lpt and Bam complex itself, given the vital role of LptD and BamA. Furthermore, the accumulation of unfolded OMPs is toxic for the cell. The first described inhibitor of OMP assembly by the Bam complex was a 15-mer peptide containing a sequence from the C-terminus of BamA that is conserved in BamA orthologues [338]. *In vitro* assays have shown that this BamA-derived peptide binds to BamD and inhibits BamA assembly, which subsequently can affect the folding of other OMPS leading to cell death [338]. The inhibitory peptide does not present whole-cell activity, due to its inability to cross the OM, and is only capable of causing growth and OM permeability defects in *E. coli* when expressed within the cell. This study suggests that designing peptidomimetic derivatives of OMP's β-signals to interfere with OMP assembly may be a valid strategy in the search for novel antibiotic leads.

The β-hairpin peptidomimetic JB-95 is potently active against several Gram-positive and Gram-negative bacteria [411]. JB-95 selectively disrupts the OM of *E. coli* without presenting lytic activity on human red blood cells; moreover, *in vivo* photolabeling experiments revealed cross-linking to several OMPs, including BamA and LptD. In cells treated with this macrocyclic peptide, depletion of many β-barrel OM proteins occurs, with the exception of BamA, and an increased expression of OM stress response genes can be observed [411]. Although these effects are consistent with Bam-inhibition, direct proof is still missing. Since JB-95 also has Gram-positive antibacterial activity, it is possible that this peptide is a membrane-acting antibiotic.

BamA is an attractive target for the development of inhibitors with antimicrobial activity due to its accessible localization at the cell surface, not requiring inhibitors to cross any bacterial membrane and thus expanding the range of molecules likely to present activity. Monoclonal antibodies (mAbs) raised against BamA have been isolated by the immunization of mice and rats with *E. coli* bacteria and the purified *E. coli* BamA protein [412]. One of these mAbs called MAB1 was identified in a screen for growth inhibition of an *E. coli* strain expressing a truncated form of LPS [412]. MAB1 binds an epitope in the external loop 4 of BamA, inhibiting the Bam-folding activity and disrupting the OM integrity, ultimately leading to cell death. Unfortunately, the clinical potential of MAB1 is limited due to a high frequency of resistance and a bactericidal activity restricted to *E. coli* strains with deeply truncated LPS, since the wild-type LPS prevents MAB1 from binding to BamA. Interestingly, resistance

mechanisms against MAB1 revealed that the β-barrel folding activity of BamA is affected by the OM fluidity, which in turn is affected by the LPS structure [412, 413]. LPS modifications thus seem to act as a determinant of the antimicrobial potency of certain molecules by modulating their attraction to the OM and altering the membrane fluidity. The anti-BamA antibody MAB1 may be a good tool to investigate the assembly of OMPs *in vivo*. Furthermore, this study highlights the potential of surface-exposed loops of BamA to be targeted by extracellular antibacterial agents.

A natural antimicrobial peptide also shown to bind an extracellular epitope in BamA is the lectin-like bacteriocin named LlpA [414]. Bacteriocins are membrane-disruptive AMPs, also known to inhibit cell wall synthesis and protein translation, secreted by bacteria as a defence mechanism against strains of their own or related species [415]. In *Pseudomonas* spp., BamA was identified as the molecular target of LlpA [414]. Resistant mutants were isolated carrying mutations mainly in the surface loop L6 of BamA, and genetic studies demonstrated that *bamA* mediates the selective killing mechanism of LlpA. In *Pseudomonas* spp., instead of possessing an immunity protein protecting the producer bacteria from LlpA's effect, immunity is conferred by a divergent sequence of the BamA surface-exposed loops that abolishes LlpA action. The bactericidal mechanism of LlpA is likely due to the disruption of BamA's activity, causing the toxic accumulation of unfolded OMPs in the periplasm. This is a novel bacteriocin killing mechanism and, promisingly, LlpAs already have proven efficacy in a murine model of *P. aeruginosa* lung infection [416]. However, though their targeted action and potency makes them attractive compounds to be developed into clinically useful antibiotics, the strain-specific activity of bacteriocins and the potential for resistance to arise may require the development of cocktails of LlpAs for an effective treatment. The surface-exposed loop 6 of BamA, which is critical for OMP folding, represents another interesting target for extracellular inhibition of this protein [417]. Unfortunately, targeting extracellular epitopes is not a viable strategy for the discovery of LptD antagonists, since all the loops essential for structure and function of LptD are inaccessible to extracellular antibacterial agents [418].

Recently, the first non-peptide based small molecule inhibitor of BamA was identified and named MRL-494 [419]. To find this molecule, a screen for compounds targeting essential processes occurring on the cell surface was performed. For this, compounds were screened for growth inhibition of a wild-type *E. coli* strain and a permeable strain defective in efflux systems. MRL-494 presented similar antibacterial potency against both strains, suggesting that it does not need to cross the OM to exert its activity. Cells treated with MRL-494 presented depletion of OMPs, suggesting BamA as a potential target; moreover, resistant mutations in *E.*

coli mapped to *bamA*, and cellular thermal shift assays showed that MRL-494 stabilizes BamA *in vivo*. MRL-494 is also active against Gram-positive organisms, causing rapid permeabilization of the cytoplasmic membrane. In Gram-negative bacteria, disruption of the IM was not observed, likely because the presence of the OM prevents MRL-494 from reaching the IM.

In a screen for murepavadin analogues with a larger spectrum of activity, an initial hit was found [420]. The investigators, in an attempt to increase potency, synthesized a series of chimaeras by chemically linking the β-hairpin peptide macrocycle of the hit molecule to the peptide macrocycle of polymyxin B (PMB), that is the portion of PMB that binds LPS [420]. This strategy yielded several chimaeras with potent bactericidal activity against worrisome bacteria such as *P. aeruginosa* and *A. baumannii*, and other multidrug-resistant Gram-negative pathogens. Since the scaffold derives from murepavadin, one would expect for these chimaeras to target LptD. Surprisingly, BamA was found to be the interacting partner. Resistant strains of *K. pneumoniae* presented mutations in several genes that included *bamA* and genes coding for LPS modifications. Additionally, when the wild-type *bamA* gene was reintroduced into the resistant strains, they recovered the sensitivity to the chimaeras. Direct binding to BamA was confirmed with *in vitro* studies, which indicated that the binding likely stabilizes BamA in a potentially inactive conformation. Still, the chimeric peptides were also shown to permeabilize both OM and IM, suggesting a direct effect on the membrane similar to polymyxins. The chimaeras have great potential in succeeding as clinical leads since preclinical investigation revealed high potency, a low frequency of resistance, low toxicity, and favourable pharmacokinetics and pharmacodynamics properties in animal models [420].

Another recently discovered antibacterial agent targeting BamA is darobactin, a compound produced by the nematode symbiont *Photorhabdus* [421]. The Gram-negative bacteria living symbiotically in the gut of nematode worms secrete antibiotics against other competing bacteria. Darobactin was found from a screen for Gram-negative antibacterial activity of *Photorhabdus* extracts and, besides the *in vitro* antibiotic activity, it is also active against important drug-resistant pathogens in animal models of infection. Several resistant *E. coli* strains harboured mutations in the *bamA* gene, and all the identified mutations were found to change amino acid residues in the same region of BamA's protein structure, thus suggesting a putative binding site for darobactin accessible from the extracellular milieu. Darobactin binding to BamA was demonstrated with *in vitro* assays and, as with the peptidomimetic chimaeras, likely stabilizes the protein in a non-functional conformation. This study highlights

the potential of bacterial symbionts of animals as natural sources for the discovery of novel antimicrobials.

Recently, the Bam complex was proven to be a valid target for the development of antivirulence compounds [422]. In uropathogenic *E. coli*, the pili are required for the colonization of host tissues and these structures are built *via* the chaperone-usher pathway, which contains an OM usher protein itself assembled by the Bam complex [356, 423]. The antiparasitic nitazoxanide was found to selectively interfere with the assembly of this usher protein by targeting the Bam complex, while not affecting the assembly of other OMPs [422]. Accordingly, sensitivity to nitazoxanide was dependent on the expression of BamB and BamE, and a resistant mutant with a point mutation in the BamD lipoprotein was isolated. Nitazoxanide thus seems to interfere with a specific function of the Bam complex specialized in the folding of the usher. By interfering with the biogenesis of adhesive surface structures, nitazoxanide derivatives have great potential to be applied in antivirulence approaches and, since nitazoxanide is an established antiparasitic drug, human toxicity and pharmacokinetic properties may be of less concern.

Preventing lipoprotein trafficking has the potential to deprive the bacterial cell of essential OM assembly machines, since lipoproteins are vital components of the Lpt, Bam, and the Lol pathway itself. Moreover, the mislocalization of some lipoproteins can be toxic for the cell [309]. The first inhibitor of the LolCDE transporter complex, called compound 2, was identified in a high-throughput phenotypic screen for *E. coli* growth inhibition [424]. The inhibitor is a pyridineimidazole and mutations conferring resistance mapped to either LolC or LolE at the interface between their periplasmic and transmembrane domains. Through biochemical transport assays, this compound was shown to inhibit the LolCDE-dependent release of lipoproteins from the IM. Despite the conservation of the LolCDE ABC transporter across Gram-negative species, the small molecule inhibitor was only active against *E. coli* and *Haemophilus influenzae*. Another LolCDE inhibitor with a pyrazole-based scaffold, and also named compound 2, was reported in the same study that identified the first LpxH inhibitor [378]. In this study, investigators developed a high-throughput screening assay, using an AmpC β-lactamase reporter strain, for the detection of compounds inhibiting the cell wall synthesis. Upon cell wall biogenesis defects, AmpC production is increased, which can be measured. In cells treated with the LolCDE-targeting compound, perturbations of the cell wall synthesis are probably due to the compromised transport of the OM lipoproteins LpoA and LpoB, which are essential for the synthesis of peptidoglycan. Unfortunately, a high frequency of resistance was detected and, given the structural similarity between both compound 2 molecules, cross-

resistance was reported. The synthetic pyrrolopyrimidinedione compound G0507, inhibitor of LolCDE, was first discovered in a screen selecting for *E. coli* growth inhibition and σ^E-induction activity [425]. G0507 was shown to cause the build-up of fully processed Lpp in the IM and to stimulate the ATPase activity of LolCDE, likely decoupling the ATPase activity from the lipoprotein-extraction activity of the transporter resulting in erratic and futile ATPase hydrolysis cycles. Given that all three reported LolCDE-inhibitors share a remarkably similar chemical structure, optimization of this scaffold may yield molecules that are more potent and thus more attractive for antibacterial therapy. As it is now, mutations in *lolC*, *lolD*, and *lolE* conferring resistance to these compounds emerge frequently, diminishing the prospects for clinical application.

LolA and LolB are essential in wild-type bacteria and, therefore, are also interesting targets in antimicrobial development. The compound MAC13243 was discovered in a screen for *E. coli* growth inhibition and LolA was identified as a potential target [426]. Accumulation of Lpp at the IM was observed upon treatment and the overexpression of LolA suppressed the killing activity of MAC13243. Furthermore, *in vitro* binding assays also pointed to LolA as the likely target [426]. Another study found that MAC13243 was prone to degradation in aqueous conditions and one of the degradation products, the *S*-(4-chlorobenzyl) isothiourea, was even more active than MAC13243 and it was a close analogue of A22, an inhibitor of the well-characterized target MreB [427]. Overproduction of LolA was again found to increase resistance, restoring the cell growth in the presence of *S*-(4-chlorobenzyl) isothiourea and A22. Moreover, NMR studies confirmed an interaction between the MAC13243 analogues and LolA [427], and increased OM permeability in LolA-depleted cells or MAC13243-treated cells was also reported [428]. Nevertheless, a recent study offered another explanation accounting for the suppressing effect of LolA overexpression upon the lethality of A22-like compounds [429]. The overproduction of LolA was shown to induce the Rcs envelope stress response and in Δ*rcsF* mutants the protective effect from LolA overexpression was lost, raising the possibility of an alternative target.

REFERENCES

1. Silver, L.L., *Challenges of antibacterial discovery.* Clin Microbiol Rev, 2011. **24**(1): p. 71-109.
2. Luepke, K.H., et al., *Past, Present, and Future of Antibacterial Economics: Increasing Bacterial Resistance, Limited Antibiotic Pipeline, and Societal Implications.* Pharmacotherapy, 2017. **37**(1): p. 71-84.
3. WHO, *2019 Antibacterial agents in clinical development: an analysis of the antibacterial clinical development pipeline.* Geneva: World Health Organization, 2019. Licence: CC BY-NC-SA 3.0 IGO.
4. Ventola, C.L., *The antibiotic resistance crisis: part 1: causes and threats.* P T, 2015. **40**(4): p. 277-83.
5. WHO, *Antibacterial agents in preclinical development: an open access database.* Geneva: World Health Organization, 2019. License: CC BY-NC-SA 3.0 IGO.
6. WHO, *Antimicrobial Resistance: Global Report on Surveillance.* Geneva: World Health Organization, 2014.
7. WHO, *Prioritization of pathogens to guide discovery, research and development of new antibiotics for drug resistant bacterial infections, including tuberculosis.* Geneva: World Health Organization, 2017. Licence: CC BY-NC-SA 3.0 IGO.
8. Tacconelli, E., et al., *Discovery, research, and development of new antibiotics: the WHO priority list of antibiotic-resistant bacteria and tuberculosis.* Lancet Infect Dis, 2018. **18**(3): p. 318-327.
9. Kaye, K.S. and J.M. Pogue, *Infections Caused by Resistant Gram-Negative Bacteria: Epidemiology and Management.* Pharmacotherapy, 2015. **35**(10): p. 949-62.
10. Silhavy, T.J., D. Kahne, and S. Walker, *The bacterial cell envelope.* Cold Spring Harb Perspect Biol, 2010. **2**(5): p. a000414.
11. Gupta, R.S., *Protein phylogenies and signature sequences: A reappraisal of evolutionary relationships among archaebacteria, eubacteria, and eukaryotes.* Microbiol Mol Biol Rev, 1998. **62**(4): p. 1435-91.
12. Nikaido, H., *Molecular basis of bacterial outer membrane permeability revisited.* Microbiol Mol Biol Rev, 2003. **67**(4): p. 593-656.
13. Gram, H.C.J., *Über die isolirte Färbung der Schizomyceten in Schnittund Trockenpräparaten.* Fortschritte der Medizin, 1884. **2**: p. 185-189.
14. Green, M.R., J. Sambrook, and J. Sambrook, *Molecular cloning : a laboratory manual*. 4th ed. 2012, Cold Spring Harbor, N.Y.: Cold Spring Harbor Laboratory Press.
15. Blattner, F.R., et al., *The complete genome sequence of Escherichia coli K-12.* Science, 1997. **277**(5331): p. 1453-62.
16. Henderson, J.C., et al., *The Power of Asymmetry: Architecture and Assembly of the Gram-Negative Outer Membrane Lipid Bilayer.* Annu Rev Microbiol, 2016. **70**: p. 255-78.
17. Raetz, C.R. and W. Dowhan, *Biosynthesis and function of phospholipids in Escherichia coli.* J Biol Chem, 1990. **265**(3): p. 1235-8.
18. Luirink, J., et al., *Biogenesis of inner membrane proteins in Escherichia coli.* Biochim Biophys Acta, 2012. **1817**(6): p. 965-76.
19. Vollmer, W., D. Blanot, and M.A. de Pedro, *Peptidoglycan structure and architecture.* FEMS Microbiol Rev, 2008. **32**(2): p. 149-67.
20. Schleifer, K.H. and O. Kandler, *Peptidoglycan types of bacterial cell walls and their taxonomic implications.* Bacteriol Rev, 1972. **36**(4): p. 407-77.
21. Holtje, J.V., *Growth of the stress-bearing and shape-maintaining murein sacculus of Escherichia coli.* Microbiol Mol Biol Rev, 1998. **62**(1): p. 181-203.
22. Matias, V.R., et al., *Cryo-transmission electron microscopy of frozen-hydrated sections of Escherichia coli and Pseudomonas aeruginosa.* J Bacteriol, 2003. **185**(20): p. 6112-8.

23. Braun, V. and U. Sieglin, *The covalent murein-lipoprotein structure of the Escherichia coli cell wall. The attachment site of the lipoprotein on the murein.* Eur J Biochem, 1970. **13**(2): p. 336-46.
24. Braun, V., *Covalent lipoprotein from the outer membrane of Escherichia coli.* Biochim Biophys Acta, 1975. **415**(3): p. 335-77.
25. Asmar, A.T., et al., *Communication across the bacterial cell envelope depends on the size of the periplasm.* PLoS Biol, 2017. **15**(12): p. e2004303.
26. Asmar, A.T. and J.F. Collet, *Lpp, the Braun lipoprotein, turns 50-major achievements and remaining issues.* FEMS Microbiol Lett, 2018. **365**(18).
27. Mathelie-Guinlet, M., et al., *Lipoprotein Lpp regulates the mechanical properties of the E. coli cell envelope.* Nat Commun, 2020. **11**(1): p. 1789.
28. Braun, V., K. Rehn, and H. Wolff, *Supramolecular structure of the rigid layer of the cell wall of Salmonella, Serratia, Proteus, and Pseudomonas fluorescens. Number of lipoprotein molecules in a membrane layer.* Biochemistry, 1970. **9**(26): p. 5041-9.
29. Halegoua, S., A. Hirashima, and M. Inouye, *Existence of a free form of a specific membrane lipoprotein in gram-negative bacteria.* J Bacteriol, 1974. **120**(3): p. 1204-8.
30. Raetz, C.R. and C. Whitfield, *Lipopolysaccharide endotoxins.* Annu Rev Biochem, 2002. **71**: p. 635-700.
31. Grabowicz, M., *Lipoproteins and Their Trafficking to the Outer Membrane.* EcoSal Plus, 2019. **8**(2).
32. Hooda, Y. and T.F. Moraes, *Translocation of lipoproteins to the surface of gram negative bacteria.* Curr Opin Struct Biol, 2018. **51**: p. 73-79.
33. Sonntag, I., et al., *Cell envelope and shape of Escherichia coli: multiple mutants missing the outer membrane lipoprotein and other major outer membrane proteins.* J Bacteriol, 1978. **136**(1): p. 280-5.
34. Wang, Y., *The function of OmpA in Escherichia coli.* Biochem Biophys Res Commun, 2002. **292**(2): p. 396-401.
35. Ishida, H., A. Garcia-Herrero, and H.J. Vogel, *The periplasmic domain of Escherichia coli outer membrane protein A can undergo a localized temperature dependent structural transition.* Biochim Biophys Acta, 2014. **1838**(12): p. 3014-24.
36. Samsudin, F., et al., *OmpA: A Flexible Clamp for Bacterial Cell Wall Attachment.* Structure, 2016. **24**(12): p. 2227-2235.
37. Choi, U. and C.R. Lee, *Distinct Roles of Outer Membrane Porins in Antibiotic Resistance and Membrane Integrity in Escherichia coli.* Front Microbiol, 2019. **10**: p. 953.
38. Fernandez, L. and R.E. Hancock, *Adaptive and mutational resistance: role of porins and efflux pumps in drug resistance.* Clin Microbiol Rev, 2012. **25**(4): p. 661-81.
39. Koebnik, R., K.P. Locher, and P. Van Gelder, *Structure and function of bacterial outer membrane proteins: barrels in a nutshell.* Mol Microbiol, 2000. **37**(2): p. 239-53.
40. Li, X.Z., P. Plesiat, and H. Nikaido, *The challenge of efflux-mediated antibiotic resistance in Gram-negative bacteria.* Clin Microbiol Rev, 2015. **28**(2): p. 337-418.
41. Delcour, A.H., *Outer membrane permeability and antibiotic resistance.* Biochim Biophys Acta, 2009. **1794**(5): p. 808-16.
42. Mach, T., et al., *Facilitated permeation of antibiotics across membrane channels--interaction of the quinolone moxifloxacin with the OmpF channel.* J Am Chem Soc, 2008. **130**(40): p. 13301-9.
43. Jaffe, A., Y.A. Chabbert, and O. Semonin, *Role of porin proteins OmpF and OmpC in the permeation of beta-lactams.* Antimicrob Agents Chemother, 1982. **22**(6): p. 942-8.
44. Perilli, M., et al., *In vitro selection and characterization of mutants in TEM-1-producing Escherichia coli by ceftazidime and ceftibuten.* J Chemother, 2007. **19**(2): p. 123-6.
45. Low, A.S., et al., *Protected environments allow parallel evolution of a bacterial pathogen in a patient subjected to long-term antibiotic therapy.* Mol Microbiol, 2001. **42**(3): p. 619-30.

46. Lou, H., et al., *Altered antibiotic transport in OmpC mutants isolated from a series of clinical strains of multi-drug resistant E. coli.* PLoS One, 2011. **6**(10): p. e25825.
47. Smani, Y., et al., *Role of OmpA in the multidrug resistance phenotype of Acinetobacter baumannii.* Antimicrob Agents Chemother, 2014. **58**(3): p. 1806-8.
48. Lister, P.D., D.J. Wolter, and N.D. Hanson, *Antibacterial-resistant Pseudomonas aeruginosa: clinical impact and complex regulation of chromosomally encoded resistance mechanisms.* Clin Microbiol Rev, 2009. **22**(4): p. 582-610.
49. Masi, M., et al., *Mechanisms of envelope permeability and antibiotic influx and efflux in Gram-negative bacteria.* Nat Microbiol, 2017. **2**: p. 17001.
50. Zgurskaya, H.I., et al., *Trans-envelope multidrug efflux pumps of Gram-negative bacteria and their synergism with the outer membrane barrier.* Res Microbiol, 2018. **169**(7-8): p. 351-356.
51. Krishnamoorthy, G., et al., *Synergy between Active Efflux and Outer Membrane Diffusion Defines Rules of Antibiotic Permeation into Gram-Negative Bacteria.* mBio, 2017. **8**(5).
52. Westfall, D.A., et al., *Bifurcation kinetics of drug uptake by Gram-negative bacteria.* PLoS One, 2017. **12**(9): p. e0184671.
53. Wright, G.D., *Bacterial resistance to antibiotics: enzymatic degradation and modification.* Adv Drug Deliv Rev, 2005. **57**(10): p. 1451-70.
54. Ruppe, E., P.L. Woerther, and F. Barbier, *Mechanisms of antimicrobial resistance in Gram-negative bacilli.* Ann Intensive Care, 2015. **5**(1): p. 61.
55. Sun, J., et al., *Plasmid-encoded tet(X) genes that confer high-level tigecycline resistance in Escherichia coli.* Nat Microbiol, 2019. **4**(9): p. 1457-1464.
56. He, T., et al., *Emergence of plasmid-mediated high-level tigecycline resistance genes in animals and humans.* Nat Microbiol, 2019. **4**(9): p. 1450-1456.
57. Sirot, J., et al., *Klebsiella pneumoniae and other Enterobacteriaceae producing novel plasmid-mediated beta-lactamases markedly active against third-generation cephalosporins: epidemiologic studies.* Rev Infect Dis, 1988. **10**(4): p. 850-9.
58. Nordmann, P., T. Naas, and L. Poirel, *Global spread of Carbapenemase-producing Enterobacteriaceae.* Emerg Infect Dis, 2011. **17**(10): p. 1791-8.
59. Logan, L.K. and R.A. Weinstein, *The Epidemiology of Carbapenem-Resistant Enterobacteriaceae: The Impact and Evolution of a Global Menace.* J Infect Dis, 2017. **215**(suppl_1): p. S28-S36.
60. Peleg, A.Y. and D.C. Hooper, *Hospital-acquired infections due to gram-negative bacteria.* N Engl J Med, 2010. **362**(19): p. 1804-13.
61. Brogden, K.A., *Antimicrobial peptides: pore formers or metabolic inhibitors in bacteria?* Nat Rev Microbiol, 2005. **3**(3): p. 238-50.
62. Giamarellou, H., *Epidemiology of infections caused by polymyxin-resistant pathogens.* Int J Antimicrob Agents, 2016. **48**(6): p. 614-621.
63. Olaitan, A.O., S. Morand, and J.M. Rolain, *Mechanisms of polymyxin resistance: acquired and intrinsic resistance in bacteria.* Front Microbiol, 2014. **5**: p. 643.
64. Moffatt, J.H., et al., *Colistin resistance in Acinetobacter baumannii is mediated by complete loss of lipopolysaccharide production.* Antimicrob Agents Chemother, 2010. **54**(12): p. 4971-7.
65. Moffatt, J.H., et al., *Insertion sequence ISAba11 is involved in colistin resistance and loss of lipopolysaccharide in Acinetobacter baumannii.* Antimicrob Agents Chemother, 2011. **55**(6): p. 3022-4.
66. Liu, Y.Y., et al., *Emergence of plasmid-mediated colistin resistance mechanism MCR-1 in animals and human beings in China: a microbiological and molecular biological study.* Lancet Infect Dis, 2016. **16**(2): p. 161-8.
67. Nang, S.C., J. Li, and T. Velkov, *The rise and spread of mcr plasmid-mediated polymyxin resistance.* Crit Rev Microbiol, 2019. **45**(2): p. 131-161.

68. Eichenberger, E.M. and J.T. Thaden, *Epidemiology and Mechanisms of Resistance of Extensively Drug Resistant Gram-Negative Bacteria.* Antibiotics (Basel), 2019. **8**(2).
69. Silver, L.L., *Multi-targeting by monotherapeutic antibacterials.* Nat Rev Drug Discov, 2007. **6**(1): p. 41-55.
70. Koulenti, D., et al., *Infections by multidrug-resistant Gram-negative Bacteria: What's new in our arsenal and what's in the pipeline?* Int J Antimicrob Agents, 2019. **53**(3): p. 211-224.
71. *The Pew Charitable Trusts. Antibiotics Currently in Global Clinical Development: https://www.pewtrusts.org/en/research-and-analysis/data-visualizations/2014/antibiotics-currently-in-clinical-development*. (accessed on 24/04/2020).
72. Tehrani, K. and N.I. Martin, *beta-lactam/beta-lactamase inhibitor combinations: an update.* Medchemcomm, 2018. **9**(9): p. 1439-1456.
73. Ehmann, D.E., et al., *Avibactam is a covalent, reversible, non-beta-lactam beta-lactamase inhibitor.* Proc Natl Acad Sci U S A, 2012. **109**(29): p. 11663-8.
74. Cahill, S.T., et al., *Cyclic Boronates Inhibit All Classes of beta-Lactamases.* Antimicrob Agents Chemother, 2017. **61**(4).
75. Zhanel, G.G., et al., *Comparison of the next-generation aminoglycoside plazomicin to gentamicin, tobramycin and amikacin.* Expert Rev Anti Infect Ther, 2012. **10**(4): p. 459-73.
76. Livermore, D.M., et al., *Activity of aminoglycosides, including ACHN-490, against carbapenem-resistant Enterobacteriaceae isolates.* J Antimicrob Chemother, 2011. **66**(1): p. 48-53.
77. Fleischmann, W.A., K.E. Greenwood-Quaintance, and R. Patel, *In Vitro Activity of Plazomicin Compared to Amikacin, Gentamicin, and Tobramycin against Multidrug-Resistant Aerobic Gram-Negative Bacilli.* Antimicrob Agents Chemother, 2020. **64**(2).
78. Lee, Y.R. and C.E. Burton, *Eravacycline, a newly approved fluorocycline.* Eur J Clin Microbiol Infect Dis, 2019. **38**(10): p. 1787-1794.
79. Sutcliffe, J.A., et al., *Antibacterial activity of eravacycline (TP-434), a novel fluorocycline, against hospital and community pathogens.* Antimicrob Agents Chemother, 2013. **57**(11): p. 5548-58.
80. Dobias, J., et al., *Activity of the novel siderophore cephalosporin cefiderocol against multidrug-resistant Gram-negative pathogens.* Eur J Clin Microbiol Infect Dis, 2017. **36**(12): p. 2319-2327.
81. Kazmierczak, K.M., et al., *In vitro activity of cefiderocol, a siderophore cephalosporin, against a recent collection of clinically relevant carbapenem-non-susceptible Gram-negative bacilli, including serine carbapenemase- and metallo-beta-lactamase-producing isolates (SIDERO-WT-2014 Study).* Int J Antimicrob Agents, 2019. **53**(2): p. 177-184.
82. Konovalova, A., D.E. Kahne, and T.J. Silhavy, *Outer Membrane Biogenesis.* Annu Rev Microbiol, 2017. **71**: p. 539-556.
83. Choi, U. and C.R. Lee, *Antimicrobial Agents That Inhibit the Outer Membrane Assembly Machines of Gram-Negative Bacteria.* J Microbiol Biotechnol, 2019. **29**(1): p. 1-10.
84. Raetz, C.R., et al., *Lipid A modification systems in gram-negative bacteria.* Annu Rev Biochem, 2007. **76**: p. 295-329.
85. Wilkinson, S.G., *Bacterial lipopolysaccharides--themes and variations.* Prog Lipid Res, 1996. **35**(3): p. 283-343.
86. Amor, K., et al., *Distribution of core oligosaccharide types in lipopolysaccharides from Escherichia coli.* Infect Immun, 2000. **68**(3): p. 1116-24.
87. Qian, J., T.A. Garrett, and C.R. Raetz, *In vitro assembly of the outer core of the lipopolysaccharide from Escherichia coli K-12 and Salmonella typhimurium.* Biochemistry, 2014. **53**(8): p. 1250-62.
88. Wang, L., Q. Wang, and P.R. Reeves, *The variation of O antigens in gram-negative bacteria.* Subcell Biochem, 2010. **53**: p. 123-52.

89. Kalynych, S., R. Morona, and M. Cygler, *Progress in understanding the assembly process of bacterial O-antigen.* FEMS Microbiol Rev, 2014. **38**(5): p. 1048-65.
90. Griffiss, J.M., et al., *The immunochemistry of neisserial LOS.* Antonie Van Leeuwenhoek, 1987. **53**(6): p. 501-7.
91. Peppler, M.S., *Two physically and serologically distinct lipopolysaccharide profiles in strains of Bordetella pertussis and their phenotype variants.* Infect Immun, 1984. **43**(1): p. 224-32.
92. Stevenson, G., et al., *Structure of the O antigen of Escherichia coli K-12 and the sequence of its rfb gene cluster.* J Bacteriol, 1994. **176**(13): p. 4144-56.
93. Steeghs, L., et al., *Meningitis bacterium is viable without endotoxin.* Nature, 1998. **392**(6675): p. 449-50.
94. Peng, D., et al., *Moraxella catarrhalis bacterium without endotoxin, a potential vaccine candidate.* Infect Immun, 2005. **73**(11): p. 7569-77.
95. Lin, L., et al., *Inhibition of LpxC protects mice from resistant Acinetobacter baumannii by modulating inflammation and enhancing phagocytosis.* mBio, 2012. **3**(5).
96. Zhang, G., T.C. Meredith, and D. Kahne, *On the essentiality of lipopolysaccharide to Gram-negative bacteria.* Curr Opin Microbiol, 2013. **16**(6): p. 779-85.
97. Ried, G., I. Hindennach, and U. Henning, *Role of lipopolysaccharide in assembly of Escherichia coli outer membrane proteins OmpA, OmpC, and OmpF.* J Bacteriol, 1990. **172**(10): p. 6048-53.
98. Schindler, H. and J.P. Rosenbusch, *Matrix protein in planar membranes: clusters of channels in a native environment and their functional reassembly.* Proc Natl Acad Sci U S A, 1981. **78**(4): p. 2302-6.
99. Kramer, R.A., et al., *Lipopolysaccharide regions involved in the activation of Escherichia coli outer membrane protease OmpT.* Eur J Biochem, 2002. **269**(6): p. 1746-52.
100. Miller, S.I., R.K. Ernst, and M.W. Bader, *LPS, TLR4 and infectious disease diversity.* Nat Rev Microbiol, 2005. **3**(1): p. 36-46.
101. Needham, B.D. and M.S. Trent, *Fortifying the barrier: the impact of lipid A remodelling on bacterial pathogenesis.* Nat Rev Microbiol, 2013. **11**(7): p. 467-81.
102. Ryu, J.K., et al., *Reconstruction of LPS Transfer Cascade Reveals Structural Determinants within LBP, CD14, and TLR4-MD2 for Efficient LPS Recognition and Transfer.* Immunity, 2017. **46**(1): p. 38-50.
103. Agnese, D.M., et al., *Human toll-like receptor 4 mutations but not CD14 polymorphisms are associated with an increased risk of gram-negative infections.* J Infect Dis, 2002. **186**(10): p. 1522-5.
104. Faber, J., et al., *A toll-like receptor 4 variant is associated with fatal outcome in children with invasive meningococcal disease.* Acta Paediatr, 2009. **98**(3): p. 548-52.
105. Lorenz, E., et al., *Relevance of mutations in the TLR4 receptor in patients with gram-negative septic shock.* Arch Intern Med, 2002. **162**(9): p. 1028-32.
106. Harvey, M. and G. Cave, *Co-administration of phospholipid emulsion with first dose bacteriocidal antibiotic may retard progression of the sepsis response in gram negative septicaemia.* Med Hypotheses, 2014. **83**(5): p. 563-5.
107. Kunsmann, L., et al., *Virulence from vesicles: Novel mechanisms of host cell injury by Escherichia coli O104:H4 outbreak strain.* Sci Rep, 2015. **5**: p. 13252.
108. Simpson, B.W. and M.S. Trent, *Pushing the envelope: LPS modifications and their consequences.* Nat Rev Microbiol, 2019. **17**(7): p. 403-416.
109. Park, B.S., et al., *The structural basis of lipopolysaccharide recognition by the TLR4-MD-2 complex.* Nature, 2009. **458**(7242): p. 1191-5.
110. Cullen, T.W., et al., *Helicobacter pylori versus the host: remodeling of the bacterial outer membrane is required for survival in the gastric mucosa.* PLoS Pathog, 2011. **7**(12): p. e1002454.

111. Mejias-Luque, R. and M. Gerhard, *Immune Evasion Strategies and Persistence of Helicobacter pylori.* Curr Top Microbiol Immunol, 2017. **400**: p. 53-71.
112. Ernst, R.K., et al., *Pseudomonas aeruginosa lipid A diversity and its recognition by Toll-like receptor 4.* J Endotoxin Res, 2003. **9**(6): p. 395-400.
113. Ernst, R.K., et al., *Unique lipid a modifications in Pseudomonas aeruginosa isolated from the airways of patients with cystic fibrosis.* J Infect Dis, 2007. **196**(7): p. 1088-92.
114. Pluschke, G., et al., *Role of the capsule and the O antigen in resistance of O18:K1 Escherichia coli to complement-mediated killing.* Infect Immun, 1983. **42**(3): p. 907-13.
115. Saldias, M.S., X. Ortega, and M.A. Valvano, *Burkholderia cenocepacia O antigen lipopolysaccharide prevents phagocytosis by macrophages and adhesion to epithelial cells.* J Med Microbiol, 2009. **58**(Pt 12): p. 1542-1548.
116. Murray, G.L., S.R. Attridge, and R. Morona, *Altering the length of the lipopolysaccharide O antigen has an impact on the interaction of Salmonella enterica serovar Typhimurium with macrophages and complement.* J Bacteriol, 2006. **188**(7): p. 2735-9.
117. Bogomolnaya, L.M., et al., *'Form variation' of the O12 antigen is critical for persistence of Salmonella Typhimurium in the murine intestine.* Mol Microbiol, 2008. **70**(5): p. 1105-19.
118. Duerr, C.U., et al., *O-antigen delays lipopolysaccharide recognition and impairs antibacterial host defense in murine intestinal epithelial cells.* PLoS Pathog, 2009. **5**(9): p. e1000567.
119. DebRoy, C., E. Roberts, and P.M. Fratamico, *Detection of O antigens in Escherichia coli.* Anim Health Res Rev, 2011. **12**(2): p. 169-85.
120. Iguchi, A., et al., *A complete view of the genetic diversity of the Escherichia coli O-antigen biosynthesis gene cluster.* DNA Res, 2015. **22**(1): p. 101-7.
121. Bertani, B. and N. Ruiz, *Function and Biogenesis of Lipopolysaccharides.* EcoSal Plus, 2018. **8**(1).
122. Raetz, C.R., et al., *Discovery of new biosynthetic pathways: the lipid A story.* J Lipid Res, 2009. **50 Suppl**: p. S103-8.
123. Anderson, M.S. and C.R. Raetz, *Biosynthesis of lipid A precursors in Escherichia coli. A cytoplasmic acyltransferase that converts UDP-N-acetylglucosamine to UDP-3-O-(R-3-hydroxymyristoyl)-N-acetylglucosamine.* J Biol Chem, 1987. **262**(11): p. 5159-69.
124. Anderson, M.S., et al., *UDP-N-acetylglucosamine acyltransferase of Escherichia coli. The first step of endotoxin biosynthesis is thermodynamically unfavorable.* J Biol Chem, 1993. **268**(26): p. 19858-65.
125. Young, K., et al., *The envA permeability/cell division gene of Escherichia coli encodes the second enzyme of lipid A biosynthesis. UDP-3-O-(R-3-hydroxymyristoyl)-N-acetylglucosamine deacetylase.* J Biol Chem, 1995. **270**(51): p. 30384-91.
126. Ogura, T., et al., *Balanced biosynthesis of major membrane components through regulated degradation of the committed enzyme of lipid A biosynthesis by the AAA protease FtsH (HflB) in Escherichia coli.* Mol Microbiol, 1999. **31**(3): p. 833-44.
127. Klein, G., et al., *Assembly of lipopolysaccharide in Escherichia coli requires the essential LapB heat shock protein.* J Biol Chem, 2014. **289**(21): p. 14829-53.
128. Kelly, T.M., et al., *The firA gene of Escherichia coli encodes UDP-3-O-(R-3-hydroxymyristoyl)-glucosamine N-acyltransferase. The third step of endotoxin biosynthesis.* J Biol Chem, 1993. **268**(26): p. 19866-74.
129. Bartling, C.M. and C.R. Raetz, *Steady-state kinetics and mechanism of LpxD, the N-acyltransferase of lipid A biosynthesis.* Biochemistry, 2008. **47**(19): p. 5290-302.
130. Babinski, K.J., S.J. Kanjilal, and C.R. Raetz, *Accumulation of the lipid A precursor UDP-2,3-diacylglucosamine in an Escherichia coli mutant lacking the lpxH gene.* J Biol Chem, 2002. **277**(29): p. 25947-56.
131. Radika, K. and C.R. Raetz, *Purification and properties of lipid A disaccharide synthase of Escherichia coli.* J Biol Chem, 1988. **263**(29): p. 14859-67.

132. Ray, B.L. and C.R. Raetz, *The biosynthesis of gram-negative endotoxin. A novel kinase in Escherichia coli membranes that incorporates the 4'-phosphate of lipid A.* J Biol Chem, 1987. **262**(3): p. 1122-8.
133. Belunis, C.J. and C.R. Raetz, *Biosynthesis of endotoxins. Purification and catalytic properties of 3-deoxy-D-manno-octulosonic acid transferase from Escherichia coli.* J Biol Chem, 1992. **267**(14): p. 9988-97.
134. Brozek, K.A. and C.R. Raetz, *Biosynthesis of lipid A in Escherichia coli. Acyl carrier protein-dependent incorporation of laurate and myristate.* J Biol Chem, 1990. **265**(26): p. 15410-7.
135. Clementz, T., J.J. Bednarski, and C.R. Raetz, *Function of the htrB high temperature requirement gene of Escherichia coli in the acylation of lipid A: HtrB catalyzed incorporation of laurate.* J Biol Chem, 1996. **271**(20): p. 12095-102.
136. Clementz, T., Z. Zhou, and C.R. Raetz, *Function of the Escherichia coli msbB gene, a multicopy suppressor of htrB knockouts, in the acylation of lipid A. Acylation by MsbB follows laurate incorporation by HtrB.* J Biol Chem, 1997. **272**(16): p. 10353-60.
137. Heinrichs, D.E., J.A. Yethon, and C. Whitfield, *Molecular basis for structural diversity in the core regions of the lipopolysaccharides of Escherichia coli and Salmonella enterica.* Mol Microbiol, 1998. **30**(2): p. 221-32.
138. Whitfield, C., N. Kaniuk, and E. Frirdich, *Molecular insights into the assembly and diversity of the outer core oligosaccharide in lipopolysaccharides from Escherichia coli and Salmonella.* J Endotoxin Res, 2003. **9**(4): p. 244-9.
139. Polissi, A. and C. Georgopoulos, *Mutational analysis and properties of the msbA gene of Escherichia coli, coding for an essential ABC family transporter.* Mol Microbiol, 1996. **20**(6): p. 1221-33.
140. Zhou, Z., et al., *Function of Escherichia coli MsbA, an essential ABC family transporter, in lipid A and phospholipid biosynthesis.* J Biol Chem, 1998. **273**(20): p. 12466-75.
141. Sorensen, P.G., et al., *Regulation of UDP-3-O-[R-3-hydroxymyristoyl]-N-acetylglucosamine deacetylase in Escherichia coli. The second enzymatic step of lipid a biosynthesis.* J Biol Chem, 1996. **271**(42): p. 25898-905.
142. Bittner, L.M., J. Arends, and F. Narberhaus, *When, how and why? Regulated proteolysis by the essential FtsH protease in Escherichia coli.* Biol Chem, 2017. **398**(5-6): p. 625-635.
143. Katz, C. and E.Z. Ron, *Dual role of FtsH in regulating lipopolysaccharide biosynthesis in Escherichia coli.* J Bacteriol, 2008. **190**(21): p. 7117-22.
144. Schakermann, M., S. Langklotz, and F. Narberhaus, *FtsH-mediated coordination of lipopolysaccharide biosynthesis in Escherichia coli correlates with the growth rate and the alarmone (p)ppGpp.* J Bacteriol, 2013. **195**(9): p. 1912-9.
145. Mahalakshmi, S., et al., *yciM is an essential gene required for regulation of lipopolysaccharide synthesis in Escherichia coli.* Mol Microbiol, 2014. **91**(1): p. 145-57.
146. Nicolaes, V., et al., *Insights into the function of YciM, a heat shock membrane protein required to maintain envelope integrity in Escherichia coli.* J Bacteriol, 2014. **196**(2): p. 300-9.
147. Dalebroux, Z.D., et al., *Delivery of cardiolipins to the Salmonella outer membrane is necessary for survival within host tissues and virulence.* Cell Host Microbe, 2015. **17**(4): p. 441-51.
148. Rossi, R.M., et al., *Cardiolipin Synthesis and Outer Membrane Localization Are Required for Shigella flexneri Virulence.* mBio, 2017. **8**(4).
149. Guest, R.L., et al., *YejM Modulates Activity of the YciM/FtsH Protease Complex To Prevent Lethal Accumulation of Lipopolysaccharide.* mBio, 2020. **11**(2).
150. Fivenson, E.M. and T.G. Bernhardt, *An Essential Membrane Protein Modulates the Proteolysis of LpxC to Control Lipopolysaccharide Synthesis in Escherichia coli.* mBio, 2020. **11**(3).
151. Nguyen, D., et al., *YejM Controls LpxC Levels by Regulating Protease Activity of the FtsH/YciM Complex of Escherichia coli.* J Bacteriol, 2020. **202**(18).
152. Clairfeuille, T., et al., *Structure of the essential inner membrane lipopolysaccharide-PbgA complex.* Nature, 2020. **584**(7821): p. 479-483.

153. Thomas, C. and R. Tampe, *Multifaceted structures and mechanisms of ABC transport systems in health and disease.* Curr Opin Struct Biol, 2018. **51**: p. 116-128.
154. Karow, M. and C. Georgopoulos, *The essential Escherichia coli msbA gene, a multicopy suppressor of null mutations in the htrB gene, is related to the universally conserved family of ATP-dependent translocators.* Mol Microbiol, 1993. **7**(1): p. 69-79.
155. Doerrler, W.T., H.S. Gibbons, and C.R. Raetz, *MsbA-dependent translocation of lipids across the inner membrane of Escherichia coli.* J Biol Chem, 2004. **279**(43): p. 45102-9.
156. Ward, A., et al., *Flexibility in the ABC transporter MsbA: Alternating access with a twist.* Proc Natl Acad Sci U S A, 2007. **104**(48): p. 19005-10.
157. Davidson, A.L., et al., *Structure, function, and evolution of bacterial ATP-binding cassette systems.* Microbiol Mol Biol Rev, 2008. **72**(2): p. 317-64, table of contents.
158. Mi, W., et al., *Structural basis of MsbA-mediated lipopolysaccharide transport.* Nature, 2017. **549**(7671): p. 233-237.
159. Ho, H., et al., *Structural basis for dual-mode inhibition of the ABC transporter MsbA.* Nature, 2018. **557**(7704): p. 196-201.
160. Gronow, S. and H. Brade, *Lipopolysaccharide biosynthesis: which steps do bacteria need to survive?* J Endotoxin Res, 2001. **7**(1): p. 3-23.
161. Meredith, T.C., et al., *Redefining the requisite lipopolysaccharide structure in Escherichia coli.* ACS Chem Biol, 2006. **1**(1): p. 33-42.
162. Mamat, U., et al., *Single amino acid substitutions in either YhjD or MsbA confer viability to 3-deoxy-d-manno-oct-2-ulosonic acid-depleted Escherichia coli.* Mol Microbiol, 2008. **67**(3): p. 633-48.
163. Klein, G., et al., *Escherichia coli K-12 Suppressor-free Mutants Lacking Early Glycosyltransferases and Late Acyltransferases: minimal lipopolysaccharide structure and induction of envelope stress response.* J Biol Chem, 2009. **284**(23): p. 15369-89.
164. Reynolds, C.M. and C.R. Raetz, *Replacement of lipopolysaccharide with free lipid A molecules in Escherichia coli mutants lacking all core sugars.* Biochemistry, 2009. **48**(40): p. 9627-40.
165. Reuter, G., et al., *The ATP binding cassette multidrug transporter LmrA and lipid transporter MsbA have overlapping substrate specificities.* J Biol Chem, 2003. **278**(37): p. 35193-8.
166. Woebking, B., et al., *Drug-lipid A interactions on the Escherichia coli ABC transporter MsbA.* J Bacteriol, 2005. **187**(18): p. 6363-9.
167. Siarheyeva, A. and F.J. Sharom, *The ABC transporter MsbA interacts with lipid A and amphipathic drugs at different sites.* Biochem J, 2009. **419**(2): p. 317-28.
168. Prost, L.R. and S.I. Miller, *The Salmonellae PhoQ sensor: mechanisms of detection of phagosome signals.* Cell Microbiol, 2008. **10**(3): p. 576-82.
169. Chen, H.D. and E.A. Groisman, *The biology of the PmrA/PmrB two-component system: the major regulator of lipopolysaccharide modifications.* Annu Rev Microbiol, 2013. **67**: p. 83-112.
170. Fernandez, L., et al., *Adaptive resistance to the "last hope" antibiotics polymyxin B and colistin in Pseudomonas aeruginosa is mediated by the novel two-component regulatory system ParR-ParS.* Antimicrob Agents Chemother, 2010. **54**(8): p. 3372-82.
171. Nowicki, E.M., et al., *Extracellular zinc induces phosphoethanolamine addition to Pseudomonas aeruginosa lipid A via the ColRS two-component system.* Mol Microbiol, 2015. **97**(1): p. 166-78.
172. Fernandez, L., et al., *The two-component system CprRS senses cationic peptides and triggers adaptive resistance in Pseudomonas aeruginosa independently of ParRS.* Antimicrob Agents Chemother, 2012. **56**(12): p. 6212-22.
173. Dalebroux, Z.D. and S.I. Miller, *Salmonellae PhoPQ regulation of the outer membrane to resist innate immunity.* Curr Opin Microbiol, 2014. **17**: p. 106-13.
174. Bader, M.W., et al., *Recognition of antimicrobial peptides by a bacterial sensor kinase.* Cell, 2005. **122**(3): p. 461-72.

175. Choi, J. and E.A. Groisman, *Acidic pH sensing in the bacterial cytoplasm is required for Salmonella virulence.* Mol Microbiol, 2016. **101**(6): p. 1024-38.
176. Choi, J. and E.A. Groisman, *Activation of master virulence regulator PhoP in acidic pH requires the Salmonella-specific protein UgtL.* Sci Signal, 2017. **10**(494).
177. Bishop, R.E., et al., *Transfer of palmitate from phospholipids to lipid A in outer membranes of gram-negative bacteria.* EMBO J, 2000. **19**(19): p. 5071-80.
178. Reynolds, C.M., et al., *An outer membrane enzyme encoded by Salmonella typhimurium lpxR that removes the 3'-acyloxyacyl moiety of lipid A.* J Biol Chem, 2006. **281**(31): p. 21974-87.
179. Trent, M.S., et al., *A PhoP/PhoQ-induced Lipase (PagL) that catalyzes 3-O-deacylation of lipid A precursors in membranes of Salmonella typhimurium.* J Biol Chem, 2001. **276**(12): p. 9083-92.
180. Kawasaki, K., R.K. Ernst, and S.I. Miller, *Inhibition of Salmonella enterica serovar Typhimurium lipopolysaccharide deacylation by aminoarabinose membrane modification.* J Bacteriol, 2005. **187**(7): p. 2448-57.
181. Kox, L.F., M.M. Wosten, and E.A. Groisman, *A small protein that mediates the activation of a two-component system by another two-component system.* EMBO J, 2000. **19**(8): p. 1861-72.
182. Kato, A. and E.A. Groisman, *Connecting two-component regulatory systems by a protein that protects a response regulator from dephosphorylation by its cognate sensor.* Genes Dev, 2004. **18**(18): p. 2302-13.
183. Rubin, E.J., et al., *PmrD is required for modifications to escherichia coli endotoxin that promote antimicrobial resistance.* Antimicrob Agents Chemother, 2015. **59**(4): p. 2051-61.
184. Perez, J.C. and E.A. Groisman, *Acid pH activation of the PmrA/PmrB two-component regulatory system of Salmonella enterica.* Mol Microbiol, 2007. **63**(1): p. 283-93.
185. Wosten, M.M., et al., *A signal transduction system that responds to extracellular iron.* Cell, 2000. **103**(1): p. 113-25.
186. Trent, M.S., et al., *An inner membrane enzyme in Salmonella and Escherichia coli that transfers 4-amino-4-deoxy-L-arabinose to lipid A: induction on polymyxin-resistant mutants and role of a novel lipid-linked donor.* J Biol Chem, 2001. **276**(46): p. 43122-31.
187. Lee, H., et al., *The PmrA-regulated pmrC gene mediates phosphoethanolamine modification of lipid A and polymyxin resistance in Salmonella enterica.* J Bacteriol, 2004. **186**(13): p. 4124-33.
188. Kato, A., et al., *Reciprocal control between a bacterium's regulatory system and the modification status of its lipopolysaccharide.* Mol Cell, 2012. **47**(6): p. 897-908.
189. Herrera, C.M., J.V. Hankins, and M.S. Trent, *Activation of PmrA inhibits LpxT-dependent phosphorylation of lipid A promoting resistance to antimicrobial peptides.* Mol Microbiol, 2010. **76**(6): p. 1444-60.
190. Lippa, A.M. and M. Goulian, *Feedback inhibition in the PhoQ/PhoP signaling system by a membrane peptide.* PLoS Genet, 2009. **5**(12): p. e1000788.
191. Moon, K. and S. Gottesman, *A PhoQ/P-regulated small RNA regulates sensitivity of Escherichia coli to antimicrobial peptides.* Mol Microbiol, 2009. **74**(6): p. 1314-30.
192. Coornaert, A., et al., *MicA sRNA links the PhoP regulon to cell envelope stress.* Mol Microbiol, 2010. **76**(2): p. 467-79.
193. Kanipes, M.I., et al., *Ca2+-induced phosphoethanolamine transfer to the outer 3-deoxy-D-manno-octulosonic acid moiety of Escherichia coli lipopolysaccharide. A novel membrane enzyme dependent upon phosphatidylethanolamine.* J Biol Chem, 2001. **276**(2): p. 1156-63.
194. Reynolds, C.M., et al., *A phosphoethanolamine transferase specific for the outer 3-deoxy-D-manno-octulosonic acid residue of Escherichia coli lipopolysaccharide. Identification of the eptB gene and Ca2+ hypersensitivity of an eptB deletion mutant.* J Biol Chem, 2005. **280**(22): p. 21202-11.
195. Murata, T., et al., *PhoPQ-mediated regulation produces a more robust permeability barrier in the outer membrane of Salmonella enterica serovar typhimurium.* J Bacteriol, 2007. **189**(20): p. 7213-22.

196. Gibbons, H.S., et al., *Oxygen requirement for the biosynthesis of the S-2-hydroxymyristate moiety in Salmonella typhimurium lipid A. Function of LpxO, A new Fe2+/alpha-ketoglutarate-dependent dioxygenase homologue.* J Biol Chem, 2000. **275**(42): p. 32940-9.
197. Gibbons, H.S., et al., *An inner membrane dioxygenase that generates the 2-hydroxymyristate moiety of Salmonella lipid A.* Biochemistry, 2008. **47**(9): p. 2814-25.
198. Fernandez, P.A., et al., *Fnr and ArcA Regulate Lipid A Hydroxylation in Salmonella Enteritidis by Controlling lpxO Expression in Response to Oxygen Availability.* Front Microbiol, 2018. **9**: p. 1220.
199. Sampson, B.A., R. Misra, and S.A. Benson, *Identification and characterization of a new gene of Escherichia coli K-12 involved in outer membrane permeability.* Genetics, 1989. **122**(3): p. 491-501.
200. Braun, M. and T.J. Silhavy, *Imp/OstA is required for cell envelope biogenesis in Escherichia coli.* Mol Microbiol, 2002. **45**(5): p. 1289-302.
201. Bos, M.P., et al., *Identification of an outer membrane protein required for the transport of lipopolysaccharide to the bacterial cell surface.* Proc Natl Acad Sci U S A, 2004. **101**(25): p. 9417-22.
202. Wu, T., et al., *Identification of a protein complex that assembles lipopolysaccharide in the outer membrane of Escherichia coli.* Proc Natl Acad Sci U S A, 2006. **103**(31): p. 11754-9.
203. Sperandeo, P., et al., *Characterization of lptA and lptB, two essential genes implicated in lipopolysaccharide transport to the outer membrane of Escherichia coli.* J Bacteriol, 2007. **189**(1): p. 244-53.
204. Tran, A.X., M.S. Trent, and C. Whitfield, *The LptA protein of Escherichia coli is a periplasmic lipid A-binding protein involved in the lipopolysaccharide export pathway.* J Biol Chem, 2008. **283**(29): p. 20342-9.
205. Sperandeo, P., et al., *Functional analysis of the protein machinery required for transport of lipopolysaccharide to the outer membrane of Escherichia coli.* J Bacteriol, 2008. **190**(13): p. 4460-9.
206. Ruiz, N., et al., *Identification of two inner-membrane proteins required for the transport of lipopolysaccharide to the outer membrane of Escherichia coli.* Proc Natl Acad Sci U S A, 2008. **105**(14): p. 5537-42.
207. Narita, S. and H. Tokuda, *Biochemical characterization of an ABC transporter LptBFGC complex required for the outer membrane sorting of lipopolysaccharides.* FEBS Lett, 2009. **583**(13): p. 2160-4.
208. Chng, S.S., et al., *Characterization of the two-protein complex in Escherichia coli responsible for lipopolysaccharide assembly at the outer membrane.* Proc Natl Acad Sci U S A, 2010. **107**(12): p. 5363-8.
209. Chng, S.S., L.S. Gronenberg, and D. Kahne, *Proteins required for lipopolysaccharide assembly in Escherichia coli form a transenvelope complex.* Biochemistry, 2010. **49**(22): p. 4565-7.
210. Chimalakonda, G., et al., *Lipoprotein LptE is required for the assembly of LptD by the beta-barrel assembly machine in the outer membrane of Escherichia coli.* Proc Natl Acad Sci U S A, 2011. **108**(6): p. 2492-7.
211. Sherman, D.J., et al., *Lipopolysaccharide is transported to the cell surface by a membrane-to-membrane protein bridge.* Science, 2018. **359**(6377): p. 798-801.
212. Okuda, S., E. Freinkman, and D. Kahne, *Cytoplasmic ATP hydrolysis powers transport of lipopolysaccharide across the periplasm in E. coli.* Science, 2012. **338**(6111): p. 1214-7.
213. Owens, T.W., et al., *Structural basis of unidirectional export of lipopolysaccharide to the cell surface.* Nature, 2019. **567**(7749): p. 550-553.
214. Li, Y., B.J. Orlando, and M. Liao, *Structural basis of lipopolysaccharide extraction by the LptB2FGC complex.* Nature, 2019. **567**(7749): p. 486-490.
215. Sperandeo, P., et al., *New insights into the Lpt machinery for lipopolysaccharide transport to the cell surface: LptA-LptC interaction and LptA stability as sensors of a properly assembled transenvelope complex.* J Bacteriol, 2011. **193**(5): p. 1042-53.

216. Tran, A.X., C. Dong, and C. Whitfield, *Structure and functional analysis of LptC, a conserved membrane protein involved in the lipopolysaccharide export pathway in Escherichia coli.* J Biol Chem, 2010. **285**(43): p. 33529-39.
217. Okuda, S., et al., *Lipopolysaccharide transport and assembly at the outer membrane: the PEZ model.* Nat Rev Microbiol, 2016. **14**(6): p. 337-45.
218. Freinkman, E., S.S. Chng, and D. Kahne, *The complex that inserts lipopolysaccharide into the bacterial outer membrane forms a two-protein plug-and-barrel.* Proc Natl Acad Sci U S A, 2011. **108**(6): p. 2486-91.
219. Dong, H., et al., *Structural basis for outer membrane lipopolysaccharide insertion.* Nature, 2014. **511**(7507): p. 52-6.
220. Qiao, S., et al., *Structural basis for lipopolysaccharide insertion in the bacterial outer membrane.* Nature, 2014. **511**(7507): p. 108-11.
221. Suits, M.D., et al., *Novel structure of the conserved gram-negative lipopolysaccharide transport protein A and mutagenesis analysis.* J Mol Biol, 2008. **380**(3): p. 476-88.
222. Dong, H., et al., *Structural and functional insights into the lipopolysaccharide ABC transporter LptB2FG.* Nat Commun, 2017. **8**(1): p. 222.
223. Luo, Q., et al., *Structural basis for lipopolysaccharide extraction by ABC transporter LptB2FG.* Nat Struct Mol Biol, 2017. **24**(5): p. 469-474.
224. Villa, R., et al., *The Escherichia coli Lpt transenvelope protein complex for lipopolysaccharide export is assembled via conserved structurally homologous domains.* J Bacteriol, 2013. **195**(5): p. 1100-8.
225. Falchi, F.A., et al., *Mutation and Suppressor Analysis of the Essential Lipopolysaccharide Transport Protein LptA Reveals Strategies To Overcome Severe Outer Membrane Permeability Defects in Escherichia coli.* J Bacteriol, 2018. **200**(2).
226. Sperandeo, P., A.M. Martorana, and A. Polissi, *The Lpt ABC transporter for lipopolysaccharide export to the cell surface.* Res Microbiol, 2019. **170**(8): p. 366-373.
227. Botos, I., et al., *Structural and Functional Characterization of the LPS Transporter LptDE from Gram-Negative Pathogens.* Structure, 2016. **24**(6): p. 965-976.
228. Sherman, D.J., et al., *Decoupling catalytic activity from biological function of the ATPase that powers lipopolysaccharide transport.* Proc Natl Acad Sci U S A, 2014. **111**(13): p. 4982-7.
229. Simpson, B.W., et al., *Identification of Residues in the Lipopolysaccharide ABC Transporter That Coordinate ATPase Activity with Extractor Function.* mBio, 2016. **7**(5).
230. May, J.M., et al., *The Antibiotic Novobiocin Binds and Activates the ATPase That Powers Lipopolysaccharide Transport.* J Am Chem Soc, 2017. **139**(48): p. 17221-17224.
231. Freinkman, E., et al., *Regulated assembly of the transenvelope protein complex required for lipopolysaccharide export.* Biochemistry, 2012. **51**(24): p. 4800-6.
232. Martorana, A.M., et al., *Functional Interaction between the Cytoplasmic ABC Protein LptB and the Inner Membrane LptC Protein, Components of the Lipopolysaccharide Transport Machinery in Escherichia coli.* J Bacteriol, 2016. **198**(16): p. 2192-203.
233. Benedet, M., et al., *The Lack of the Essential LptC Protein in the Trans-Envelope Lipopolysaccharide Transport Machine Is Circumvented by Suppressor Mutations in LptF, an Inner Membrane Component of the Escherichia coli Transporter.* PLoS One, 2016. **11**(8): p. e0161354.
234. Hamad, M.A., et al., *Aminoarabinose is essential for lipopolysaccharide export and intrinsic antimicrobial peptide resistance in Burkholderia cenocepacia(dagger).* Mol Microbiol, 2012. **85**(5): p. 962-74.
235. Bertani, B.R., et al., *A cluster of residues in the lipopolysaccharide exporter that selects substrate variants for transport to the outer membrane.* Mol Microbiol, 2018. **109**(4): p. 541-554.
236. Ortega, X.P., et al., *A putative gene cluster for aminoarabinose biosynthesis is essential for Burkholderia cenocepacia viability.* J Bacteriol, 2007. **189**(9): p. 3639-44.

237. Laguri, C., et al., *Interaction of lipopolysaccharides at intermolecular sites of the periplasmic Lpt transport assembly.* Sci Rep, 2017. **7**(1): p. 9715.
238. Schultz, K.M. and C.S. Klug, *Characterization of and lipopolysaccharide binding to the E. coli LptC protein dimer.* Protein Sci, 2018. **27**(2): p. 381-389.
239. Schultz, K.M., T.J. Lundquist, and C.S. Klug, *Lipopolysaccharide binding to the periplasmic protein LptA.* Protein Sci, 2017. **26**(8): p. 1517-1523.
240. Hicks, G. and Z. Jia, *Structural Basis for the Lipopolysaccharide Export Activity of the Bacterial Lipopolysaccharide Transport System.* Int J Mol Sci, 2018. **19**(9).
241. Merten, J.A., K.M. Schultz, and C.S. Klug, *Concentration-dependent oligomerization and oligomeric arrangement of LptA.* Protein Sci, 2012. **21**(2): p. 211-8.
242. Santambrogio, C., et al., *LptA assembles into rod-like oligomers involving disorder-to-order transitions.* J Am Soc Mass Spectrom, 2013. **24**(10): p. 1593-602.
243. Schultz, K.M., J.B. Feix, and C.S. Klug, *Disruption of LptA oligomerization and affinity of the LptA-LptC interaction.* Protein Sci, 2013. **22**(11): p. 1639-45.
244. Martorana, A.M., et al., *Complex transcriptional organization regulates an Escherichia coli locus implicated in lipopolysaccharide biogenesis.* Res Microbiol, 2011. **162**(5): p. 470-82.
245. Ruiz, N., et al., *Nonconsecutive disulfide bond formation in an essential integral outer membrane protein.* Proc Natl Acad Sci U S A, 2010. **107**(27): p. 12245-50.
246. Bos, M.P. and J. Tommassen, *The LptD chaperone LptE is not directly involved in lipopolysaccharide transport in Neisseria meningitidis.* J Biol Chem, 2011. **286**(33): p. 28688-96.
247. Chng, S.S., et al., *Disulfide rearrangement triggered by translocon assembly controls lipopolysaccharide export.* Science, 2012. **337**(6102): p. 1665-8.
248. Grabowicz, M., J. Yeh, and T.J. Silhavy, *Dominant negative lptE mutation that supports a role for LptE as a plug in the LptD barrel.* J Bacteriol, 2013. **195**(6): p. 1327-34.
249. Malojcic, G., et al., *LptE binds to and alters the physical state of LPS to catalyze its assembly at the cell surface.* Proc Natl Acad Sci U S A, 2014. **111**(26): p. 9467-72.
250. Gu, Y., et al., *Lipopolysaccharide is inserted into the outer membrane through an intramembrane hole, a lumen gate, and the lateral opening of LptD.* Structure, 2015. **23**(3): p. 496-504.
251. Li, X., et al., *Trapped lipopolysaccharide and LptD intermediates reveal lipopolysaccharide translocation steps across the Escherichia coli outer membrane.* Sci Rep, 2015. **5**: p. 11883.
252. Xie, R., R.J. Taylor, and D. Kahne, *Outer Membrane Translocon Communicates with Inner Membrane ATPase To Stop Lipopolysaccharide Transport.* J Am Chem Soc, 2018. **140**(40): p. 12691-12694.
253. Dowhan, W., *A retrospective: use of Escherichia coli as a vehicle to study phospholipid synthesis and function.* Biochim Biophys Acta, 2013. **1831**(3): p. 471-94.
254. Shrivastava, R. and S.S. Chng, *Lipid trafficking across the Gram-negative cell envelope.* J Biol Chem, 2019. **294**(39): p. 14175-14184.
255. Demchick, P. and A.L. Koch, *The permeability of the wall fabric of Escherichia coli and Bacillus subtilis.* J Bacteriol, 1996. **178**(3): p. 768-73.
256. Kulp, A. and M.J. Kuehn, *Biological functions and biogenesis of secreted bacterial outer membrane vesicles.* Annu Rev Microbiol, 2010. **64**: p. 163-84.
257. Bayer, M.E., *Areas of adhesion between wall and membrane of Escherichia coli.* J Gen Microbiol, 1968. **53**(3): p. 395-404.
258. Bayer, M.E., *Zones of membrane adhesion in the cryofixed envelope of Escherichia coli.* J Struct Biol, 1991. **107**(3): p. 268-80.
259. Kellenberger, E., *The 'Bayer bridges' confronted with results from improved electron microscopy methods.* Mol Microbiol, 1990. **4**(5): p. 697-705.
260. Hobot, J.A., et al., *Periplasmic gel: new concept resulting from the reinvestigation of bacterial cell envelope ultrastructure by new methods.* J Bacteriol, 1984. **160**(1): p. 143-52.

261. Dubochet, J., et al., *Electron microscopy of frozen-hydrated bacteria.* J Bacteriol, 1983. **155**(1): p. 381-90.
262. Donohue-Rolfe, A.M. and M. Schaechter, *Translocation of phospholipids from the inner to the outer membrane of Escherichia coli.* Proc Natl Acad Sci U S A, 1980. **77**(4): p. 1867-71.
263. Jones, N.C. and M.J. Osborn, *Translocation of phospholipids between the outer and inner membranes of Salmonella typhimurium.* J Biol Chem, 1977. **252**(20): p. 7405-12.
264. Langley, K.E., E. Hawrot, and E.P. Kennedy, *Membrane assembly: movement of phosphatidylserine between the cytoplasmic and outer membranes of Escherichia coli.* J Bacteriol, 1982. **152**(3): p. 1033-41.
265. De Lay, N.R. and J.E. Cronan, *Genetic interaction between the Escherichia coli AcpT phosphopantetheinyl transferase and the YejM inner membrane protein.* Genetics, 2008. **178**(3): p. 1327-37.
266. Shrivastava, R., X. Jiang, and S.S. Chng, *Outer membrane lipid homeostasis via retrograde phospholipid transport in Escherichia coli.* Mol Microbiol, 2017. **106**(3): p. 395-408.
267. Gerding, M.A., et al., *The trans-envelope Tol-Pal complex is part of the cell division machinery and required for proper outer-membrane invagination during cell constriction in E. coli.* Mol Microbiol, 2007. **63**(4): p. 1008-25.
268. Petiti, M., et al., *Tol Energy-Driven Localization of Pal and Anchoring to the Peptidoglycan Promote Outer-Membrane Constriction.* J Mol Biol, 2019. **431**(17): p. 3275-3288.
269. Cascales, E., et al., *Proton motive force drives the interaction of the inner membrane TolA and outer membrane pal proteins in Escherichia coli.* Mol Microbiol, 2000. **38**(4): p. 904-15.
270. Germon, P., et al., *Energy-dependent conformational change in the TolA protein of Escherichia coli involves its N-terminal domain, TolQ, and TolR.* J Bacteriol, 2001. **183**(14): p. 4110-4.
271. Godlewska, R., et al., *Peptidoglycan-associated lipoprotein (Pal) of Gram-negative bacteria: function, structure, role in pathogenesis and potential application in immunoprophylaxis.* FEMS Microbiol Lett, 2009. **298**(1): p. 1-11.
272. Walburger, A., C. Lazdunski, and Y. Corda, *The Tol/Pal system function requires an interaction between the C-terminal domain of TolA and the N-terminal domain of TolB.* Mol Microbiol, 2002. **44**(3): p. 695-708.
273. Nikaido, H., *Restoring permeability barrier function to outer membrane.* Chem Biol, 2005. **12**(5): p. 507-9.
274. Ruiz, N., et al., *Probing the barrier function of the outer membrane with chemical conditionality.* ACS Chem Biol, 2006. **1**(6): p. 385-95.
275. Dekker, N., *Outer-membrane phospholipase A: known structure, unknown biological function.* Mol Microbiol, 2000. **35**(4): p. 711-7.
276. Snijder, H.J., et al., *Structural evidence for dimerization-regulated activation of an integral membrane phospholipase.* Nature, 1999. **401**(6754): p. 717-21.
277. May, K.L. and T.J. Silhavy, *The Escherichia coli Phospholipase PldA Regulates Outer Membrane Homeostasis via Lipid Signaling.* mBio, 2018. **9**(2).
278. Guo, L., et al., *Lipid A acylation and bacterial resistance against vertebrate antimicrobial peptides.* Cell, 1998. **95**(2): p. 189-98.
279. Bishop, R.E., *The lipid A palmitoyltransferase PagP: molecular mechanisms and role in bacterial pathogenesis.* Mol Microbiol, 2005. **57**(4): p. 900-12.
280. Malinverni, J.C. and T.J. Silhavy, *An ABC transport system that maintains lipid asymmetry in the gram-negative outer membrane.* Proc Natl Acad Sci U S A, 2009. **106**(19): p. 8009-14.
281. Chong, Z.S., W.F. Woo, and S.S. Chng, *Osmoporin OmpC forms a complex with MlaA to maintain outer membrane lipid asymmetry in Escherichia coli.* Mol Microbiol, 2015. **98**(6): p. 1133-46.
282. Ekiert, D.C., et al., *Architectures of Lipid Transport Systems for the Bacterial Outer Membrane.* Cell, 2017. **169**(2): p. 273-285 e17.

283. Ercan, B., et al., *Characterization of Interactions and Phospholipid Transfer between Substrate Binding Proteins of the OmpC-Mla System.* Biochemistry, 2019. **58**(2): p. 114-119.
284. Abellon-Ruiz, J., et al., *Structural basis for maintenance of bacterial outer membrane lipid asymmetry.* Nat Microbiol, 2017. **2**(12): p. 1616-1623.
285. Yeow, J., et al., *The architecture of the OmpC-MlaA complex sheds light on the maintenance of outer membrane lipid asymmetry in Escherichia coli.* J Biol Chem, 2018. **293**(29): p. 11325-11340.
286. Thong, S., et al., *Defining key roles for auxiliary proteins in an ABC transporter that maintains bacterial outer membrane lipid asymmetry.* Elife, 2016. **5**.
287. Sutterlin, H.A., et al., *Disruption of lipid homeostasis in the Gram-negative cell envelope activates a novel cell death pathway.* Proc Natl Acad Sci U S A, 2016. **113**(11): p. E1565-74.
288. Nakayama, T. and Q.M. Zhang-Akiyama, *pqiABC and yebST, Putative mce Operons of Escherichia coli, Encode Transport Pathways and Contribute to Membrane Integrity.* J Bacteriol, 2017. **199**(1).
289. Isom, G.L., et al., *MCE domain proteins: conserved inner membrane lipid-binding proteins required for outer membrane homeostasis.* Sci Rep, 2017. **7**(1): p. 8608.
290. Konovalova, A. and T.J. Silhavy, *Outer membrane lipoprotein biogenesis: Lol is not the end.* Philos Trans R Soc Lond B Biol Sci, 2015. **370**(1679).
291. Shruthi, H., M.M. Babu, and K. Sankaran, *TAT-pathway-dependent lipoproteins as a niche-based adaptation in prokaryotes.* J Mol Evol, 2010. **70**(4): p. 359-70.
292. Kudva, R., et al., *Protein translocation across the inner membrane of Gram-negative bacteria: the Sec and Tat dependent protein transport pathways.* Res Microbiol, 2013. **164**(6): p. 505-34.
293. von Heijne, G., *The structure of signal peptides from bacterial lipoproteins.* Protein Eng, 1989. **2**(7): p. 531-4.
294. Hayashi, S. and H.C. Wu, *Lipoproteins in bacteria.* J Bioenerg Biomembr, 1990. **22**(3): p. 451-71.
295. Horler, R.S., et al., *EchoLOCATION: an in silico analysis of the subcellular locations of Escherichia coli proteins and comparison with experimentally derived locations.* Bioinformatics, 2009. **25**(2): p. 163-6.
296. Terada, M., et al., *Lipoprotein sorting signals evaluated as the LolA-dependent release of lipoproteins from the cytoplasmic membrane of Escherichia coli.* J Biol Chem, 2001. **276**(50): p. 47690-4.
297. Okuda, S. and H. Tokuda, *Lipoprotein sorting in bacteria.* Annu Rev Microbiol, 2011. **65**: p. 239-59.
298. Armbruster, K.M. and T.C. Meredith, *Identification of the Lyso-Form N-Acyl Intramolecular Transferase in Low-GC Firmicutes.* J Bacteriol, 2017. **199**(11).
299. Narita, S. and H. Tokuda, *Overexpression of LolCDE allows deletion of the Escherichia coli gene encoding apolipoprotein N-acyltransferase.* J Bacteriol, 2011. **193**(18): p. 4832-40.
300. LoVullo, E.D., et al., *Revisiting the Gram-negative lipoprotein paradigm.* J Bacteriol, 2015. **197**(10): p. 1705-15.
301. Yakushi, T., et al., *A new ABC transporter mediating the detachment of lipid-modified proteins from membranes.* Nat Cell Biol, 2000. **2**(4): p. 212-8.
302. Ito, Y., et al., *A novel ligand bound ABC transporter, LolCDE, provides insights into the molecular mechanisms underlying membrane detachment of bacterial lipoproteins.* Mol Microbiol, 2006. **62**(4): p. 1064-75.
303. Taniguchi, N. and H. Tokuda, *Molecular events involved in a single cycle of ligand transfer from an ATP binding cassette transporter, LolCDE, to a molecular chaperone, LolA.* J Biol Chem, 2008. **283**(13): p. 8538-44.
304. Mizutani, M., et al., *Functional differentiation of structurally similar membrane subunits of the ABC transporter LolCDE complex.* FEBS Lett, 2013. **587**(1): p. 23-9.

305. Kaplan, E., et al., *Insights into bacterial lipoprotein trafficking from a structure of LolA bound to the LolC periplasmic domain.* Proc Natl Acad Sci U S A, 2018. **115**(31): p. E7389-E7397.
306. Okuda, S. and H. Tokuda, *Model of mouth-to-mouth transfer of bacterial lipoproteins through inner membrane LolC, periplasmic LolA, and outer membrane LolB.* Proc Natl Acad Sci U S A, 2009. **106**(14): p. 5877-82.
307. Paradis-Bleau, C., et al., *Lipoprotein cofactors located in the outer membrane activate bacterial cell wall polymerases.* Cell, 2010. **143**(7): p. 1110-20.
308. Typas, A., et al., *Regulation of peptidoglycan synthesis by outer-membrane proteins.* Cell, 2010. **143**(7): p. 1097-109.
309. Tanaka, K., S.I. Matsuyama, and H. Tokuda, *Deletion of lolB, encoding an outer membrane lipoprotein, is lethal for Escherichia coli and causes accumulation of lipoprotein localization intermediates in the periplasm.* J Bacteriol, 2001. **183**(22): p. 6538-42.
310. Grabowicz, M. and T.J. Silhavy, *Redefining the essential trafficking pathway for outer membrane lipoproteins.* Proc Natl Acad Sci U S A, 2017. **114**(18): p. 4769-4774.
311. Leyton, D.L., A.E. Rossiter, and I.R. Henderson, *From self sufficiency to dependence: mechanisms and factors important for autotransporter biogenesis.* Nat Rev Microbiol, 2012. **10**(3): p. 213-25.
312. Cho, S.H., et al., *Detecting envelope stress by monitoring beta-barrel assembly.* Cell, 2014. **159**(7): p. 1652-64.
313. Konovalova, A., et al., *Transmembrane domain of surface-exposed outer membrane lipoprotein RcsF is threaded through the lumen of beta-barrel proteins.* Proc Natl Acad Sci U S A, 2014. **111**(41): p. E4350-8.
314. Hooda, Y., et al., *Slam is an outer membrane protein that is required for the surface display of lipidated virulence factors in Neisseria.* Nat Microbiol, 2016. **1**: p. 16009.
315. Fairman, J.W., N. Noinaj, and S.K. Buchanan, *The structural biology of beta-barrel membrane proteins: a summary of recent reports.* Curr Opin Struct Biol, 2011. **21**(4): p. 523-31.
316. Onufryk, C., et al., *Characterization of six lipoproteins in the sigmaE regulon.* J Bacteriol, 2005. **187**(13): p. 4552-61.
317. Ruiz, N., et al., *Chemical conditionality: a genetic strategy to probe organelle assembly.* Cell, 2005. **121**(2): p. 307-17.
318. Sklar, J.G., et al., *Lipoprotein SmpA is a component of the YaeT complex that assembles outer membrane proteins in Escherichia coli.* Proc Natl Acad Sci U S A, 2007. **104**(15): p. 6400-5.
319. Voulhoux, R., et al., *Role of a highly conserved bacterial protein in outer membrane protein assembly.* Science, 2003. **299**(5604): p. 262-5.
320. Noinaj, N., et al., *Structural insight into the biogenesis of beta-barrel membrane proteins.* Nature, 2013. **501**(7467): p. 385-90.
321. Albrecht, R., et al., *Structure of BamA, an essential factor in outer membrane protein biogenesis.* Acta Crystallogr D Biol Crystallogr, 2014. **70**(Pt 6): p. 1779-89.
322. Ni, D., et al., *Structural and functional analysis of the beta-barrel domain of BamA from Escherichia coli.* FASEB J, 2014. **28**(6): p. 2677-85.
323. Gu, Y., et al., *Structural basis of outer membrane protein insertion by the BAM complex.* Nature, 2016. **531**(7592): p. 64-9.
324. Danoff, E.J. and K.G. Fleming, *Membrane defects accelerate outer membrane beta-barrel protein folding.* Biochemistry, 2015. **54**(2): p. 97-9.
325. Gessmann, D., et al., *Outer membrane beta-barrel protein folding is physically controlled by periplasmic lipid head groups and BamA.* Proc Natl Acad Sci U S A, 2014. **111**(16): p. 5878-83.
326. Schiffrin, B., et al., *Effects of Periplasmic Chaperones and Membrane Thickness on BamA-Catalyzed Outer-Membrane Protein Folding.* J Mol Biol, 2017. **429**(23): p. 3776-3792.
327. Kim, S., et al., *Structure and function of an essential component of the outer membrane protein assembly machine.* Science, 2007. **317**(5840): p. 961-4.

328. Gatzeva-Topalova, P.Z., et al., *Structure and flexibility of the complete periplasmic domain of BamA: the protein insertion machine of the outer membrane.* Structure, 2010. **18**(11): p. 1492-501.
329. Bakelar, J., S.K. Buchanan, and N. Noinaj, *The structure of the beta-barrel assembly machinery complex.* Science, 2016. **351**(6269): p. 180-6.
330. Ricci, D.P., et al., *Activation of the Escherichia coli beta-barrel assembly machine (Bam) is required for essential components to interact properly with substrate.* Proc Natl Acad Sci U S A, 2012. **109**(9): p. 3487-91.
331. Vuong, P., et al., *Analysis of YfgL and YaeT interactions through bioinformatics, mutagenesis, and biochemistry.* J Bacteriol, 2008. **190**(5): p. 1507-17.
332. Han, L., et al., *Structure of the BAM complex and its implications for biogenesis of outer-membrane proteins.* Nat Struct Mol Biol, 2016. **23**(3): p. 192-6.
333. Iadanza, M.G., et al., *Lateral opening in the intact beta-barrel assembly machinery captured by cryo-EM.* Nat Commun, 2016. **7**: p. 12865.
334. Malinverni, J.C., et al., *YfiO stabilizes the YaeT complex and is essential for outer membrane protein assembly in Escherichia coli.* Mol Microbiol, 2006. **61**(1): p. 151-64.
335. Remaut, H. and G. Waksman, *Protein-protein interaction through beta-strand addition.* Trends Biochem Sci, 2006. **31**(8): p. 436-44.
336. Heuck, A., A. Schleiffer, and T. Clausen, *Augmenting beta-augmentation: structural basis of how BamB binds BamA and may support folding of outer membrane proteins.* J Mol Biol, 2011. **406**(5): p. 659-66.
337. Sandoval, C.M., et al., *Crystal structure of BamD: an essential component of the beta-Barrel assembly machinery of gram-negative bacteria.* J Mol Biol, 2011. **409**(3): p. 348-57.
338. Hagan, C.L., J.S. Wzorek, and D. Kahne, *Inhibition of the beta-barrel assembly machine by a peptide that binds BamD.* Proc Natl Acad Sci U S A, 2015. **112**(7): p. 2011-6.
339. Lee, J., et al., *Substrate binding to BamD triggers a conformational change in BamA to control membrane insertion.* Proc Natl Acad Sci U S A, 2018. **115**(10): p. 2359-2364.
340. Robert, V., et al., *Assembly factor Omp85 recognizes its outer membrane protein substrates by a species-specific C-terminal motif.* PLoS Biol, 2006. **4**(11): p. e377.
341. Paramasivam, N., M. Habeck, and D. Linke, *Is the C-terminal insertional signal in Gram-negative bacterial outer membrane proteins species-specific or not?* BMC Genomics, 2012. **13**: p. 510.
342. Rigel, N.W., D.P. Ricci, and T.J. Silhavy, *Conformation-specific labeling of BamA and suppressor analysis suggest a cyclic mechanism for beta-barrel assembly in Escherichia coli.* Proc Natl Acad Sci U S A, 2013. **110**(13): p. 5151-6.
343. McCabe, A.L., et al., *Conformational Changes That Coordinate the Activity of BamA and BamD Allowing beta-Barrel Assembly.* J Bacteriol, 2017. **199**(20).
344. Misra, R., R. Stikeleather, and R. Gabriele, *In vivo roles of BamA, BamB and BamD in the biogenesis of BamA, a core protein of the beta-barrel assembly machine of Escherichia coli.* J Mol Biol, 2015. **427**(5): p. 1061-74.
345. Chen, Z., et al., *Structural basis for the interaction of BamB with the POTRA3-4 domains of BamA.* Acta Crystallogr D Struct Biol, 2016. **72**(Pt 2): p. 236-44.
346. Jansen, K.B., S.L. Baker, and M.C. Sousa, *Crystal structure of BamB bound to a periplasmic domain fragment of BamA, the central component of the beta-barrel assembly machine.* J Biol Chem, 2015. **290**(4): p. 2126-36.
347. Hagan, C.L., D.B. Westwood, and D. Kahne, *bam Lipoproteins Assemble BamA in vitro.* Biochemistry, 2013. **52**(35): p. 6108-13.
348. Charlson, E.S., J.N. Werner, and R. Misra, *Differential effects of yfgL mutation on Escherichia coli outer membrane proteins and lipopolysaccharide.* J Bacteriol, 2006. **188**(20): p. 7186-94.

349. Hsieh, P.F., et al., *The Klebsiella pneumoniae YfgL (BamB) lipoprotein contributes to outer membrane protein biogenesis, type-1 fimbriae expression, anti-phagocytosis, and in vivo virulence.* Virulence, 2016. **7**(5): p. 587-601.
350. Gunasinghe, S.D., et al., *The WD40 Protein BamB Mediates Coupling of BAM Complexes into Assembly Precincts in the Bacterial Outer Membrane.* Cell Rep, 2018. **23**(9): p. 2782-2794.
351. Dekker, N., et al., *In vitro folding of Escherichia coli outer-membrane phospholipase A.* Eur J Biochem, 1995. **232**(1): p. 214-9.
352. Kleinschmidt, J.H. and L.K. Tamm, *Folding intermediates of a beta-barrel membrane protein. Kinetic evidence for a multi-step membrane insertion mechanism.* Biochemistry, 1996. **35**(40): p. 12993-3000.
353. Burgess, N.K., et al., *Beta-barrel proteins that reside in the Escherichia coli outer membrane in vivo demonstrate varied folding behavior in vitro.* J Biol Chem, 2008. **283**(39): p. 26748-58.
354. Ricci, D.P. and T.J. Silhavy, *Outer Membrane Protein Insertion by the beta-barrel Assembly Machine.* EcoSal Plus, 2019. **8**(2).
355. Schiffrin, B., D.J. Brockwell, and S.E. Radford, *Outer membrane protein folding from an energy landscape perspective.* BMC Biol, 2017. **15**(1): p. 123.
356. Ranava, D., et al., *Bacterial machineries for the assembly of membrane-embedded beta-barrel proteins.* FEMS Microbiol Lett, 2018. **365**(10).
357. Hohr, A.I.C., et al., *Membrane protein insertion through a mitochondrial beta-barrel gate.* Science, 2018. **359**(6373).
358. Doyle, M.T. and H.D. Bernstein, *Bacterial outer membrane proteins assemble via asymmetric interactions with the BamA beta-barrel.* Nat Commun, 2019. **10**(1): p. 3358.
359. Lee, J., et al., *Formation of a beta-barrel membrane protein is catalyzed by the interior surface of the assembly machine protein BamA.* Elife, 2019. **8**.
360. Tomasek, D., et al., *Structure of a nascent membrane protein as it folds on the BAM complex.* Nature, 2020.
361. Ieva, R., et al., *Sequential and spatially restricted interactions of assembly factors with an autotransporter beta domain.* Proc Natl Acad Sci U S A, 2011. **108**(31): p. E383-91.
362. Lee, J., et al., *Characterization of a stalled complex on the beta-barrel assembly machine.* Proc Natl Acad Sci U S A, 2016. **113**(31): p. 8717-22.
363. Hammond, S.M., *Inhibitors of lipopolysaccharide biosynthesis impair the virulence potential of Escherichia coli.* FEMS Microbiol Lett, 1992. **100**(1-3): p. 293-7.
364. Erwin, A.L., *Antibacterial Drug Discovery Targeting the Lipopolysaccharide Biosynthetic Enzyme LpxC.* Cold Spring Harb Perspect Med, 2016. **6**(7).
365. Onishi, H.R., et al., *Antibacterial agents that inhibit lipid A biosynthesis.* Science, 1996. **274**(5289): p. 980-2.
366. Clements, J.M., et al., *Antibacterial activities and characterization of novel inhibitors of LpxC.* Antimicrob Agents Chemother, 2002. **46**(6): p. 1793-9.
367. Kline, T., et al., *Potent, novel in vitro inhibitors of the Pseudomonas aeruginosa deacetylase LpxC.* J Med Chem, 2002. **45**(14): p. 3112-29.
368. Mdluli, K.E., et al., *Molecular validation of LpxC as an antibacterial drug target in Pseudomonas aeruginosa.* Antimicrob Agents Chemother, 2006. **50**(6): p. 2178-84.
369. McClerren, A.L., et al., *A slow, tight-binding inhibitor of the zinc-dependent deacetylase LpxC of lipid A biosynthesis with antibiotic activity comparable to ciprofloxacin.* Biochemistry, 2005. **44**(50): p. 16574-83.
370. Piizzi, G., et al., *Design, Synthesis, and Properties of a Potent Inhibitor of Pseudomonas aeruginosa Deacetylase LpxC.* J Med Chem, 2017. **60**(12): p. 5002-5014.
371. Williams, A.H., et al., *Structure of UDP-N-acetylglucosamine acyltransferase with a bound antibacterial pentadecapeptide.* Proc Natl Acad Sci U S A, 2006. **103**(29): p. 10877-82.
372. Benson, R.E., et al., *Intracellular expression of Peptide fusions for demonstration of protein essentiality in bacteria.* Antimicrob Agents Chemother, 2003. **47**(9): p. 2875-81.

373. Jenkins, R.J. and G.D. Dotson, *Dual targeting antibacterial peptide inhibitor of early lipid A biosynthesis.* ACS Chem Biol, 2012. **7**(7): p. 1170-7.
374. Jenkins, R.J., et al., *Structural basis for the recognition of peptide RJPXD33 by acyltransferases in lipid A biosynthesis.* J Biol Chem, 2014. **289**(22): p. 15527-35.
375. Postma, T.M. and R.J.M. Liskamp, *Triple-targeting Gram-negative selective antimicrobial peptides capable of disrupting the cell membrane and lipid A biosynthesis.* RSC Advances, 2016. **6**(70): p. 65418-65421.
376. Richie, D.L., et al., *Toxic Accumulation of LPS Pathway Intermediates Underlies the Requirement of LpxH for Growth of Acinetobacter baumannii ATCC 19606.* PLoS One, 2016. **11**(8): p. e0160918.
377. Wei, J.R., et al., *LpxK Is Essential for Growth of Acinetobacter baumannii ATCC 19606: Relationship to Toxic Accumulation of Lipid A Pathway Intermediates.* mSphere, 2017. **2**(4).
378. Nayar, A.S., et al., *Novel antibacterial targets and compounds revealed by a high-throughput cell wall reporter assay.* J Bacteriol, 2015. **197**(10): p. 1726-34.
379. Lee, M., et al., *Structure-Activity Relationship of Sulfonyl Piperazine LpxH Inhibitors Analyzed by an LpxE-Coupled Malachite Green Assay.* ACS Infect Dis, 2019. **5**(4): p. 641-651.
380. Smyth, K.M. and A. Marchant, *Conservation of the 2-keto-3-deoxymanno-octulosonic acid (Kdo) biosynthesis pathway between plants and bacteria.* Carbohydr Res, 2013. **380**: p. 70-5.
381. Baasov, T., et al., *Catalytic mechanism of 3-deoxy-D-manno-2-octulosonate-8-phosphate synthase. The use of synthetic analogues to probe the structure of the putative reaction intermediate.* Eur J Biochem, 1993. **217**(3): p. 991-9.
382. Heyes, D.J., et al., *Structure-based mechanism of CMP-2-keto-3-deoxymanno-octulonic acid synthetase: convergent evolution of a sugar-activating enzyme with DNA/RNA polymerases.* J Biol Chem, 2009. **284**(51): p. 35514-23.
383. Cipolla, L., et al., *New targets for antibacterial design: Kdo biosynthesis and LPS machinery transport to the cell surface.* Curr Med Chem, 2011. **18**(6): p. 830-52.
384. Claesson, A., et al., *Design and synthesis of peptide derivatives of a 3-deoxy-D-manno-2-octulosonic acid (KDO) analogue as novel antibacterial agents acting upon lipopolysaccharide biosynthesis.* J Med Chem, 1987. **30**(12): p. 2309-13.
385. Claesson, A., et al., *A 2-deoxy analogue of KDO as the first inhibitor of the enzyme CMP-KDO synthetase.* Biochem Biophys Res Commun, 1987. **143**(3): p. 1063-8.
386. Birck, M.R., T.P. Holler, and R.W. Woodard, *Identification of a slow tight-binding inhibitor of 3-deoxy-D-manno-octulosonic acid 8-phosphate synthase.* J Am Chem Soc, 2000. **122**(38): p. 9334–9335.
387. Gao, Z., et al., *High-Throughput "FP-Tag" Assay for the Identification of Glycosyltransferase Inhibitors.* J Am Chem Soc, 2019. **141**(6): p. 2201-2204.
388. Ahmad, S., et al., *Toward novel inhibitors against KdsB: a highly specific and selective broad-spectrum bacterial enzyme.* J Biomol Struct Dyn, 2019. **37**(5): p. 1326-1345.
389. Alexander, M.K., et al., *Disrupting Gram-Negative Bacterial Outer Membrane Biosynthesis through Inhibition of the Lipopolysaccharide Transporter MsbA.* Antimicrob Agents Chemother, 2018. **62**(11).
390. Zhang, G., et al., *Cell-based screen for discovering lipopolysaccharide biogenesis inhibitors.* Proc Natl Acad Sci U S A, 2018. **115**(26): p. 6834-6839.
391. Harris, T.L., et al., *Small molecule downregulation of PmrAB reverses lipid A modification and breaks colistin resistance.* ACS Chem Biol, 2014. **9**(1): p. 122-7.
392. Kline, T., et al., *Synthesis of and evaluation of lipid A modification by 4-substituted 4-deoxy arabinose analogs as potential inhibitors of bacterial polymyxin resistance.* Bioorg Med Chem Lett, 2008. **18**(4): p. 1507-10.
393. Srinivas, N., et al., *Peptidomimetic antibiotics target outer-membrane biogenesis in Pseudomonas aeruginosa.* Science, 2010. **327**(5968): p. 1010-3.

394. Shankaramma, S.C., et al., *Macrocyclic hairpin mimetics of the cationic antimicrobial peptide protegrin I: a new family of broad-spectrum antibiotics.* Chembiochem, 2002. **3**(11): p. 1126-33.
395. Robinson, J.A., et al., *Properties and structure-activity studies of cyclic beta-hairpin peptidomimetics based on the cationic antimicrobial peptide protegrin I.* Bioorg Med Chem, 2005. **13**(6): p. 2055-64.
396. Werneburg, M., et al., *Inhibition of lipopolysaccharide transport to the outer membrane in Pseudomonas aeruginosa by peptidomimetic antibiotics.* Chembiochem, 2012. **13**(12): p. 1767-75.
397. Martin-Loeches, I., G.E. Dale, and A. Torres, *Murepavadin: a new antibiotic class in the pipeline.* Expert Rev Anti Infect Ther, 2018. **16**(4): p. 259-268.
398. Wach, A., K. Dembowsky, and G.E. Dale, *Pharmacokinetics and Safety of Intravenous Murepavadin Infusion in Healthy Adult Subjects Administered Single and Multiple Ascending Doses.* Antimicrob Agents Chemother, 2018. **62**(4).
399. Andolina, G., et al., *A Peptidomimetic Antibiotic Interacts with the Periplasmic Domain of LptD from Pseudomonas aeruginosa.* ACS Chem Biol, 2018. **13**(3): p. 666-675.
400. Polyphor AG. *Polyphor closes the Phase III PRISM studies of murepavadin intravenous formulation and evaluates further product improvement options:* https://www.polyphor.com/news/corporate-news-details/?newsid=1800485. (accessed on 16/08/2020).
401. Polyphor AG. *Inhaled Murepavadin:* https://www.polyphor.com/pol7080/. (accessed on 16/08/2020).
402. Vetterli, S.U., et al., *Thanatin targets the intermembrane protein complex required for lipopolysaccharide transport in Escherichia coli.* Sci Adv, 2018. **4**(11): p. eaau2634.
403. Fehlbaum, P., et al., *Structure-activity analysis of thanatin, a 21-residue inducible insect defense peptide with sequence homology to frog skin antimicrobial peptides.* Proc Natl Acad Sci U S A, 1996. **93**(3): p. 1221-5.
404. Ma, B., et al., *The Disulfide Bond of the Peptide Thanatin Is Dispensible for Its Antimicrobial Activity In Vivo and In Vitro.* Antimicrob Agents Chemother, 2016. **60**(7): p. 4283-9.
405. Ma, B., et al., *The antimicrobial peptide thanatin disrupts the bacterial outer membrane and inactivates the NDM-1 metallo-beta-lactamase.* Nat Commun, 2019. **10**(1): p. 3517.
406. Zhang, X., et al., *Identification of an anti-Gram-negative bacteria agent disrupting the interaction between lipopolysaccharide transporters LptA and LptC.* Int J Antimicrob Agents, 2019. **53**(4): p. 442-448.
407. De La Fuente, R., et al., *Small molecules with antimicrobial activity against E. coli and P. aeruginosa identified by high-throughput screening.* Br J Pharmacol, 2006. **149**(5): p. 551-9.
408. Gronenberg, L.S. and D. Kahne, *Development of an activity assay for discovery of inhibitors of lipopolysaccharide transport.* J Am Chem Soc, 2010. **132**(8): p. 2518-9.
409. Sherman, D.J., et al., *Validation of inhibitors of an ABC transporter required to transport lipopolysaccharide to the cell surface in Escherichia coli.* Bioorg Med Chem, 2013. **21**(16): p. 4846-51.
410. Mandler, M.D., et al., *Novobiocin Enhances Polymyxin Activity by Stimulating Lipopolysaccharide Transport.* J Am Chem Soc, 2018. **140**(22): p. 6749-6753.
411. Urfer, M., et al., *A Peptidomimetic Antibiotic Targets Outer Membrane Proteins and Disrupts Selectively the Outer Membrane in Escherichia coli.* J Biol Chem, 2016. **291**(4): p. 1921-32.
412. Storek, K.M., et al., *Monoclonal antibody targeting the beta-barrel assembly machine of Escherichia coli is bactericidal.* Proc Natl Acad Sci U S A, 2018. **115**(14): p. 3692-3697.
413. Storek, K.M., et al., *The Escherichia coli beta-Barrel Assembly Machinery Is Sensitized to Perturbations under High Membrane Fluidity.* J Bacteriol, 2019. **201**(1).
414. Ghequire, M.G.K., et al., *Hitting with a BAM: Selective Killing by Lectin-Like Bacteriocins.* mBio, 2018. **9**(2).

415. Cavera, V.L., et al., *Bacteriocins and their position in the next wave of conventional antibiotics.* Int J Antimicrob Agents, 2015. **46**(5): p. 494-501.
416. McCaughey, L.C., et al., *Efficacy of species-specific protein antibiotics in a murine model of acute Pseudomonas aeruginosa lung infection.* Sci Rep, 2016. **6**: p. 30201.
417. Leonard-Rivera, M. and R. Misra, *Conserved residues of the putative L6 loop of Escherichia coli BamA play a critical role in the assembly of beta-barrel outer membrane proteins, including that of BamA itself.* J Bacteriol, 2012. **194**(17): p. 4662-8.
418. Storek, K.M., et al., *Massive antibody discovery used to probe structure-function relationships of the essential outer membrane protein LptD.* Elife, 2019. **8**.
419. Hart, E.M., et al., *A small-molecule inhibitor of BamA impervious to efflux and the outer membrane permeability barrier.* Proc Natl Acad Sci U S A, 2019. **116**(43): p. 21748-21757.
420. Luther, A., et al., *Chimeric peptidomimetic antibiotics against Gram-negative bacteria.* Nature, 2019. **576**(7787): p. 452-458.
421. Imai, Y., et al., *A new antibiotic selectively kills Gram-negative pathogens.* Nature, 2019. **576**(7787): p. 459-464.
422. Psonis, J.J., et al., *The small molecule nitazoxanide selectively disrupts BAM-mediated folding of the outer membrane usher protein.* J Biol Chem, 2019. **294**(39): p. 14357-14369.
423. Werneburg, G.T. and D.G. Thanassi, *Pili Assembled by the Chaperone/Usher Pathway in Escherichia coli and Salmonella.* EcoSal Plus, 2018. **8**(1).
424. McLeod, S.M., et al., *Small-molecule inhibitors of gram-negative lipoprotein trafficking discovered by phenotypic screening.* J Bacteriol, 2015. **197**(6): p. 1075-82.
425. Nickerson, N.N., et al., *A Novel Inhibitor of the LolCDE ABC Transporter Essential for Lipoprotein Trafficking in Gram-Negative Bacteria.* Antimicrob Agents Chemother, 2018. **62**(4).
426. Pathania, R., et al., *Chemical genomics in Escherichia coli identifies an inhibitor of bacterial lipoprotein targeting.* Nat Chem Biol, 2009. **5**(11): p. 849-56.
427. Barker, C.A., et al., *Degradation of MAC13243 and studies of the interaction of resulting thiourea compounds with the lipoprotein targeting chaperone LolA.* Bioorg Med Chem Lett, 2013. **23**(8): p. 2426-31.
428. Muheim, C., et al., *Increasing the permeability of Escherichia coli using MAC13243.* Sci Rep, 2017. **7**(1): p. 17629.
429. Buss, J.A., et al., *Pathway-Directed Screen for Inhibitors of the Bacterial Cell Elongation Machinery.* Antimicrob Agents Chemother, 2019. **63**(1).

PART II. RESULTS

AIM OF THE PROJECT

The outer membrane (OM) of Gram-negative bacteria is an asymmetric lipid bilayer containing phospholipids in the inner leaflet and lipopolysaccharide (LPS) in the outer leaflet. The tight packing of LPS and its amphipathic nature, which account for the great barrier-like properties of the OM, explain why the development of new antibiotics to treat infections caused by Gram-negative bacteria has been so difficult. Among the sophisticated molecular machines assembling the OM, our research is focused on machinery that transports LPS to the OM, the LPS transport (Lpt) machinery. In *E. coli*, the Lpt system is composed of seven essential proteins spanning the cell envelope: the ABC transporter $LptB_2FGC$ powers the LPS extraction from the inner membrane (IM) and its transport along the periplasmic bridge, comprising LptA, to the OM LptDE translocon, which assembles LPS on the cell surface. The Lpt complex operates as a single device since the depletion of any component leads to the accumulation of LPS at the outer leaflet of the IM and results in increased OM permeability and OM defects.

The research project of this thesis focuses on two main topics: elucidating the mechanism behind thanatin's antibacterial activity, and the characterization of a mutant six-component Lpt machinery that is functional without LptC.

Thanatin, a host-defence antimicrobial peptide first isolated more than twenty years ago, was only recently discovered to target the Lpt machinery. Spontaneous thanatin-resistant mutants presenting LptA as the only mutated gene were isolated by Vetterli *et al*. (2018) and, through NMR studies, they showed that this peptide binds to the N-terminal β-strand of LptA. This region is involved in LptA dimerization and its interaction with LptC within the periplasmic bridge. Therefore, to test whether the antibacterial activity of thanatin is due to the inhibition of LptA interaction with itself or with LptC, we implemented the Bacterial Adenylate Cyclase Two-Hybrid (BACTH) system to detect these interactions in the periplasm and investigate thanatin's target. To provide additional evidence of an effect on the LPS transport, we assessed the LptA levels in cells treated with thanatin and whether we could observe the accumulation of LPS modified with colanic acid (CA), since both degradation of LptA and CA-modified LPS are indicative of LPS transport defects.

To gain further insight into thanatin's effect on the integrity of the cell envelope, we investigated whether this peptide could induce the *lptAp1*, *eptAp*, and *ldtDp* promoters. The *lptAp1* is a σ^E-dependent promoter only activated upon LPS biogenesis defects (Martorana *et al*., 2011), and the promoter of *ldtD* has been shown to be activated when the LPS synthesis is inhibited (Morè *et al*., 2019). The promoter of *eptA* was tested to probe if thanatin could induce

two-component systems that regulate LPS modifications, specifically the PmrAB system which modifies the phosphates of lipid A with positively charged groups.

Although all seven Lpt proteins have been shown to be essential, viable mutants lacking LptC but carrying suppressor mutations at the residue R212 in the periplasmic domain of LptF were isolated by our group, and the substitution R212G was shown to restore cell viability and OM permeability to a nearly wild-type level (Benedet *et al*., 2016). Interestingly, LptC was recently proposed to have a regulatory role on the $LptB_2FGC$ transporter by modulating its ATPase activity (Owens *et al*., 2019; Li *et al*., 2019), thus adding to the mystery of how the suppressor mutants can survive without LptC.

In the second part of this project, we sought to clarify how the cell can bypass LptC and its regulatory role in the machinery by studying the mechanism of suppression by $LptF^{R212G}$. For this, we investigated whether a six-component Lpt complex was assembled and whether it involved a direct interaction between $LptF^{R212G}$ and LptA. Moreover, we analysed the ATPase activity of the mutant IM complex in comparison to the wild type and examined the interaction networks around the residue R212 of LptF in the $LptB_2FG$ and $LptB_2FGC$ complexes in order to gain an understanding into the role of LptC in the machinery and how the $lptF^{R212G}$ allele turns LptC dispensable.

1. Thanatin impairs Lpt complex assembly

1.1 Manuscript 1 (published)

frontiers in Microbiology

ORIGINAL RESEARCH
published: 13 May 2020
doi: 10.3389/fmicb.2020.00909

Thanatin Impairs Lipopolysaccharide Transport Complex Assembly by Targeting LptC–LptA Interaction and Decreasing LptA Stability

Elisabete C. C. M. Moura[1], Tiago Baeta[2†], Alessandra Romanelli[3†], Cedric Laguri[2], Alessandra M. Martorana[1], Emanuela Erba[3], Jean-Pierre Simorre[2], Paola Sperandeo[1] and Alessandra Polissi[1]**

[1] Dipartimento di Scienze Farmacologiche e Biomolecolari, Università degli Studi di Milano, Milan, Italy, [2] Université Grenoble Alpes, CNRS, CEA, IBS, Grenoble, France, [3] Dipartimento di Scienze Farmaceutiche, Università degli Studi di Milano, Milan, Italy

OPEN ACCESS

Edited by:
Paolo Visca,
Roma Tre University, Italy

Reviewed by:
Changjiang Dong,
University of East Anglia,
United Kingdom
Candice Klug,
Medical College of Wisconsin,
United States

***Correspondence:**
Paola Sperandeo
paola.sperandeo@unimi.it
Alessandra Polissi
alessandra.polissi@unimi.it

† These authors have contributed equally to this work

Specialty section:
This article was submitted to Antimicrobials, Resistance and Chemotherapy, a section of the journal Frontiers in Microbiology

Received: 04 February 2020
Accepted: 17 April 2020
Published: 13 May 2020

Citation:
Moura ECCM, Baeta T, Romanelli A, Laguri C, Martorana AM, Erba E, Simorre J-P, Sperandeo P and Polissi A (2020) Thanatin Impairs Lipopolysaccharide Transport Complex Assembly by Targeting LptC–LptA Interaction and Decreasing LptA Stability. Front. Microbiol. 11:909. doi: 10.3389/fmicb.2020.00909

The outer membrane (OM) of Gram-negative bacteria is a highly selective permeability barrier due to its asymmetric structure with lipopolysaccharide (LPS) in the outer leaflet. In *Escherichia coli*, LPS is transported to the cell surface by the LPS transport (Lpt) system composed of seven essential proteins forming a transenvelope bridge. Transport is powered by the ABC transporter $LptB_2FGC$, which extracts LPS from the inner membrane (IM) and transfers it, through LptC protein, to the periplasmic protein LptA. Then, LptA delivers LPS to the OM LptDE translocon for final assembly at the cell surface. The Lpt protein machinery operates as a single device, since depletion of any component leads to the accumulation of a modified LPS decorated with repeating units of colanic acid at the IM outer leaflet. Moreover, correct machine assembly is essential for LPS transit and disruption of the Lpt complex results in LptA degradation. Due to its vital role in cell physiology, the Lpt system represents a good target for antimicrobial drugs. Thanatin is a naturally occurring antimicrobial peptide reported to cause defects in membrane assembly and demonstrated *in vitro* to bind to the N-terminal β-strand of LptA. Since this region is involved in both LptA dimerization and interaction with LptC, we wanted to elucidate the mechanism of inhibition of thanatin and discriminate whether its antibacterial effect is exerted by the disruption of the interaction of LptA with itself or with LptC. For this purpose, we here implemented the Bacterial Adenylate Cyclase Two-Hybrid (BACTH) system to probe *in vivo* the Lpt interactome in the periplasm. With this system, we found that thanatin targets both LptC–LptA and LptA–LptA interactions, with a greater inhibitory effect on the former. We confirmed *in vitro* the disruption of LptC–LptA interaction using two different biophysical techniques. Finally, we observed that in cells treated with thanatin, LptA undergoes degradation and LPS decorated with colanic acid accumulates. These data further support inhibition or disruption of Lpt complex assembly as the main killing mechanism of thanatin against Gram-negative bacteria.

Keywords: bacterial cell wall, lipopolysaccharide, Lpt system, thanatin, antimicrobial peptides, BACTH technique, NMR

INTRODUCTION

The emergence and spread of multidrug resistant pathogens pose an alarming threat to human and animal health worldwide. The old classes of antibiotics are becoming ineffective at killing an increasing number of pathogens and the decline in the discovery and development of new drugs, experienced in recent years, is seriously eroding the ability of clinicians to control infectious diseases, making the identification of new antimicrobial compounds with novel mechanisms of action an urgent need (Tacconelli et al., 2018). This situation is even more worrisome for Gram-negative pathogens since they are endowed with an asymmetric outer membrane (OM), surrounding the inner membrane (IM) and delimiting a peptidoglycan-containing periplasmic space, that protects them from harmful hydrophobic compounds such as antibiotics (Nikaido, 2003). The peculiar permeability barrier properties of the OM are conferred by the presence of a layer of tightly packed molecules of lipopolysaccharide (LPS) in its outer leaflet (Raetz and Whitfield, 2002; Silhavy et al., 2010). LPS consists of three covalently linked moieties: lipid A, the conserved hydrophobic anchor of the molecule in the membrane; a core oligosaccharide; and a somewhat variable polysaccharide chain, termed *O* antigen (Raetz and Whitfield, 2002). The biosynthesis of the lipid A-core domain takes place at the cytoplasmic side of the IM, whereas the assembly of mature LPS occurs at the periplasmic side of the IM, after flipping of the lipid A-core across the IM by the essential transporter MsbA (Polissi and Georgopoulos, 1996; Raetz and Whitfield, 2002; Doerrler et al., 2004).

Translocation of LPS from the IM to the OM, across the periplasm, requires the activity of the LPS transport (Lpt) machinery. This assembly is a conserved multiprotein complex composed, in *Escherichia coli*, of seven essential proteins (LptA-G) that bridges the IM and OM (Wu et al., 2006; Sperandeo et al., 2007, 2008; Ruiz et al., 2008; Freinkman et al., 2012) (**Figure 1A**). The Lpt partners are organized in three sub-complexes, located in each cell envelope compartment (IM, periplasm, and OM), that interact with each other to allow the transport of LPS to the OM, shielding the hydrophobic moieties of lipid A in the hydrophilic environment of the periplasm (Sperandeo et al., 2008). At the IM, the ABC transporter $LptB_2FGC$ provides the energy for LPS extraction from the IM (Okuda et al., 2012; Li et al., 2019; Owens et al., 2019). The unconventional subunit LptC plays a dual role in the transporter, regulating the ATPase activity and providing the docking site for the periplasmic protein LptA at the membrane (Sperandeo et al., 2011; Owens et al., 2019). After extraction, LPS is transferred from LptC to LptA (Tran et al., 2010; Okuda et al., 2012), that then interacts at the OM with the periplasmic domain of LptD forming the bridge that connects the IM and OM (Okuda et al., 2016). LptA has the tendency to oligomerize *in vitro* (Suits et al., 2008; Merten et al., 2012; Santambrogio et al., 2013); however, the number of LptA monomers that constitute the Lpt bridge is still not known. At the OM, the translocon composed of the β-barrel protein LptD and the lipoprotein LptE receives LPS from LptA for its final assembly at the cell surface (Freinkman et al., 2011; Dong et al., 2014; Qiao et al., 2014). The interaction between the Lpt proteins is crucial in building a functional machinery (Sperandeo et al., 2011; Falchi et al., 2018) and is mediated by a conserved domain with a peculiar structural architecture (the β-jellyroll fold) shared by all the periplasmic domains of the Lpt proteins (LptF, LptG, LptC, LptA, and LptD) (Suits et al., 2008; Tran et al., 2010; Qiao et al., 2014). Alignment of the β-jellyroll folds of LptF, LptC, LptA, and LptD in a C-terminal-to-N-terminal arrangement is thought to allow the formation of a hydrophobic groove that spans the periplasm and accommodates the acyl chains of the LPS molecules during transport (Villa et al., 2013; Okuda et al., 2016; Sperandeo et al., 2019). Inhibition of bridge formation, as a consequence of Lpt protein depletion in conditional expression mutants or due to mutations that interfere with protein–protein interactions at any level in the system, results in cell growth arrest and blocking of Lpt, with accumulation of newly synthesized LPS in the IM and formation of membranous bodies in the periplasm (Wu et al., 2006; Sperandeo et al., 2007, 2008; Ruiz et al., 2008). Accumulated LPS molecules can be decorated at the periplasmic side of the IM by the addition of colanic acid units (Majdalani and Gottesman, 2005; Sperandeo et al., 2008, 2011). Overall, the Lpt mechanism mediated by the Lpt machinery has been compared to that of a PEZ candy dispenser, where a spring at the base of the dispenser loads the candy into the tube and pushes them up to the cap, which then opens to release them to the customer (Okuda et al., 2016). Interestingly, when the Lpt bridge is not properly assembled, LptA undergoes degradation, suggesting that the steady-state level of LptA in the cell, together with the appearance of colanic acid-modified LPS, are diagnostic of Lpt defects (Sperandeo et al., 2011).

Due to its relevance in Gram-negative bacteria cell physiology, LPS biogenesis can be considered a promising target for the development of novel antibacterial molecules. Potent inhibitors of the lipid A biosynthesis were identified in past studies and are continuously in development (Simpson and Trent, 2019). Moreover, two compounds targeting the MsbA-mediated IM translocation process have been recently reported (Ho et al., 2018; Zhang et al., 2018). However, the only inhibitor of LPS biogenesis to have entered, so far, Phase III trials is Murepavadin, a macrocyclic peptidomimetic selectively directed against *Pseudomonas aeruginosa* LptD (Srinivas et al., 2010; Lehman and Grabowicz, 2019). Unfortunately, the clinical trials have been suspended recently due to nephrotoxicity (Lehman and Grabowicz, 2019). Nevertheless, the identification of Murepavadin highlights the Lpt machinery as a good target for the discovery of molecules endowed with antibacterial activity.

Very recently, a screening strategy based on the yeast two-hybrid (YTH) system has allowed the isolation of a compound, IMB-881, that disrupts LptC–LptA interaction, exerting bactericidal activity against *E. coli* and other Enterobacterial species (Zhang et al., 2019).

Here we show the implementation of the Bacterial Adenylate Cyclase Two-Hybrid (BACTH) system (Karimova et al., 1998), based on the interaction-mediated reconstitution of the adenylate cyclase activity in *E. coli*, to allow the detection of LptC–LptA and LptA–LptA interactions in their native environment, the periplasm. We successfully reconstituted both interactions and

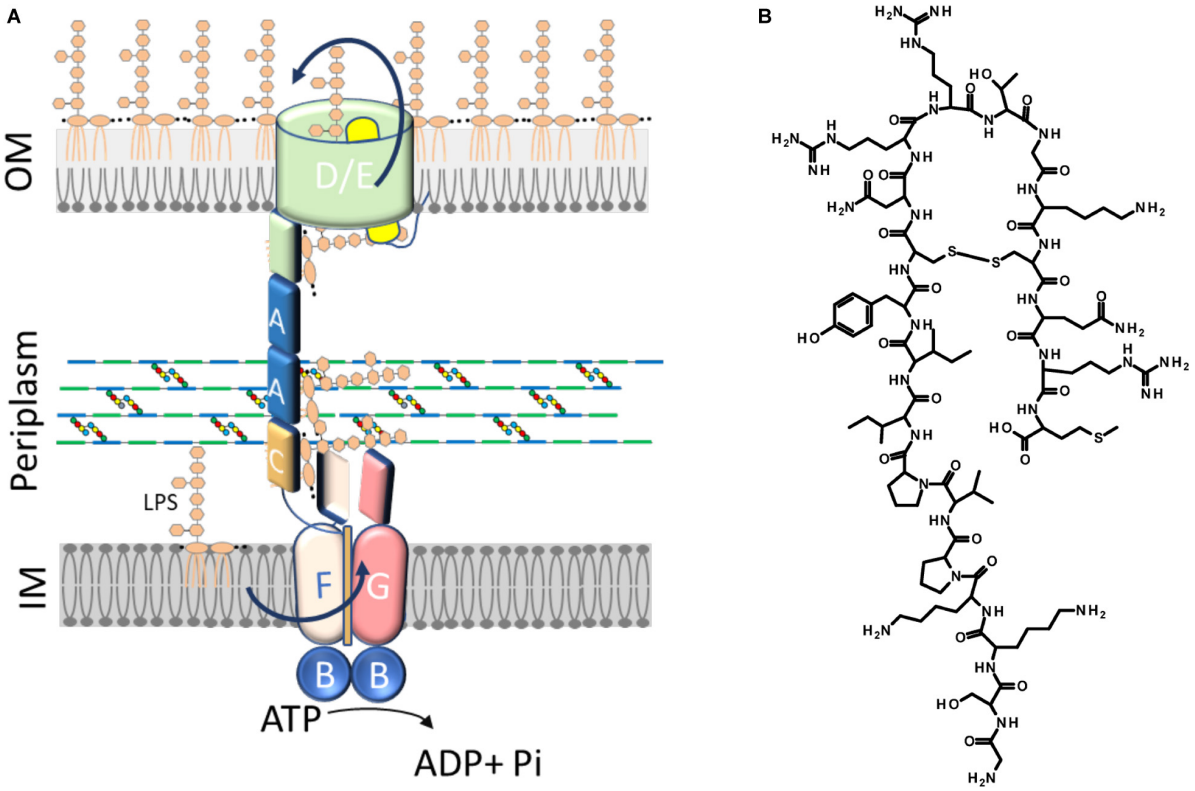

FIGURE 1 | The Lpt machinery and thanatin. **(A)** The lipopolysaccharide transport system in *Escherichia coli* consists of a seven-protein complex organized in an inner membrane (IM) ABC transporter ($LptB_2FGC$) and an outer membrane (OM) translocon (LptDE) connected by a periplasmic protein, LptA, that bridges the membranes. LptA is anchored to the IM through its interaction with LptC. The number of LptA molecules forming the bridge is not known. For clarity, only two molecules of LptA are depicted. **(B)** Structure of thanatin.

exploited this system to more thoroughly investigate the effect of the antimicrobial peptide thanatin.

Thanatin is a 21-residue inducible cationic defense peptide isolated from the hemipteran insect *Podisus maculiventris*, that contains one disulfide bond and exhibits a broad range of antibacterial and antifungal activity (Fehlbaum et al., 1996) (**Figure 1B**).

Important new insights into thanatin's mode of action against Gram-negative bacteria have been provided by a recent work showing that thanatin binds to *E. coli* LptA and LptD *in vivo* and *in vitro* (Vetterli et al., 2018). Accordingly, spontaneous thanatin-resistant mutants isolated in the same work share a single point mutation in the *lptA* gene, strongly indicating LptA as the major target of thanatin. Analysis of the nuclear magnetic resonance (NMR) structure of the LptA–thanatin complex reveals that the interaction occurs at the N-terminal β-strand of the β-jellyroll of LptA, region involved in LptA interaction with LptC and/or with another monomer of LptA (Suits et al., 2008; Freinkman et al., 2012). It has been thus speculated that thanatin might exert its antibacterial activity by interfering with the interactions established by LptA within the Lpt bridge (Vetterli et al., 2018). However, no evidence supporting this hypothesis has been published yet.

Our investigation provides more insights into thanatin's mode of action against Gram-negative bacteria showing that it interferes with LptC–LptA interaction *in vivo*. Disruption of the Lpt protein bridge is further supported by LptA degradation and appearance of LPS modified by colanic acid in thanatin treated cells. The results of this work strongly validate the assembly of the Lpt machinery as a promising target for the development of a novel class of antibacterial or adjuvant drugs.

MATERIALS AND METHODS

Bacterial Strains and Media

Escherichia coli strains and plasmids used in this study are listed in **Table 1**. AM604 genomic DNA was used as template for PCR and the XL1-Blue strain was used in all cloning steps. The strain MG1655 was used in the study of LptA stability and in the analysis of LPS profiles. BACTH assays were performed with the *E. coli* Δ*cya* strain BTH101 (Karimova et al., 1998; Ouellette et al., 2017). The strains M15/pREP4 and BL21(DE3) were used in the purification of $LptC_{24-191}$ (Sperandeo et al., 2011) and $LptA_m$ (Laguri et al., 2017), respectively. Bacteria were grown in Luria–Bertani (LB) medium (10 g/L tryptone, 5 g/L yeast extract, 10 g/L NaCl) or LB-agar medium (LB

medium with 10 g/L agar). When required, antibiotics or inducer were added at the following concentrations: ampicillin at 100 μg/mL, spectinomycin at 50 μg/mL, isopropyl-β-D-thiogalactopyranoside (IPTG) at 0.5 mM.

Plasmid Construction

To construct the recombinant plasmids used in the BACTH assay (listed in **Table 1**), the genes encoding the Lpt proteins of interest (or their subdomains) were PCR-amplified using the appropriate primer pairs, as listed in **Table 2**. The PCR products were then digested with the indicated restriction enzymes and subcloned into the corresponding sites of the pSTM25 and pUTM18C vectors. These BACTH vectors, expressing the T25 and T18 fragments of the adenylate cyclase toxin of *Bordetella pertussis* fused at their C-terminal ends with the first transmembrane domain of the *E. coli* OppB protein (TM), were employed in order to study protein interactions in the periplasm (Ouellette et al., 2014). In the recombinant plasmids pST25-LptC and pUT18C-LptC, full-length LptC (comprising its own transmembrane domain) was fused at the C-terminal end of the T25 and T18 fragments, respectively. MalE, LptA, and $LptA_m$ were fused to the C-terminal end of TM to originate the constructs pUTM18C-MalE, pSTM25-LptA, pUTM18C-LptA, pSTM25-$LptA_m$, and pUTM18C-$LptA_m$. The recombinant plasmids pSTM25-$LptA^{Q62L}$, pUTM18C-$LptA^{Q62L}$, and pUTM18C-$LptA_m{}^{Q62L}$ were constructed by using a Q5 site-directed mutagenesis kit (New England Biolabs) with the primer pair AP733-AP734. Transformation was performed in XL1-Blue electrocompetent cells and transformants were selected at 30°C on LB plates supplemented with the appropriate antibiotics (ampicillin or spectinomycin), and 0.4% glucose to repress expression. All the cloned DNA regions obtained by PCR were verified by sequencing.

Bacterial Adenylate Cyclase Two-Hybrid (BACTH) Assay

To study protein–protein interactions with the BACTH system, electrocompetent BTH101 cells were co-transformed with each pair of plasmids to be tested (**Figure 2A**), plated onto LB plates containing selective antibiotics (100 μg/mL ampicillin and 50 μg/mL spectinomycin) and incubated at 30°C for 24–48 h. Interaction efficiencies were quantified by determining the β-galactosidase activities in 96-well microtiter plates according to a protocol adapted from Paschos et al. (2011). For this measurement, at least eight clones from each plasmid combination were analyzed for β-galactosidase activity in two independent experiments. Each clone was inoculated in 1 mL of LB medium supplemented with antibiotics and 0.5 mM IPTG for overnight induction. The β-galactosidase activity was measured from 20 μL culture diluted in 80 μL PM2 buffer (70 mM Na_2HPO_4. $12H_20$, 30 mM NaH_2PO_4. H_2O, 1 mM $MgSO_4$, 0.2 mM $MnSO_4$, pH 7.0) containing 8 mg/mL *ortho*-nitrophenyl-β-galactoside (ONPG), 0.01% SDS, and 50 mM β-mercaptoethanol. Reaction mixtures were incubated at room temperature for 20–30 min or until a sufficiently yellow color had developed, and the reactions were stopped with 100 μL 1 M Na_2CO_3. The optical densities at 420 and 550 nm were recorded for each sample using a plate reader (EnSpire Multimode Plate Reader, PerkinElmer) and the specific activity was calculated with the formula: Miller units = $[OD_{420} - (1.75 \times OD_{550})]/[t \times OD_{600} \times (\text{volume in mL})] \times 1000$, where OD_{600} is the optical density at 600 nm after overnight incubation and t is the time in minutes needed for color formation.

Peptide Synthesis

Peptides were synthesized on a 0.1 mmol scale on a Wang resin 0.99 mmol/g. The first amino acid was attached to the resin following a protocol described in the literature (Avitabile et al., 2019). The peptides were then elongated on a Liberty Blue CEM synthesizer using standard protocols. At the end of the synthesis, the peptides were cleaved from the resin and protecting groups were removed by treating the resin with a solution of TFA/thioanisol/H_2O 95/2.5/2.5 v/v/v for 2 h. The peptides were then lyophilized. Wild type (WT) peptide was cyclized as reported by Fehlbaum et al. (1996). Peptides were purified by RP-HPLC on a Jupiter 10μ Proteo 90A° (100 × 21.20 mm) column using a gradient of CH_3CN (0.1% TFA) in H_2O (0.1% TFA) from 10 to 50% in 20 min and analyzed on a Vydamass C18 100A 5μ 150 × 4.6 mm column with the same gradient. Peptides were characterized by mass spectrometry on a Thermo Scientific LCQ Fleet ion trap. Pure peptides were then lyophilized three times, the first to eliminate HPLC solvents, the second from a solution 6/4 v/v H_2O /CH_3COOH, and the third in water.

Thanatin WT Cyclic

Sequence: GSKKPVPIIYCNRRTGKCQRM
Calculated mass (Da): 2433.95; found (Da): 1217.08 $[M+2H]^{2+}$; 812.33 $[M+3H]^{3+}$; 609.29 $[M+4H]^{4+}$

Thanatin Scramble (Scr)

Sequence: YVCIRMNKISPKQRTPGGRCK
Calculated mass (Da): 2435.95; found (Da): 1219.02 $[M+2H]^{2+}$; 813.47 $[M+3H]^{3+}$; 610.50 $[M+4H]^{4+}$

Determination of Minimal Inhibitory Concentration (MIC)

The minimal inhibitory concentration (MIC) values of thanatin, thanatin scramble, and vancomycin (as a positive control) were assessed with a protocol adapted from Wiegand et al. (2008) using 96-well microtiter plates. Stationary phase cultures of the *E. coli* WT strain MG1655 (Blattner et al., 1997), the permeabilized mutants AS19 (Sekiguchi and Iida, 1967) and NR698 (Ruiz et al., 2005), and the BACTH strain BTH101 (Karimova et al., 1998; Ouellette et al., 2017) grown at 37°C in LB medium, were diluted in fresh medium adjusting the OD_{600} to a value of 0.05 and incubated in the presence of twofold decreasing concentrations of the compounds ranging from 64 μg/mL to 62.5 ng/mL. After 24 h of incubation at 37°C, the OD_{600} was measured by a plate reader (EnSpire Multimode Plate Reader, PerkinElmer). The MIC value was determined as the lowest concentration of compound leading to no detectable growth.

TABLE 1 | *Escherichia coli* strains and plasmids.

Strain or plasmid	Relevant genotype or description		Source or references
Strains			
MG1655	K-12, F^- λ^- *ilvG*$^-$ *rfb-50 rph-1*		Blattner et al., 1997
AM604	MC4100 ara $^+$		Wu et al., 2006
AS19	*E. coli* strain B, hyperpermeable strain		Sekiguchi and Iida, 1967
NR698	*imp4213*		Ruiz et al., 2005
XL1-Blue	*recA1 endA1 gyrA96* (Nal^R) *thi-1 hsdR17 supE44 relA1 lac* [F' *proAB lacI*^{q}*ZΔM15* Tn*10* (Tet^R)]		NEB
BTH101	F^- *cya-99 araD139 galE15 galK16 rpsL1* (*Str*^{R}) *hsdR2 mcrA1 mcrB1*		Karimova et al., 1998; Ouellette et al., 2017
M15/pREP4	F^- *lac thi mtl*/pREP4		QIAGEN
BL21(DE3)	F^- *ompT gal dcm lon hsdS*$_B$(r_B^- m_B^-) (λDE3 *[lacI lacUV5-T7 gene 1 ind1 Sam7 nin5]*)		Studier and Moffatt, 1986
Plasmids		ori	
pSTM25	*aadA* P_{lac}::*t25-TM*	p15A	Ouellette et al., 2014
pUTM18C	*bla* P_{lac}::*t18-TM*	ColE1	Ouellette et al., 2014
pUTM18C-MalE	*malE* sequence (residues 27–396) cloned downstream T18-TM	ColE1	This study
pSTM25-LptA$_m$	*lptA* sequence (residues 28–159) cloned downstream T25-TM	p15A	This study
pUTM18C-LptA$_m$	*lptA* sequence (residues 28–159) cloned downstream T18-TM	ColE1	This study
pUTM18C-LptA$_m^{Q62L}$	*lptA* sequence (residues 28–159) bearing a Q-to-L mutation at position 62 cloned downstream T18-TM	ColE1	This study
pSTM25-LptA	*lptA* sequence (residues 28–185) cloned downstream T25-TM	p15A	This study
pSTM25-LptA^{Q62L}	*lptA* sequence (residues 28–185) bearing a Q-to-L mutation at position 62 cloned downstream T25-TM	p15A	This study
pUTM18C-LptA	*lptA* sequence (residues 28–185) cloned downstream T18-TM	ColE1	This study
pUTM18C-LptA^{Q62L}	*lptA* sequence (residues 28–185) bearing a Q-to-L mutation at position 62 cloned downstream T18-TM	ColE1	This study
pST25-LptC	*lptC* full-length sequence cloned downstream T25	p15A	This study
pUT18C-LptC	*lptC* full-length sequence cloned downstream T18	ColE1	This study
pQEsH-*lptC*	pQE30 (QIAGEN) derivative, expresses His_6-$LptC_{24-191}$; *bla*		Sperandeo et al., 2011
pET-LptAΔ$_{160-185}$ –H	*pT7-lptA*Δ$_{160-185}$ -His_6; *bla*		Laguri et al., 2017

TABLE 2 | Oligonucleotides.

Name		Sequence (5′–3′)[a]	Used to make
AP576	Reverse	attgtggatccTTAAGGCTGAGTTTGTTTG	*lptC* cloning in pSTM25 and pUTM18C; BamHI
AP579	Forward	taatgtcgacgAAAATCGAAGAAGGTAAACTG	*malE* cloning in pUTM18C; SalI
AP580	Reverse	aaggatctagaTTACTTGGTGATACGAGTCTGC	*malE* cloning in pUTM18C; XbaI
AP581	Forward	gagacgagctcgGTAACCGGAGACACTGATCAG	*lptA* and *lptA*$_m$ cloning in pUTM18C; SacI
AP582	Reverse	gagaggaattcTTAATTACCCTTCTTCTGTGC	*lptA* cloning in pUTM18C; EcoRI
AP665	Reverse	gagaggaattcTTAGCGCTTGCCTTTGTCG	*lptA*$_m$ cloning in pUTM18C; EcoRI
AP666	Forward	aaggatctagagGTAACCGGAGACACTGATCAG	*lptA* cloning in pSTM25; XbaI
AP667	Reverse	attgtggatccTTAATTACCCTTCTTCTGTGC	*lptA* cloning in pSTM25; BamHI
AP688	Reverse	attgtggatccTTAGCGCTTGCCTTTGTCG	*lptA*$_m$ cloning in pSTM25; BamHI
AP689	Forward	gaagatctgcagggATGAGTAAAGCCAGACGTTG	*lptC* cloning in pSTM25; PstI
AP690	Forward	gaagatctgcaggATGAGTAAAGCCAGACGTTG	*lptC* cloning in pUTM18C; PstI
AP733	Forward	ATCGTCACC**CTG**GGCACCATC	Q62L mutagenesis in *lptA*
AP734	Reverse	GACATTACCGGTAAAGGTAACC	Q62L mutagenesis in *lptA*

[a] *E. coli genomic sequence in uppercase; restriction sites in underlined lowercase; codon mutated by site-directed mutagenesis in bold.*

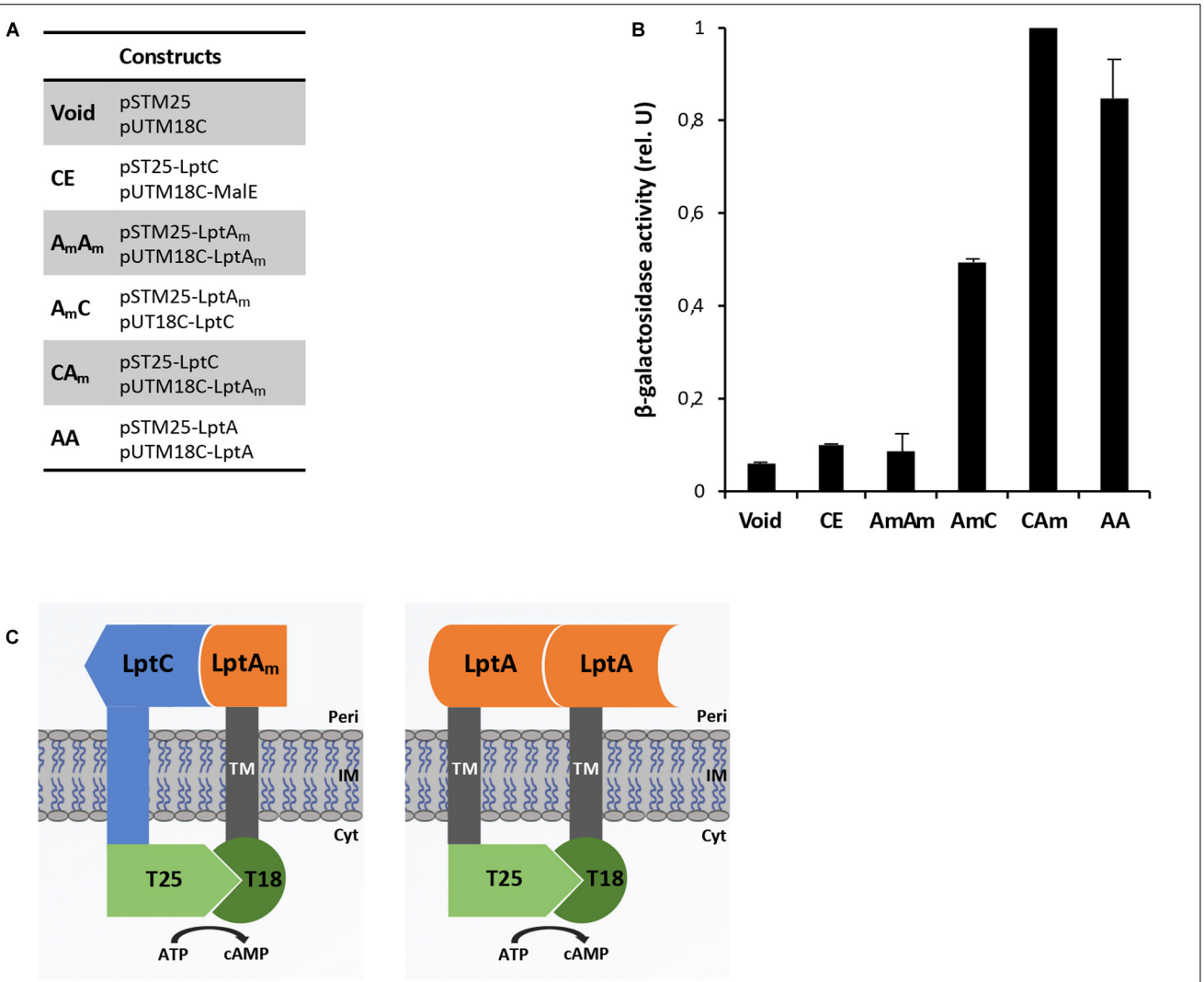

FIGURE 2 | BACTH analysis of interactions between the tested combinations. **(A)** List of constructs co-expressed in the BTH101 strain for BACTH analysis. **(B)** β-Galactosidase activities are the results of at least two independent experiments in cells grown overnight in selective medium supplemented with IPTG. All values were normalized by the average activity obtained for T25LptC–TM18LptA$_m$ (CA$_m$) interaction. Each bar represents the mean value with standard deviation. **(C)** Schematic representation of the interactions T25LptC–TM18LptA$_m$ (CA$_m$) and TM25LptA–TM18LptA (AA). Full length LptC and truncated LptA were cloned in frame to the T25 and T18 fragments, respectively (left diagram). Full length LptA was fused in frame to both adenylate cyclase fragments (right diagram). TM indicates the transmembrane domain of OppB from *E. coli*. Peri, periplasm; IM, inner membrane; Cyt, cytoplasm.

Analysis of Thanatin's Effect on Lpt Protein Interactions Using the BACTH Assay

To assess thanatin's effect on the periplasmic interactions LptA–LptA and LptC–LptA$_m$, at least four clones from each combination were cultured in LB medium supplemented with antibiotics at 37°C to an OD$_{600}$ around 1.0. These precultures were used to inoculate 1 mL of LB medium supplemented with antibiotics, 0.5 mM IPTG, and thanatin at different concentrations to an OD$_{600}$ of 0.05; and the cultures were incubated for 18 h (overnight) at 30°C. After overnight induction of the expression of the hybrid proteins, the β-galactosidase activities were determined. For the clones expressing the BACTH combination T25LptC-TM18LptA$_m$, thanatin was tested at 0.7, 1.0, and 1.4 μg/mL. For the TM25LptA–TM18LptA pair, a higher concentration of thanatin could be added to the cultures without affecting bacterial growth; thus, values of 0.7, 1.0, 1.4, and 2.8 μg/mL were tested. A scrambled version of thanatin (Scr) was also employed in this assay at the same concentrations as a control for the specificity of interaction inhibition.

Protein Production and Purification

Escherichia coli LptC lacking the first 23 residues of the transmembrane domain was expressed from a plasmid (LptC pQESH, QIAGEN) with an N-terminal His-Tag and purified as described (Laguri et al., 2017). LptC was expressed in ^{15}N enriched deuterated medium with specific ^{13}C-^{1}H labeling of

Isoleucines δ1 and Leucine and Valine proR methyl groups according to standard protocols (Kerfah et al., 2015) with NMRbio precursors[1]. LptA$_m$ coding for residues 28–159 followed by a SGRVEHHHHHH TAG in a pET21b vector was expressed and purified as described (Laguri et al., 2017). Both proteins were exchanged to 50 mM Na_2HPO_4 pH 8.0, 150 mM NaCl buffer.

NMR Spectroscopy

Nuclear magnetic resonance experiments were recorded at 25°C on Bruker 600 MHz spectrometer equipped with a triple resonance cryoprobe. 2D-[^{1}H, ^{13}C]-methyl-SOFAST experiments were recorded to follow LptC methyl groups on LptC $^{15}N^2H$ and ^{13}C-^1H specifically labeled on Iδ1, Lδ1, and Vγ1 at 20 μM prepared in 50 mM Na_2HPO_4 pH 8.0, 150 mM NaCl buffer with 10% D_2O. Unlabeled LptA$_m$ at 40 μM prepared in the exact same buffer was added to LptC to achieve 100% of LptC complexed with LptA$_m$. Thanatin or Scr at 42 μM was added to the complex and interaction experiments were followed using 2D-[^{1}H, ^{13}C]-methyl-SOFAST experiments. NMR experiments were processed and analyzed using Topspin 3.2 and CcpNmr 2.4.

Biacore Experiments

Surface plasmon resonance (SPR) experiments were performed on a Biacore T200 with a CM3 chip. HBS-P+ and HBS-N buffers (GE Healthcare) were used for immobilization and interactions, respectively. 66 Resonance units (RUs) of LptA$_m$ were immobilized on a flow cell by the amine (EDC-NHS) coupling method followed by ethanolamine saturation, with a flow cell modified only with EDC-NHS-ethanolamine as reference for subtractions. For interactions, protein and ligands were diluted in HBS-N running buffer and regeneration between injections achieved with a 30 s pulse of 10 mM HCl. Sensorgrams shown were subtracted with the reference flow cell as well as with injection of buffer alone. Determination of LptC–LptA$_m$ Kd was performed by injecting increasing concentrations of LptC (5.6–100 μM) over immobilized LptA$_m$. Kinetics analysis of the data was unsuccessful due to very fast association, and the Kd was determined from steady-state binding levels obtained at the end of the association phase with Bioeval software (GE Healthcare).

Determination of LptA, LptD, and LptB Steady-State Levels Upon Thanatin Treatment

LptA, LptD, and LptB (as loading control) steady-state levels were assessed in the MG1655 strain by western blot analysis with polyclonal antibodies raised in rabbit against LptA, LptD, and LptB. Bacterial cultures were grown at 37°C in LB medium. At OD_{600} 0.1, the cells were treated or not with 5.25 μg/mL of thanatin (1.5 × MIC). Cell growth was monitored by measuring the OD_{600} value at 30-min intervals and viability was determined by quantifying the colony-forming units (CFU) at 1-h intervals during a time period of 4 h. Whole-cell extracts for protein analysis were collected and harvested by centrifugation (5000 *g*, 10 min) 20, 30, 40, 60, and 120 min after treatment with thanatin. The cell pellets were resuspended in a volume (in mL) of SDS Laemmli buffer equal to 1/24 of the total optical density of the sample. The samples were boiled for 5 min and equal volumes (15 μL) were separated by 12.5% SDS-PAGE. Proteins were transferred onto nitrocellulose membranes (GE Healthcare), and immunodecoration was performed as previously described (Sperandeo et al., 2007). Polyclonal antibodies raised against LptA (GenScript Corporation), LptD (GenScript Corporation), and LptB (kindly provided by D. Kahne and N. Ruiz) were used as primary antibodies at dilutions of 1:1,000, 1:500, and 1:10,000, respectively. As secondary antibody, goat anti-rabbit immunoglobulin (Li-Cor) was used at a dilution of 1:15,000. Bands were visualized by an Odyssey Fc imaging system (Li-Cor GmbH).

LPS Analysis From Whole-Cell Extracts

Whole-cell extract samples for LPS analysis were obtained as described in the previous section. For LPS visualization, equal volumes (20 μL) of whole-cell extracts were digested with 6 μg of proteinase K (Sigma–Aldrich) at 60°C for 1 h and then separated by 18% Tricine SDS-PAGE (Lesse et al., 1990). Immunodecoration was performed using anti-LPS core WN1 222-5 monoclonal antibodies (Hycult Biotech) at a dilution of 1:500. As secondary antibody, goat anti-mouse immunoglobulin G-peroxidase (HRP) conjugate (Sigma–Aldrich) was used at a dilution of 1:5000.

RESULTS

Adaptation of the BACTH Assay for the Detection of Lpt Protein Interactions in the Periplasm

The BACTH system was implemented in this work to allow the detection *in vivo* of two crucial protein-protein interactions within the Lpt interactome, namely, LptC–LptA and LptA–LptA. The BACTH assay is based on the interaction-mediated reconstitution of the adenylate cyclase activity of the toxin of *B. pertussis*, whose catalytic domain can be divided in two complementary fragments, T25 and T18 (Karimova et al., 1998; Battesti and Bouveret, 2012). In this work, we used the BACTH vectors expressing these fragments fused in frame with the first transmembrane domain of the *E. coli* OppB protein (TM) (pSTM25 and pUTM18C). These plasmids allow expression of the targeted protein domains fused to TM25 and TM18 into the periplasm (Ouellette et al., 2014) which reflects the physiological environment of the tested interactions. To detect LptA–LptA dimerization, LptA was subcloned into both BACTH vectors at the C-terminal end of the TM, originating the hybrid TM25LptA and TM18LptA proteins. To detect LptC–LptA association, we fused at the C-terminal end of the TM a truncated monomeric version of LptA, referred to as LptA$_m$, that lacks the last C-terminal β-strand and is not able to self-oligomerize, although still functional *in vivo* (Laguri et al., 2017). We decided to use LptA$_m$ to avoid titration of the fusion protein caused by

[1]http://www.nmr-bio.com/

interaction of LptA with itself, leading to a decrease in the β-galactosidase signal when testing LptC–LptA interaction with the BACTH technique. Full-length LptC was subcloned into both pSTM25 and pUTM18C vectors, in frame with the C-terminal end of the adenylate cyclase fragments, to obtain the constructs T25LptC and T18LptC.

As negative controls for the assay, we used: (i) the combination between the void plasmids pSTM25 and pUTM18C; (ii) the non-productive LptA$_m$–LptA$_m$ association; and (iii) the association LptC–MalE, between LptC and the unrelated periplasmic binding subunit of the *E. coli* maltose transporter, MalE (Davidson et al., 1992; Ehrmann et al., 1998). Constructs were transformed into the adenylate cyclase-deficient strain BTH101 and the efficiency of interaction between the various protein fusions was quantified by measuring the β-galactosidase activity. The results for the BACTH complementation assay are presented in **Figures 2A,B**. As expected, LptC–MalE combination did not produce a positive interaction signal, confirming that the BACTH system is suitable to detect specific interactions occurring in the periplasm. Also, truncated LptA was confirmed to be unable to oligomerize. We successfully detected *in vivo* the LptC–LptA$_m$ interaction and the dimerization of LptA (schematic representation in **Figure 2C**). The signal obtained for the pair T25LptC–TM18LptA$_m$ (CA$_m$) was twofold higher than the one obtained for the complementary combination TM25LptA$_m$–T18LptC (A$_m$C). This effect is not surprising since it was previously reported that β-galactosidase measurements may significantly vary according to the T25 and T18 combination chosen for the BACTH assay (Ouellette et al., 2017). Indeed, when testing the LptC–LptA$_m$ interaction, hybrid LptA$_m$ can be titrated away from the reaction by interaction through its N-terminal with native LptA. This effect is likely even more significant in the TM25LptA$_m$–T18LptC configuration, where LptA$_m$ is expressed from a low-copy number vector (pSTM25), thus further diminishing the number of hybrid LptA$_m$ proteins free to interact with LptC and accounting for the lower β-galactosidase signal observed in A$_m$C combination. Therefore, we decided to use the pair of constructs T25LptC–TM18LptA$_m$ in further tests. It should be noted that in our assay, the interaction of full-length LptA with itself (LptA–LptA) produced a lower β-galactosidase activity signal compared to LptC–LptA$_m$. This is consistent with previously published *in vitro* measurements revealing that the affinity between LptA and LptC is stronger than the affinity for LptA oligomerization (Schultz et al., 2013).

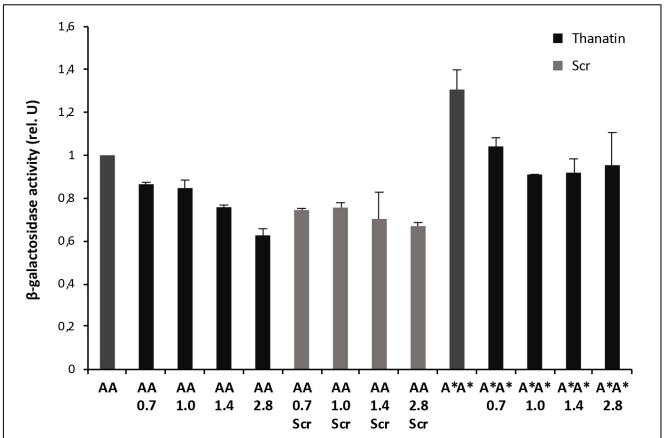

FIGURE 3 | Thanatin's effect on LptA–LptA (AA) and LptA^{Q62L}–LptA^{Q62L} (A*A*) interactions. Thanatin and thanatin scramble (Scr) were tested at concentrations ranging from 0.7 to 2.8 μg/mL. All values were normalized by the average activity obtained for the untreated LptA–LptA interaction. Values are averages of at least eight technical replicates from two independent experiments ± standard deviation.

Thanatin Inhibits LptC–LptA$_m$ and LptA–LptA Interactions *in vivo*

Interaction between the antibacterial peptide thanatin and LptA was recently demonstrated and NMR experiments clearly showed that the N-terminal strand of the β-hairpin of thanatin docks in parallel orientation onto the first N-terminal β-strand of the β-jellyroll of LptA (Vetterli et al., 2018). It is well known from structural studies that dimerization of LptA monomers with themselves or with LptC involves the N-terminal edge strand of the β-jellyroll of LptA (Suits et al., 2008; Schultz et al., 2013; Laguri et al., 2017). Thanatin's binding site therefore overlaps with the interaction site of LptA with another LptA subunit in the homodimer LptA–LptA and with LptC in the heterodimer LptA–LptC, suggesting a possible mechanism for the antibacterial activity. We thus analyzed the effect of thanatin on these interactions with the adapted BACTH assay and used a scrambled version of thanatin, characterized by the same amino acid composition but with a different sequence (thanatin scramble, Scr), as specificity control (**Figures 3**, **4**). The MIC of thanatin and thanatin scramble was assessed against WT MG1655, and permeabilized AS19 and NR698 *E. coli* strains. The MIC values were 1.8–3.5 and above 64 μg/mL for thanatin and thanatin scramble, respectively, when tested against the WT MG1655 strain (**Table 3**). Slightly lower MIC values were obtained for thanatin when tested against the permeabilized *E. coli* mutants (0.1–0.4 μg/mL). On the contrary, no significant difference relative to the WT strain was observed in the MIC values of thanatin scramble when tested against the permeabilized mutant strains, suggesting that the lower activity of the peptide cannot be attributed to its inability to cross the OM barrier.

To explore whether thanatin's antibacterial activity is due to the inhibition of LptA interaction with itself or with LptC, we evaluated the effect of increasing sub-MIC concentrations of the peptide on the TM25LptA–TM18LptA and T25LptC–TM18LptA$_m$ associations and the results are presented in **Figures 3**, **4**, respectively. After overnight induction of the fusion proteins in the presence of thanatin, we could observe inhibition not only of LptA–LptA dimerization but also of LptC–LptA$_m$ interaction, but the inhibitory effect was much greater on the latter. A clear dose-dependent response could only be observed in the inhibition of LptC–LptA$_m$ interaction. The thanatin scramble was not capable of disrupting these periplasmic interactions in a dose-dependent manner, indicating that this is an effect specific to thanatin secondary and tertiary structures rather than to any cationic peptide with the same amino acid composition.

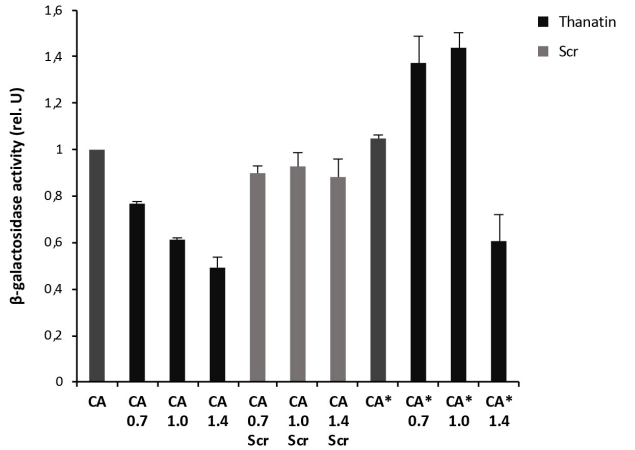

FIGURE 4 | Thanatin's effect on LptC–LptA$_m$ (CA) and LptC–LptA$_m{}^{Q62L}$ (CA*) interactions. Thanatin and thanatin scramble (Scr) were tested at concentrations ranging from 0.7 to 1.4 μg/mL. All values were normalized by the average activity obtained for the untreated interaction LptC–LptA$_m$. Values are averages of at least eight technical replicates from two independent experiments ± standard deviation.

TABLE 3 | Minimal inhibitory concentrations (MICs) in μg/mL of thanatin, thanatin scramble, and vancomycin.

	MIC (μg/mL)		
Strains	**Thanatin**	**Thanatin scramble**	**Vancomycin**
MG1655	1.8–3.5	>64	>64
AS19	0.1–0.2	64	4.0–8.0
NR698	0.1–0.4	32–64	0.5–1.0
BTH101	3.5	>64	>64

Compounds were tested against wild-type (MG1655) and permeable (AS19 and NR698) Escherichia coli strains. The BTH101 strain used in the BACTH assay was also tested. The data are representative of three biological replicates.

We also tested a previously isolated thanatin-resistant mutant presenting a glutamine to leucine substitution at position 62 in the LptA protein (*lptA*^{Q62L} allele) (Vetterli et al., 2018). The *lptA-Q62L* mutation was introduced into the BACTH constructs and tested as described above (**Figures 3**, **4**). The data obtained suggest that Q62L mutation in LptA specifically impairs the ability of thanatin to disrupt LptC–LptA$_m{}^{Q62L}$ (CA*) association, since the peptide is not effective against CA* at concentrations at which it is active against the WT CA pair, namely, 0.7 and 1 μg/mL (**Figure 4**). It should be noted that Q62L mutation exerts an unexpected stabilizing effect on LptA^{Q62L}–LptA^{Q62L} (A*A*) interaction, resulting in a β-galactosidase signal higher than that of the WT LptA–LptA combination. This effect is abolished upon treatment with thanatin, although not in a dose-dependent manner (**Figure 3**). Residue Q62 is not directly involved in the interaction of LptA with another LptA monomer, LptC, or with thanatin but belongs to a loop of the β-jellyroll of LptA that comes into contact with the short N-terminal α-helix of the WT protein upon thanatin interaction (Vetterli et al., 2018). This effect could be explained assuming that Q62L mutation induces a conformational change in the N-terminal region of LptA, which alters the way all these three interactions occur. Since thanatin's binding site overlaps the binding site of LptA with another LptA protein, if the Q62L mutation somehow alters thanatin's binding, then it is possible that it also alters the interaction of LptA^{Q62L} with itself, perhaps by strengthening it.

A similar stabilizing effect is also observed when testing the LptC–LptA$_m{}^{Q62L}$ combination. However, in this case, the effect is observed only upon treatment with low concentrations of thanatin, since the β-galactosidase signal of non-treated CA* is comparable to that of the WT (**Figure 4**). This suggests that LptA$_m{}^{Q62L}$ is still able to bind thanatin and this binding determines a conformational change in the protein that somehow enhances the stability of LptC–LptA$_m{}^{Q62L}$ complex. At higher thanatin concentrations, however, it seems that the inhibitory effect of the peptide on LptC–LptA$_m{}^{Q62L}$ prevails over the stabilizing effect. This could be explained by hypothesizing that Q62L mutation in LptA creates a secondary high-affinity binding site for thanatin. According to this hypothesis, when low concentrations of thanatin are added, thanatin binds to the high-affinity site, leaving the binding site for LptC unoccupied (and possibly stabilizing LptC–LptA$_m{}^{Q62L}$ complex). On the contrary, when higher concentrations of thanatin are used, all the available binding sites are occupied, thus impairing LptC–LptA complex formation.

Thanatin Disrupts LptC–LptA$_m$ Interaction *in vitro*

Thanatin's ability to interfere with LptC–LptA complex formation was assessed by NMR and SPR. For these assays, the monomeric version of LptA (LptA$_m$) was used to neglect the oligomerization of LptA. ^{1}H-^{13}C NMR of the specifically labeled Isoleucines of LptC efficiently report on the interaction with LptA (Laguri et al., 2017). In particular, Isoleucines 175 (175Ile) and 184 (184Ile) δ1 methyl groups at the C-terminus of LptC and in the vicinity of the binding interface change chemical shifts upon formation of the complex with LptA$_m$ (**Figure 5A**, left panel). After adding thanatin to the LptC–LptA$_m$ complex, we observed that 175Ile and 184Ile peaks completely shifted to a frequency corresponding to free LptC, indicating a total disruption of LptC–LptA$_m$ dimers (**Figure 5A**, right panel). The same experiment performed with the thanatin scramble (Scr) showed no disruption of the LptC–LptA$_m$ complex, suggesting specific competition and disruption of the binding interface by the thanatin (**Figure 5A**, right panel).

Complex disruption was also probed by SPR, in which the surface of a chip was functionalized with LptA$_m$. First, we confirmed the binding of LptC to the immobilized LptA$_m$ (**Supplementary Figure S1**A) and we determined the Kd of the interaction (Kd = 80 ± 44 μM). Then, to assess thanatin's effect, we injected thanatin over LptA$_m$ and confirmed stable interaction with LptA$_m$ on the surface, followed by the injection of LptC (**Figure 5B**, upper panels). We observed that, upon LptC injection, the response values decreased in a dose-dependent manner to the thanatin injected in the system (in concentrations up to 1 μM), indicating fewer surface-free LptA$_m$ epitopes

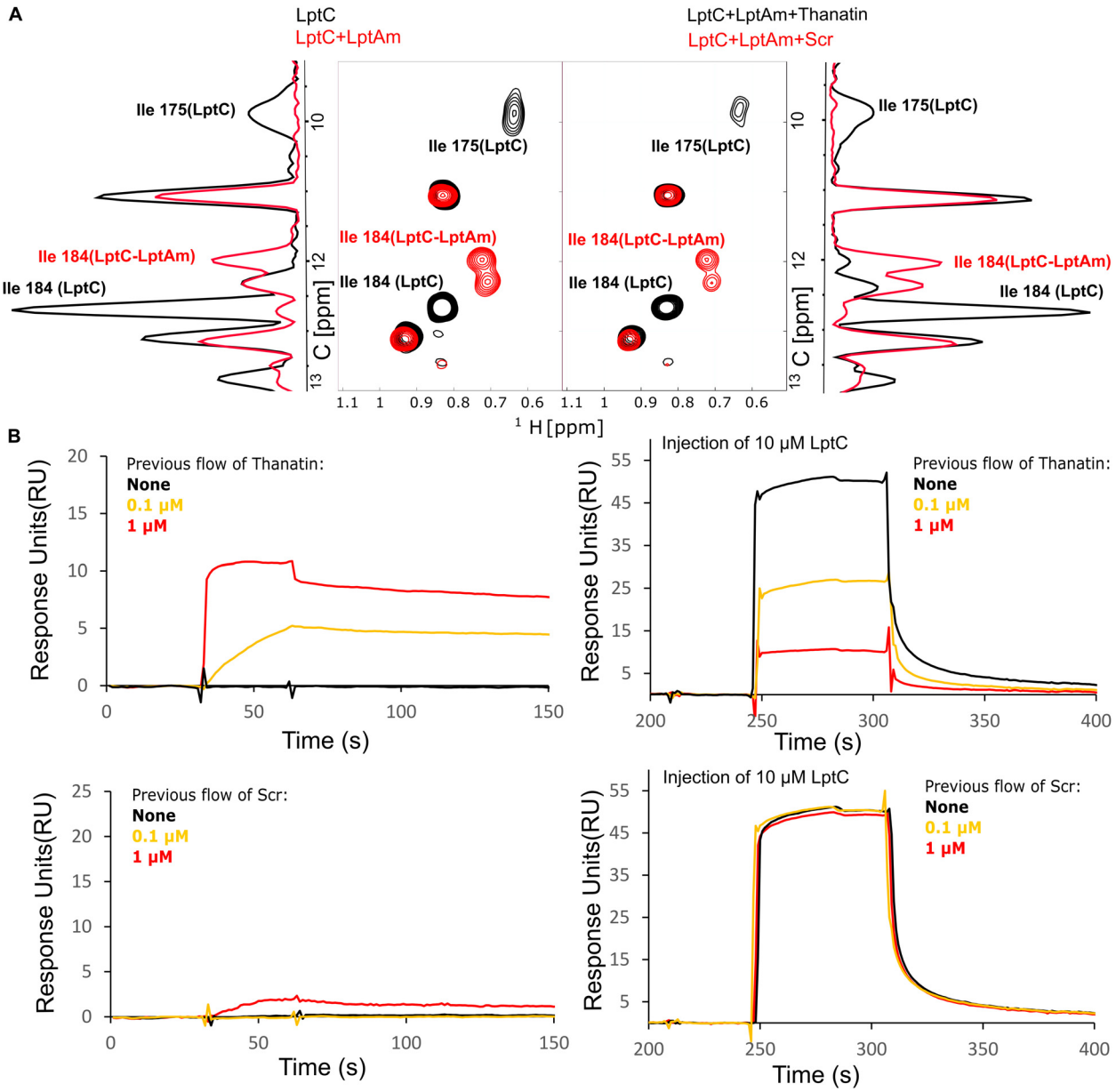

FIGURE 5 | LptC–LptA interaction is specifically disrupted by thanatin. **(A)** [^{1}H, ^{13}C]-correlation spectra of methyl labeled LptC in absence (black) and presence (red) of two molar equivalents of LptA$_m$, focused on Isoleucines in black for signals corresponding to isolated LptC and in red for LptC in complex with LptA$_m$ (left panel). A 1D-^{13}C projection of the 2D experiment is shown on the side for clarity. On the right panel, addition of thanatin disrupts LptC–LptA$_m$ interaction originating signals characteristic of LptC alone (black). Thanatin scramble (Scr) did not change LptC–LptA$_m$ spectra, indicating intact LptC–LptA$_m$ complexes (red). **(B)** Monitoring of LptC–LptA$_m$ interaction upon thanatin treatment by SPR. (Left panels) Thanatin or Scr were injected over surface-immobilized LptA$_m$, with concentrations following a color-code in bold: 0 (black), 0.1 µM (yellow), or 1 µM (red). Thanatin interacts strongly with LptA$_m$ presenting rapid association and slow dissociation. (Right panels) For clarity, after previous injections with the same concentrations of thanatin/Scr, sensorgrams were readjusted to 0, followed by LptC injection at 10 µM and recording. Binding of LptC to immobilized LptA$_m$ is reduced with increasing thanatin concentrations previously flowed (maximum at 1 µM), while Scr displays no effect.

available to interact with LptC (**Figure 5B**, upper right panel). The same experiment with the scrambled version showed no or little binding of Scr to immobilized LptA$_m$ and hence no effect on LptC binding (**Figure 5B**, lower panels), further demonstrating a specific effect of thanatin in preventing the formation of LptC–LptA$_m$ complex.

Thanatin Treatment Results in LptA Degradation and LPS Modification

Depletion of components of the IM and OM Lpt sub-complexes results in LptA degradation, which has been proposed to be a marker of incorrect complex assembly (Sperandeo et al., 2011).

We reasoned that the disruption of LptC–LptA interaction by thanatin treatment could impair Lpt complex assembly. Therefore, we evaluated the LptA steady-state levels in *E. coli* WT cells upon treatment with thanatin. Samples were taken at different time points within 2 h from MG1655 cultures grown in the presence or absence of thanatin at 5.25 μg/mL (1.5 × MIC) and analyzed by western blotting using anti-LptA antibodies. The abundance of LptD, the OM docking element of LptA, was also assessed and the level of LptB was used as a sample loading control. Culture growth and cell viability were monitored by OD_{600} measurement and determination of CFU, respectively, for a time span of 4 h. In cultures treated with thanatin, we observed a decrease in the OD_{600} with minor effect on cell viability (**Figure 6A**). As shown in **Figure 6B**, substantial LptA degradation occurs within 60 min of incubation with thanatin and, after 120 min, the steady-state level of LptA is very low and almost undetectable with our antibody preparation. The abundance of LptD did not change over time, indicating that the steady-state level of this OM component is not affected by thanatin treatment. The decrease in LptA level suggests that the IM and OM are not properly bridged when cells are treated with thanatin.

Depletion of any Lpt component leads to the accumulation of LPS decorated with colanic acid repeating units at the IM outer leaflet (Ruiz et al., 2008; Sperandeo et al., 2008). This phenotype is diagnostic of defects in Lpt occurring after MsbA-mediated flipping of lipid A-core across the IM. We therefore tested whether treatment with thanatin would induce similar LPS modifications. As shown in **Figure 6C**, LPS decorated with colanic acid, migrating as ladder-like bands in gel electrophoresis, was detected 120 min after adding thanatin to the culture; no LPS modification was observed in untreated cells. These data suggest that thanatin, by disrupting the LptC–LptA interaction, impairs Lpt complex assembly leading to the accumulation of LPS at the periplasmic side of the IM, where it is decorated with colanic acid. The observed LPS profile, together with the LptA degradation kinetic, strongly suggests that the disruption of the Lpt protein bridge could be the major killing mechanism of thanatin against Gram-negative bacteria.

DISCUSSION

The LPS export pathway is a valuable target for novel antibiotic discovery. Murepavadin, a macrocyclic peptidomimetic, has thus far been the most promising antibiotic candidate targeting the Lpt machinery. It was originally identified from a library of structural mimics of class I CAMP (cationic antimicrobial peptide) protegrin and later found to target the β-barrel OM protein LptD (Srinivas et al., 2010; Werneburg et al., 2012; Andolina et al., 2018).

Recent efforts to target the Lpt pathway have led to the identification, through a YTH assay, of IMB-881 as a synthetic molecule inhibiting LptC–LptA interaction (Zhang et al., 2019). The inhibitory activity of IMB-881 further suggests that interfering with the Lpt interactome is a good strategy to prevent Lpt to the cell surface. Nevertheless, in the YTH system, LptC–LptA interaction occurs in the cytoplasm of a yeast cell, and molecules active in this system may not be able to permeate the bacterial OM. To improve the screening system, we here implemented the BACTH assay (Karimova et al., 1998; Ouellette et al., 2014, 2017) that enables targeting of Lpt protein interactions in their native environment, preserving both protein functionality and folding state. This bacterial two-hybrid technique was used to probe LpC–LptA and LptA–LptA interactions. LptC has an important structural role in the Lpt machinery as it serves as the docking site for LptA binding to the IM $LptB_2FGC$ complex (Sperandeo et al., 2011; Freinkman et al., 2012). Indeed, mutations in LptC compromising interaction with LptA are lethal (Sperandeo et al., 2011; Villa et al., 2013). LptA molecules have a strong tendency to oligomerize in solution (Suits et al., 2008; Merten et al., 2012; Santambrogio et al., 2013) but we still do not know whether LptA self-oligomerization has a physiological relevance, since a monomeric LptA is still able to partially support cell growth (Laguri et al., 2017). In the BACTH assay, LptC–LptA interaction appears stronger than LptA–LptA dimerization, in line with the reported *in vitro* affinities (Schultz et al., 2013); however, we cannot exclude that the observed lower β-galactosidase signal could also be due to the formation of non-productive interactions between LptA molecules fused to the same (T25 or T18) adenylate cyclase fragment. The assay seems robust as no association is detected between unrelated non-interacting proteins: LptC and the maltose periplasmic binding protein MalE (Davidson et al., 1992) or between oligomerization deficient $LptA_m$ proteins (Laguri et al., 2017).

The BACTH system was also employed to explore the mechanism of action of thanatin, an antimicrobial peptide recently shown to bind the first β-strand of LptA (Vetterli et al., 2018). Thanatin inhibits LptC–LptA interaction in a dose-dependent manner, whereas very little and non-dose dependent inhibitory effect is observed against LptA–LptA association. LptA first N-terminal β-strand is a key determinant interacting with the C-terminal region of LptC or the C-terminal region of another LptA in head-to-tail LptA self-oligomerization (Freinkman et al., 2012; Laguri et al., 2017). LptC and LptA share a very similar protein architecture, despite no amino acid sequence similarity (Tran et al., 2010; Villa et al., 2013); indeed, in the LptC–$LptA_m$ complex, LptC precisely occupies the same position as LptA in the LptA oligomer (Laguri et al., 2017). Interestingly, thanatin seems able to discriminate between the two different interactions that LptA is implicated on via its N-terminal region and could, therefore, also serve as a tool to probe the different interactions occurring within the Lpt periplasmic protein bridge. This result is in agreement with earlier data showing that the enantiomeric form of thanatin (D-thanatin) is nearly inactive against Gram-negative strains, suggesting that a stereospecific recognition by a cellular target is required for thanatin to exert its antibacterial effect (Fehlbaum et al., 1996).

A scrambled version of thanatin, that maintains the overall peptide amino acid composition and charge, loses the antibacterial activity, fails to disrupt the LptC–LptA interaction *in vivo* (BACTH assay) and *in vitro* (NMR), and does not bind to $LptA_m$ (SPR analyses). These data further support a specific action of thanatin in binding to LptA and in competing with LptC for the formation of the LptC–LptA complex. Thanatin scramble

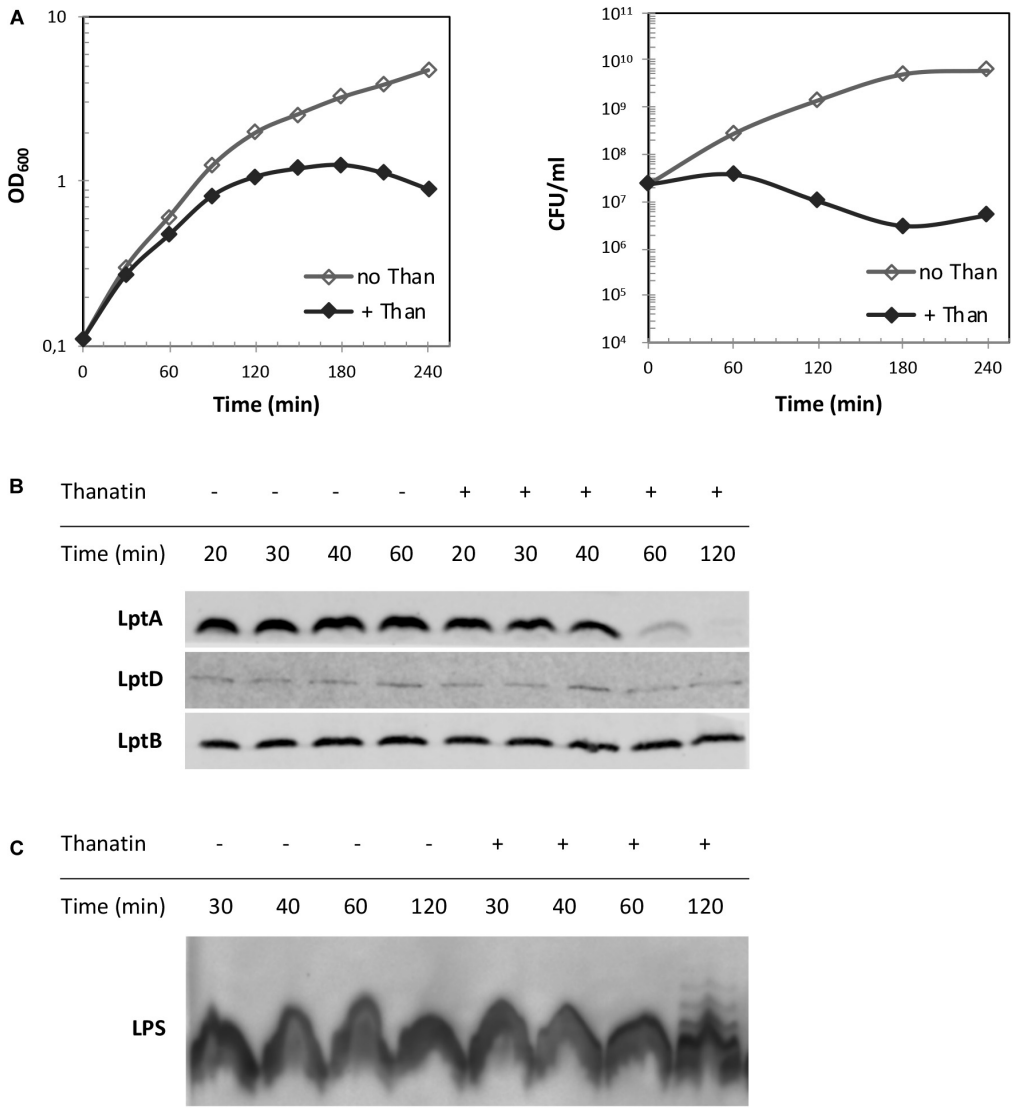

FIGURE 6 | LptA steady-state level and LPS profile upon treatment with thanatin. **(A)** Growth curves of wild type strain MG1655 in the presence (+ Than) and absence (no Than) of thanatin at 5.25 μg/mL (1.5 × MIC) concentration. Growth was monitored by measuring the OD_{600} (left panel) and by determining CFU/mL (right panel). **(B)** Western blot analysis to reveal LptA steady-state levels. Samples were collected 20, 30, 40, 60, and 120 min after treatment with thanatin. Whole-cell extracts were prepared and analyzed by western blot with anti-LptA, anti-LptD, anti-LptB (as loading control) antibodies. An equal amount of cells (0.36 OD_{600} units) was loaded into each lane. **(C)** Western blot analysis to reveal LPS profiles. Whole-cell extracts obtained 30, 40, 60, and 120 min after treatment with thanatin were incubated with proteinase K and analyzed by western blot with anti-LPS antibodies. An equal amount of cells (0.48 OD_{600}) was loaded into each lane. Results shown are representative of three independent experiments.

does not display antibacterial activity against permeabilized *E. coli* strains, strongly suggesting that the lack of activity of the scrambled peptide is not due to its inability to reach its target in the periplasm.

It has been reported that *E. coli* cells carrying $LptA^{Q62L}$ amino acid substitution become resistant to thanatin (Vetterli et al., 2018). Residue Q62 does not appear to be implicated in thanatin binding and the mechanism underlying resistance is still unknown. LptC–$LptA^{Q62L}$ interaction is not inhibited by thanatin in the BACTH assay and, surprisingly, it appears stronger in the presence of the peptide. In the case of the interaction between $LptA^{Q62L}$ mutant proteins, the dimerization seems stronger than that observed between WT LptA, even in the absence of thanatin. We can speculate that Q62L mutation somehow alters the stability of both LptC–LptA and LptA–LptA complexes, affecting the binding of thanatin to LptA. However, it is difficult to explain these results since neither the effect of the Q62L substitution on LptA structure nor the mechanism of thanatin resistance are known.

Previous *in vitro* data revealed that besides LptA, thanatin binds to the LptDE complex in the low nanomolar range and, furthermore, its binding site in LptA has been shown by

modeling studies to be highly conserved in the periplasmic domain of LptD (Robinson, 2019). This suggests that thanatin can inhibit multiple protein–protein interactions required for the Lpt complex assembly. It was not possible to test the periplasmic domain of LptD in the BACTH assay, since expression of a folded and functional LptD is strictly dependent on the expression and interaction with LptE (Chng et al., 2010). Nevertheless, the isolation of suppressor mutants exclusively at the N-terminal region of LptA (Vetterli et al., 2018), that is not involved in the LptA–LptD interaction, and the ability of the LptA$_m$ mutant protein, lacking the C-terminal β-strand implicated in both LptA–LptA and LptA–LptD interactions, to partially support the cell growth (Laguri et al., 2017) suggest that LptC–LptA interaction is thanatin's main target.

Thanatin has been related to the group of CAMPs that kill bacteria by cell agglutination. In the host organism, this class of antimicrobial peptides does not permeabilize bacterial cell membranes but rather interacts with LPS or peptidoglycan, favoring cell aggregation and bacterial removal by phagocytosis (Shai, 2002; Jung et al., 2012; Pulido et al., 2012). Thanatin has indeed been shown to bind LPS *in vitro* and promote cell agglutination as a result of cell surface charge neutralization (Sinha et al., 2017). Recently, the comparison of thanatin's affinity to LPS relative to Ca^{2+} and Mg^{2+} revealed that thanatin displaces divalent cations from LPS *in vivo* promoting LPS shedding from bacterial cells at concentrations 10-fold higher than the MIC, increasing OM permeability (Ma et al., 2019). Interestingly, the same study reports that thanatin is able to inhibit the enzymatic activity of New Delhi metallo-β-lactamase-1 (NMD-1), responsible for the resistance to β-lactam antibiotics in several multidrug resistant strains, by binding to the active site of the enzyme with higher affinity than Zn^{2+}, displacing it and reversing carbapenem resistance. This evidences that, alongside a killing effect on Gram-negative pathogens based on OM permeabilization, thanatin may help restoring the activity of β-lactam antibiotics in multidrug resistant pathogens (Ma et al., 2019).

In the reported BACTH assay, inhibition of LptC–LptA interaction is observed at sub-MIC concentrations of thanatin, a condition that does not inhibit the growth of cells expressing LptC and LptA$_m$ protein fusions. Based on our data, we propose that LPS binding is employed by thanatin as a self-promoted mechanism of entry in the periplasm of bacterial cells where the LptA target resides. Supporting this hypothesis is the finding of a mutated version of thanatin, where Arg 13 and Arg 14 residues have been substituted by Ala, that presents reduced LPS binding affinity and loses the antibacterial activity (Sinha et al., 2017).

In *E. coli* cells treated with thanatin, LptA undergoes degradation and LPS is decorated with colanic acid. Notably, these phenotypes are observed in cells where LPS export machinery disassembles and transport of LPS molecules is impaired due to mutations in any of the Lpt complex components (Sperandeo et al., 2008, 2011). These data suggest that the main mechanism of action of thanatin occurring at MIC concentration is the disassembly of the Lpt machinery and consequently the blocking of LPS transport.

Overall, our results highlight OM biogenesis as an excellent target for novel antibiotic discovery. Thanatin joins the increasing list of molecules that disrupt the assembly of the OM with diverse mechanisms (Hart et al., 2019; Imai et al., 2019; Lehman and Grabowicz, 2019; Psonis et al., 2019). Based on their mechanisms, these compounds could be employed not only to fight multidrug resistant pathogens but also in combination with existing antibiotics not sufficiently effective.

DATA AVAILABILITY STATEMENT

All datasets generated for this study are included in the article/**Supplementary Material**.

AUTHOR CONTRIBUTIONS

EM performed the BACTH assays and *in vivo* experiments. TB and CL performed NMR and SPR experiments. AR and EE designed and synthetized the peptides. AP, PS, AM, and EM designed the *in vivo* experiments. J-PS, CL, and TB designed the NMR and SPR experiments. EM, AP, PS, CL, TB, and AR wrote the manuscript. All the authors reviewed and approved the manuscript.

FUNDING

AP, J-PS, CL, TB, and EM were supported by the Train2Target project granted from the European Union's Horizon 2020 Research and Innovation Program under the Marie Skłodowska-Curie grant agreement #721484. PS was supported by the Italian Ministry of Education, University and Research, (FABBR)-MIUR 2017, Funding for the financing of basic research activities.

ACKNOWLEDGMENTS

This work used the platforms of the Grenoble Instruct-ERIC center (ISBG; UMS 3518 CNRS-CEA-UGA-EMBL) within the Grenoble Partnership for Structural Biology (PSB), supported by FRISBI (ANR-10-INBS-05-02) and GRAL, financed within the University Grenoble Alpes graduate school (Ecoles Universitaires de Recherche) CBH-EUR-GS (ANR-17-EURE-0003). The authors acknowledge the SPR/BLI platform personal, Jean-Baptiste REISER Ph.D., and Anne Chouquet, for their help and assistance.

SUPPLEMENTARY MATERIAL

The Supplementary Material for this article can be found online at: https://www.frontiersin.org/articles/10.3389/fmicb.2020.00909/full#supplementary-material

FIGURE S1 | SPR of LptC–LptA$_m$ interaction and its disruption by thanatin. **(A)** Determination of LptC–LptA$_m$ dissociation constant. Left panel: Sensorgrams of LptC injected at different concentrations over immobilized LptA$_m$. Right panel: Steady-state analysis of LptC–LptA$_m$ interaction. **(B)** Raw Sensorgrams of the data presented in **Figure 5B**.

REFERENCES

Andolina, G., Bencze, L. C., Zerbe, K., Muller, M., Steinmann, J., Kocherla, H., et al. (2018). A peptidomimetic antibiotic interacts with the periplasmic domain of LptD from *Pseudomonas aeruginosa*. *ACS Chem Biol.* 13, 666–675. doi: 10.1021/acschembio.7b00822

Avitabile, C., Diaferia, C., Roviello, V., Altamura, D., Giannini, C., Vitagliano, L., et al. (2019). Fluorescence and morphology of self-assembled nucleobases and their diphenylalanine hybrid aggregates. *Chemistry* 25, 14850–14857. doi: 10.1002/chem.201902709

Battesti, A., and Bouveret, E. (2012). The bacterial two-hybrid system based on adenylate cyclase reconstitution in *Escherichia coli*. *Methods* 58, 325–334. doi: 10.1016/j.ymeth.2012.07.018

Blattner, F. R., Plunkett, G., Bloch, C. A., Perna, N. T., Burland, V., Riley, M., et al. (1997). The complete genome sequence of *Escherichia coli* K-12. *Science* 277, 1453–1462. doi: 10.1126/science.277.5331.1453

Chng, S. S., Ruiz, N., Chimalakonda, G., Silhavy, T. J., and Kahne, D. (2010). Characterization of the two-protein complex in *Escherichia coli* responsible for lipopolysaccharide assembly at the outer membrane. *Proc. Natl. Acad. Sci. U.S.A.* 107, 5363–5368. doi: 10.1073/pnas.0912872107

Davidson, A. L., Shuman, H. A., and Nikaido, H. (1992). Mechanism of maltose transport in *Escherichia coli*: transmembrane signaling by periplasmic binding proteins. *Proc. Natl. Acad. Sci. U.S.A.* 89, 2360–2364. doi: 10.1073/pnas.89.6.2360

Doerrler, W. T., Gibbons, H. S., and Raetz, C. R. (2004). MsbA-dependent translocation of lipids across the inner membrane of *Escherichia coli*. *J. Biol. Chem.* 279, 45102–45109. doi: 10.1074/jbc.M408106200

Dong, H., Xiang, Q., Gu, Y., Wang, Z., Paterson, N. G., Stansfeld, P. J., et al. (2014). Structural basis for outer membrane lipopolysaccharide insertion. *Nature* 511, 52–56. doi: 10.1038/nature13464

Ehrmann, M., Ehrle, R., Hofmann, E., Boos, W., and Schlosser, A. (1998). The ABC maltose transporter. *Mol. Microbiol.* 29, 685–694. doi: 10.1046/j.1365-2958.1998.00915.x

Falchi, F. A., Maccagni, E. A., Puccio, S., Peano, C., De Castro, C., Palmigiano, A., et al. (2018). Mutation and suppressor analysis of the essential lipopolysaccharide transport protein LptA reveals strategies to overcome severe outer membrane permeability defects in *Escherichia coli*. *J. Bacteriol.* 200:e487-17. doi: 10.1128/jb.00487-17

Fehlbaum, P., Bulet, P., Chernysh, S., Briand, J. P., Roussel, J. P., Letellier, L., et al. (1996). Structure-activity analysis of thanatin, a 21-residue inducible insect defense peptide with sequence homology to frog skin antimicrobial peptides. *Proc. Natl. Acad. Sci. U.S.A.* 93, 1221–1225. doi: 10.1073/pnas.93.3.1221

Freinkman, E., Chng, S. S., and Kahne, D. (2011). The complex that inserts lipopolysaccharide into the bacterial outer membrane forms a two-protein plug-and-barrel. *Proc. Natl. Acad. Sci. U.S.A.* 108, 2486–2491. doi: 10.1073/pnas.1015617108

Freinkman, E., Okuda, S., Ruiz, N., and Kahne, D. (2012). Regulated assembly of the transenvelope protein complex required for lipopolysaccharide export. *Biochemistry* 51, 4800–4806. doi: 10.1021/bi300592c

Hart, E. M., Mitchell, A. M., Konovalova, A., Grabowicz, M., Sheng, J., Han, X., et al. (2019). A small-molecule inhibitor of BamA impervious to efflux and the outer membrane permeability barrier. *Proc. Natl. Acad. Sci. U.S.A.* 116, 21748–21757. doi: 10.1073/pnas.1912345116

Ho, H., Miu, A., Alexander, M. K., Garcia, N. K., Oh, A., Zilberleyb, I., et al. (2018). Structural basis for dual-mode inhibition of the ABC transporter MsbA. *Nature* 557, 196–201. doi: 10.1038/s41586-018-0083-5

Imai, Y., Meyer, K. J., Iinishi, A., Favre-Godal, Q., Green, R., Manuse, S., et al. (2019). A new antibiotic selectively kills Gram-negative pathogens. *Nature* 576, 459–464. doi: 10.1038/s41586-019-1791-1

Jung, S., Sonnichsen, F. D., Hung, C. W., Tholey, A., Boidin-Wichlacz, C., Haeusgen, W., et al. (2012). Macin family of antimicrobial proteins combines antimicrobial and nerve repair activities. *J. Biol. Chem.* 287, 14246–14258. doi: 10.1074/jbc.M111.336495

Karimova, G., Pidoux, J., Ullmann, A., and Ladant, D. (1998). A bacterial two-hybrid system based on a reconstituted signal transduction pathway. *Proc. Natl. Acad. Sci. U.S.A.* 95, 5752–5756. doi: 10.1073/pnas.95.10.5752

Kerfah, R., Plevin, M. J., Sounier, R., Gans, P., and Boisbouvier, J. (2015). Methyl-specific isotopic labeling: a molecular tool box for solution NMR studies of large proteins. *Curr. Opin. Struct. Biol.* 32, 113–122. doi: 10.1016/j.sbi.2015.03.009

Laguri, C., Sperandeo, P., Pounot, K., Ayala, I., Silipo, A., Bougault, C. M., et al. (2017). Interaction of lipopolysaccharides at intermolecular sites of the periplasmic Lpt transport assembly. *Sci. Rep.* 7:9715. doi: 10.1038/s41598-017-10136-0

Lehman, K. M., and Grabowicz, M. (2019). Countering gram-negative antibiotic resistance: recent progress in disrupting the outer membrane with novel therapeutics. *Antibiotics (Basel.)* 8:E163. doi: 10.3390/antibiotics8040163

Lesse, A. J., Campagnari, A. A., Bittner, W. E., and Apicella, M. A. (1990). Increased resolution of lipopolysaccharides and lipooligosaccharides utilizing tricine-sodium dodecyl sulfate-polyacrylamide gel electrophoresis. *J. Immunol. Methods* 126, 109–117.

Li, Y., Orlando, B. J., and Liao, M. (2019). Structural basis of lipopolysaccharide extraction by the LptB2FGC complex. *Nature* 567, 486–490. doi: 10.1038/s41586-019-1025-6

Ma, B., Fang, C., Lu, L., Wang, M., Xue, X., Zhou, Y., et al. (2019). The antimicrobial peptide thanatin disrupts the bacterial outer membrane and inactivates the NDM-1 metallo-beta-lactamase. *Nat. Commun.* 10:3517. doi: 10.1038/s41467-019-11503-3

Majdalani, N., and Gottesman, S. (2005). The Rcs phosphorelay: a complex signal transduction system. *Annu. Rev. Microbiol.* 59, 379–405. doi: 10.1146/annurev.micro.59.050405.101230

Merten, J. A., Schultz, K. M., and Klug, C. S. (2012). Concentration-dependent oligomerization and oligomeric arrangement of LptA. *Protein Sci.* 21, 211–218. doi: 10.1002/pro.2004

Nikaido, H. (2003). Molecular Basis of Bacterial Outer Membrane Permeability Revisited. *Microbiol. Mol. Biol. Rev.* 67, 593–656. doi: 10.1128/mmbr.67.4.593-656.2003

Okuda, S., Freinkman, E., and Kahne, D. (2012). Cytoplasmic ATP hydrolysis powers transport of lipopolysaccharide across the periplasm in *E. coli*. *Science* 338, 1214–1217. doi: 10.1126/science.1228984

Okuda, S., Sherman, D. J., Silhavy, T. J., Ruiz, N., and Kahne, D. (2016). Lipopolysaccharide transport and assembly at the outer membrane: the PEZ model. *Nat. Rev. Microbiol.* 14, 337–345. doi: 10.1038/nrmicro.2016.25

Ouellette, S. P., Gauliard, E., Antosova, Z., and Ladant, D. (2014). A gateway((R))-compatible bacterial adenylate cyclase-based two-hybrid system. *Environ. Microbiol. Rep.* 6, 259–267. doi: 10.1111/1758-2229.12123

Ouellette, S. P., Karimova, G., Davi, M., and Ladant, D. (2017). Analysis of membrane protein interactions with a bacterial adenylate cyclase-based two-hybrid (BACTH) technique. *Curr. Protoc. Mol. Biol.* 118, 21–20. doi: 10.1002/cpmb.36

Owens, T. W., Taylor, R. J., Pahil, K. S., Bertani, B. R., Ruiz, N., Kruse, A. C., et al. (2019). Structural basis of unidirectional export of lipopolysaccharide to the cell surface. *Nature* 567, 550–553. doi: 10.1038/s41586-019-1039-0

Paschos, A., den Hartigh, A., Smith, M. A., Atluri, V. L., Sivanesan, D., Tsolis, R. M., et al. (2011). An in vivo high-throughput screening approach targeting the type IV secretion system component VirB8 identified inhibitors of Brucella abortus 2308 proliferation. *Infect. Immun.* 79, 1033–1043. doi: 10.1128/iai.00993-10

Polissi, A., and Georgopoulos, C. (1996). Mutational analysis and properties of the msbA gene of *Escherichia coli*, coding for an essential ABC family transporter. *Mol. Microbiol.* 20, 1221–1233.

Psonis, J. J., Chahales, P., Henderson, N. S., Rigel, N. W., Hoffman, P. S., and Thanassi, D. G. (2019). The small molecule nitazoxanide selectively disrupts BAM-mediated folding of the outer membrane usher protein. *J. Biol. Chem.* 294, 14357–14369. doi: 10.1074/jbc.RA119.009616

Pulido, D., Moussaoui, M., Andreu, D., Nogues, M. V., Torrent, M., and Boix, E. (2012). Antimicrobial action and cell agglutination by the eosinophil cationic protein are modulated by the cell wall lipopolysaccharide structure. *Antimicrob. Agents Chemother.* 56, 2378–2385. doi: 10.1128/aac.06107-11

Qiao, S., Luo, Q., Zhao, Y., Zhang, X. C., and Huang, Y. (2014). Structural basis for lipopolysaccharide insertion in the bacterial outer membrane. *Nature* 511, 108–111. doi: 10.1038/nature13484

Raetz, C. R., and Whitfield, C. (2002). Lipopolysaccharide endotoxins. *Annu. Rev. Biochem.* 71, 635–700. doi: 10.1146/annurev.biochem.71.110601.135414

Robinson, J. A. (2019). Folded synthetic peptides and other molecules targeting outer membrane protein complexes in gram-negative bacteria. *Front. Chem.* 7:45. doi: 10.3389/fchem.2019.00045

Ruiz, N., Falcone, B., Kahne, D., and Silhavy, T. J. (2005). Chemical conditionality: a genetic strategy to probe organelle assembly. *Cell* 121, 307–317. doi: 10.1016/j.cell.2005.02.014

Ruiz, N., Gronenberg, L. S., Kahne, D., and Silhavy, T. J. (2008). Identification of two inner-membrane proteins required for the transport of lipopolysaccharide to the outer membrane of *Escherichia coli*. *Proc. Natl. Acad. Sci. U.S.A.* 105, 5537–5542. doi: 10.1073/pnas.0801196105

Santambrogio, C., Sperandeo, P., Villa, R., Sobott, F., Polissi, A., and Grandori, R. (2013). LptA assembles into rod-like oligomers involving disorder-to-order transitions. *J. Am. Soc. Mass Spectrom.* 24, 1593–1602. doi: 10.1007/s13361-013-0687-9

Schultz, K. M., Feix, J. B., and Klug, C. S. (2013). Disruption of LptA oligomerization and affinity of the LptA-LptC interaction. *Protein Sci.* 22, 1639–1645. doi: 10.1002/pro.2369

Sekiguchi, M., and Iida, S. (1967). Mutants of *Escherichia coli* permeable to actinomycin. *Proc. Natl. Acad. Sci. U.S.A.* 58, 2315–2320. doi: 10.1073/pnas.58.6.2315

Shai, Y. (2002). Mode of action of membrane active antimicrobial peptides. *Biopolymers* 66, 236–248. doi: 10.1002/bip.10260

Silhavy, T. J., Kahne, D., and Walker, S. (2010). The bacterial cell envelope. *Cold Spring Harb. Perspect. Biol.* 2:a000414. doi: 10.1101/cshperspect.a000414

Simpson, B. W., and Trent, M. S. (2019). Pushing the envelope: LPS modifications and their consequences. *Nat. Rev. Microbiol.* 17, 403–416. doi: 10.1038/s41579-019-0201-x

Sinha, S., Zheng, L., Mu, Y., Ng, W. J., and Bhattacharjya, S. (2017). Structure and interactions of A host defense antimicrobial peptide thanatin in lipopolysaccharide micelles reveal mechanism of bacterial cell agglutination. *Sci. Rep.* 7:17795. doi: 10.1038/s41598-017-18102-6

Sperandeo, P., Cescutti, R., Villa, R., Di Benedetto, C., Candia, D., Deho, G., et al. (2007). Characterization of lptA and lptB, two essential genes implicated in lipopolysaccharide transport to the outer membrane of *Escherichia coli*. *J. Bacteriol.* 189, 244–253. doi: 10.1128/jb.01126-06

Sperandeo, P., Lau, F. K., Carpentieri, A., De Castro, C., Molinaro, A., Deho, G., et al. (2008). Functional analysis of the protein machinery required for transport of lipopolysaccharide to the outer membrane of *Escherichia coli*. *J. Bacteriol.* 190, 4460–4469. doi: 10.1128/jb.00270-08

Sperandeo, P., Martorana, A. M., and Polissi, A. (2019). The Lpt ABC transporter for lipopolysaccharide export to the cell surface. *Res. Microbiol.* 170, 366–373. doi: 10.1016/j.resmic.2019.07.005

Sperandeo, P., Villa, R., Martorana, A. M., Samalikova, M., Grandori, R., Deho, G., et al. (2011). New insights into the Lpt machinery for lipopolysaccharide transport to the cell surface: LptA-LptC interaction and LptA stability as sensors of a properly assembled transenvelope complex. *J. Bacteriol.* 193, 1042–1053. doi: 10.1128/jb.01037-10

Srinivas, N., Jetter, P., Ueberbacher, B. J., Werneburg, M., Zerbe, K., Steinmann, J., et al. (2010). Peptidomimetic antibiotics target outer-membrane biogenesis in *Pseudomonas aeruginosa*. *Science* 327, 1010–1013. doi: 10.1126/science.1182749

Studier, F. W., and Moffatt, B. A. (1986). Use of bacteriophage T7 RNA polymerase to direct selective high-level expression of cloned genes. *J. Mol. Biol.* 189, 113–130.

Suits, M. D. L., Sperandeo, P., Dehò, G., Polissi, A., and Jia, Z. (2008). Novel structure of the conserved gram-negative lipopolysaccharide transport protein A and mutagenesis analysis. *J. Mol. Biol.* 380, 476–488. doi: 10.1016/j.jmb.2008.04.045

Tacconelli, E., Carrara, E., Savoldi, A., Harbarth, S., Mendelson, M., Monnet, D. L., et al. (2018). Discovery, research, and development of new antibiotics: the WHO priority list of antibiotic-resistant bacteria and tuberculosis. *Lancet Infect. Dis.* 18, 318–327. doi: 10.1016/s1473-3099(17)30753-3

Tran, A. X., Dong, C., and Whitfield, C. (2010). Structure and functional analysis of LptC, a conserved membrane protein involved in the lipopolysaccharide export pathway in *Escherichia coli*. *J. Biol. Chem.* 285, 33529–33539. doi: 10.1074/jbc.M110.144709

Vetterli, S. U., Zerbe, K., Muller, M., Urfer, M., Mondal, M., Wang, S., et al. (2018). Thanatin targets the intermembrane protein complex required for lipopolysaccharide transport in *Escherichia coli*. *Sci. Adv.* 4:eaau2634. doi: 10.1126/sciadv.aau2634

Villa, R., Martorana, A. M., Okuda, S., Gourlay, L. J., Nardini, M., Sperandeo, P., et al. (2013). The *Escherichia coli* Lpt transenvelope protein complex for lipopolysaccharide export is assembled via conserved structurally homologous domains. *J. Bacteriol.* 195, 1100–1108. doi: 10.1128/jb.02057-12

Werneburg, M., Zerbe, K., Juhas, M., Bigler, L., Stalder, U., Kaech, A., et al. (2012). Inhibition of lipopolysaccharide transport to the outer membrane in *Pseudomonas aeruginosa* by peptidomimetic antibiotics. *Chembiochem* 13, 1767–1775. doi: 10.1002/cbic.201200276

Wiegand, I., Hilpert, K., and Hancock, R. E. (2008). Agar and broth dilution methods to determine the minimal inhibitory concentration (MIC) of antimicrobial substances. *Nat. Protoc.* 3, 163–175. doi: 10.1038/nprot.2007.521

Wu, T., McCandlish, A. C., Gronenberg, L. S., Chng, S. S., Silhavy, T. J., and Kahne, D. (2006). Identification of a protein complex that assembles lipopolysaccharide in the outer membrane of *Escherichia coli*. *Proc. Natl. Acad. Sci. U.S.A.* 103, 11754–11759. doi: 10.1073/pnas.0604744103

Zhang, G., Baidin, V., Pahil, K. S., Moison, E., Tomasek, D., Ramadoss, N. S., et al. (2018). Cell-based screen for discovering lipopolysaccharide biogenesis inhibitors. *Proc. Natl. Acad. Sci. U.S.A.* 115, 6834–6839. doi: 10.1073/pnas.1804670115

Zhang, X., Li, Y., Wang, W., Zhang, J., Lin, Y., Hong, B., et al. (2019). Identification of an anti-Gram-negative bacteria agent disrupting the interaction between lipopolysaccharide transporters LptA and LptC. *Int. J. Antimicrob. Agents* 53, 442–448. doi: 10.1016/j.ijantimicag.2018.11.016

Conflict of Interest: The authors declare that the research was conducted in the absence of any commercial or financial relationships that could be construed as a potential conflict of interest.

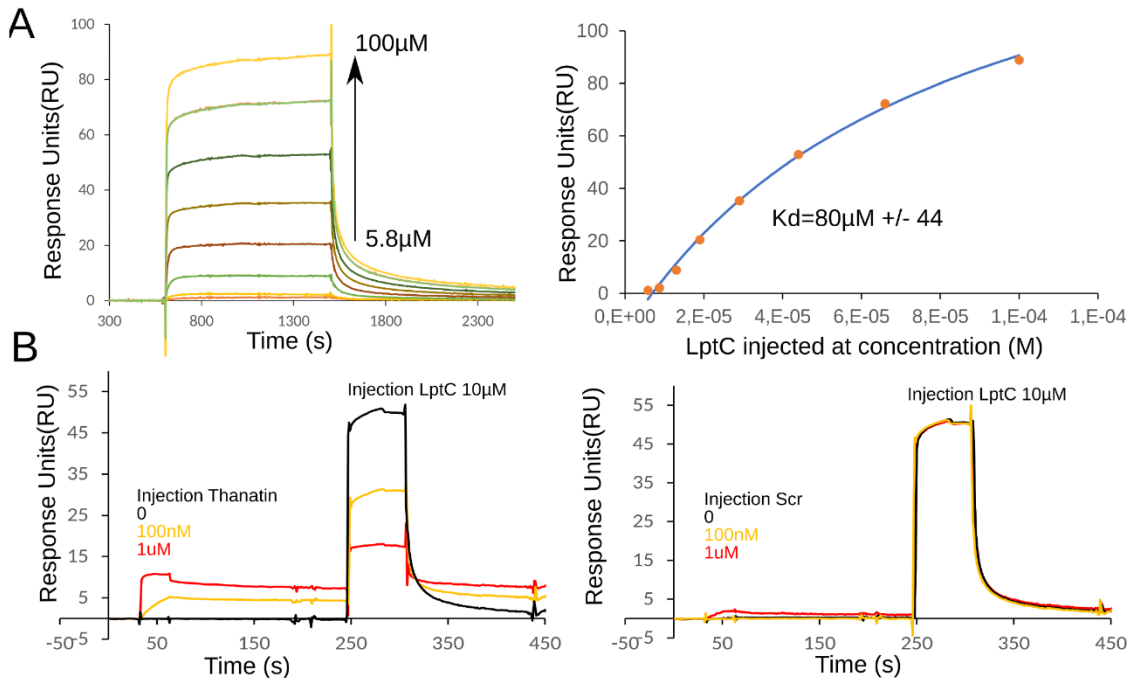
A
Response Units(RU)
100µM
5.8µM
Time (s)
Kd=80µM +/- 44
LptC injected at concentration (M)
B
Injection LptC 10µM
Injection Thanatin
0
100nM
1uM
Injection Scr
Time (s)

Figure S1

1.2 Additional unpublished data

The additional results here presented are complementary to the published study on thanatin's ability to disrupt Lpt periplasmic interactions. This work was performed to further explore thanatin's effect on the integrity of the bacterial cell envelope.

1.2.1 Checkerboard synergy assays

Thanatin was shown in Manuscript 1 to inhibit LptC-LptA and LptA-LptA interactions, causing the degradation of LptA, likely as a consequence of the destabilization of the Lpt bridge architecture. The disruption of the Lpt complex and the arrest of LPS transport lead to OM permeability defects. Therefore, we tested thanatin for antibacterial synergy with three antibiotics (vancomycin, bacitracin, rifampicin) that have a limited ability to penetrate an integral OM, and are thus normally inactive against Gram-negative bacteria. Rifampicin is an antibiotic that permeates the IM to reach its target, the RNA polymerase, while vancomycin and bacitracin inhibit the cell wall synthesis in the periplasm [1].

The checkerboard titration method is a commonly used technique to assess synergy of antimicrobial combinations [2]. Checkerboard assays were conducted against the wild-type MG1655 *E. coli* strain (**Figure 1**), and the fractional inhibitory concentration (FIC) index was calculated for each compound combination as described in Materials and Methods. An FIC index (FIC_I) of 0.31 was obtained for both thanatin/vancomycin and thanatin/bacitracin combinations. For thanatin/rifampicin, the FIC_I was determined to be 0.38. Since an FIC index equal to 0.5 or lower indicates synergism [2], these data suggest that thanatin potentiates the antibacterial effect of all three tested antibiotics, possibly by increasing their entry into the cell due to a compromised OM.

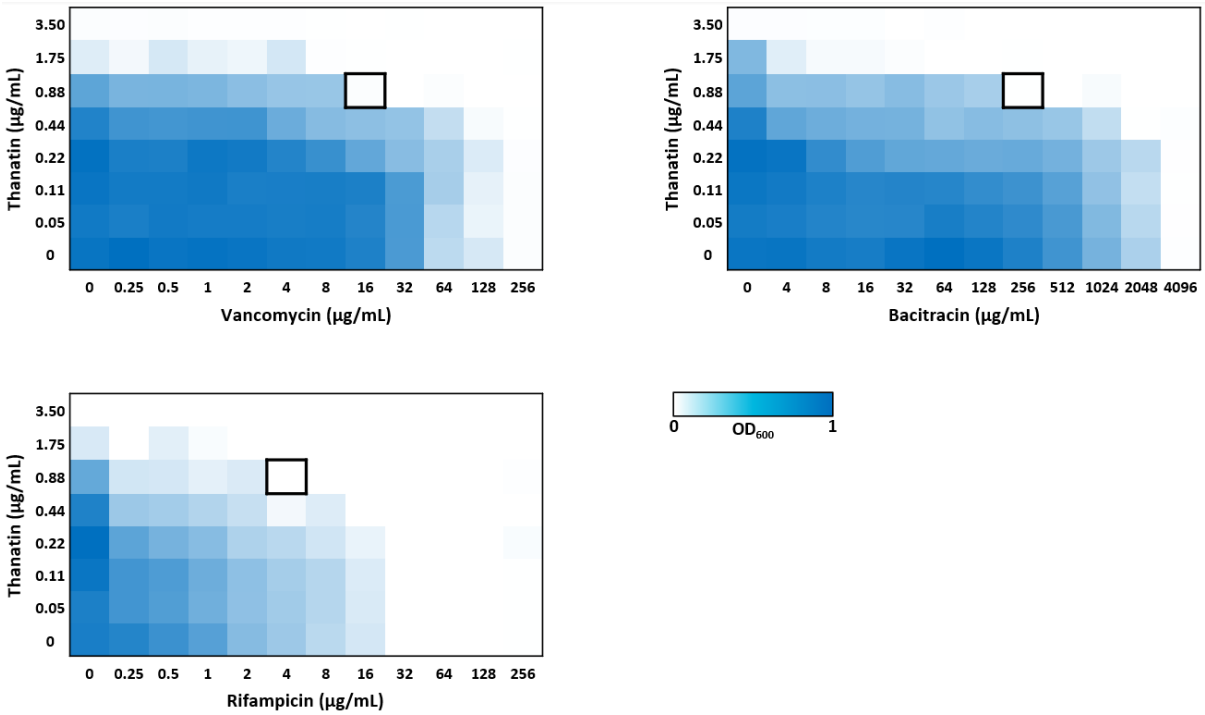

Figure 1. Checkerboard assays against the wild-type *E. coli* strain MG1655. Thanatin was tested in combination with vancomycin, bacitracin, and rifampicin. The FIC index was calculated for the well delimited by the black square. The data are representative of two biological replicates.

1.2.2 Envelope stress response activation in thanatin-treated cells

1.2.2.1 Introduction

The bacterial cell envelope is a vital protective barrier against the environment and, thus, the biogenesis and integrity of this multi-layered structure are tightly surveilled by dedicated stress response pathways [3]. Envelope stress responses (ESRs) detect envelope damages caused by environmental or chemical assaults and respond by altering the transcriptome in order to recover and maintain cell envelope integrity. The most relevant ESRs are σ^E, Cpx, and Rcs (**Figure 2**).

The σ^E stress response system senses perturbations in the OM and activation of this pathway generally occurs upon the periplasmic accumulation of misfolded OMPs or mislocalized LPS [4]. Modifications in the LPS structure and intermediates of the LPS transport and biosynthesis have been shown to activate the σ^E response [4-6]. Other inducing cues include oxidative stress, acid stress, heat shock, hypo-osmotic shock, biofilm formation, and carbon starvation [7]. The σ^E factor is kept in an inactive form by the anti-σ factor RseA, a single-pass IM protein. When unfolded or misfolded OMPs accumulate in the periplasm, they bind to DegS, an IM protease, that cleaves RseA. This proteolytic reaction is inhibited by RseB, which is bound to RseA. The displacement of RseB from RseA for full activation of σ^E has been proposed to occur by i) the binding of LPS acyl chains to RseB [4], and/or ii) the interaction with unfolded OMPs [8]. The cleavage of RseA triggers a proteolytic cascade that ultimately frees σ^E to activate the transcription of genes involved in the biosynthesis, transport and/or assembly of the OM components (LPS, OMPs, phospholipids) and of periplasmic chaperones and proteases [3]. Activation of σ^E also increases the transcription of small RNAs (sRNAs), such as MicA and RybB, that downregulate OMP synthesis, and MicL that reduces Lpp levels.

Unlike σ^E that makes use of a proteolysis cascade, the Cpx (conjugative pilus expression) stress response uses a two-component system (TCS) for inter-compartment signalling, where CpxA is the IM sensory histidine kinase and CpxR is the cognate DNA-binding response regulator [3]. The Cpx system seems to be primarily focused on protecting the integrity of the IM. Cpx is activated by a broad array of conditions and the common inducing signals are defects in protein secretion across the IM, and the presence of misfolded IM and periplasmic proteins. Inducers of the pathway include, amongst other stresses, changes in osmolarity,

alkaline pH, exposure to copper or ethanol, alterations in the IM phospholipid composition, defects in the peptidoglycan cell wall, antimicrobial peptides, adhesion of the cell to hydrophobic surfaces, and aberrant expression of the Pap pilus [3, 7]. In response to stress signals, conformational changes in the periplasmic sensor domain of CpxA induce the auto-phosphorylation of the cytoplasmic histidine kinase domain. CpxA then phosphorylates CpxR to activate it for transcriptional regulation. In the absence of stress, CpxA functions as a phosphatase to deactivate CpxR. CpxP, which belongs to the Cpx regulon, provides negative feedback on the stress pathway by binding to the periplasmic domain of CpxA. The activation of Cpx is also modulated by the OM lipoprotein NlpE. Upon OM lipoprotein trafficking defects, NlpE accumulates in the IM activating Cpx [9, 10]. Moreover, NlpE is required for sensing adhesion to hydrophobic surfaces [11]. The Cpx response leads to the increased expression of peptidoglycan-modifying proteins (such as LdtD), envelope protein folding and degradation factors, genes involved in antimicrobial resistance and virulence factors, while it downregulates the expression of IM non-essential protein complexes, such as the electron transport chain complexes [3, 7]. The Cpx system directly inhibits σ^E by preventing its production; moreover, it also represses OMP synthesis. CpxR has also been shown to upregulate the production of RprA, a sRNA highly induced by the Rcs stress response system that, in turn, downregulates the transcription of strong CpxR-dependent promoters [12].

The Rcs (regulator of capsule synthesis) system detects modifications in the LPS charge or in the fluidity of the LPS layer, responds to defects in peptidoglycan biosynthesis and lipoprotein trafficking, and senses the loss of periplasmic osmoprotectant sugars [3]. The Rcs phosphorelay signalling cascade is more complex than the Cpx TCS [13]. The OM lipoprotein RcsF is the sensor protein of the system, detecting stresses occurring at the OM and periplasm. In activating conditions, RcsF interacts with the IM protein IgaA, the negative regulator of the pathway, to relieve IgaA's inhibition on RcsC and RcsD. RcsC is the IM histidine kinase that phosphorylates the IM phosphotransferase RcsD, which then transfers a phosphate to the response regulator RcsB. RcsB forms homodimers or heterodimers with the auxiliary regulator RcsA to regulate the transcription of the Rcs regulon [13]. The expression of genes involved in biofilm formation and production of colanic acid capsule is increased, while genes involved in motility are repressed, reducing flagella production [14-16]. The overproduction of colanic acid, a major outcome of Rcs activation, helps to protect the bacteria from antimicrobial peptides that damage the LPS surface layer [17].

In addition to the ESRs, other systems can alter the cell envelope in response to environmental stimuli in order for the cell to adapt to changing conditions. Examples of these

pathways include the TCSs PhoPQ and PmrAB (also named BasSR in *E. coli*) that control the expression of LPS-modifying enzymes (see Chapter 2, section 2.1.4 of the Introduction). In *Salmonella enterica* and *E. coli*, the two TCSs are linked by the connector protein PmrD [18-20]. Modifications induced by these systems allow the stabilization of the OM in a challenging environment. The PhoPQ TCS is linked to the σ^E stress response by the sRNA MicA, which is produced upon the activation of σ^E and downregulates the *phoPQ* transcript [21].

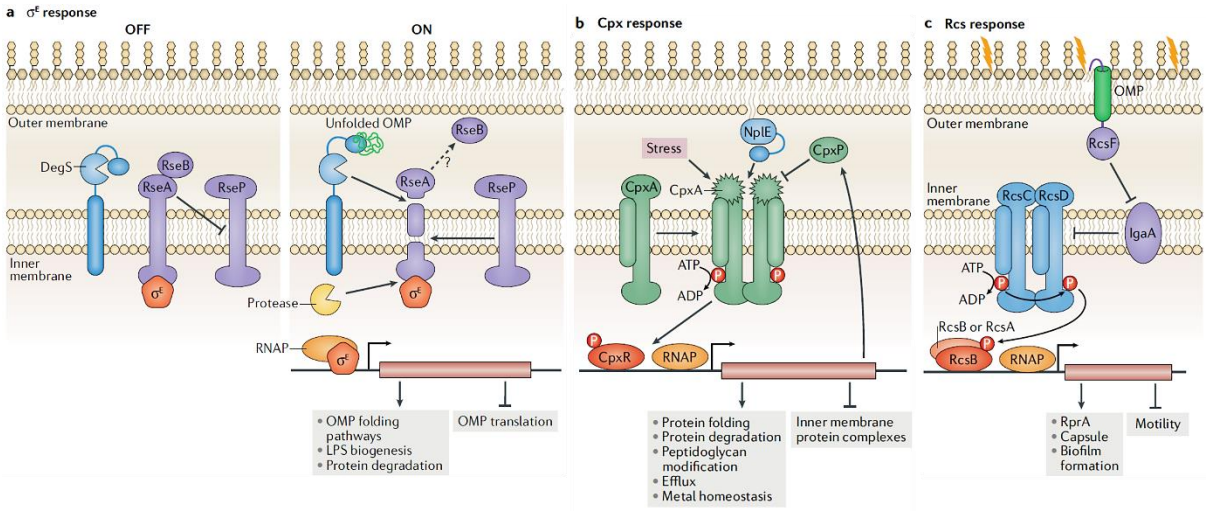

Figure 2. The σ^E, Cpx, and Rcs envelope stress responses of *Escherichia coli* (adapted from [3]). See text for details.

1.2.2.2 Induction of the *lptAp1* promoter

The *E. coli yrbG-lptB* locus encodes genes involved in the biosynthesis and transport of LPS, namely, *kdsC* and *kdsD* for the biosynthesis of Kdo residues; and *lptC*, *lptA*, and *lptB* for the LPS transport [22]. Three intralocus promoters have been identified (*yrbGp*, *kdsCp*, *lptAp*), and the *lptAp* region is itself composed of the two overlapping promoters *lptAp1* and *lptAp2* [23]. The *lptAp1* was shown to be an unconventional σ^E-dependent promoter that only responds to conditions affecting LPS biogenesis, thus inferring a LPS-specific σ^E-dependent signalling pathway [24, 25]. Since the depletion of Lpt proteins was shown to induce the *lptAp1* promoter [25], we wondered if the disruption of Lpt interactions caused by thanatin could have a similar effect. Therefore, we tested the induction of *lptAp1* by treating wild-type *E. coli* BW25113 cells, previously transformed with the pAM8 plasmid carrying a *lptAp1-lacZ* fusion [25], with thanatin at the same concentration used in the LptA stability studies presented in Manuscript 1

(5.25 µg/mL), which corresponds to 0.75 × MIC against BW25113, and with 5.25 µg/mL thanatin scramble (Scr), as a negative control. We treated the same cells with 25 mM ammonium metavanadate, as a positive control. Polymyxin B (PMB), a cationic antimicrobial peptide known to disturb the LPS layer, was also tested at 0.25 µg/mL (0.5 × MIC against BW25113). We could not perform treatment with PMB at 0.75 × MIC because of the extensive cell lysis occurring in this condition and hampering sample collection. Samples were taken at 0.5 h, 1 h, and 2 h of treatment and tested for β-galactosidase activity; a sample from a non-treated culture was also collected. To analyse the data, the signal obtained for the non-treated sample was subtracted from the β-galactosidase activities of the treated samples to eliminate the contribution of the overlapping *lptAp2* constitutive promoter to the signal.

The results are presented in **Figure 3**. As expected, Scr was unable to induce the promoter. On the contrary, PMB causes a maximum induction of *lptAp1* after 0.5 h of treatment, with a signal intensity comparable to the positive control ammonium metavanadate. This indicates a rapid and direct effect of PMB on the activation of *lptAp1*. With thanatin, however, a strong signal for the induction of the promoter was only observed after 2 h of incubation. Delayed response to thanatin is suggestive of a secondary effect that takes place in the cell and induces strongly *lptAp1*. Ammonium metavanadate also greatly induces the promoter after 2 h-induction, and thus suggests that prolonged incubation with this compound is more harmful for the cells. Alternatively, ammonium metavanadate might have both a direct and indirect effect.

Since thanatin induces strongly *lptAp1* after 2 h of treatment, the same time point at which we observed the appearance of LPS decorated with colanic acid (see Manuscript 1), we postulated that these two effects could be related. Accordingly, in cells treated with ammonium metavanadate, the production of LPS decorated with colanic acid has been previously detected [25]. To test this hypothesis, we performed the same assay with the *E. coli* PS135 strain, which is unable to synthesise colanic acid (CA) due to the deletion of *wcaJ*, and the results are presented in **Figure 4**. Interestingly, when the biosynthesis of CA is interrupted and LPS cannot be decorated with this sugar, thanatin's ability to induce *lptAp1* is abolished. Ammonium metavanadate is still able to induce *lptAp1* after 2 h-incubation, albeit less strongly, possibly because it affects also other cellular processes in addition to inducing LPS decoration with CA. Surprisingly, in the PS135 strain, not only is activation of *lptAp1* by PMB not repressed, but it also increases with time.

These results suggest that PMB and thanatin induce *lptAp1* by different mechanisms. Moreover, in thanatin-treated cells the modification of LPS with CA seems to be the inducing cue of the *lptAp1* promoter. LPS modifications have indeed been shown to activate σ^E-stress

response [5]. Therefore, it is possible that the bacterial cell modulates the expression of *lptAB* in response to the production of CA-modified LPS, which is indicative of LPS transport defects, to restore LPS trafficking to the OM. As proposed by Martorana *et al*., internal promoters in the *yrbG-lptB* locus, that encodes genes for both LPS synthesis and transport [22], may allow differential expression of these genes according to the needs of the bacterial cell under various physiological and environmental conditions.

The production of CA is tightly regulated by the Rcs phosphorelay system [13, 26], implying a link between this stress response and the regulation of the *lptAp1* promoter.

Antimicrobial peptides such as PMB have been reported to activate the transcription of the Rcs regulon *via* RcsF in *S. enterica* [27]. Using sublethal concentrations of PMB, Farris *et al*. observed a rapid induction of Rcs, with a peak activation within ten minutes, that was subsequently reduced in parallel with membrane repair. PMB has a rapid permeabilizing effect on the OM, which accounts for the activation of the Rcs system within minutes of exposure [27]. Assuming that it is the overproduction of CA that helps to stabilise the OM after exposure to sublethal concentrations of PMB, which subsequently reduces Rcs activation, we can speculate that in an *E. coli* strain unable to synthesize CA, the damage to the OM by PMB is not counteracted. If this is the case, Rcs induction would never be reduced and this could explain why *lptAp1* activation increases over time. Further experiments are required to clarify if there is indeed such a link between Rcs activation and the induction of *lptAp1*.

Upon exposure to thanatin, it is possible that changes in the OM caused by thanatin activate the Rcs transcriptional response, either directly by interacting with LPS and disrupting the OM [28], which would trigger a rapid induction of Rcs, or indirectly by LPS transport inhibition, to which a delayed activation may be observed. Indeed, thanatin was shown to induce the Rcs system (Luirink J. personal communication). Interestingly, it has been reported that the blocking of lipoprotein trafficking, due to the depletion of Lol proteins, induces Rcs-dependent expression of LolA, the periplasmic chaperone of the pathway [29]. Whether *lptAp1* induction is likewise dependent on Rcs activation requires further investigation.

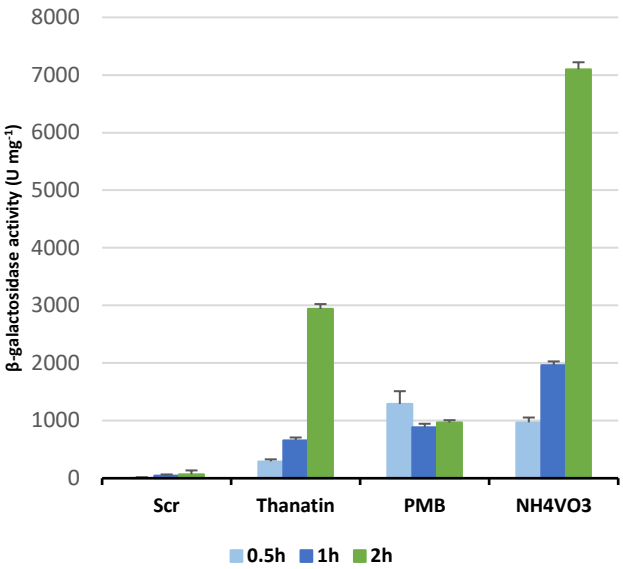

Figure 3. Induction of the *lptAp1* promoter in the BW25113 strain. β-galactosidase activity expressed from *lptAp1-lacZ* fusions upon 0.5 h, 1 h, and 2 h of treatment with 5.25 µg/mL of thanatin and thanatin scramble (Scr), 0.25 µg/mL of polymyxin B (PMB), and 25 mM NH_4VO_3. Each bar represents the mean value with standard deviation of the β-galactosidase activities obtained in two independent experiments. The signal obtained for the non-treated sample was subtracted from the β-galactosidase activity values of the treated samples.

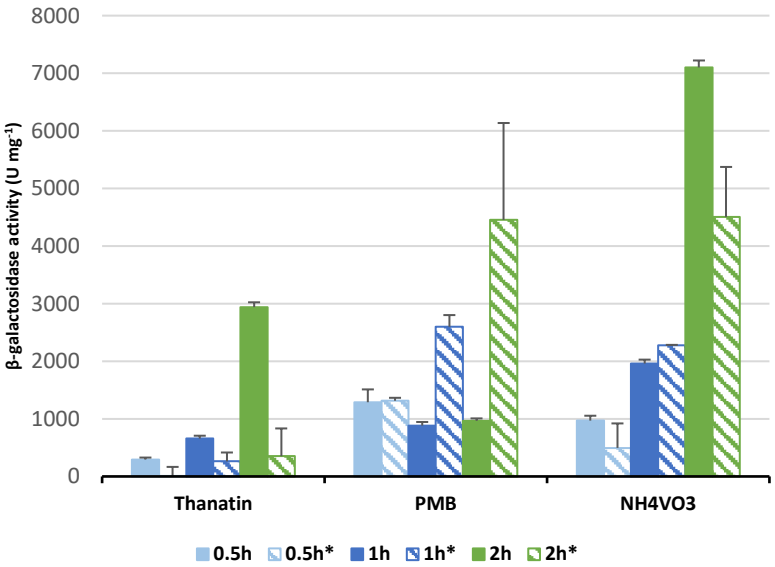

Figure 4. Induction of the *lptAp1* promoter in the PS135 strain in comparison to the wild-type BW25113 strain. β-galactosidase activity expressed from *lptAp1-lacZ* fusions in BW25113 (full bars) and PS135 (striped bars) upon 0.5 h, 1 h, and 2 h of treatment with thanatin at 5.25 µg/mL, 0.25 µg/mL polymyxin B (PMB), and 25 mM NH_4VO_3. Each bar represents the mean value with standard deviation of the β-galactosidase activities obtained in two independent experiments. The signal obtained for the non-treated sample was subtracted from the β-galactosidase activity values of the treated samples.

1.2.2.3 Induction of the *eptA* promoter

In response to environmental stressors, bacteria can alter the lipid A moiety in order to fortify the OM and allow their survival [30]. Intricate TCS protein networks sense diverse stimuli and upregulate the transcription of genes that will help adjust the cell envelope to the new environmental conditions. In *E. coli* and *Salmonella* spp., the PhoPQ and PmrAB systems regulate the expression of genes encoding enzymes that modify the acylation and the phosphates of lipid A, respectively (please refer to Chapter 2, section 2.1.4 of the Introduction for further details). The TCS PmrAB masks the lipid A phosphates with positively charged groups by upregulating ArnT and EptA, enzymes that modify the lipid A with aminoarabinose (L-Ara4N) and phosphoethanolamine (PEtN), respectively [31, 32]. In *Salmonella* and *E. coli*, activation of PmrAB promotes resistance to AMPs, including PMB, by reducing the net negative charge of the OM [20, 33]. Activation of PmrAB is in part mediated by the second TCS PhoPQ, *via* the PmrD protein [20, 34].

To test the induction of the PmrAB system by thanatin, we monitored the induction of the representative *eptA* promoter. *E. coli* BW25113 cells carrying the plasmid with the reporter fusion *eptAp-lacZ* were treated with thanatin at 5.25 µg/mL (0.75 × MIC against BW25113), and with 5.25 µg/mL thanatin scramble (Scr), as a negative control. PMB, known to induce the PhoPQ and PmrAB systems in *Salmonella* Typhimurium [35], was also tested at 0.25 µg/mL (0.5 × MIC against BW25113). As a positive control, we treated the cells with 200 µM $FeSO_4$ since the IM histidine kinase PmrB senses high levels of iron [36]. Samples were taken at 0.5 h, 1 h, and 2 h of treatment and tested for β-galactosidase activity; a sample from a non-treated culture was also collected.

As shown in **Figure 5**, Scr did not affect the *eptA* promoter. A β-galactosidase activity signal for the induction of *eptAp* could be detected after 30 minutes of treatment with $FeSO_4$, supporting a direct role in the activation of PmrB. Upon thanatin treatment, a strong β-galactosidase activity could only be observed after 2 h-exposure whereas, surprisingly, PMB did not activate *eptAp* at any time point. From these results it appears that: i) either PMB does not activate in *E. coli* PhoPQ and consequently neither PmrAB, or ii) it activates PhoPQ but the activation of PmrAB is decoupled from PhoPQ. In *E. coli*, the L-Ara4N substituent, added by ArnT to the lipid A, is well-characterized in its contribution to PMB resistance [31, 37-39]. On the other hand, literature on the role of PEtN modifications is less abundant and most of the research work has been performed in *S.* Typhimurium.

According to the work from Rubin *et al*. [20], PmrD is required in *E. coli* for LPS modifications that confer resistance to PMB to occur, indicating some degree of PhoPQ-dependence for PmrAB activation. However, they also found that in the absence of PhoPQ, *pmrD* is still transcriptionally active under low Mg^{2+} conditions, suggesting a yet unknown system or factor able to induce the expression of *pmrD*. Perhaps, thanatin is activating this second system responsible for the PhoPQ-independent transcriptional activation of *pmrD*. Moreover, induction of this yet to be identified system could occur upon a secondary cellular effect caused by thanatin, much like *lptAp1* activation seems to be due to the decoration of LPS with CA consequent to the inhibition of LPS transport. Interestingly, an EptA homologous protein called EptB, present in both *E. coli* and *S.* Typhimurium, is under the control of the σ^E transcription factor [40]. This enzyme also transfers a PEtN group to LPS but unlike EptA, it does not modify the phosphates and instead adds the PEtN moiety to the second Kdo sugar of the core oligosaccharide [41, 42]. Perhaps the *eptA* gene could also be under the control of an ESR that is activated by thanatin and not PMB.

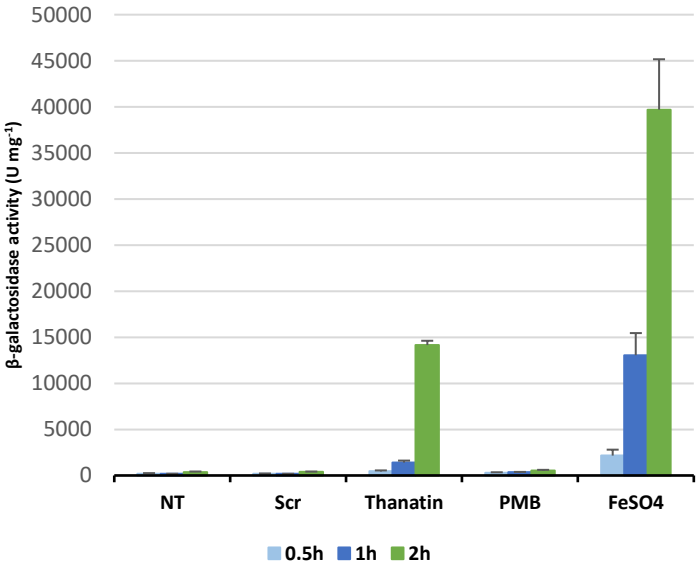

Figure 5. The *eptA* promoter is activated by thanatin. β-galactosidase activity expressed from *eptAp-lacZ* fusions in BW25113 cells upon 0.5 h, 1 h, and 2 h of treatment with or without 5.25 µg/mL of thanatin and thanatin scramble (Scr), 0.25 µg/mL of polymyxin B (PMB), and 200 µM $FeSO_4$. Each bar represents the mean value with standard deviation of the β-galactosidase activities obtained in two independent experiments. NT, no treatment.

1.2.2.4 Induction of the *ldtD* promoter

The peptidoglycan cell wall, which confers shape and osmotic stability to the cell, is formed by repeating units of the disaccharide N-acetyl glucosamine–N-acetyl muramic acid crosslinked by short peptides [43]. In *E. coli*, the stem peptides are composed of L-alanine, D-glutamic acid, L-meso-diaminopalmelic acid (mDAP), and two D-alanines [44, 45]. The vast majority of cross-links are of the DD or 4-3 type, occurring between the D-Alanine residue at position 4 and the mDAP at position 3 of the acceptor muropeptide. The DD-transpeptidation is performed by the DD-TPase activity of the class A Penicillin Binding Proteins (PBPs) PBP1A and PBP1B, and class B PBP2 and PBP3 [46]. The stem peptides can also be crosslinked in a 3-3 or LD-type configuration between two mDAP residues of adjacent strands in a reaction catalysed by LD-transpeptidases (LDTs); in normal, non-stress, conditions LD-transpeptidation occurs at very low levels (2-10%) [47]. In *E. coli*, six LDTs have been identified so far and they can be divided according to their function. LdtA, LdtB, and LdtC covalently attach Lpp to mDAP residues of the peptidoglycan (PG) cell wall [48]; while LdtD and LdtE catalyse 3-3 crosslinking [49]. LdtF does not possess LD-TPase activity and it seems to stimulate the activity of both LdtD and LdtE [50]. LD-transpeptidation has been associated with resistance to β-lactams since the alternative crosslinking mechanism prevents the action of these antibiotics, with the exception of carbapenems [51-54]. Interestingly, upon defects in the LPS transport, peptidoglycan remodelling *via* an increase in 3-3 cross-links occurs [50]. Strengthening the PG cell wall seems to help *E. coli* cells at avoiding cell lysis when the integrity of the OM is compromised. Morè *et al*. have suggested that LdtD together with PBP1B and PBP6a form a dedicated PG repair machine that runs a PG remodelling program to counteract damages to the OM [50].

Since LdtD was specifically expressed in response to the disruption of LPS transport, caused by either the depletion of LptC or cell exposure to a LpxC-inhibitor [50], we tested if thanatin could induce the expression of LdtD. For this, we treated *E. coli* BW25113 cells, previously transformed with the plasmid pRS415-*ldtDp* carrying a transcriptional fusion of the promoter region of *ldtD* to *lacZ* [50], with thanatin at 5.25 µg/mL (0.75 × MIC against BW25113), and with 5.25 µg/mL thanatin scramble (Scr), as a negative control. EDTA, a chelating agent known to perturb the LPS layer [55] and shown to induce *ldtDp* (Polissi A. personal communication), was also used at 5 mM as a positive control. The β-galactosidase activity was measured from samples taken at 0.5 h, 1 h, and 2 h of treatment; samples from a non-treated culture were also collected.

As shown in **Figure 6**, the signals for β-galactosidase activity obtained with Scr were comparable to the non-treated culture; therefore, we considered that Scr did not have an effect on the promoter. EDTA did not strongly induce *ldtDp*. It is possible that, at the concentration of 5 mM, the damage caused by EDTA upon the LPS layer is not very pronounced, or it is with some success counteracted by cellular systems that modify the envelope. Consequently, in the experimental conditions used, EDTA does not strongly activate the PG remodelling machinery formed by LdtD, PBP1B, and PBP6a. Activation of the *ldtD* promoter by thanatin is discernible at one hour of incubation and reaches a strong signal after two hours. At one hour of treatment with thanatin, LptA undergoes degradation and two hours after exposure, LPS decorated with CA accumulates and LptA can no longer be detected (see Manuscript 1). This seems to correlate with a strong induction of *ldtDp* observed only after two hours since, at this time point, the transport of LPS to the OM is deeply perturbed by thanatin, evidenced by the accumulation of LPS at the IM where it is decorated with CA. Taken together, these results are diagnostic of severe LPS transport defects.

The expression of peptidoglycan-modifying enzymes such as LdtD is induced by the Cpx envelope stress response [56, 57], and this ESR has been reported to be activated by inhibitors of the ABC transporter MsbA that block the LPS transport [58]. Thanatin also activates the Cpx stress response (Luirink J. personal communication). Further studies will elucidate whether the induction of the *ldtD* promoter by thanatin is dependent on Cpx activation.

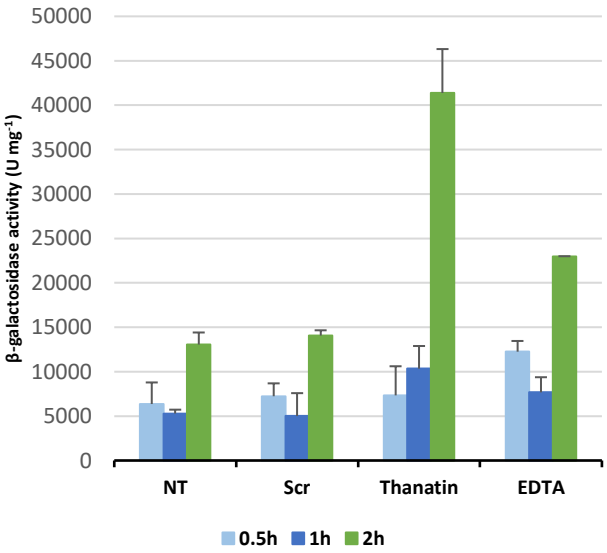

Figure 6. The *ldtD* promoter is activated by thanatin. β-galactosidase activity expressed from *ldtDp-lacZ* fusions in BW25113 cells upon 0.5 h, 1 h, and 2 h of treatment with or without 5.25 µg/mL of thanatin and thanatin scramble (Scr), and 5 mM EDTA. Each bar represents the mean value with standard deviation of the β-galactosidase activities obtained in two independent experiments. NT, no treatment.

1.2.3 Additional materials and methods

Bacterial strains and media

The *E. coli* strains and plasmids used in the additional experiments are listed in **Table 1**, and the oligonucleotides are listed in **Table 2**. The wild-type strain MG1655 was used in the checkerboard synergy assays. The wild-type strain BW25113 was used to study the activation of the promoters *lptAp1*, *eptAp*, and *ldtDp*, and the mutant strain PS135 was also employed in the study of *lptAp1* activation. Luria-Bertani (LB) medium (10 g/L tryptone, 5 g/L yeast extract, 10 g/L NaCl) supplemented with 100 µg/mL ampicillin was used to grow the bacteria for the study of *lptAp1* and *eptAp* activation. LD medium (10 g/L tryptone, 5 g/L yeast extract, 5 g/L NaCl) without antibiotic was used to grow the bacteria for the study of *ldtDp* activation; the overnight preculture was supplemented with 100 µg/mL ampicillin.

Checkerboard synergy assays

The checkerboard broth microdilution assays were performed in 96-well microtiter plates against the strain MG1655. Thanatin, with concentrations starting at 3.5 µg/mL, was tested in combination with the antibiotics bacitracin (starting concentration 4096 µg/mL), vancomycin and rifampicin (starting concentrations 256 µg/mL). A stationary phase bacterial culture, grown at 37°C in LB medium, was diluted in fresh medium adjusting the OD_{600} to a value of 0.05 and incubated in the presence of concentration gradients of the three compound combinations. After 24 h of incubation at 37°C, the OD_{600} was measured by a plate reader (EnSpire Multimode Plate Reader, PerkinElmer). The FIC index (FIC_I) was calculated for the well presenting no detectable bacterial growth at the lowest concentration of the tested antibiotic when combined with 0.25 × MIC of thanatin. The FIC of each compound was calculated by dividing the concentration in that well by the MIC of the drug alone. The FIC_I for each drug combination was obtained by the sum of the individual FIC values, and it was considered synergistic when ≤ 0.5 [2].

Plasmid construction

To construct the plasmid pRS415-*eptAp*, the promoter region of *eptA* was PCR-amplified from the genomic MG1655 DNA with the primer pair AP540/AP541, as presented in **Table 2**. The PCR product was then digested with the indicated restriction enzymes and subcloned into the corresponding site of the pRS415 vector. The insert was verified by sequencing.

Growth conditions for the induction of the promoters

The induction of the promoters with the different stress agents was performed with a protocol adapted from [25]. Briefly, to test the induction of *lptAp1* and *eptAp*, the bacterial cultures were grown at 37°C in LB medium supplemented with ampicillin until an OD_{600} of 0.2, and diluted 2-fold by transferring 5 mL of the culture to prewarmed falcon tubes containing 5 mL LB medium supplemented with ampicillin and with or without the stress agent. Incubation at 37°C was resumed and samples were collected at 0.5 h, 1 h, and 2 h of treatment to test for β-galactosidase activity.

To test the induction of the *ldtD* promoter, the bacterial culture was grown at 37°C in LD medium until an OD_{600} of 0.1 and split into 20 mL subcultures in prewarmed flasks containing or not the stress agent. Incubation at 37°C was continued and samples were collected at 0.5 h, 1 h, and 2 h of treatment to test for β-galactosidase activity.

β-galactosidase activity assay

β-galactosidase activity assays were performed with a protocol adapted from [59]. One or two mL of culture were collected, pelleted by centrifugation (3000 g, 10 min at 4°C), and resuspended in 1 mL PM2 buffer (70 mM Na_2HPO_4 . $12H_20$, 30 mM NaH_2PO_4 . H_2O, 1 mM $MgSO_4$, 0.2 mM $MnSO_4$, pH 7.0). After recording the OD_{600} for each sample, the cells were permeabilized with 30 µL of 0.1% SDS and 50 µL of chloroform, vortexed two times for ten seconds and equilibrated for two minutes. Aliquots of 0.1 to 0.4 mL of permeabilized cells were added to 1 mL (final volume) of PM2 buffer containing 100 mM β-mercaptoethanol, and placed at 30ºC for 5 min. A control tube to serve as a blank was also prepared. The enzymatic reaction was started by adding 200 µL of 0.4% *ortho*-nitrophenyl-β-galactoside (ONPG) (ONPG dissolved in PM2 buffer and pre-equilibrated at 30ºC) and stopped after one minute with 500 µL 1M Na_2CO_3. The optical densities at 420 nm and 550 nm were recorded. For each sample, the values of optical density at 600 nm, 420 nm, and 550 nm were recorded using a plate reader (EnSpire Multimode Plate Reader, PerkinElmer). The specific activity was expressed as nmoles of ONPG hydrolysed per min per mg of dry weight bacteria.

Table 1 *Escherichia coli* K-12 strains and plasmids

Strain or plasmid	Relevant genotype or description	Source or Reference
Strains		
MG1655	K-12, F⁻ λ⁻ *ilvG⁻ rfb-50 rph-1*	[60]
BW25113	Δ(*araD-araB*)*567* Δ*lacZ4787*(::*rrnB-3*) λ⁻ *rph-1* Δ(*rhaD-rhaB*)*568 hsdR514*	[61]
PS135	AM604 Δ*wcaJ*::*cat*	[62]
Plasmids		
pRS415	pBR322 derivative, carries the entire *lac* operon without the promoter; *bla*	[63]
pAM8	pRS415 derivative, harbours *E. coli* 3341138 – 3341434 fragment; *bla*	[25]
pRS415-*eptAp*	pRS415 derivative, expresses LacZ from the *eptA* promoter region; *bla*	This study
pRS415-*ldtDp*	pRS415 derivative, expresses LacZ from the *ldtD* promoter region; *bla*	[50]

Table 2 Oligonucleotides

Name		Sequence (5'-3')[a]	Used to make
AP540	Forward	gtattccggaattcGGGTAAAGCACGCCCGGCATATCTGGC	*eptAp* cloning in pRS415; EcoRI
AP541	Reverse	tctatcgcggatccGCACGGTGTTTCCATCGAACAAAGTGC	*eptAp* cloning in pRS415; BamHI

[a] *E. coli* genomic sequence in uppercase; restriction sites in underlined lowercase.

1.2.4 References

1. Silver, L.L., *Multi-targeting by monotherapeutic antibacterials.* Nat Rev Drug Discov, 2007. **6**(1): p. 41-55.
2. Brennan-Krohn, T. and J.E. Kirby, *When One Drug Is Not Enough: Context, Methodology, and Future Prospects in Antibacterial Synergy Testing.* Clin Lab Med, 2019. **39**(3): p. 345-358.
3. Mitchell, A.M. and T.J. Silhavy, *Envelope stress responses: balancing damage repair and toxicity.* Nat Rev Microbiol, 2019. **17**(7): p. 417-428.
4. Lima, S., et al., *Dual molecular signals mediate the bacterial response to outer-membrane stress.* Science, 2013. **340**(6134): p. 837-41.
5. Tam, C. and D. Missiakas, *Changes in lipopolysaccharide structure induce the sigma(E)-dependent response of Escherichia coli.* Mol Microbiol, 2005. **55**(5): p. 1403-12.
6. Klein, G., et al., *Escherichia coli K-12 Suppressor-free Mutants Lacking Early Glycosyltransferases and Late Acyltransferases: minimal lipopolysaccharide structure and induction of envelope stress response.* J Biol Chem, 2009. **284**(23): p. 15369-89.
7. Hews, C.L., et al., *Maintaining Integrity Under Stress: Envelope Stress Response Regulation of Pathogenesis in Gram-Negative Bacteria.* Front Cell Infect Microbiol, 2019. **9**: p. 313.
8. Chaba, R., et al., *Signal integration by DegS and RseB governs the σ E-mediated envelope stress response in Escherichia coli.* Proc Natl Acad Sci U S A, 2011. **108**(5): p. 2106-11.
9. May, K.L., et al., *A Stress Response Monitoring Lipoprotein Trafficking to the Outer Membrane.* mBio, 2019. **10**(3).
10. Delhaye, A., G. Laloux, and J.F. Collet, *The Lipoprotein NlpE Is a Cpx Sensor That Serves as a Sentinel for Protein Sorting and Folding Defects in the Escherichia coli Envelope.* J Bacteriol, 2019. **201**(10).
11. Otto, K. and T.J. Silhavy, *Surface sensing and adhesion of Escherichia coli controlled by the Cpx-signaling pathway.* Proc Natl Acad Sci U S A, 2002. **99**(4): p. 2287-92.
12. Vogt, S.L., et al., *The Cpx envelope stress response regulates and is regulated by small noncoding RNAs.* J Bacteriol, 2014. **196**(24): p. 4229-38.
13. Wall, E., N. Majdalani, and S. Gottesman, *The Complex Rcs Regulatory Cascade.* Annu Rev Microbiol, 2018. **72**: p. 111-139.
14. Ferrieres, L., et al., *The yjbEFGH locus in Escherichia coli K-12 is an operon encoding proteins involved in exopolysaccharide production.* Microbiology, 2007. **153**(Pt 4): p. 1070-1080.
15. Wehland, M. and F. Bernhard, *The RcsAB box. Characterization of a new operator essential for the regulation of exopolysaccharide biosynthesis in enteric bacteria.* J Biol Chem, 2000. **275**(10): p. 7013-20.
16. Francez-Charlot, A., et al., *RcsCDB His-Asp phosphorelay system negatively regulates the flhDC operon in Escherichia coli.* Mol Microbiol, 2003. **49**(3): p. 823-32.
17. Gruenheid, S. and H. Le Moual, *Resistance to antimicrobial peptides in Gram-negative bacteria.* FEMS Microbiol Lett, 2012. **330**(2): p. 81-9.
18. Kox, L.F., M.M. Wosten, and E.A. Groisman, *A small protein that mediates the activation of a two-component system by another two-component system.* EMBO J, 2000. **19**(8): p. 1861-72.
19. Kato, A. and E.A. Groisman, *Connecting two-component regulatory systems by a protein that protects a response regulator from dephosphorylation by its cognate sensor.* Genes Dev, 2004. **18**(18): p. 2302-13.
20. Rubin, E.J., et al., *PmrD is required for modifications to escherichia coli endotoxin that promote antimicrobial resistance.* Antimicrob Agents Chemother, 2015. **59**(4): p. 2051-61.
21. Coornaert, A., et al., *MicA sRNA links the PhoP regulon to cell envelope stress.* Mol Microbiol, 2010. **76**(2): p. 467-79.
22. Sperandeo, P., G. Deho, and A. Polissi, *The lipopolysaccharide transport system of Gram-negative bacteria.* Biochim Biophys Acta, 2009. **1791**(7): p. 594-602.

23. Sperandeo, P., et al., *Non-essential KDO biosynthesis and new essential cell envelope biogenesis genes in the Escherichia coli yrbG-yhbG locus.* Res Microbiol, 2006. **157**(6): p. 547-58.
24. Sperandeo, P., et al., *Characterization of lptA and lptB, two essential genes implicated in lipopolysaccharide transport to the outer membrane of Escherichia coli.* J Bacteriol, 2007. **189**(1): p. 244-53.
25. Martorana, A.M., et al., *Complex transcriptional organization regulates an Escherichia coli locus implicated in lipopolysaccharide biogenesis.* Res Microbiol, 2011. **162**(5): p. 470-82.
26. Gottesman, S., P. Trisler, and A. Torres-Cabassa, *Regulation of capsular polysaccharide synthesis in Escherichia coli K-12: characterization of three regulatory genes.* J Bacteriol, 1985. **162**(3): p. 1111-9.
27. Farris, C., et al., *Antimicrobial peptides activate the Rcs regulon through the outer membrane lipoprotein RcsF.* J Bacteriol, 2010. **192**(19): p. 4894-903.
28. Ma, B., et al., *The antimicrobial peptide thanatin disrupts the bacterial outer membrane and inactivates the NDM-1 metallo-beta-lactamase.* Nat Commun, 2019. **10**(1): p. 3517.
29. Tao, K., S. Narita, and H. Tokuda, *Defective lipoprotein sorting induces lolA expression through the Rcs stress response phosphorelay system.* J Bacteriol, 2012. **194**(14): p. 3643-50.
30. Simpson, B.W. and M.S. Trent, *Pushing the envelope: LPS modifications and their consequences.* Nat Rev Microbiol, 2019. **17**(7): p. 403-416.
31. Trent, M.S., et al., *An inner membrane enzyme in Salmonella and Escherichia coli that transfers 4-amino-4-deoxy-L-arabinose to lipid A: induction on polymyxin-resistant mutants and role of a novel lipid-linked donor.* J Biol Chem, 2001. **276**(46): p. 43122-31.
32. Lee, H., et al., *The PmrA-regulated pmrC gene mediates phosphoethanolamine modification of lipid A and polymyxin resistance in Salmonella enterica.* J Bacteriol, 2004. **186**(13): p. 4124-33.
33. Herrera, C.M., J.V. Hankins, and M.S. Trent, *Activation of PmrA inhibits LpxT-dependent phosphorylation of lipid A promoting resistance to antimicrobial peptides.* Mol Microbiol, 2010. **76**(6): p. 1444-60.
34. Hagiwara, D., T. Yamashino, and T. Mizuno, *A Genome-wide view of the Escherichia coli BasS-BasR two-component system implicated in iron-responses.* Biosci Biotechnol Biochem, 2004. **68**(8): p. 1758-67.
35. Richards, S.M., et al., *Cationic antimicrobial peptides serve as activation signals for the Salmonella Typhimurium PhoPQ and PmrAB regulons in vitro and in vivo.* Front Cell Infect Microbiol, 2012. **2**: p. 102.
36. Wosten, M.M., et al., *A signal transduction system that responds to extracellular iron.* Cell, 2000. **103**(1): p. 113-25.
37. Breazeale, S.D., et al., *A formyltransferase required for polymyxin resistance in Escherichia coli and the modification of lipid A with 4-Amino-4-deoxy-L-arabinose. Identification and function oF UDP-4-deoxy-4-formamido-L-arabinose.* J Biol Chem, 2005. **280**(14): p. 14154-67.
38. Alteri, C.J., et al., *The broadly conserved regulator PhoP links pathogen virulence and membrane potential in Escherichia coli.* Mol Microbiol, 2011. **82**(1): p. 145-63.
39. Raetz, C.R., et al., *Lipid A modification systems in gram-negative bacteria.* Annu Rev Biochem, 2007. **76**: p. 295-329.
40. Figueroa-Bossi, N., et al., *Loss of Hfq activates the sigmaE-dependent envelope stress response in Salmonella enterica.* Mol Microbiol, 2006. **62**(3): p. 838-52.
41. Kanipes, M.I., et al., *Ca2+-induced phosphoethanolamine transfer to the outer 3-deoxy-D-manno-octulosonic acid moiety of Escherichia coli lipopolysaccharide. A novel membrane enzyme dependent upon phosphatidylethanolamine.* J Biol Chem, 2001. **276**(2): p. 1156-63.
42. Reynolds, C.M., et al., *A phosphoethanolamine transferase specific for the outer 3-deoxy-D-manno-octulosonic acid residue of Escherichia coli lipopolysaccharide. Identification of the eptB gene and Ca2+ hypersensitivity of an eptB deletion mutant.* J Biol Chem, 2005. **280**(22): p. 21202-11.

43. Vollmer, W., D. Blanot, and M.A. de Pedro, *Peptidoglycan structure and architecture.* FEMS Microbiol Rev, 2008. **32**(2): p. 149-67.
44. Schleifer, K.H. and O. Kandler, *Peptidoglycan types of bacterial cell walls and their taxonomic implications.* Bacteriol Rev, 1972. **36**(4): p. 407-77.
45. Holtje, J.V., *Growth of the stress-bearing and shape-maintaining murein sacculus of Escherichia coli.* Microbiol Mol Biol Rev, 1998. **62**(1): p. 181-203.
46. Sauvage, E., et al., *The penicillin-binding proteins: structure and role in peptidoglycan biosynthesis.* FEMS Microbiol Rev, 2008. **32**(2): p. 234-58.
47. Glauner, B., J.V. Holtje, and U. Schwarz, *The composition of the murein of Escherichia coli.* J Biol Chem, 1988. **263**(21): p. 10088-95.
48. Magnet, S., et al., *Identification of the L,D-transpeptidases responsible for attachment of the Braun lipoprotein to Escherichia coli peptidoglycan.* J Bacteriol, 2007. **189**(10): p. 3927-31.
49. Magnet, S., et al., *Identification of the L,D-transpeptidases for peptidoglycan cross-linking in Escherichia coli.* J Bacteriol, 2008. **190**(13): p. 4782-5.
50. More, N., et al., *Peptidoglycan Remodeling Enables Escherichia coli To Survive Severe Outer Membrane Assembly Defect.* mBio, 2019. **10**(1).
51. Mainardi, J.L., et al., *Evolution of peptidoglycan biosynthesis under the selective pressure of antibiotics in Gram-positive bacteria.* FEMS Microbiol Rev, 2008. **32**(2): p. 386-408.
52. Gupta, R., et al., *The Mycobacterium tuberculosis protein LdtMt2 is a nonclassical transpeptidase required for virulence and resistance to amoxicillin.* Nat Med, 2010. **16**(4): p. 466-9.
53. Ealand, C.S., E.E. Machowski, and B.D. Kana, *beta-lactam resistance: The role of low molecular weight penicillin binding proteins, beta-lactamases and ld-transpeptidases in bacteria associated with respiratory tract infections.* IUBMB Life, 2018. **70**(9): p. 855-868.
54. Mainardi, J.L., et al., *Unexpected inhibition of peptidoglycan LD-transpeptidase from Enterococcus faecium by the beta-lactam imipenem.* J Biol Chem, 2007. **282**(42): p. 30414-22.
55. Vaara, M., *Agents that increase the permeability of the outer membrane.* Microbiol Rev, 1992. **56**(3): p. 395-411.
56. Bernal-Cabas, M., J.A. Ayala, and T.L. Raivio, *The Cpx envelope stress response modifies peptidoglycan cross-linking via the L,D-transpeptidase LdtD and the novel protein YgaU.* J Bacteriol, 2015. **197**(3): p. 603-14.
57. Delhaye, A., J.F. Collet, and G. Laloux, *Fine-Tuning of the Cpx Envelope Stress Response Is Required for Cell Wall Homeostasis in Escherichia coli.* mBio, 2016. **7**(1): p. e00047-16.
58. Alexander, M.K., et al., *Disrupting Gram-Negative Bacterial Outer Membrane Biosynthesis through Inhibition of the Lipopolysaccharide Transporter MsbA.* Antimicrob Agents Chemother, 2018. **62**(11).
59. Miller, J.H., *A short course in bacterial genetics : a laboratory manual and handbook for Escherichia coli and related bacteria*. 1992, Plainview, N.Y.: Cold Spring Harbor Laboratory Press.
60. Blattner, F.R., et al., *The complete genome sequence of Escherichia coli K-12.* Science, 1997. **277**(5331): p. 1453-62.
61. Datsenko, K.A. and B.L. Wanner, *One-step inactivation of chromosomal genes in Escherichia coli K-12 using PCR products.* Proc Natl Acad Sci U S A, 2000. **97**(12): p. 6640-5.
62. Falchi, F.A., et al., *Mutation and Suppressor Analysis of the Essential Lipopolysaccharide Transport Protein LptA Reveals Strategies To Overcome Severe Outer Membrane Permeability Defects in Escherichia coli.* J Bacteriol, 2018. **200**(2).
63. Simons, R.W., F. Houman, and N. Kleckner, *Improved single and multicopy lac-based cloning vectors for protein and operon fusions.* Gene, 1987. **53**(1): p. 85-96.

2. Manuscript 2 (unpublished draft)

Foreword

The following work here presented was mainly performed by Federica Falchi, the lead author of Manuscript 2. This work was carried out in collaboration with the laboratory of Jean-Pierre Simorre and, from his group, Tiago Baeta and Cedric Laguri obtained the SEC-MALLS and SPR data. As contributing author, I performed the molecular cloning and protein purification of protein complexes used in the ATPase activity assays. I also contributed to setting up the experimental conditions for SEC-MALLS and SPR data collection.

A LptF suppressor mutation reveals a checkpoint control for the correct assembly of the Lpt machinery

Federica A. Falchi[1a], Tiago Baeta[2,#], Elisabete C. C. M. Moura[1,#], Cedric Laguri[2], Jean-Pierre Simorre[2], Alessandra Polissi[1], Paola Sperandeo[1]*

[1]Dipartimento di Scienze Farmacologiche e Biomolecolari, Università degli Studi di Milano, Milan, Italy

[2]Univ. Grenoble Alpes, CNRS, CEA, IBS, F-38000 Grenoble, France

[a] Current address: Dipartimento di Bioscienze, Università degli Studi di Milano, Milan, Italy

# contributed equally to the present work

*** Correspondence:**

Dr. Paola Sperandeo

paola.sperandeo@unimi.it

ABSTRACT

Lipopolysaccharides (LPS) are essential components of the outer membrane (OM) of many Gram-negative bacteria that provide a barrier against the entry of toxic molecules. In *Escherichia coli*, LPS is exported to the cell surface by seven essential proteins (LptA-G) that form a transenvelope complex. At the inner membrane, the ATP-binding cassette (ABC) transporter $LptB_2FG$, associated with LptC, powers LPS extraction from the membrane and its transfer to the periplasmic LptA protein. LptC interacts both with $LptB_2FG$ and LptA and regulates the ATPase activity of $LptB_2FG$, but its precise role in the transport remains unclear.

A genetic screen has previously identified mutants at a residue (R212) of LptF that are viable in absence of LptC, suggesting that this position at the interface of the LptF/LptC complex is key in LPS transport. Here, we provide *in vivo* and *in vitro* evidence that LptF R212G mutant assembles a six-component machinery by interacting with LptA in the absence of LptC, and that the mutation does not interfere with LptC recruitment. Furthermore, we show that loss of charge and steric hindrance at position 212 of LptF accounts for the independence of the mutants towards LptC. R212 mutation, located in the periplasm at the interface with LptC also abolishes regulation of the $LptB_2FG$ ATPase activity by LptC and LptA. Overall, this study suggests that R212 position is a checkpoint in the Lpt system that signals proper assembly of the $LptB_2FGC$ transporter with LptA.

INTRODUCTION

The hallmark of Gram-negative bacteria is their tripartite cell envelope constituted by two concentric membranes delimiting an aqueous space, the periplasm, that contains a thin layer of peptidoglycan [1]. The inner membrane (IM) is a canonical phospholipid bilayer, whose role is to confine cytoplasmic components; in contrast, the outer membrane (OM) is highly asymmetric with phospholipids in the inner leaflet and lipopolysaccharide (LPS) in the outer leaflet of its bilayer [1, 2]. The presence of tightly packed LPS molecules exclusively in the outer leaflet of the OM accounts for its peculiar permeability proprieties, and protects Gram-negative bacteria from noxious agents, such as antibiotics, enabling the colonization of different and hostile environments [3]. Accordingly, LPS is an essential structure in most Gram-negative organisms [4], and defects in the integrity of the LPS layer increase their sensitivity to several antibiotics [3]. Therefore, a deeper understanding of the molecular mechanisms that drive the building of the OM is fundamental for the development of novel strategies to fight bacterial infections.

LPS is a complex amphipathic molecule consisting of an acylated bis-phosphorylated di-glucosamine anchor (the lipid A), linked to a conserved oligosaccharide chain (the core), which can be further decorated by the addition of a highly variable polysaccharide (the O antigen) [5]. The lipid A-core moiety of LPS is synthesized and assembled at the cytoplasmic side of the IM and is then flipped across the IM by the action of the essential ATP-binding cassette (ABC) transporter MsbA, to gain periplasmic orientation [5-7]. Following the addition of the O antigen and other chemical modifications at the periplasmic side of the IM, mature LPS molecules need to be extracted from the membrane and transported through the aqueous periplasmic space to be finally assembled at the outer side of the OM. This process requires an energy input from the cytoplasm to facilitate extraction of the acyl chains of lipid A from the IM, and to allow the transport of the amphipathic LPS molecules in the hydrophilic environment of the periplasm towards the outer leaflet of the OM against a concentration gradient [8].]. All these tasks are accomplished by a multiprotein machinery named Lpt (from Lipopolysaccharide transport), that couples the energy harnessed from the ATP binding and hydrolysis in the cytoplasm to the establishment of a continuous stream of LPS molecules through a channel that connects the IM to the OM [9].

The Lpt machinery is composed of seven essential proteins in *Escherichia coli* (LptA to G), with variable degrees of conservation among Gram-negative bacteria, that are organized in

three sub-complexes spanning all compartments of the cell: at the IM, a dimer of the ATP-binding protein LptB is associated with the transmembrane proteins LptF and LptG, and with the bitopic protein LptC, to form an unconventional ABC transporter responsible for energising the LPS detachment from the IM [10-13].

The energy provided by $LptB_2FGC$ is also employed to move LPS molecules into the hydrophobic interior of a periplasmic bridge formed by the N-to-C terminal interaction of the structurally similar β-jellyroll domains found in LptC [14-16], the entirely periplasmic protein LptA [17, 18], and the N-terminal domain of LptD, the ß-barrel OM protein that, in complex with the lipoprotein LptE, constitutes the translocon for final insertion of LPS in the OM [19, 20]. The relevance of LptCAD bridge formation has been recently demonstrated by showing that LptA is required *in vitro* to connect vesicles bearing the IM and OM Lpt subcomplexes, thus allowing LPS trafficking between them [21]. Accordingly, each protein of the bridge was previously shown to directly interact with LPS [22, 23]. It is important to note that the same β-jellyroll architecture has also been found in the periplasmic domains of both LptF and LptG, suggestive of the possible paths for LPS during transport [24, 25]. The mechanism for LPS transport by the Lpt system has been compared to the movement of candies in a PEZ candy dispenser, where the stack of candies is pushed into the tube by a spring at the bottom of the dispenser. Similarly, the energy provided by $LptB_2FGC$ creates a stream of LPS molecules moving through the hydrophobic grove of LptCAD in the periplasm to be finally inserted in the OM by LptDE [26].

Recent structural data have revealed that, before the extraction from the IM, LPS is accommodated into a hydrophobic cavity formed by the transmembrane helices of LptF and LptG, and the interaction between the charged moieties of lipid A and a cluster of residues in the first transmembrane helix of LptG is responsible for the early recognition of the substrate by the transporter [11, 27]. Interestingly, the transmembrane helix of LptC interdigitates between the transmembrane helices of LptF and LptG, contributing to the formation of the cavity [11-13]. In this structural architecture, the periplasmic domain of LptC is associated in a head-to-tail fashion with the β-jellyroll domain of LptF, from which it receives LPS [11]. From the data available so far, the β-jellyroll domain of LptG seems to not be involved in LPS transport, at least under laboratory conditions. Despite the wealth of structural information gained recently, the mechanism that couples energy production by $LptB_2FGC$ with LPS movement into the machinery, as well as the role of LptC in the transporter, still await to be elucidated.

LptC is an unconventional subunit of the $LptB_2FGC$ ABC transporter, whose presence has been shown to decrease the ATPase activity of the transporter [11, 12, 21]. The inhibitory activity of LptC has been associated to its transmembrane domain, despite this region being dispensable for bacterial growth under laboratory conditions, but what exactly this inhibition means for the function of the machinery is still not clear [28]. To gain a better understanding into the function of LptC, we performed a selection for suppressor mutations that overcome the lethality of the deletion of *lptC*, upon conditions of LptA overexpression [29]. From this screen, we isolated a class of mutants bearing a substitution of the residue R212 in the β-jellyroll domain of LptF [29]. The existence of this class of mutants suggested that mutations in a specific region of LptF might enable LptA to substitute for LptC in the assembly of the Lpt machinery, prompting us to better characterize these mutants.

In this work, we show that the specific mutation R212G in LptF allows the formation of a six-component transenvelope machinery through the direct interaction of the β-jellyroll domain of LptF with LptA. Structural observations coupled to site-directed mutagenesis, alongside the measurement of the ATPase activity of purified wild-type and mutant $LptB_2FG$ complexes in the presence or absence of LptC, allow us to propose a mechanism for the suppression of Δ*lptC* by the $lptF^{R212G}$ allele. According to this model, $LptB_2FGC$ IM complex would control LPS flow to the periplasmic bridge *via* a dynamic network of interaction occurring between LptF and LptC, creating a path for LPS delivery to LptA. In the absence of LptC, the R212G mutation would reshuffle such interaction network to allow direct transfer of LPS from LptF to LptA.

MATERIALS AND METHODS

Bacterial strains and growth conditions

E. coli bacterial strains used in this study are listed in **Table 1**. Unless otherwise stated, bacteria were grown at 37°C in Luria-Bertani (LB) [30] and, when required, 100 μg/mL ampicillin, 30 μg/mL chloramphenicol, 25 μg/mL kanamycin, 50 μg/mL spectinomycin were added. Solid media were prepared as described above with 1% (w/v) agar.

Plasmid construction

All plasmids are listed in **Table 2**. To construct any plasmid, the desired gene or DNA fragment was amplified by PCR from the DNA template using primers listed in **Table 3**. The amplified fragment was digested with appropriate restriction enzymes (New England Biolabs) and inserted into the same sites of a carrying vector. Amber mutant variants were generated by site-directed mutagenesis using QuickChange II Site-Directed Mutagenesis Kit (Agilent Technologies) or Q5 Site-Directed Mutagenesis Kit (NEB). All cloned DNA regions obtained by PCR were sequenced to rule out the presence of mutations.

Affinity purification of membrane Lpt complexes

Membrane Lpt complexes were affinity purified from strains expressing His-tagged LptB from pET23/42 LptB plasmid or His-tagged LptC from pET23/42 LptC plasmid as described in Chng *et al*. [20]. As negative control a strain containing pET23/42 was used.

In vivo UV-Photocrosslinking

In vivo site-specific UV-Photocrosslinking and whole-cell lysate analysis. Amber codons were introduced into pGS445 and pGS451 plasmids, harbouring *lptFGAB* and *lptF*^{R212G}*GAB*, respectively, pEVOL-Spn vector [31, 32] was used to incorporate *p*-benzoyl-L-phenylalanine (*p*Bpa) into LptF or LptF^{R212G}. Plasmids carrying amber mutations were used to transform AM604 strain. Diploid strains were used for all experiments and the protocol was modified from Simpson *et al*. [33]. Briefly, overnight cultures were diluted in 10 mL of LB medium containing 0.45 mM *p*BPA (Bachem) and 0.2% arabinose to an optical density at 600 nm (OD_{600}) of 0.1. Strains were grown to an OD_{600} of 0.5-0.7. A total amount of 1 OD of cells was transferred to a 6-well flat-bottom cell culture plate (Greiner bio-one) and irradiated for 10 min with a UV lamp (365 nm). An additional sample corresponding to 1 OD of cells was used as

UV-untreated control. Samples were then TCA precipitated, resuspended in 100 µl of sample buffer (SB) 1x for SDS−PAGE and analysed by western blotting using anti-LptA and anti-LptF antibodies.

In vivo UV-Photocrosslinking followed by affinity purification. Amber codons were introduced in pET23/42 LptF-His or pET23/42 LptF^{R212G}-His plasmids expressing C-terminal His-tagged LptF or LptF^{R212G}, respectively, and pSup-BpaRS-6TRN was used to introduce *p*BPA at the specified positions. The assay was performed as described in Owens *et al*. (2019), with minor modifications. Overnight cultures of were diluted 1:100 into 200 mL of LB medium supplemented with 0.7 mM *p*BPA and suitable antibiotics and grown to midlog phase at 30°C. Each culture was split in half, and each sample was pelleted, resuspended in 4 mL of ice-cold PBS and either used directly or irradiated with UV light at 365 nm for 10 min. All cells were collected and resuspended in 4 mL of ice-cold Buffer A [20 mM Tris (pH 7.4), 300 mM NaCl, 5 mM $MgCl_2$ and 15 mM imidazole] containing 1% ZW 3-14 (Fluka), 100 µg/mL lysozyme, 1 mM phenylmethanesulfonyl fluoride (PMSF), and 50 µg/mL DNase I, lysed by sonication and centrifuged at 4000 g, 10 min, to remove unbroken cells. Then, Nickel affinity purification was performed. 0.5 mL of Ni-NTA resin suspension (Qiagen) was pre-equilibrated with 5 mL of Buffer A. The mixture was loaded onto the column and allowed to drain by gravity. The column was washed with 1 mL of Buffer A and 2 x 5 mL of Buffer B [20 mM Tris (pH 7.4), 300 mM NaCl, 20 mM imidazole, 0.1% ZW 3-14] and eluted with 2 x 0.75 mL of Buffer C [20 mM Tris (pH 7.4), 300 mM NaCl, 200 mM imidazole, 0.1% ZW 3-14]. The eluate was then TCA precipitated, resuspended in 80 µL of sample buffer (SB) 1x for SDS−PAGE and immunoblotting.

Purification of LptB$_2$FG and LptB$_2$FGC complexes

To overexpress and purify the IM Lpt complex with or without LptC, KRX cells were transformed with pCDFDuet vector expressing full-length LptB, LptF, LptG or LptB, LptF^{R212G}, LptG, and with or without pBAD/HisA-LptC expressing LptC fused to a C-terminal His tag. Cultures were grown in 1 L of LB medium to an OD_{600} of 0.8 at 37°C. Expression was induced with 0.02% L-rhamnose and 0.02% arabinose for 3 h at 37°C. Cells were harvested by centrifugation at 4°C, 5000 g, 20 min and stored at -80°C. The cell pellets were resuspended in Lysis buffer [50 mM Tris HCl pH 7.4, 300 mM NaCl, 1 mM $MgCl_2$] supplemented with 1 mM phenylmethanesulfonyl fluoride (PMSF) (Sigma-Aldrich), 100 µg/mL lysozyme and 50 µg/mL DNaseI. The cells were disrupted by a single passage through a cell disruptor (One Shot

model; Constant Systems Ltd.) at a pressure of 22,000 lb/in^2. Unbroken cells were removed by centrifugation at 4500 g for 15 min and membranes were isolated by ultracentrifugation at 100,000 g for 1 h. Membranes were resuspended and solubilized in 20 mL of Resuspension buffer [20 mM Tris-HCl (pH 7.4), 300 mM NaCl, 5 mM $MgCl_2$, 10% (vol/vol) glycerol, 1% (wt/vol) *n*-dodecyl-β-D-maltopyranoside (DDM, Sigma), 2 mM ATP] at 4°C for 1 h, followed by centrifugation at 100,000 g for 30 min. The supernatant was supplied with 2 mM imidazole and rocked for 1 h with 1 mL of TALON metal affinity resin (Clontech), pre-equilibrated with Affinity buffer [20 mM Tris-HCl (pH 7.4), 300 mM NaCl, 5 mM $MgCl_2$, 10% (vol/vol) glycerol, 0.05% (wt/vol) DDM]. The column was washed with 20 column volumes (cv) of Affinity buffer plus 2 mM imidazole and 10 cv of Affinity buffer plus 10 mM imidazole. Proteins were eluted with 8 cv of affinity buffer plus 100 mM imidazole and the eluate was concentrated up to 2 mL with an Amicon centrifugation filter, 10-kDa molecular weight cut-off (MWCO, Amicon Ultra; Millipore). The buffer was changed to Exchange buffer [20 mM Tris-HCl pH 7.4, 300 mM NaCl, 0.05% (wt/vol) DDM] and the sample was concentrated up to 0.4 mL as above. The protein concentration was determined by Bradford assay (Thermo Fisher) using bovine serum albumin as a standard and samples were loaded on SDS-PAGE and Coomassie stained. For the purification of the $LptB_2FG$ complex, an additional step of size exclusion chromatography was performed before determining protein concentration. The $LptB_2FG$ concentrated eluate was applied to a HiLoad 16/600 Superdex 200 gel filtration column pre-equilibrated with 20 mM Tris-HCl pH 7.4, 300 mM NaCl, 0.05% (wt/vol) DDM. Peak fractions were combined and concentrated with an Amicon 100-kDa molecular weight cut-off centrifugation filter (Amicon Ultra; Millipore).

Purification of ΔTM LptC ($LptC_{\Delta 1\text{-}23}$) and $LptA_m$

E. coli LptC lacking the first 23 residues of the transmembrane domain was expressed from a plasmid (LptC pQESH, QIAGEN) with an N-terminal His-Tag and purified as described by Laguri *et al*. [15].

$LptA_m$ coding for residues 1–159 followed by a SGRVEHHHHHH TAG in a pET21b-derived vector was expressed and purified as described by Laguri *et al*. [15].

ATPase activity assay

The ATPase activity of 0.2 μM $LptB_2FG$ and $LptB_2F^{R212G}G$ purified complexes, or 0.1 μM $LptB_2FGC$ and $LptB_2F^{R212G}GC$ purified complexes, was measured in 50 mM Tris-HCl, pH 8.0,

500 mM NaCl, 10% glycerol, 0.01% DDM. LptA or soluble LptC were added at 20 x molar ratio. The reaction was started at room temperature by the addition of 5 mM ATP/$MgCl_2$. Aliquots (15 µL) were taken at 0, 5, 10, 20, 40, and 60 minutes and mixed with the same volume of 12% SDS to stop the reaction. The amounts of inorganic phosphate were determined according to the method reported in Chifflet *et al*. [34].

Absorbance was read at 850 nm using the EnSpire Multimode Plate Reader (PerkinElmer). The assay was repeated three times for each condition and the results were analysed with GraphPad Prism (GraphPad Software, Inc., San Diego, CA, USA). Plotted data represents the mean value of 3 replicates, error bars indicate the standard deviation. Initial rates are the slope of the linear region of the graph (t = 5 min). Significance was evaluated with t-test or One-way ANOVA and post-hoc Tukey HSD analysis.

$\alpha = 0.05$, *, $P<0.05$; **, $P<0.01$; ****, $P<0.001$; ns, not significant.

SDS-PAGE and immunoblotting

Home-made 10%, 12.5% or 15% polyacrylamide gels and Tris-glycine running buffer were used for SDS-PAGE/immunoblotting experiments [35]. For immunoblotting, proteins were transferred onto nitrocellulose or PVDF membranes (Hybond ECL; GE Healthcare). Mouse monoclonal anti-His (Sigma-Aldrich) was used at 1:3,000 dilution. Polyclonal sera against LptA [36], LptC [37], LptD [37] and LptF [28] (GenScript) were used at dilutions of 1:1,000, 1:3,000, 1:5,000 and 1:10,000 respectively. Polyclonal serum anti-LptB [37] (kindly provided by D. Kahne and N. Ruiz) was used at dilution of 1:10,000. As secondary antibodies, anti-rabbit and anti-mouse immunoglobulins (Li-Cor) were used at a dilution of 1:15,000 and bands were detected using an Odissey Fc imaging system (Li-Cor). LptF crosslinking was visualized using a goat anti-rabbit IgG HRP-conjugated secondary antibody (Sigma-Aldrich). Filters were developed with the Cyanagen Westar ηC Ultra 2.0 reagent and detected using an Odissey Fc imaging system (Li-Cor).

Surface Plasmon Resonance binding assay

$LptB_2FG$ and $LptB_2F^{R212G}G$ purified in DDM were immobilized onto a CM5 chip in a T200 instrument (GE Healthcare) through standard EDC/NHS method in 10 mM MES pH 6.0, 300 µM DDM at 21°C. About 4000 RU of immobilized protein was achieved. $LptA_m$ was injected at different concentrations in 20 mM Tris, 150 mM NaCl, 300 µM DDM, pH 8.0 buffer. The sensorchip was regenerated between two injections with 10 s NaOH 10 mM, 300 µM DDM

pulses. Sensorgrams accounting from buffer alone and from a control sensorchip were subtracted prior to analysis. Kd was determined with the BiaEval software considering steady state binding prior to dissociation.

SEC-MALLS (Size Exclusion Chromatography - Multiple Angle Laser Light Scattering)

$LptB_2FG$ and $LptB_2F^{R212G}G$ purified in DDM were injected (40 µL volume at 8 µM) alone or in presence of 50 µM of ΔTM LptC or $LptA_m$ in 20 mM Tris, 150 mM NaCl 0.05% DDM buffer at 25°C on a Superdex S200 (10/300GL) connected to an HPLC-Multi Angle light scattering (DynaPro Nanostar), refraction index (Optilab rex) and Optical density detectors (SPD-M20A). Data analysis is performed with ASTRA 5.4.3.20 software (WYATT). Two-component analysis with the protein conjugate method was used for determination of DDM micelle and protein complexes masses.

RESULTS

LptF^{R212G} mutant assembles a six-component Lpt machinery

The *E. coli* LptC protein is an essential structural component of the Lpt bridge connecting the IM ABC transporter LptB$_2$FG with the periplasmic LptA protein [16, 38]. In a previous work, we showed that three amino acid substitutions at residue R212 of LptF, namely R212G, R212S, and R212C (collectively defined as *lptF*^{SupC} mutants), are able to suppress the lethal phenotype of Δ*lptC* mutants, provided that LptA is overexpressed [29]. Among the *lptF*^{SupC} mutants, we focused on the *lptF*^{R212G} allele because it restores not only cell viability but also OM permeability of Δ*lptC* cells to a nearly wild-type level [29]. R212 is located in the LptF β-jellyroll periplasmic domain oriented towards the interior of the cavity at the interface with LptC (**Figure 1**); this suggests that the suppressor mutants can assemble a functional six-component Lpt machine [11, 29].

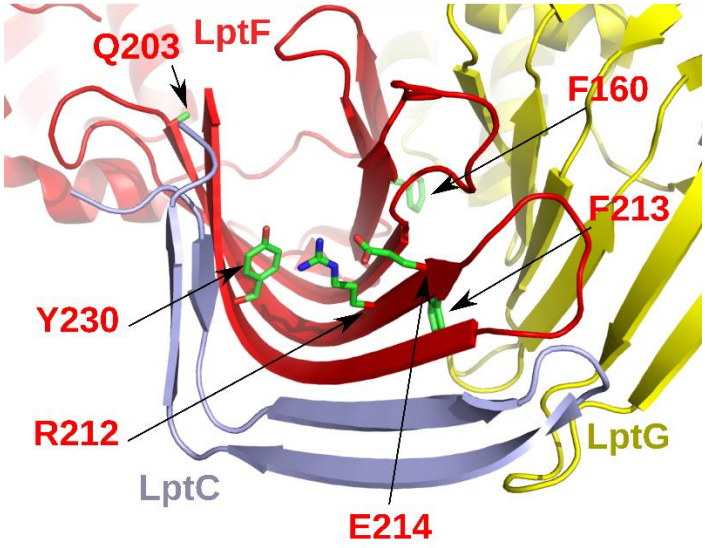

Figure 1 Ribbon representation of a detail of LptF periplasmic domain in LptB$_2$FGC structure (PDB 6MIT). LptC is coloured grey, LptF red and LptG yellow. Residues are depicted as sticks.

To assess the assembly of the Lpt complex in the *lptF*^{R212G} mutant in the absence of LptC, an *in vivo* pull-down assay was performed [16]. Total membranes were prepared from an equal cell number of *lptC*$^{+}$ parental strain (bearing Δ*lptCA* allele complemented by an IPTG-inducible *tacp*-driven copy of *lptC* and *lptA* genes) and the Δ*lptC lptF*^{R212G} suppressor mutant (bearing Δ*lptCA* allele complemented by a *tacp*-driven copy of *lptA*), both ectopically expressing C-terminally His-tagged LptB (LptB-H). After DDM-solubilization, membrane

proteins were subjected to affinity chromatography using LptB-H as bait. As negative control, affinity purification was carried out from solubilized membranes of *lptC*$^{+}$ cells transformed with the empty vector. Affinity purified samples were analysed by SDS-PAGE followed by immunoblotting with a panel of specific antibodies to assess the co-purification of IM and OM Lpt proteins. Notably, in the Δ*lptC lptF*^{R212G} suppressor mutant, LptB-H co-purified LptA, LptD and LptF^{R212G}, the latter with slightly lower affinity compared to the wild-type strain (**Figure 2A**), suggesting that in Δ*lptC lptF*^{R212G} mutant the IM and OM Lpt sub-complexes are physically connected. LptC was not enriched in affinity-purified membranes from Δ*lptC lptF*^{R212G} cells and, as expected, *lptC*$^{+}$ cells assemble the canonical seven-component Lpt machine. It thus appears that the R212G amino acid substitution in LptF can bypass the requirement of LptC and allows the assembly of a six-component Lpt machine in cells overexpressing LptA. These data suggest that in the Δ*lptC lptF*^{R212G} mutant, IM and OM are connected by a LptFAD transenvelope bridge.

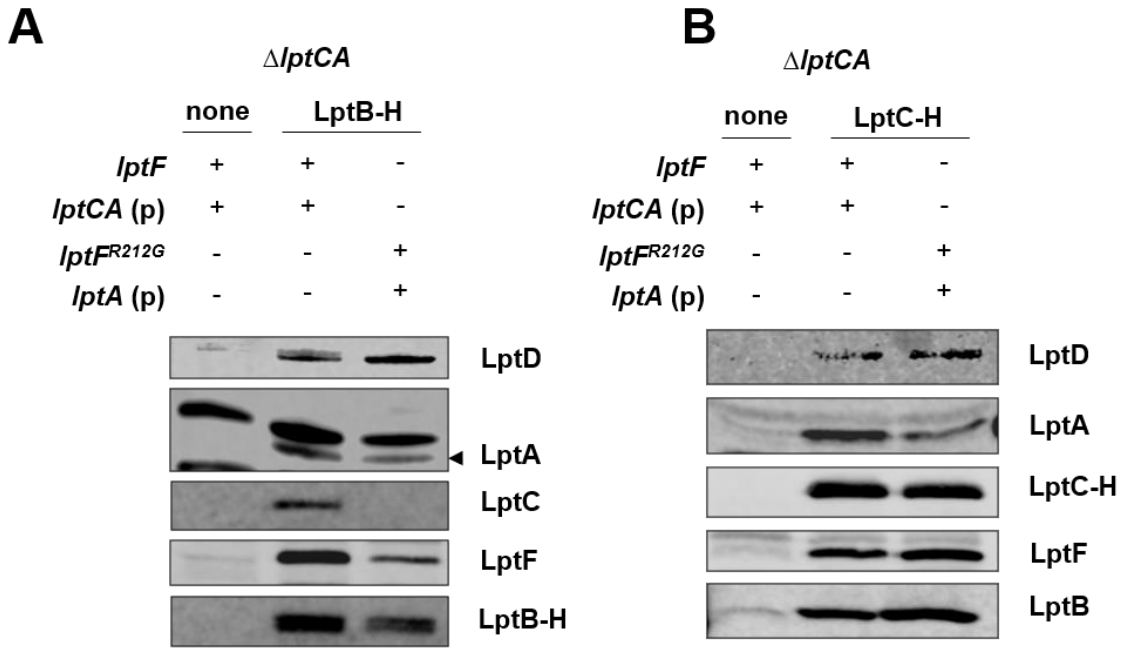

Figure 2 LptF^{R212G} assembles the Lpt machinery in cells deleted for *lptC*. Δ*lptCA* cells (KG286.06 and KG295.01) carrying wild-type or mutant *lptF* alleles (*lptF*, *lptF*^{R212G} respectively) and ectopically expressing *lptA* (p) from pGS321 or *lptCA* (p) from pGS404 were transformed with pET23/42 derived plasmids expressing His tagged *lptB* (LptB-H, **panel A**) or *lptC* (LptC-H, **panel B**). Total membranes from an equal number of cells were prepared and subjected to affinity chromatography. Immunoblot analyses with the indicated antibodies are shown. None: void plasmid control.

We previously showed that suppressor mutations in *lptF* are compatible with the presence of LptC and that LptF^{SupC} proteins are functional in a seven-component Lpt machine [29]. Therefore, we assessed whether LptC is recruited in the Lpt complex in *lptF*^{R212G} cells. Pull-down from solubilized membranes of *lptC*$^{+}$ and Δ*lptC lptF*^{R212G} strains, ectopically expressing a C-terminally His-tagged version of LptC (LptC-H), was performed. As negative control, we used the *lptC*$^{+}$ strain transformed with the empty vector. Affinity purified samples were analysed as described above. As shown in **Figure 2B**, LptC-H copurified the IM Lpt components LptB and LptF, as well as LptA and the OM Lpt component LptD in both *lptF*$^{+}$ and *lptF*^{R212G} backgrounds, suggesting that wild-type LptC can be assembled in the Lpt mutant machinery when LptF^{R212G} is present. To confirm this *in vitro*, and to exclude the formation of an LptB$_2$FGC complex only through the N-terminal membrane anchor of LptC, LptB$_2$FG and LptB$_2$F^{R212G}G, containing a His-tagged LptB, were overexpressed and purified in DDM micelles. The proper assembly of the two purified complexes was assessed by SEC-MALLS, a technique that determines the molecular weight and size of heterocomplexes, which confirmed the predicted mass of 134 kDa. When a soluble version of LptC lacking the transmembrane helix (ΔTM LptC [38]) was added to either the wild-type or R212G complexes, an increase in the size of the complex confirmed that the strong interaction of LptC through the β-jellyroll was maintained in the LptB$_2$F^{R212G}G complex (**Figure 3**). We can therefore conclude that LptF^{R212G} does not impair LptC interaction with the LptB$_2$F^{R212G}G mutated complex and is compatible with the formation of the canonical seven-component Lpt machine.

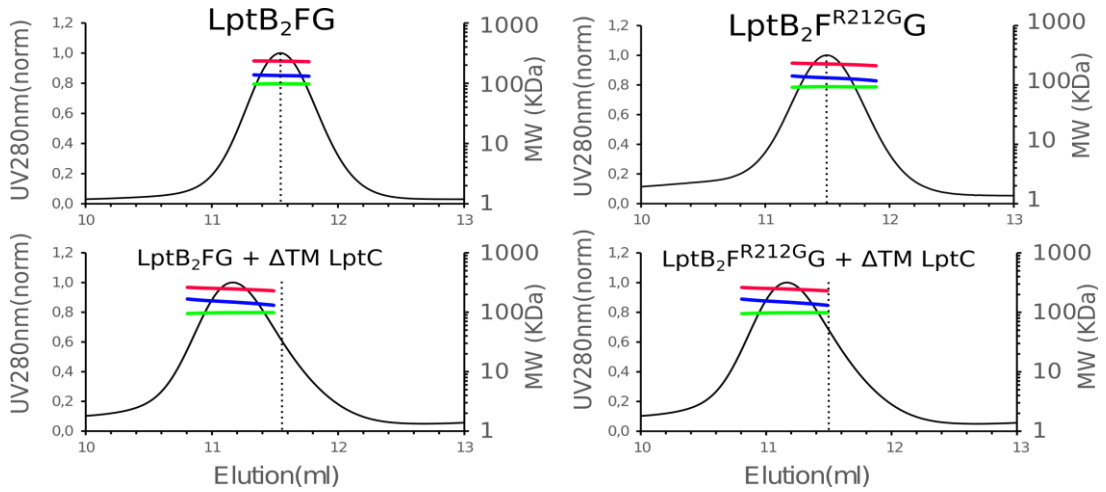

Figure 3 LptBF^{R212G}G forms a stable complex with ΔTM LptC *in vitro*. SEC-MALLS elution profiles of DDM-purified LpB$_2$FG and LpB$_2$F^{R212G}G complexes alone (upper panels) and 1:1 mixtures of LpB$_2$FG:ΔTM LptC and LptB$_2$F^{R212G}G:ΔTM LptC (lower panels). Dotted line indicates the elution volume corresponding to 134 kDa.

LptF^{R212G} directly interacts with LptA in the absence of LptC

In the canonical Lpt machine, LptC interacts directly with LptA and provides the IM docking site for the formation of the Lpt periplasmic bridge [15, 16, 38]. We postulated that in *lptF^{SupC}* cells lacking LptC, the IM LptB$_2$F^{R212G}G complex might interact directly with LptA, possibly *via* a direct binding of LptF^{SupC} to LptA. To test this hypothesis, we carried out site-specific crosslinking by incorporating the UV photo-crosslinkable amino acid *p*-benzoylphenylalanine (*p*BPA) at specific sites in LptF and LptF^{R212G}. *p*BPA was incorporated in residues around R212, based on their orientation in the hypothetical interaction interface with LptA (**Figure 1**) [11, 12], and the appearance of UV-dependent crosslinked products was assessed by immunoblot assays using anti-LptA antibodies. We replaced residues F213 and E214 because they are adjacent to the suppressor site R212 on the β7 strand of the β-jellyroll domain of LptF and have different orientations with respect to the hydrophobic cavity; Y230 was replaced since it points towards the interior of the cavity at the C-terminal end of the LptF periplasmic domain (β9 strand) (**Figure 1**). Finally, we selected Q203 since, despite more distant, is oriented towards the interior of the cavity, and F160 because it lies on the β2 strand, pointing outwards. Site-specific mutagenesis of *lptF* and *lptF^{R212G}* for *p*BPA incorporation was carried out in pGS445 and in pGS451 plasmids, carrying *lptF^{+}* and *lptF^{R212G}* alleles, respectively, and expressing LptG and LptAB at comparable levels from the same *tacp* promoter. The mutagenized plasmids were introduced into *lptC^{+} lptF^{+}* AM604 strain. All *p*BPA-encoding alleles are functional since they can complement the conditional *araBp-lptFG* mutant NR1113 [39] under non-permissive conditions (data not shown).

Initially, photo-crosslinking experiments were performed on whole-cell extracts. As shown in **Table 4** and **Figure S1**, UV-dependent crosslinked products with a mass compatible to that expected for the LptF-LptA complex were detected only in cells expressing LptF$^{R212G\text{-}Y230pBPA}$. This suggests that in the suppressor mutant *lptF^{R212G}* lacking LptC, the periplasmic bridge is formed by a direct interaction of the C-terminal end of the LptF periplasmic domain with LptA. To further probe LptF^{R212G}-LptA interaction, we performed *in vivo* photo-crosslinking in AM604 cells expressing LptA from a *tacp* promoter and *p*BPA substituted variants of the C-terminally His-tagged LptF proteins (LptF-H or LptF^{R212G}-H) from the leaky expression plasmid pET23/42, according to a previously described procedure [11]. As negative control, LptF-H carrying F213*p*BPA-encoding allele was used, since the side chain of this residue points towards the opposite orientation of the hydrophobic LptF β-jellyroll cavity with respect to R212. Whole-cell lysates were affinity-purified, concentrated by TCA precipitation

and analyzed by SDS-PAGE followed by immunoblotting using anti-LptA and anti-LptF antibodies. As shown in **Figure 4A**, we detected UV-dependent LptF-LptA crosslinking products only when LptF$^{R212G\text{-}Y230pBPA}$ was used as bait, further supporting the notion of a direct interaction between LptF and LptA in *lptF^{SupC}* mutants.

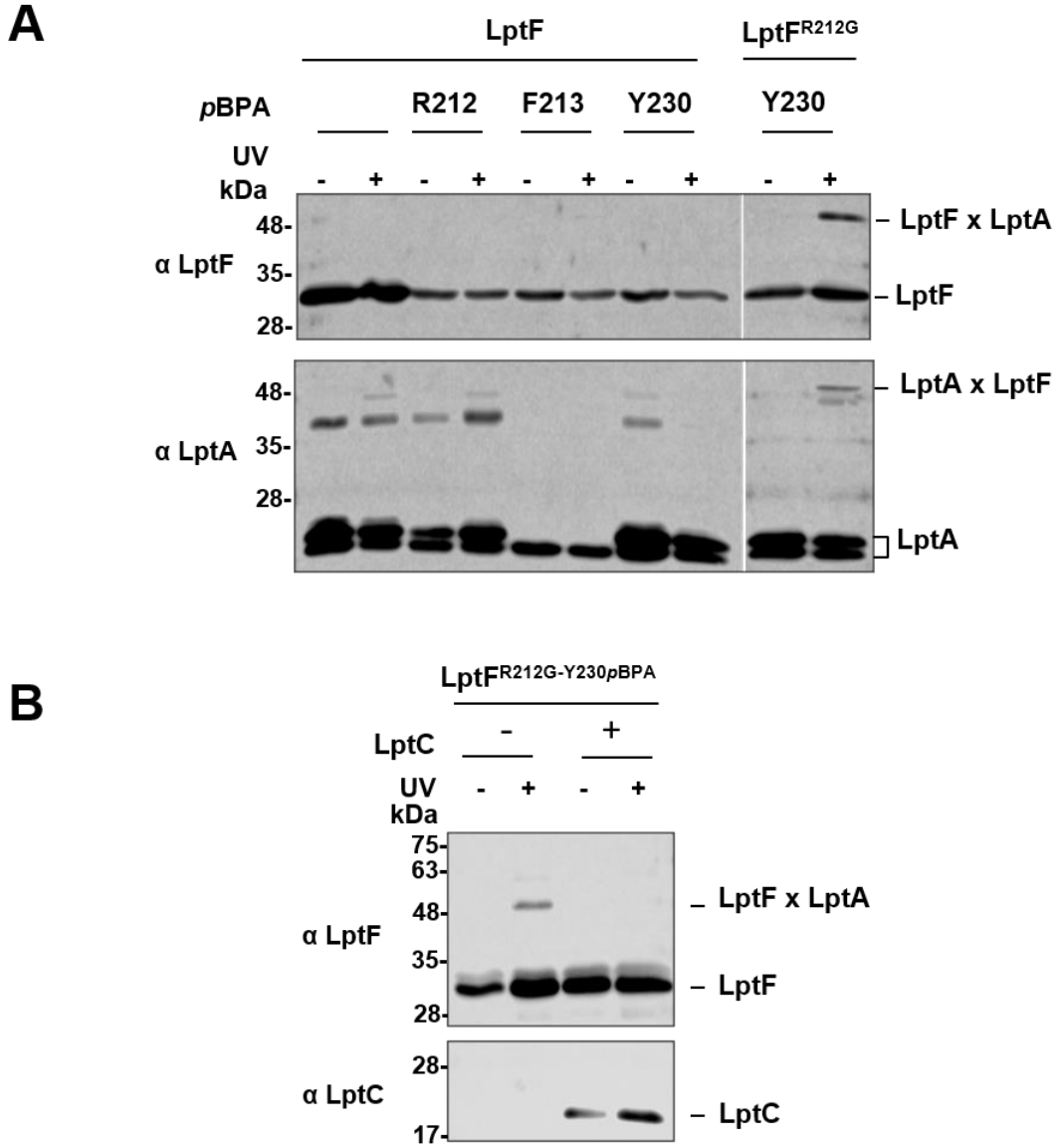

Figure 4 Mutant LptF^{R212G} interacts with LptA and interaction is lost in the presence of ectopically expressed LptC. **(A)** *In vivo* photo-crosslinking followed by nickel-affinity chromatography from solubilized whole-cell lysate expressing the indicated *p*BPA-containing LptF-His mutants from pET23/42 derived plasmids as bait and LptA from pGS323. UV-dependent photo-crosslinking to LptA was detected with anti-LptA and anti-LptF antibodies. **(B)** *In vivo* photo-crosslinking followed by nickel-affinity chromatography from solubilized whole-cell lysate expressing LptF$^{R212G\text{-}Y230pPBA}$-His (LptF$^{R212G\text{-}Y230pBPA}$) and LptA or LptCA from pGS323 and pGS308, respectively. UV-dependent photo-crosslinking to LptA was detected with anti-LptF and anti-LptC antibodies.

We previously observed that re-introduction of a wild-type copy of *lptC* completely restored the OM permeability defects of the *lptF*^{SupC} mutants [29]. In line with this observation, pull-down experiments (**Figure 2B**) show that LptC can be assembled in the Lpt complex expressing LptF^{R212G}. We therefore evaluated whether overexpression of LptC impacted on LptF^{R212G}-LptA crosslinking. To this end, we introduced pBAD/HisA-LptC plasmid [10], in which *lptC* is expressed from the inducible *araBp* promoter, into wild-type AM604 cells ectopically expressing *lptFG-lptAB* and *lptF*^{R212G}*G-lptAB* operons from the *tacp* promoter, and carrying the above mentioned *p*BPA substitutions. UV-dependent crosslinking adducts were assessed in whole-cell extract samples by immunoblotting using anti-LptA antibodies. As shown in **Table 4** and **Figure S1**, LptF^{R212G}-LptA crosslinking was abolished by LptC overexpression. This result was confirmed by photo-crosslinking assay followed by affinity chromatography from solubilized cell lysate ectopically expressing LptF^{R212G}-H and LptA or LptCA (**Figure 4B**). Interestingly, immunoblotting using anti-LptC antibodies failed to detect a LptC-LptF^{R212G}-H crosslinking product, suggesting that residue Y230 is not directly involved in LptF^{R212G}-LptC interaction, at least in the presence of LptA. Accordingly, Y230 has not been included among the residues mediating LptF-LptC interaction in the wild-type complex in a recently published paper [11].

SEC-MALLS analysis of purified LptB$_2$FG and LptB$_2$F^{R212G}G complexes in the presence of the monomeric version of LptA (LptA$_m$, deleted of residues from 160 to 181 [15]) did not allow copurification of LptA with any of the complexes, suggesting that the interaction of LptB$_2$FG with LptA is much weaker than with LptC. We thus designed an interaction assay by Surface Plasmon Resonance (SPR). LptB$_2$FG and LptB$_2$F^{R212G}G were covalently immobilized and increasing concentrations of monomeric LptA were flowed over the surface (**Figure S2**). Concentration-dependent response was observed, consistent with an interaction with both LptB$_2$FG and LptB$_2$F^{R212G}G. SPR profiles could be fitted at equilibrium and the estimated Kd values of LptA$_m$ are 74 and 81 µM for LptB$_2$FG and LptB$_2$F^{R212G}G, respectively. These values are consistent with the inability to co-purify LptA with LptB$_2$FG or LptB$_2$F^{R212G}G *in vitro*.

Loss of net charge and steric hindrance of LptF residue 212 is necessary to compensate for the lack of LptC

To gain more insights into the suppression mechanism, we wanted to explore the chemical determinants that allow LptF^{SupC} mutants to compensate for the lack of LptC. R212 appears well-conserved among γ-proteobacteria (**Figure S3**), suggesting that this position might have a crucial role in the function of LptF. Furthermore, since the Δ*lptC* suppressor mutations rely on the replacement of the positive charge of the polar amphipathic amino acid R212 by a neutral amino acid with reduced steric hindrance, it might be possible that the replacement disrupts an interaction that somehow makes LptC essential for LPS transport. On the other hand, R212 residue has been recently shown to directly interact with LPS [11], suggesting that, in the wild-type strain, the positive charge of R212 might be engaged in an interaction with the negative charge of the phosphate residues of lipid A. However, the position of R212 at the bottom of the groove formed by LptFCAD periplasmic domains makes this hypothesis unlikely.

We therefore investigated whether the suppression of Δ*lptC* lethal phenotype requires either the loss of R212 positive charge or the reduction of the steric hindrance of its side chain. We reasoned that if suppression requires the disruption of a salt-bridge pair within the LptF protein, introduction of a negative charge should result in phenotypic suppression as well. On the contrary, if reduction of the steric hindrance plays a role in suppression, introduction of a residue with a bulkier side chain should result in loss of phenotypic suppression. We thus generated *lptF* mutant alleles on the plasmid pGS445 (expressing *lptFG-lptAB* operons from the *tacp* promoter) by substituting the positively charged R212 residue with the negatively charged glutamic acid (R212E) or with asparagine (R212N), which has an increased steric hindrance relative to the originally selected compensatory mutations though maintaining its polar nature. The resulting plasmids pGS501 (*lptF^{R212E}G-lptAB*) and pGS502 (*lptF^{R212N}G-lptAB*) express functional LptF proteins, as judged by their ability to complement the growth of the arabinose-dependent conditional *lptFG* mutant NR1113 [39] under non-permissive conditions (**Figure 5**, upper panel). However, both *lptF^{R212E}* and *lptF^{R212N}* alleles could not support the growth of LptC depleted cells, while *lptF^{R212G}* did (**Figure 5**, lower panel). Overall, we conclude that suppression of the lethal phenotype of *lptF^{SupC}* mutants is achieved by the loss of net charge and reduction of the steric hindrance in the side chain of LptF residue 212.

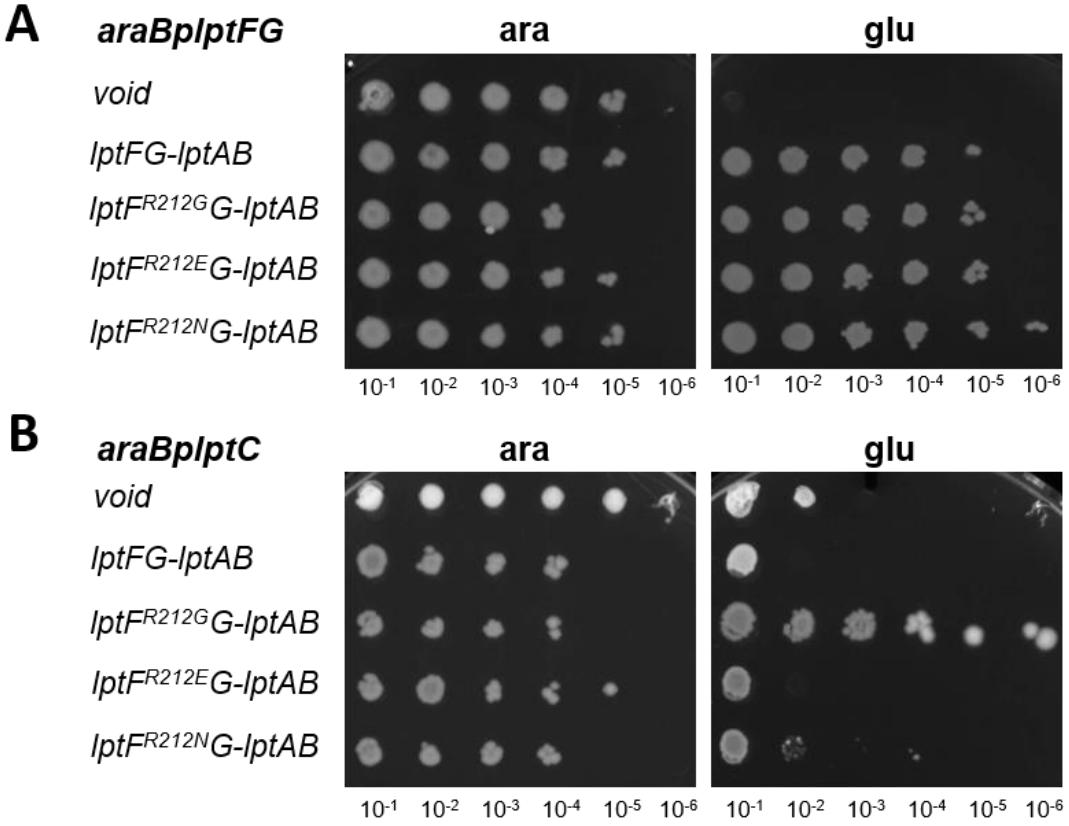

Figure 5 Complementation of *lptC* or *lptFG* depleted cells by different *lptF*^{R212} alleles. Cultures of NR1113 (*araBplptFG*) **(A)** and FL905 (*araBplptC*) **(B)** strains transformed with pGS445 derivatives expressing the *lpt* genes listed on the left were grown in LB-arabinose, serially diluted 1:10 in microtiter wells, and replica-plated onto agar plates with either arabinose 0.2% (ara) or glucose 0.2% (glu) to induce or fully repress the *araBp* promoter, respectively. Serial dilutions are indicated on bottom of the panels. void: cells transformed with pGS100 plasmid not expressing Lpt proteins.

$LptF^{R212G}$ mutation impacts on the activity of the $LptB_2FG$ or $LptB_2FGC$ complexes.

$LptB_2FG$ harnesses the energy of the ATP hydrolysis for the detachment of LPS from the periplasmic side of the IM and its funneling into the periplasmic Lpt bridge [40]. The transmembrane helix of LptC is responsible for modulating ATP hydrolysis and coupling it with LPS transport through a recently described unconventional mechanism [11, 12]. To better understand how a mutation at residue R212 of LptF allows bacteria to survive and transport LPS in the absence of LptC, we purified recombinant $LptB_2FG$ and $LptB_2F^{R212G}G$ complexes from detergent-solubilized membranes and compared their ability to hydrolyze ATP. As shown in **Figure 6A**, the wild-type and mutated IM complexes displayed similar ATPase activity. Although we could not detect a difference in the initial rate of the reaction between wild-type and mutant $LptB_2FG$ within the first five minutes, there is a clearly distinct time-dependence in the phosphate release between the two complexes, indicative of a decreased ATPase activity of the mutant complex (**Figure S4**). When we compared the ATPase activity of $LptB_2FGC$ and $LptB_2F^{R212G}GC$ complexes co-purified from the C-terminally His-tagged LptC, we observed that the wild-type complex was less active than the complex containing $LptF^{R212G}$ (**Figure 6B**).

In the wild-type strain, besides its regulatory activity on the $LptB_2FG$ ABC transporter, LptC binds LptA thus providing the IM docking site for periplasmic protein bridge formation [15, 38]. We therefore explored the ability of LptA to modulate the ATPase activity of detergent-purified wild-type and mutant $LptB_2FG$ and $LptB_2FGC$ complexes. We chose to use the monomeric version of LptA ($LptA_m$ [15]) to avoid artifacts resulting from LptA oligomerization. We tested 20:1 $LptA_m$: complexes molar ratio to ensure a significant number of complexes containing LptA. Surprisingly, the presence of $LptA_m$ stimulated the ATPase activity of the wild-type $LptB_2FGC$ complex, that reached a rate of ATP hydrolysis comparable to that of $LptB_2FGC$ containing $LptF^{R212G}$. On the contrary, $LptA_m$ altered neither the ATPase activity of $LptB_2F^{R212G}GC$ complex, nor that of the wild-type and mutant $LptB_2FG$ complexes (**Figure 6B**). Notably, when a soluble LptC version lacking the N-terminal transmembrane helix, referred as ΔTM LptC in this study ($LptC_{\Delta 1\text{-}23}$ [38]), was added to wild-type $LptB_2FG$ and mutant $LptB_2F^{R212G}G$ complexes at 20:1 molar ratio, only the ATPase activity of the wild-type complex was stimulated (**Figure 6A**).

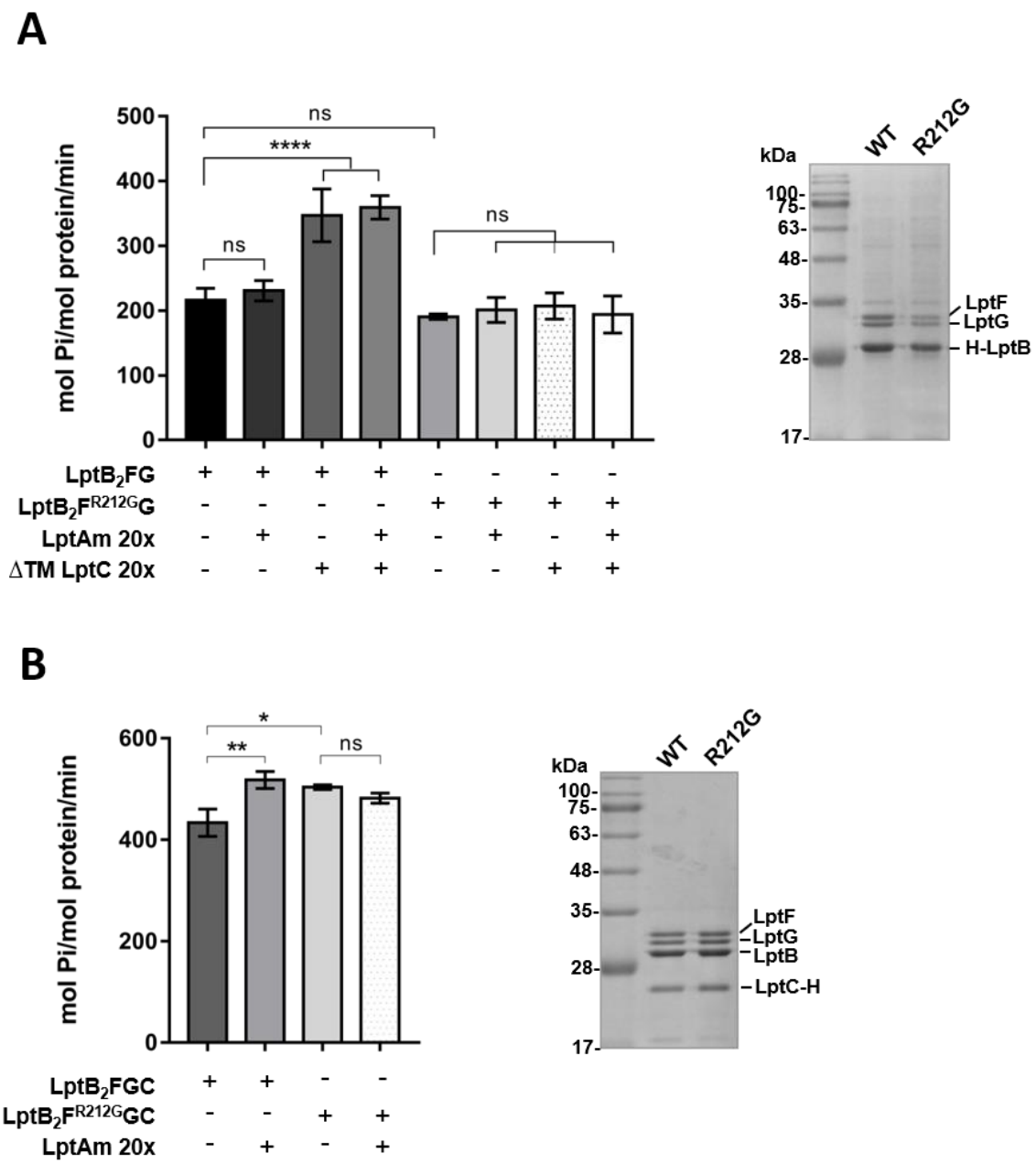

Figure 6 ATPase activity of wild-type and mutant $LptB_2FG$ and $LptB_2FGC$ complexes. **(A)** $LptB_2FG$ and $LptB_2F^{R212G}G$ were purified from DDM-solubilized membranes using His-LptB (H-LptB) from pCDFDuet-His_6LptBFG and pCDFDuet-His_6LptBF^{R212G}G as bait. The ATPase activity was assessed by measuring the inorganic phosphate release over time, using 0.2 μM purified complexes. **(B)** $LptB_2FGC$ and $LptB_2F^{R212G}GC$ complexes were purified from cells expressing pCDFDuet-LptBFG or pCDFDuet-LptBF^{R212G}G using LptC-His (LptC-H) from pET23/42-LptC-His as bait. The ATPase activity was measured using 0.1 μM complexes. Data are the initial rate of ATP hydrolysis, calculated within 5 minutes. When indicated, complexes were incubated with 20x molar excess of monomeric LptA ($LptA_m$) and/or ΔTM LptC ($LptC_{\Delta 1\text{-}23}$). Error bars, s. d. ($n$ = 3 technical replicates). On the right, SDS-PAGE analysis of purified complexes.

DISCUSSION

We previously isolated a class of suppressor mutants bearing the deletion of the *lptC* gene [29]. The viability of these suppressors was strictly dependent upon the presence of specific amino acid substitutions at the position 212 of LptF and the ectopic overexpression of LptA from a plasmid. Based on these observations we postulated that the *lptF*^{R212G} allele would enable an extra copy of LptA to substitute for LptC, through the abolishment of an unknown mechanism that makes the presence of LptC essential for LPS transport and cell viability [29]. The existence of this class of mutants prompted us to investigate whether six-component Lpt complexes, containing the mutant LptF variants and lacking LptC, were assembled in the suppressor mutants. Amongst the suppressors originally isolated, we selected for further characterization the mutation (R212G) that almost completely suppresses the defects observed in the *lptC* deletion mutants. Indeed, *lptF*^{R212G} still shows some OM permeability defects, as demonstrated by its sensitivity to novobiocin at concentrations that the wild type tolerates.

We found that in cells overexpressing LptA, unlike its wild-type counterpart, the LptF^{R212G} mutant protein can be assembled in a six-component transenvelope complex, suggesting that in this mutant LptA can directly interact with LptF. LptF might intrinsically be able to interact with LptA but, in a wild-type Lpt machinery, its higher affinity for LptC, revealed by SEC-MALLS experiments, accounts for the LptFCA architecture of the periplasmic bridge. Initially, we had hypothesized that R212 mutations could decrease the affinity of LptF for LptC favouring its interaction with LptA; however, the affinities of LptF and LptF^{R212G} for LptA were found to be similar by SPR. LptB$_2$F^{R212G}G still forms a stable complex with ΔTM LptC *in vitro* and, when present, LptC can still be assembled in a LptF^{R212G}-containing seven-component complex *in vivo*. Moreover, the functionality of LptB$_2$F^{R212G}GC is comparable to that of the wild type, since the OM permeability is completely restored in strains producing the mutant complexes [29]. Overall, these results suggest that, although residue R212 lies at the interaction interface with LptC (**Figure 7**), its substitution with a Glycine neither impairs the LptF-LptC interaction nor increases LptF affinity for LptA, at least *in vitro*. Nevertheless, it appears that R212G mutation enables LpF^{R212G} to interact with LptA through residue Y230, as assessed by UV-photocrosslinking experiments. Since R212G mutation does not increase LptF affinity for LptA, we speculate that this interaction can be favoured by LPS transit through the gateway formed by the two proteins. Y230 is crucial for the functionality of the Lpt transporter since its mutation to glutamic acid (E) is lethal for the cells [13], supporting its involvement in

an essential interaction within the transporter. Interestingly, when LptC is assembled in the complex containing $LptF^{R212G}$, the interaction between Y230 and LptA is abolished but LptC does not substitute for LptA in this interaction. This evidence indicates that, in the presence of LptC, residue Y230 is not involved in $LptF^{R212G}$-LptC interaction, in line with what we and others observed for the wild-type LptF [11].

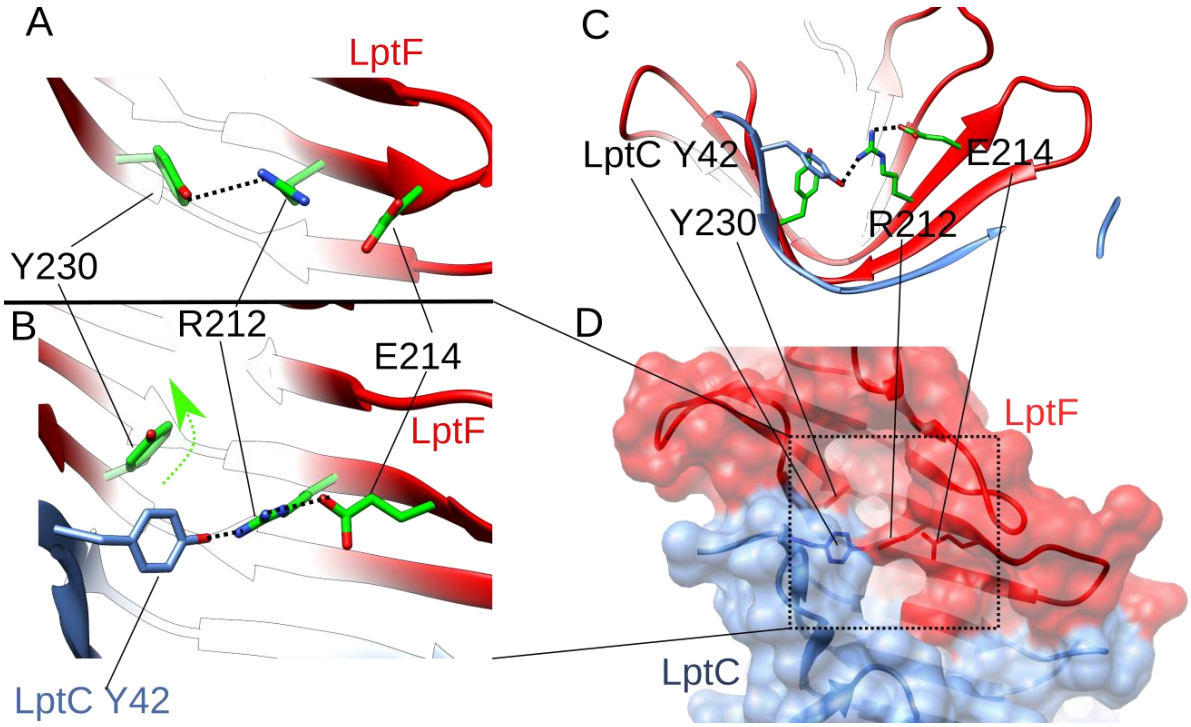

Figure 7 The presence of LptC in $LptB_2FGC$ complex alters the interaction network of LptF R212 residue. **(A)** Interactions of LptF R212 residue with Y230 in $LptB_2FG$ (PDB 5X5Y). **(B)** LptF R212 interaction with Y230 is replaced by LptC Y42 residue in the $LptB_2FGC$ complex (PDB:6MIT with LptC in blue) and LptF Y230 is flipped towards LptF. **(C)** The $LptB_2FGC$ complex is oriented such as LPS flow is towards the viewer. LptF R212 residue is on the path of LPS flow [11]. In **(D)** the same complex tilted with LptF and LptC represented in surface.

It has been recently shown that residue 212 is involved in LptF-LPS interaction [11]. Positively charged residues in other Lpt proteins have been shown to be involved in the formation of salt-bridge interactions with the negatively charged phosphates of lipid A; an example is K34 residue in the first transmembrane helix of LptG, that contributes to forming the cavity for early LPS binding by $LptB_2FGC$ [13, 27]. However, the location of R212 residue at the bottom of the concave cleft in the β-jellyroll of LptF is not in favour of an interaction with the phosphates of the lipid A. We propose that the presence of a positive charge (R212)

in a region of the protein that is mainly hydrophobic and likely involved in the interaction with the hydrophobic tails of lipid A could prevent LPS progression into the hydrophobic groove of the bridge formed by LptF and LptA, unless LptC is present (**Figure 7**). According to this hypothesis, R212 would work as a checkpoint for the transport of LPS in the periplasmic bridge. In line with this, charge inversion of the side chain of residue 212, through the introduction of a glutamic acid (E), or introduction of a bulkier, polar residue abolished the suppression of Δ*lptC* allele lethality, although still preserving the functionality of the mutant LptF protein in the presence of LptC. These data support the idea that the presence of LptC is required, through R212, to somehow facilitate LPS release by LptF. This mechanism would allow the release of LPS from the IM only when the LptCAD bridge is correctly assembled to ensure efficient transport of LPS through the periplasm and to avoid LPS mistargeting. Such a checkpoint for the transport of LPS across the periplasmic bridge would parallel mechanisms that avoid the assembly of a defective periplasmic LptCAD protein bridge. The $LptC^{G56V}$ mutant, which is proficient in LptA-interaction *in vitro* but defective in its association with the $LptB_2FG$ complex, fails to recruit LptA to the transenvelope complex [28]. A similar control system hampers the recruitment of LptA by the LptD protein whose maturation resulted in the non-correct formation of the disulfide bonds between the N-terminal β-jellyroll and the C-terminal β-barrel domains of the protein [16, 41]. Unfortunately, no structural information is available that describes the position of lipid A into the periplasmic domain of LptF; therefore, we can only speculate on the interaction between LptF R212 residue and LPS.

The comparison among the available structures of the $LptB_2FG$ complex in the presence and absence of LptC reveals that R212 is involved in different interaction networks. Notably, in the presence of LptC, R212 is engaged, probably *via* hydrogen bonding or cation-Pi interaction, with the aromatic residue 42 (Y42 in *Enterobacter cloacae*, or F42 of *Vibrio cholerae*) of LptC; on the contrary, in the structures of complexes lacking LptC, R212 is involved in an intramolecular interaction with Y230 (**Figure 7 A,B,C**). This observation suggests that the presence of LptC would prevent the interaction between residues Y230 and R212 in LptF, leaving residue Y230 free to interact with LPS. We can speculate that in the suppressor mutants lacking LptC, mutations that abolish the positive charge and the steric hindrance of LptF residue 212 would prevent Y230 from making this intramolecular interaction, leaving Y230 free to be engaged in other interactions. LPS would then be free to transit in the gateway created by novel intermolecular interactions.

Another important question related to the suppression mechanism by $LptF^{R212G}$ is the regulatory role proposed for the transmembrane helix of LptC, based on its position between

the transmembrane helices of LptF and LptG, where it induces an enlargement of the cavity of $LptB_2FGC$ that accommodates LPS before detachment from the IM, and on its ability to decrease the ATPase activity rate of the transporter [11, 12, 21]. Since the $LptB_2F^{R212G}G$ complex lacks the transmembrane helix of LptC, we sought to compare the ATP hydrolysis rate of wild-type and mutant $LptB_2FG$ complexes, associated or not with LptC. We could not detect a difference in the initial rate of the reaction between wild-type and mutant $LptB_2FG$ complexes within the initial minutes of the reaction; however, there is a clearly different time-dependence in the phosphate release between the two complexes, indicative of a decreased ATPase activity of the mutant complex (**Figure S4**). Interestingly, incubation with a soluble LptC version lacking the N-terminal transmembrane helix, but not with LptA, stimulates the ATPase activity of the wild-type complex, suggesting that a proper interaction with the periplasmic domain of LptF generates a conformational change that can somehow be transmitted to LptB, modulating the rate of ATP hydrolysis. Surprisingly, neither incubation with soluble LptC nor with LptA affects the activity of the mutant complex, suggesting that interaction with $LptF^{R212G}$ cannot be "signalled" to LptB. The different ATP hydrolysis rates observed between wild-type and mutant $LptB_2FGC$, containing the full-length LptC protein, suggest that the transmembrane helix of LptC is not able to exert its inhibitory activity in the presence of $LptF^{R212G}$. In line with what we observed with the addition of soluble LptC, incubation with LptA stimulates the activity of the wild-type $LptB_2FGC$ complex but not that of the mutant one, indicating that $LptB_2FGCA$ assembly relieves the inhibitory activity of LptC in the wild-type complex.

The absence of $LptF^{R212}$ allows unregulated transfer of LPS to LptA and clearly underlines the role of LptC-LptF junction in regulating the activity of LPS transport. LptC, located both at the entry of LPS into the $LptB_2FG$ inner membrane complex and at its exit, appears more and more as a key regulator of the LPS transfer.

FUNDING

AP, JPS, CL, ECCMM, and TB were supported by the Train2Target project granted from the European Union's Horizon 2020 research and innovation program under the Marie Sklodowska-Curie grant agreement #721484. PS was supported by the Italian Ministry of Education, University and Research, (FABBR)-MIUR 2017, Funding for the financing of basic research activities.

ACKNOWLEDGEMENTS

This work used the platforms of the Grenoble Instruct-ERIC center (ISBG ; UMS 3518 CNRS-CEA-UGA-EMBL) within the Grenoble Partnership for Structural Biology (PSB), supported by FRISBI (ANR-10-INBS-05-02) and GRAL, financed within the University Grenoble Alpes graduate school (Ecoles Universitaires de Recherche) CBH-EUR-GS (ANR-17-EURE-0003). We thank Aline Le Roy and Christine Ebel, for assistance with access to the Protein Analysis On Line (PAOL) platform and the SPR/BLI platform personal, Jean-Baptiste REISER Ph.D. and Anne Chouquet, for their help and assistance. The authors acknowledge Isabel Ayala and Karine Giandoreggio-Barranco for great technical assistance.

Table 1 *Escherichia coli* strains.

Strain	Relevant Characteristics		Reference/Source
	Chromosomal	**Plasmid**	
AM604	MC4100 Ara^{+}		[42]
DH5α	Δ(*argF-lac169*) 80d*lacZ58*(M15) *glnV44*(AS) λ^{-} *rfbD1 gyrA96 recA1 endA1 spoT1 thi-1 hsdR17*		[43]
FL905	AM604 ϕ(*kan araC araBp-lptC*)*1*		[44]
KG286.06/pGS404	*rpsL150* Δ*lptCA*	*ptac-lptCA cat*	[29]
KG295.01/pGS321	*rpsL150* Δ*lptCA lptF*^{R212G}	*ptac-lptA cat*	[29]
KRX	[F', *tra*D36, Δ*omp*P, *pro*A+B+, *lac*Iq, Δ(*lac*Z)M15] Δ*omp*T, *end*A1, *rec*A1, *gyr*A96, *thi*-1, *hsd*R17 (rK–, mK+), e14– (McrA–), *rel*A1, *sup*E44, Δ(*lac-pro*AB), Δ(*rha*BAD)::T7 gene 1		Promega
NEB® 5-alpha	*fhuA2 (argF-lacZ)U169 phoA glnV44 80 (lacZ)*M15 *gyrA96 recA1 relA1 endA1 thi-1 hsdR17*		New England Biolabs (NEB)
NR1113	Δ(λattlom)::*bla araBp-lptFG* Δ*lptFG*		[39]
XL1blue	F^{-} λ^{-} *recA1 endA1 gyrA96 thi-1 hsdR17 supE44 relA1 lac* {F'*proAB, lacI*q*Z* Δ*M15* Tn*10*(Tet^{R})}		Agilent Technologies
MG1655	K-12, F^{-} λ^{-} *ilvG*$^{-}$ *rfb-50 rph-1*		[45]

Table 2 Plasmids.

Plasmid	Relevant Characteristics[a]	Construction/Origin
pBAD/His A LptC	pBAD/His A derivative encoding LptC with replacement of Ser at position 2 to Gly to introduce a NcoI site; Amp^R	[10]
pCDFDuet-LptBHis_6FG	pCDFDuet-1 (Novagen) derivative encoding full-length LptB with a C-terminal His_6 tag, and full-length LptF and LptG; Spn^R	[10]
pCDFDuet-His_6LptBFG	pCDFDuet-LptBHis_6FG derivative encoding full-length LptB with a N-terminal His_6 tag, and full-length LptF and LptG	His_6-LptB was PCR amplified with AP707-AP708 oligos from MG1655 genomic DNA and cloned into NcoI-EcoRI sites
pCDFDuet-His_6LptBF^{R212G}G	pCDFDuet-His_6LptBFG derivative encoding full-length LptB with a N-terminal His_6 tag, and full-length $LptF^{R212G}$ and LptG	By site-directed mutagenesis using oligos AP613-AP614
pCDFDuet-LptBFG	pCDFDuet-His_6LptBFG derivative encoding full-length LptB, LptF, and LptG	LptB was PCR amplified with AP599-AP655 oligos from MG1655 genomic DNA and cloned into NcoI-EcoRI sites
pCDFDuet-LptBF^{R212G}G	pCDFDuet-His_6LptBF^{R212G}G derivative encoding full-length LptB, $LptF^{R212G}$, and LptG	LptB was PCR amplified with AP599-AP655 oligos from MG1655 genomic DNA and cloned into NcoI-EcoRI sites
pBAD/His A LptC-His	pBAD/His A LptC derivative encoding LptC with a C-terminal His_8 tag	LptC-His was PCR amplified with AP656-AP657 oligos from pET23/42 LptC-His and cloned into NcoI-HindIII sites
pET23/42	pET23a(+) with multiple cloning sites of pET42a(+), T7 promoter; Amp^R	[20]
pET23/42 LptB-His	encodes full-length LptB with a C-terminal His_8 tag	This work
pET23/42 LptC-His	encodes full-length LptC with a C-terminal His_8 tag	[20]
pET23/42 LptF-His	encodes full-length LptF with a C-terminal His_8 tag	This work
pET23/42 $LptF^{R212G}$-His	encodes full-length $LptF^{R212G}$ with a C-terminal His_8 tag	This work
pET30b $LptF^{R212E}$G	pET30b-*lptF*^{R212E} *lptG*, T7 promoter; Kan^R	Laboratory collection

pET30b LptF^{R212N}G	pET30b-*lptF^{R212N} lptG*, T7 promoter; Kan^{R}	Laboratory collection
pEVOL	*aaRS*, tRNACUA opt, p15A origin; Cam^{R}	[32]
pEVOL-Spn	pEVOL derivative; Spn^{R}	This work
pGS100	pGZ119EH derivative, contains TIR sequence downstream of *ptac*; Cam^{R}	[46]
pGS308	*ptac-lptCA, kan, oriV*$_{ColD}$	[29]
pGS323	*ptac-lptA, kan, oriV*$_{ColD}$	[29]
pGS445	pGS100 derivative, *ptac- lptFG_lptAB*	[29]
pGS451	pGS100 derivative, *ptac- lptF^{R212G}G_lptAB*	[29]
pGS501	pGS445 derivative, *ptac- lptF^{R212E}G_lptAB*	This work
pGS502	pGS445 derivative, *ptac- lptF^{R212N}G_lptAB*	This work
pSup- BpaRS-6TRN	*Mj tyrRS*, tRNA $_{CUA}$, p15A origin; Cam^{R}	[47]
pQEsH-*lptC*	pQE30 (QIAGEN) derivative, expresses His$_6$-LptC$_{24-191}$; Amp^{R}	[38]
pET-LptAΔ$_{160-185}$ –H	*pT7-lptAΔ$_{160-185}$* -His$_6$; Amp^{R}	[15]

[a] Amp^{R}, ampicillin resistance; Spn^{R}, spectinomycin resistance; Kan^{R}, kanamycin resistance; Cam^{R}, chloramphenicol resistance

Table 3 Oligonucleotides.

Name	Sequence[a]	Notes
Plasmid construction		
AP450	acacctcgagTCTGAAGTCTTCCCCAAG	pET23/42 LptB-His construction with AP479; XhoI
AP479	acaccatatgGCAACATTAACTGCAAAGAAC	pET23/42 LptB-His construction with AP450; NdeI
AP573	cggaattccgCAGGTATCCGGTAAACGG	pEVOL-Spn construction with AP574; EcoRI
AP574	cggaattccgGCGGCTATTTAACGACCC	pEVOL-Spn construction with AP573; EcoRI
AP599	catgccatggCAACATTAACTGCAAAG	pCDFDuet-LptBFG and pCDFDuet-LptBF^{R212G}G construction with AP655; NcoI
AP613	ACCAGGGAACGGGCTTCGAAGGC	pCDFDuet-His$_6$LptBF^{R212G}G by site-directed mutagenesis
AP614	TGAGAGTGACGACCTGGGAG	pCDFDuet-His$_6$LptBF^{R212G}G by site-directed mutagenesis
AP655	gagaggaattcTCAGAGTCTGAAGTCTTCCC	pCDFDuet-LptBFG and pCDFDuet-LptBF^{R212G}G construction with AP599; EcoRI
AP656	catgccatggGTAAAGCCAGACGTTGGGTT	pBAD/His A LptC-His construction with AP657; NcoI
AP657	cccaagcttTTAGTGGTGGTGGTGGTG	pBAD/His A LptC-His construction with AP656; HindIII
AP707	tataccatggGCCATCATCATCATCATCACGGAATGGCAACATTA ACTGCAAAGAACC	pCDFDuet-His$_6$LptBFG construction with AP708; NcoI
AP708	tatagaattcTCAGAGTCTGAAGTCTTCCCCAAGGTATACACG	pCDFDuet-His$_6$LptBFG construction with AP707; EcoRI
FG3195	gataggaattcaccGTGATAATCATAAGATATCTGG	pGS501 and pGS502 construction with FG3196, using as template pET30b LptF^{R212E}G and pET30b LptF^{R212N}G, respectively; EcoRI
FG3196	ggctagtctagaTTACGATTTTCTCATTAACAGC	pGS501 and pGS502 construction with FG3195, using as template pET30b LptF^{R212E}G and pET30b LptF^{R212N}G, respectively; XbaI
FG3295	ctggcatatgATAATCATAAGATATCTGGTGCGG	pET23/42 LptF-His and pET23/42 LptF^{R212G}-His construction with FG3296; NdeI

FG3296	atatctcgagCACCGCTCCTTTACGCGA	pET23/42 LptF-His and pET23/42 LptF^{R212G}-His construction with FG3295; XhoI

Generation of LptF amber mutants

AP500	CACTCTCAACCAGGGAACGtagTTCGAAGGCACTGCATTG	LptF amber mutant generation with AP501; **R212am**
AP501	CAATGCAGTGCCTTCGAActaCGTTCCCTGGTTGAGAGTG	LptF amber mutant generation with AP500; **R212am**
AP512	TGGCAGCTCGGTGCTGtagATCGAAAGCGTTGACG	LptF and LptF^{R212G} amber mutants generation with AP513; **F160am**
AP513	CGTCAACGCTTTCGATctaCAGCACCGAGCTGCCA	LptF and LptF^{R212G} amber mutants generation with AP512; **F160am**
AP514	CTGCGCGACGGCTCCtagGTCGTCACTCTCAAC	LptF and LptF^{R212G} amber mutants generation with AP515; **Q203am**
AP515	GTTGAGAGTGACGACctaGGAGCCGTCGCGCAG	LptF and LptF^{R212G} amber mutants generation with AP514; **Q203am**
AP518	ACCAGGGAACGCGCTTCtagGGCACTGCATTGTTACG	LptF amber mutant generation with AP519; **E214am**
AP519	CGTAACAATGCAGTGCCctaGAAGCGCGTTCCCTGGT	LptF amber mutant generation with AP518; **E214am**
AP524	CTCAACCAGGGAACGGGCtagGAAGGCACTGCATTGTTAC	LptF^{R212G} amber mutant generation with AP525; **F213am**
AP525	GTAACAATGCAGTGCCTTCctaGCCCGTTCCCTGGTTGAG	LptF^{R212G} amber mutant generation with AP524; **F213am**
AP603	AACGGGCTTCtagGGCACTGCAT	LptF^{R212G} amber mutant generation with AP604; **E214am**
AP604	CCCTGGTTGAGAGTGACG	LptF^{R212G} amber mutant generation with AP603; **E214am**
AP605	CTTCCAGGATtagCAGGCGATCA	LptF and LptF^{R212G} amber mutants generation with AP606; **Y230am**
AP606	TCCGTAATGCGGAAATCAC	LptF and LptF^{R212G} amber mutants generation with AP605; **Y230am**

[a] Upper case letters, sequence present in the template; lower case letters, additional/modified sequence not present in the template; restriction sites are underlined.

Table 4 Summary of LptF *in vivo* photo-crosslinking experiments.

LptF[a]	Amber mutation	LptC overexpression[b]	XL-LptA
wt	none	-	NO
		+	NO
	F160am	-	NO
		+	nt
	Q203am	-	NO
		+	NO
	R212am	-	NO
		+	NO
	E214am	-	NO
		+	NO
	Y230am	-	NO
		+	NO
R212G	none	-	NO
		+	NO
	F160am	-	NO
		+	nt
	Q203am	-	NO
		+	NO
	F213am	-	NO
		+	nt
	E214am	-	NO
		+	NO
	Y230am	-	YES
		+	NO

[a] LptF variant expressed from a high-copy number plasmid

[b] when indicated with +, LptC was expressed from pBADHisA vector; nt, not tested

REFERENCES

1. Silhavy, T.J., D. Kahne, and S. Walker, *The bacterial cell envelope.* Cold Spring Harb Perspect Biol, 2010. **2**(5): p. a000414.
2. Henderson, J.C., et al., *The Power of Asymmetry: Architecture and Assembly of the Gram-Negative Outer Membrane Lipid Bilayer.* Annu Rev Microbiol, 2016. **70**: p. 255-78.
3. Nikaido, H., *Molecular basis of bacterial outer membrane permeability revisited.* Microbiol Mol Biol Rev, 2003. **67**(4): p. 593-656.
4. Zhang, G., T.C. Meredith, and D. Kahne, *On the essentiality of lipopolysaccharide to Gram-negative bacteria.* Curr Opin Microbiol, 2013. **16**(6): p. 779-85.
5. Raetz, C.R. and C. Whitfield, *Lipopolysaccharide endotoxins.* Annu Rev Biochem, 2002. **71**: p. 635-700.
6. Mi, W., et al., *Structural basis of MsbA-mediated lipopolysaccharide transport.* Nature, 2017. **549**(7671): p. 233-237.
7. Doerrler, W.T., H.S. Gibbons, and C.R. Raetz, *MsbA-dependent translocation of lipids across the inner membrane of Escherichia coli.* J Biol Chem, 2004. **279**(43): p. 45102-9.
8. Sperandeo, P., A.M. Martorana, and A. Polissi, *Lipopolysaccharide Biosynthesis and Transport to the Outer Membrane of Gram-Negative Bacteria.* Subcell Biochem, 2019. **92**: p. 9-37.
9. Sperandeo, P., A.M. Martorana, and A. Polissi, *The Lpt ABC transporter for lipopolysaccharide export to the cell surface.* Res Microbiol, 2019. **170**(8): p. 366-373.
10. Narita, S. and H. Tokuda, *Biochemical characterization of an ABC transporter LptBFGC complex required for the outer membrane sorting of lipopolysaccharides.* FEBS Lett, 2009. **583**(13): p. 2160-4.
11. Owens, T.W., et al., *Structural basis of unidirectional export of lipopolysaccharide to the cell surface.* Nature, 2019. **567**(7749): p. 550-553.
12. Li, Y., B.J. Orlando, and M. Liao, *Structural basis of lipopolysaccharide extraction by the LptB2FGC complex.* Nature, 2019. **567**(7749): p. 486-490.
13. Tang, X., et al., *Cryo-EM structures of lipopolysaccharide transporter LptB2FGC in lipopolysaccharide or AMP-PNP-bound states reveal its transport mechanism.* Nat Commun, 2019. **10**(1): p. 4175.
14. Tran, A.X., C. Dong, and C. Whitfield, *Structure and functional analysis of LptC, a conserved membrane protein involved in the lipopolysaccharide export pathway in Escherichia coli.* J Biol Chem, 2010. **285**(43): p. 33529-39.
15. Laguri, C., et al., *Interaction of lipopolysaccharides at intermolecular sites of the periplasmic Lpt transport assembly.* Sci Rep, 2017. **7**(1): p. 9715.
16. Freinkman, E., et al., *Regulated assembly of the transenvelope protein complex required for lipopolysaccharide export.* Biochemistry, 2012. **51**(24): p. 4800-6.
17. Sperandeo, P., et al., *Characterization of lptA and lptB, two essential genes implicated in lipopolysaccharide transport to the outer membrane of Escherichia coli.* J Bacteriol, 2007. **189**(1): p. 244-53.
18. Suits, M.D., et al., *Novel structure of the conserved gram-negative lipopolysaccharide transport protein A and mutagenesis analysis.* J Mol Biol, 2008. **380**(3): p. 476-88.
19. Dong, H., et al., *Structural basis for outer membrane lipopolysaccharide insertion.* Nature, 2014. **511**(7507): p. 52-6.
20. Chng, S.S., et al., *Characterization of the two-protein complex in Escherichia coli responsible for lipopolysaccharide assembly at the outer membrane.* Proc Natl Acad Sci U S A, 2010. **107**(12): p. 5363-8.
21. Sherman, D.J., et al., *Lipopolysaccharide is transported to the cell surface by a membrane-to-membrane protein bridge.* Science, 2018. **359**(6377): p. 798-801.
22. Okuda, S., E. Freinkman, and D. Kahne, *Cytoplasmic ATP hydrolysis powers transport of lipopolysaccharide across the periplasm in E. coli.* Science, 2012. **338**(6111): p. 1214-7.

23. Gu, Y., et al., *Lipopolysaccharide is inserted into the outer membrane through an intramembrane hole, a lumen gate, and the lateral opening of LptD.* Structure, 2015. **23**(3): p. 496-504.
24. Luo, Q., et al., *Structural basis for lipopolysaccharide extraction by ABC transporter LptB2FG.* Nat Struct Mol Biol, 2017. **24**(5): p. 469-474.
25. Dong, H., et al., *Structural and functional insights into the lipopolysaccharide ABC transporter LptB2FG.* Nat Commun, 2017. **8**(1): p. 222.
26. Okuda, S., et al., *Lipopolysaccharide transport and assembly at the outer membrane: the PEZ model.* Nat Rev Microbiol, 2016. **14**(6): p. 337-45.
27. Bertani, B.R., et al., *A cluster of residues in the lipopolysaccharide exporter that selects substrate variants for transport to the outer membrane.* Mol Microbiol, 2018. **109**(4): p. 541-554.
28. Villa, R., et al., *The Escherichia coli Lpt transenvelope protein complex for lipopolysaccharide export is assembled via conserved structurally homologous domains.* J Bacteriol, 2013. **195**(5): p. 1100-8.
29. Benedet, M., et al., *The Lack of the Essential LptC Protein in the Trans-Envelope Lipopolysaccharide Transport Machine Is Circumvented by Suppressor Mutations in LptF, an Inner Membrane Component of the Escherichia coli Transporter.* PLoS One, 2016. **11**(8): p. e0161354.
30. Bertani, G., *Studies on lysogenesis. I. The mode of phage liberation by lysogenic Escherichia coli.* J Bacteriol, 1951. **62**(3): p. 293-300.
31. Cho, S.H., et al., *Detecting envelope stress by monitoring beta-barrel assembly.* Cell, 2014. **159**(7): p. 1652-64.
32. Young, T.S., et al., *An enhanced system for unnatural amino acid mutagenesis in E. coli.* J Mol Biol, 2010. **395**(2): p. 361-74.
33. Simpson, B.W., et al., *Identification of Residues in the Lipopolysaccharide ABC Transporter That Coordinate ATPase Activity with Extractor Function.* mBio, 2016. **7**(5).
34. Chifflet, S., et al., *A method for the determination of inorganic phosphate in the presence of labile organic phosphate and high concentrations of protein: application to lens ATPases.* Anal Biochem, 1988. **168**(1): p. 1-4.
35. Laemmli, U.K., F. Beguin, and G. Gujer-Kellenberger, *A factor preventing the major head protein of bacteriophage T4 from random aggregation.* J Mol Biol, 1970. **47**(1): p. 69-85.
36. Falchi, F.A., et al., *Mutation and Suppressor Analysis of the Essential Lipopolysaccharide Transport Protein LptA Reveals Strategies To Overcome Severe Outer Membrane Permeability Defects in Escherichia coli.* J Bacteriol, 2018. **200**(2).
37. Martorana, A.M., et al., *Functional Interaction between the Cytoplasmic ABC Protein LptB and the Inner Membrane LptC Protein, Components of the Lipopolysaccharide Transport Machinery in Escherichia coli.* J Bacteriol, 2016. **198**(16): p. 2192-203.
38. Sperandeo, P., et al., *New insights into the Lpt machinery for lipopolysaccharide transport to the cell surface: LptA-LptC interaction and LptA stability as sensors of a properly assembled transenvelope complex.* J Bacteriol, 2011. **193**(5): p. 1042-53.
39. Ruiz, N., et al., *Identification of two inner-membrane proteins required for the transport of lipopolysaccharide to the outer membrane of Escherichia coli.* Proc Natl Acad Sci U S A, 2008. **105**(14): p. 5537-42.
40. Sperandeo, P., A.M. Martorana, and A. Polissi, *The lipopolysaccharide transport (Lpt) machinery: A nonconventional transporter for lipopolysaccharide assembly at the outer membrane of Gram-negative bacteria.* J Biol Chem, 2017. **292**(44): p. 17981-17990.
41. Chng, S.S., et al., *Disulfide rearrangement triggered by translocon assembly controls lipopolysaccharide export.* Science, 2012. **337**(6102): p. 1665-8.
42. Wu, T., et al., *Identification of a protein complex that assembles lipopolysaccharide in the outer membrane of Escherichia coli.* Proc Natl Acad Sci U S A, 2006. **103**(31): p. 11754-9.
43. Hanahan, D., *Studies on transformation of Escherichia coli with plasmids.* J Mol Biol, 1983. **166**(4): p. 557-80.

44. Sperandeo, P., et al., *Functional analysis of the protein machinery required for transport of lipopolysaccharide to the outer membrane of Escherichia coli.* J Bacteriol, 2008. **190**(13): p. 4460-9.
45. Blattner, F.R., et al., *The complete genome sequence of Escherichia coli K-12.* Science, 1997. **277**(5331): p. 1453-62.
46. Sperandeo, P., et al., *Non-essential KDO biosynthesis and new essential cell envelope biogenesis genes in the Escherichia coli yrbG-yhbG locus.* Res Microbiol, 2006. **157**(6): p. 547-58.
47. Ryu, Y. and P.G. Schultz, *Efficient incorporation of unnatural amino acids into proteins in Escherichia coli.* Nat Methods, 2006. **3**(4): p. 263-5.

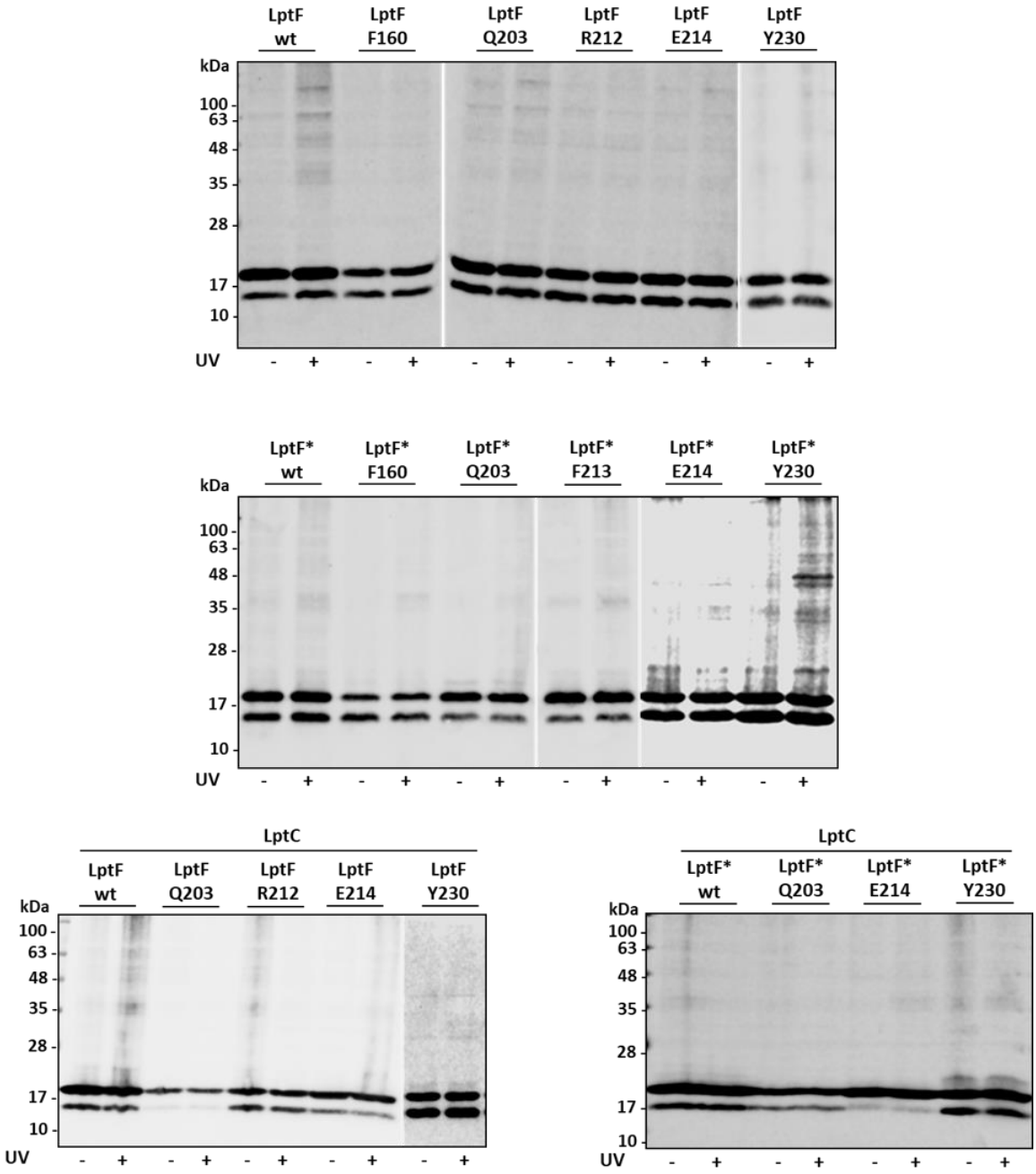

Figure S1 Mutant LptF^{R212G} interacts with LptA and interaction is lost in the presence of ectopically expressed LptC. Specific amino acid positions in LptF and LptF R212G (LptF*) were mutated to incorporate *p*BPA. Amber codons were introduced into *lptF* gene in pGS445 and pGS451 plasmids, harbouring *lptFGAB* and *lptF*^{R212G}*GAB*, respectively. To assess the effect of LptC overexpression, cells were transformed with plasmid pBAD/HisA-LptC expressing LptC fused to a C-terminal His tag. Crosslinking products were detected in TCA precipitated whole-cell extracts, separated onto SDS-PAGE followed by immunoblotting with anti-LptA antibodies. Only residue Y230 in mutant LptF^{R212G} protein crosslinked to LptA upon UV-irradiation, and this interaction was abolished by LptC overexpression.

A

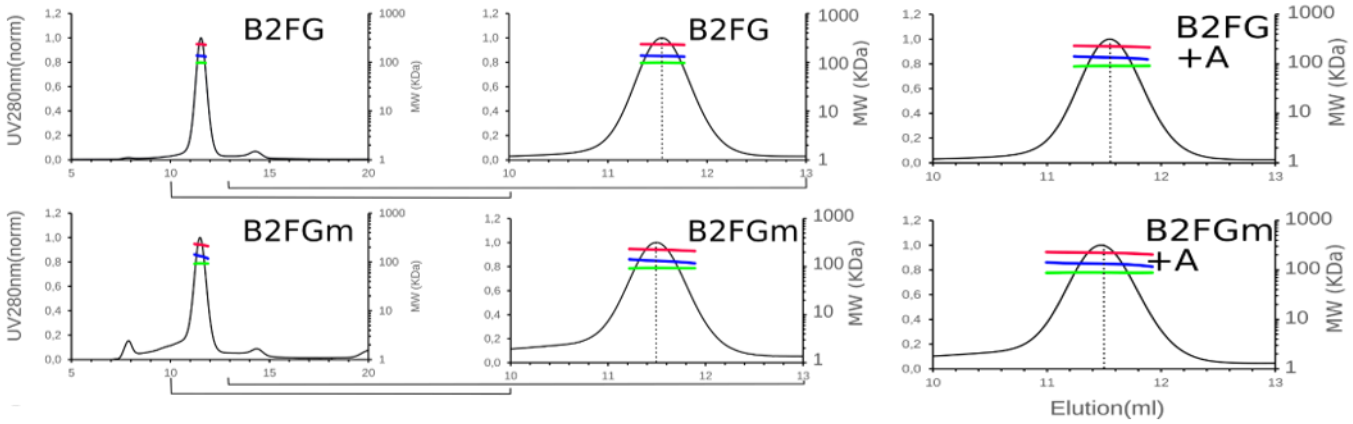
B2FG
B2FG
B2FG +A
B2FGm
B2FGm
B2FGm +A
UV280nm(norm)
MW (KDa)
Elution(ml)

B

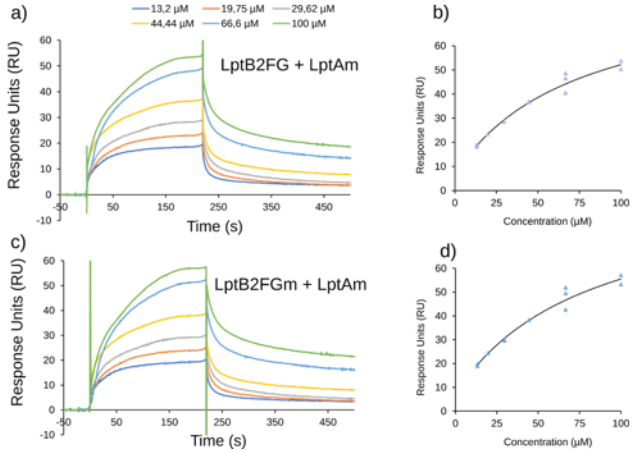
a)
b)
c)
d)
13,2 µM
19,75 µM
29,62 µM
44,44 µM
66,6 µM
100 µM
LptB2FG + LptAm
LptB2FGm + LptAm
Response Units (RU)
Time (s)
Concentration (µM)

Figure S2

Figure S2 $LptB_2F^{R212G}G$ does not form a stable complex with $LptA_m$ *in vitro*. **(A)** SEC-MALLS elution profiles of DDM-purified LpB_2FG and $LpB_2F^{R212G}G$ complexes alone (left panels) and 1:1 mixtures of LpB_2FG:$LptA_m$ and $LptB_2F^{R212G}G$:$LptA_m$ (right panels). Dotted line indicates the elution volume corresponding to 134 kDa. **(B)** Determination of the dissociation constants of the interactions $LptB_2FG$-$LptA_m$ and $LptB_2F^{R212G}G$-$LptA_m$ by SPR. Left panels: Sensorgrams of $LptA_m$ injected at increasing concentrations over immobilized $LptB_2FG$ (upper left panel) and $LptB_2F^{R212G}G$ (lower left panel). Right panels: Steady-state analysis of $LptB_2FG$-$LptA_m$ and $LptB_2F^{R212G}G$-$LptA_m$ interactions.

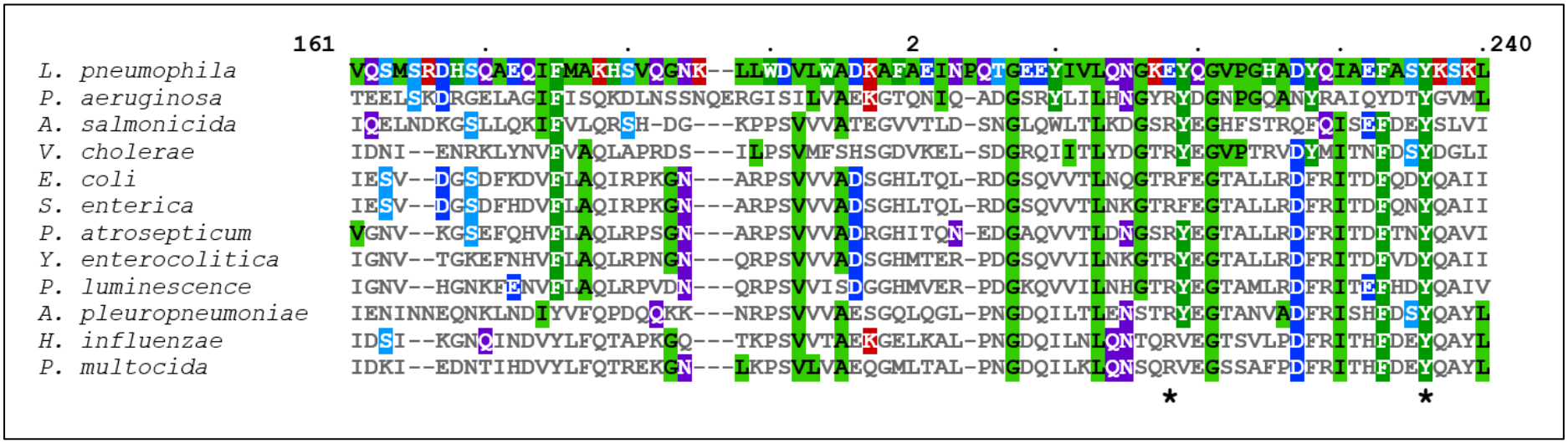

Figure S3 *Escherichia coli* LptF residues R212 and Y230 are conserved among γ-Proteobacteria. Multiple sequence alignment between the relevant region of the periplasmic domain of LptF orthologues from 12 γ-Proteobacteria by ClustalO and then coloured in MView (https://www.ebi.ac.uk/Tools/msa/clustalo/). Uniprot accession numbers are provided in brackets as follow: *E. coli* (LPTC_ECOLI), *Salmonella enterica* (A9N767_SALPB), *Pectobacterium atrosepticum* (Q6DAG2_PECAS), *Yersinia enterocolitica* (A1JRC3_YERE8), *Photorhabdus luminescens* (0Q7N059_PHOLL), *Haemophilus influenzae* (Q4QLE6_HAEI8), *Pasteurella multocida* (V4PYQ4_PASMD), *Actinobacillus pleuropneumoniae* (A3MZ56_ACTP2), *Vibrio cholerae* O1 (C3NV80_VIBCJ), *Aeromonas salmonicida* (A4SHX4_AERS4), *Pseudomonas aeruginosa* PAO1 (Q9HVV8_PSEAE), *Legionella pneumophila* (D5TAY1_LEGP2). The conserved residues R212 and Y230 of the *E. coli* are indicated by asterisks.

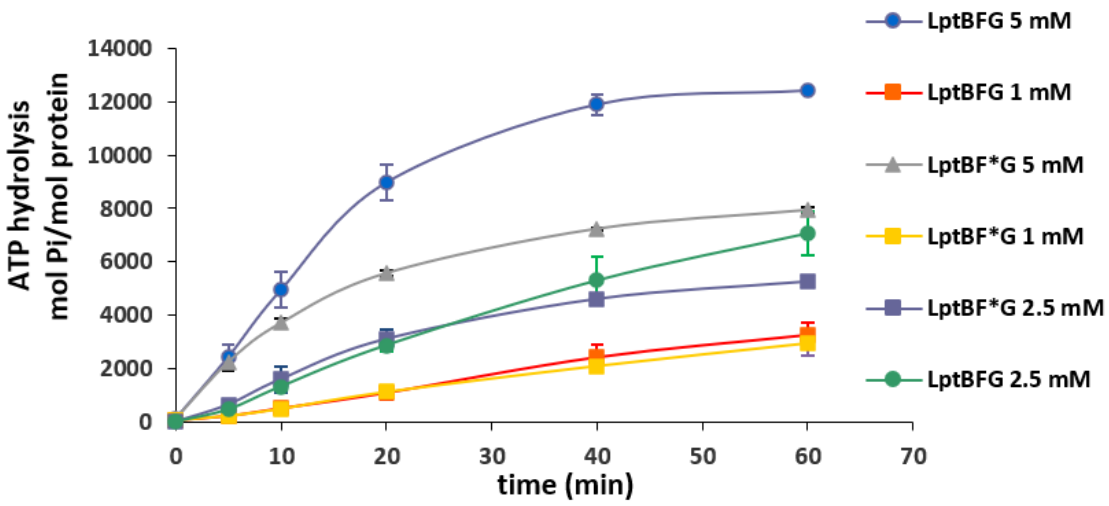

Figure S4 ATPase activity of $LptB_2FG$ and $LptB_2F^{R212G}G$ complexes at different ATP concentrations. $LptB_2F^{R212G}G$ (LptBF*G) displays the same initial rate as $LptB_2FG$ at different substrate concentrations, but the maximum product concentration released by $LptB_2F^{R212G}G$ is lower than $LptB_2FG$. $LptB_2FG$ and $LptB_2F^{R212G}G$ were purified as described in Figure 6 legend. The time-course for product formation (single turnover enzyme kinetics) was assessed by measuring the inorganic phosphate release over time, using 0.2 μM purified complexes. Error bars, s. d. (n = 3 technical replicates).

CONCLUSIONS and FUTURE DIRECTIONS

Given its vital function in protecting the cell from external attacks, the outer membrane (OM) of Gram-negative organisms has been gathering increased attention in the field of antibiotic discovery (see Chapter 3 for details). Murepavadin, a macrocyclic peptidomimetic, validated the Lpt machine as a target in drug development and, recently, thanatin was reported as the first natural product to act on the Lpt system [1]. Two different mechanisms have been proposed for thanatin's antibacterial activity. While Vetterli *et al*. have proposed that thanatin targets the machinery that transports LPS to the cell surface [1], Ma *et al*. have suggested that thanatin permeabilizes the OM by competitively displacing cations, thus causing the release of LPS [2]. The results presented in this thesis support the first mechanism above, i.e., that the antibacterial activity is mainly the outcome of thanatin's interference upon the Lpt machine.

We successfully implemented the Bacterial Adenylate Cyclase Two-Hybrid (BACTH) system to detect Lpt interactions in the periplasm and, using this technique, we showed that thanatin disrupts the Lpt bridge *in vivo* by inhibiting the LptC-LptA and LptA-LptA interactions. Moreover, we observed LptA degradation and the accumulation of LPS decorated with colanic acid (CA) in cells treated with thanatin, further evidencing the disruption of LPS transport [3]. Studying the induction of the *lptAp1* promoter, we observed that thanatin does not activate this promoter in cells unable to synthesise CA. Therefore, we propose that it is the build-up of CA-modified LPS that induces *lptAp1* in thanatin-treated cells. Although *lptAp1* is a σ^E-dependent promoter, the fact that its activation is also dependent on the production of CA is indicative of a link to the Rcs envelope stress response (ESR), and raises the possibility of *lptAp1* requiring both stress responses to be activated. Future work will investigate if indeed *lptAp1* activation only occurs upon LPS-related stresses that activate both σ^E and Rcs responses. Thanatin was also shown to induce the promoter of *ldtD*, suggesting that it induces the remodelling of the peptidoglycan layer. This is a defence mechanism employed by the cell when faced with a severely compromised OM, which can result from a defective LPS biogenesis [4].

We also investigated if thanatin could activate the two-component system (TCS) PmrAB (also known as BasSR in *E. coli*) by monitoring the induction of the *eptA* promoter. Interestingly, the promoter was activated by thanatin but not by the well-known peptide antibiotic polymyxin B (PMB). Thus, the bacterial cell responds very differently to thanatin and PMB, with PMB also activating *lptAp1* differently than thanatin. This may reflect distinct

bacterial killing mechanisms for the two AMPs. In *E. coli*, the dependence of PmrAB on PhoPQ activation is still not clear. Despite the close phylogenetical relationship between *Salmonella* and *E. coli*, more studies using *E. coli* are necessary to elucidate the TCSs PhoPQ and PmrAB and their interconnection in this organism. Therefore, research efforts should be directed towards this topic. It will be interesting to test in the future if, in cells treated with thanatin, the *arn* operon is equally induced and whether the induction of the TCS PhoPQ and the protein PmrD are required for *eptAp* activation. At the moment, it is not clear if the induction of *eptAp* is occurring directly because the cell senses a cationic antimicrobial peptide or if it is due to defects in the LPS transport, which activate other systems that modify the biogenesis of the cell envelope, such as the ESRs. Interestingly, in *Citrobacter rodentium*, the activity of EptA (also known as PmrC) was found to reduce the production of outer membrane vesicles and, in *Salmonella enterica*, lipid A species with modified phosphates were shown to be more likely retained in the OM [5, 6]. These studies support the important role of LPS modifications in the regulation of OM biogenesis.

From our results, we can conclude that thanatin interferes with the biogenesis of the LPS outer layer by perturbing the transport of LPS through the periplasm, which leads to other cellular responses such as increased LptA expression *via lptAp1* activation, the modification of LPS, and possibly the remodelling of the peptidoglycan cell wall. Moreover, thanatin is likely to activate the three main ESRs, i.e., σ^E, Rcs, and Cpx; although direct evidence is lacking. Considered together, our results demonstrate the complexity of pathways and signalling networks monitoring and changing the cell envelope so that the bacterial cell can endure against assaults upon its protective wall. Additionally, thanatin was proven to be a great probe for getting insights into fundamental biological processes in the *E. coli* cell.

Thanatin and derivative molecules have the potential to be used as novel antimicrobials alone or in combinational therapy as potentiators, by enhancing the efficacy of antibiotics usually unable to penetrate the OM, as it was evidenced by the synergism observed with vancomycin, bacitracin, and rifampicin (see Additional unpublished data). Thanatin is a promising starting point for the rational design of antibacterial compounds with several molecular targets. We showed that this peptide inhibits the LptC-LptA and LptA-LptA interactions and, according to Vetterli *et al*., it also likely targets the LptA-LptD interaction. Therefore, thanatin can disrupt the Lpt bridge at several contact points, reducing the likelihood of resistance to emerge. Targeting a dynamic network of protein-protein interactions is an encouraging strategy for novel antibiotic development.

The exact role of the bitopic protein LptC in the unconventional ABC transporter $LptB_2FGC$ had remained elusive until very recently when Owens *et al*. and Li *et al*. published structural data on the transporter, which finally shed some light into the function of LptC [7, 8]. We had started the work presented in this thesis when little was known about the role of LptC, besides its periplasmic domain being essential and the transmembrane region being dispensable in laboratory conditions. The aforementioned structural studies helped us to understand that the transmembrane helix of LptC has a regulatory role on the ATPase activity of the transporter, possibly allowing an efficient coupling between LPS transport and ATP hydrolysis.

Our group had previously isolated suppressor mutants carrying a mutation in residue R212 of the β-jellyroll of LptF that allowed the survival of the bacteria when *lptC* was deleted [9]. We sought to elucidate how the R212G mutation in LptF abolishes the requirement of both the periplasmic domain of LptC, which is directly involved in the transfer of LPS to LptA, and the transmembrane domain, which modulates the ATPase activity of the transporter. First, we observed with UV-photocrosslinking that $LptBF^{R212G}G$ complex can directly interact with LptA, thus bypassing the need for the β-jellyroll domain of LptC. Secondly, from our ATPase activity data, the mutant complex seems to already be in an energy-efficient state for the transport of LPS, hence not requiring the transmembrane domain of LptC to modulate its activity.

Analysing the interaction networks of the IM wild-type and mutant complexes, we discovered intramolecular interactions that may control the flow of LPS through the machinery. In the wild-type complex where LptC is present, the conserved residue Y230 of LptF is free to interact with LPS. However, in the absence of LptC, this residue interacts with R212, possibly hampering LPS release from LptF. In the mutant complex, which functions without LptC, the arginine 212 is replaced with a glycine, abolishing the interaction with Y230 and leaving this residue free to engage with LptA. Briefly, the R212G mutation determines conformational changes and reshuffling of intramolecular interactions that allow the machinery to bypass the need for LptC and directly transfer LPS to LptA.

Future work will concentrate on unravelling exactly how LptC regulates the activity of the ABC transporter, and how it couples the ATP binding and hydrolysis in the cytoplasm to the extraction of LPS from the membrane. Since our experiments were performed using DDM-purified IM complexes, systems that can provide a more native environment may be more suitable for the study of the $LptB_2FGC$ complex, as they can more accurately translate to what might really be happening *in vivo*.

It is not yet known whether the Lpt machinery operates in the same way in strains producing O antigen. Furthermore, it is not clear how important the periplasmic domain of LptG is in the system. Although the structure of each of the seven proteins forming the Lpt machine has been solved, the transenvelope complex has yet to be seen, and the exact stoichiometry of LptA monomers in the bridge remains a mystery. Overall, further work needs to be done to fully understand how this machine works and how it is regulated.

References

1. Vetterli, S.U., et al., *Thanatin targets the intermembrane protein complex required for lipopolysaccharide transport in Escherichia coli.* Sci Adv, 2018. **4**(11): p. eaau2634.
2. Ma, B., et al., *The antimicrobial peptide thanatin disrupts the bacterial outer membrane and inactivates the NDM-1 metallo-beta-lactamase.* Nat Commun, 2019. **10**(1): p. 3517.
3. Sperandeo, P., et al., *Functional analysis of the protein machinery required for transport of lipopolysaccharide to the outer membrane of Escherichia coli.* J Bacteriol, 2008. **190**(13): p. 4460-9.
4. More, N., et al., *Peptidoglycan Remodeling Enables Escherichia coli To Survive Severe Outer Membrane Assembly Defect.* mBio, 2019. **10**(1).
5. Sinha, A., et al., *PmrC (EptA) and CptA Negatively Affect Outer Membrane Vesicle Production in Citrobacter rodentium.* J Bacteriol, 2019. **201**(7).
6. Bonnington, K.E. and M.J. Kuehn, *Outer Membrane Vesicle Production Facilitates LPS Remodeling and Outer Membrane Maintenance in Salmonella during Environmental Transitions.* mBio, 2016. **7**(5).
7. Owens, T.W., et al., *Structural basis of unidirectional export of lipopolysaccharide to the cell surface.* Nature, 2019. **567**(7749): p. 550-553.
8. Li, Y., B.J. Orlando, and M. Liao, *Structural basis of lipopolysaccharide extraction by the LptB2FGC complex.* Nature, 2019. **567**(7749): p. 486-490.
9. Benedet, M., et al., *The Lack of the Essential LptC Protein in the Trans-Envelope Lipopolysaccharide Transport Machine Is Circumvented by Suppressor Mutations in LptF, an Inner Membrane Component of the Escherichia coli Transporter.* PLoS One, 2016. **11**(8): p. e0161354.